2017

Cardiac and Mitochondrial Dysfunction during Diabetes Mellitus: Examination of Mitochondrial Import Mechanisms

Danielle Lee Shepherd

Cardiac and Mitochondrial Dysfunction during Diabetes Mellitus: Examination of Mitochondrial Import Mechanisms

Danielle Lee Shepherd

Dissertation submitted to the School of Medicine at West Virginia University in partial fulfillment of the requirements for the degree of

Doctor of Philosophy
In
Exercise Physiology

John M. Hollander, Ph.D., Chair
Stephen E. Alway, Ph.D.
Emidio E. Pistilli, Ph.D.
I. Mark Olfert, Ph.D.
S. Jamal Mustafa, Ph.D.
Division of Exercise Physiology
Morgantown, West Virginia
2016

Key Words: Diabetes mellitus, Mitochondria, Import, miRNA

ABSTRACT

Cardiac and Mitochondrial Dysfunction during Diabetes Mellitus: Examination of Mitochondrial Import Mechanisms

Danielle Lee Shepherd

Approximately 9% of the United States population is diagnosed with diabetes mellitus (DM), which is comprised of 2 distinct pathologies: type 1 diabetes mellitus (T1DM) and type 2 diabetes mellitus (T2DM). T1DM, which is caused by insufficient insulin production, affects approximately 5% of diabetic patients, while T2DM results from insulin resistance and affects 95% of all diabetic patients. Within diabetic patients, cardiac complications, such as diabetic cardiomyopathy, are the leading cause of morbidity and mortality. The mitochondrion has been implicated as an underlying factor in the etiology and progression of the cardiac contractile deficits and cardiac failure that accompany DM. The study of cardiac mitochondria is further complicated by the presence of two distinct mitochondrial subpopulations residing within the cardiomyocyte. The pool of mitochondria existing beneath the sarcolemmal membrane are termed the subsarcolemmal mitochondria (SSM), while the group that exists between the myofibrils is called the interfibrillar mitochondria (IFM). Assessment of mitochondrial subpopulations has revealed differential impact to both physiological and pathological stimuli. Specifically, during DM, the IFM are most impacted during T1DM, with the SSM being most impacted under T2DM pathological insult. During DM, proteomic analyses by our laboratory and others reveal decreased abundance of nuclear-encoded mitochondrial proteins essential for processes such as oxidative phosphorylation, fatty acid oxidation and tricarboxylic acid cycle in the subpopulation predominantly impacted by the DM type. Further, our laboratory has previously shown import efficiency to be down in the T1DM IFM, which could play a role in the proteomic dysregulation. Approximately 99% of the mitochondrial proteome is composed of nuclear-encoded proteins imported into the mitochondrion via a complicated mechanism of translocation that coordinates both the outer and inner mitochondrial membranes, thus highlighting the importance of studying the nuclear-encoded mitochondrial protein import process during pathological states. To date, evaluation of the diabetic heart using a highly sensitive echocardiographic analysis software in order to assess subtle changes in left ventricular function prior to overt contractile dysfunction during DM has not been completed. Additionally, the differential proteomic alterations in mitochondrial subpopulations resulting from distinct DM pathologies and the evaluation of inefficient nuclear-encoded mitochondrial protein import due to decrements in a key import constituent in the mitochondrial subpopulation predominantly affected, mitochondrial heat shock protein 70 (mtHsp70), have not been completed. Further, the mechanisms involved in miRNA import into the mitochondrion during DM remains limited. Therefore, the goal of the following studies was to examine subpopulation-specific mitochondrial proteome disruption stemming from inefficient nuclear-encoded mitochondrial protein import and/or increased miRNA influx into the mitochondrion, thus leading to increased contractile dysfunction during DM. T1DM was induced in 6-week-old mice with multiple low-dose (50mg/kg) streptozotocin (STZ) injections for 5 consecutive days. Hyperglycemia was confirmed and echocardiography performed at weeks 1, 3 and 6 post-diabetic onset. Conventional analyses revealed cardiac contractile deficits relative to control at 6-weeks post-T1DM onset. In contrast, short- and long-axis analyses using the speckle-tracking based strain analysis software demonstrated changes in the LV myocardium as early as

1-week post-diabetic onset. These findings show that analysis of myocardial function using speckle-tracking based strain analyses could provide a more precise method for evaluating cardiac contractile dysfunction during the progression of different pathological states. Our laboratory has previously shown that proteomic alterations specific to the T2DM SSM and T1DM IFM occur, potentially due to a decrement in nuclear-encoded mitochondrial protein import. Because mtHsp70, an essential component in the import of nuclear-encoded proteins into the mitochondrion is consistently down during DM, we generated a novel transgenic line with a cardiac-specific overexpression of mtHsp70. We subjected this line to STZ to generate a T1DM mouse model with mtHsp70 overexpression. Further, we utilized the db/db mouse model for T2DM and with a novel ovarian transplantation procedure, we were able to generate an increased abundance of mtHsp70 db/db and control animals, which were approximately 20-weeks-old before hearts were excised and mitochondrial subpopulations isolated. When assessing nuclear-encoded mitochondrial protein import efficiency in the mitochondrial subpopulations during both types of DM, we found decrements to this process in the SSM of T2DM mice and IFM of T1DM mice, which was subsequently restored with mtHsp70 overexpression. Further, alterations to the most impacted mitochondrial subpopulations proteome were noted, with mtHsp70 affording protection. Additionally, we also found mtHsp70 protein content to be down in the T1DM and T2DM human heart. These findings support the rationale for the use of mtHsp70 as a mitochondrial-targeted therapeutic capable of protecting the mitochondrial subpopulation most impacted during the different types of DM. Interestingly, the mitochondrial proteome could also be affected by redistribution of microRNAs (miRNAs) during a pathological setting. MiRNAs are able to regulate protein expression via transcriptional and translational repression and are suggested to be located within the mitochondrion. Our laboratory has previously shown detrimental impact to the IFM due to redistribution of miR-141 and miR-378 during T1DM. This emphasizes the importance of studying how miRNA are able to translocate into the mitochondrion, a mechanism that currently remains unknown. Therefore, we assessed the involvement of polynucleotide phosphorylase (PNPase), a protein located in the mitochondrial intermembrane space, in the import of miRNA into the mitochondrion. We found PNPase to be associated with argonaute 2 (Ago2), a component of the RNA-induced silencing complex (RISC). PNPase was found to have an increased expression in the SSM during T2DM, along with an increased association with Ago2. PNPase protein expression is also significantly increased in mitochondria from T2DM human patients. Further, an increased presence of miR-378 within the mitochondrion was noted, which corresponded to a decrease in ATP6 protein content and ATP synthase function. Overexpression of PNPase in the HL-1 cardiomyocyte cell line revealed similar results. These findings show for the first time a potential component involved in the mechanism of miRNA import into the mitochondrion. Overall, the studies highlighted above indicate that speckle-tracking based strain analyses provide a mechanism to detect subtle changes in LV myocardial function during the progression of DM. Further, through manipulating mtHsp70, the driving force behind nuclear-encoded mitochondrial protein import, we highlight the novel therapeutic paradigm in which multiple dysfunctional processes are corrected through a single protein target capable of restoring mitochondrial and cardiac contractile function independent of DM type. We have shown for the first time a potential constituent involved in the complicated import process of miRNA into the mitochondrion. In conclusion, targeted therapeutics generated to correct disrupted mitochondrial mechanisms during DM, may provide cardiac benefit via reduced mitochondrial dysfunction and preservation of the mitochondrial proteome, ultimately leading to restored cardiac function and a better quality of life for diabetic patients.

AKNOWLEDGEMENTS

I would like to thank everyone involved in my education and professional development throughout my tenure at West Virginia University. First, I would like to acknowledge my advisor and mentor, Dr. John Hollander. Thank you for your support and guidance that helped me to grow both professionally and personally. Thank you for spending the time to help me learn how to think outside of the box and to further develop my critical thinking skills. I would also like to thank my committee members Dr. Stephen Alway, Dr. Emidio Pistilli, Dr. I. Mark Olfert and Dr. S. Jamal Mustafa for their critical input and investment in both my research and my professional interests, as well as their support for my future career endeavors.

Next, I would like to thank all of my colleagues at West Virginia University. I would like to thank the past and present members of the Hollander laboratory: Dr. Walter Baseler, Dr. Dharendra Thapa, Dr. Rajaganapathi Jagannathan, Sara Lewis and Seth Stine. I want to sincerely thank Quincy Hathaway and Mark Pinti for all of the chalk talk sessions and encouragement, as well as Kristen Hughes and Shruthi Sreekumar for making me laugh even during the tough and frustrating times. A special thank you to the honorary Hollander lab member, Tyler Pizzute, for all of the coffee and encouragement you provided. Additionally, I would like to thank Janelle Stricker and Sarah McLaughlin for their support and advice during my time here. A special thank you to the Office of the Graduate Research and Education and the Division of Exercise Physiology for their unending support. Specifically, thank you Dr. Fred Minnear for your support and your tough love to help me to grow into the person that I am today. Thank you to my colleagues and running/triathlon training buddies, Lindsey Bishop and Michelle Bedenbaugh. Without the two of you, I would not have experienced some of my fondest outside of laboratory memories during graduate school, so thank you for getting me out of the lab. To Dr. Tara Croston, you have been one of my greatest supporters and friends throughout this process. Thank you for always being there and guiding me when I needed you while you were in the lab and after you graduated. Last, but certainly not least, thank you Dr. Cody Nichols. I will forever be grateful for the time we had together as labmates, roommates, and always tied as my lab husband and most importantly, friend and brother. You truly helped me to grow scientifically, professionally and personally. My time at West Virginia University would not have been as great without you, so thank you for everything and all of the memories we created.

I would like to thank my family for their unwavering support and confidence in me during my graduate career, even though I always kept them on their toes for when I would finish going to school. Without the support from my father and mother, George and Karen, along with my stepparents, Mark and Barb, I would not have gotten to where I am today. All of you were there through the good and hard times, so thank you for the encouragement. Thank you also to my extended family for always asking, “Are you done with school?” and supporting me through the entire process. Thank you to some of the most important people in my life, Rozzy Lauderback, Rachel Matheny, Alissa McBurney, Sarah Perley and Alysia Arrowood for helping me through the tough times during graduate school and encouraging me to finish strong. I am eternally grateful for you always having faith in me, even when I did not have faith in myself. I am truly blessed to have each one of you in my life.

DEDICATION

To My Parents: George and Karen

Thank you for always providing me with support throughout all of my life endeavors. Thank you for encouraging me to be my best and do my best at all times. In particular, thank you for your support throughout my entire academic career. I love you both.

LIST OF ABBREVIATIONS

AA	Anterior Apex
AB	Anterior Base
ACEi	Angiotensin-Converting Enzyme Inhibitor
ADP	Adenosine Diphosphate
AF	Anterior Free
AGO	Argonaute
AM	Anterior Mid
ANOVA	Analysis of Variance
AS	Anterior Septum
ATP	Adenosine Triphosphate
B-Mode	Brightness Mode
BPM	Beats Per Minute
C, Ctl	Control
Ca^{2+}	Calcium
CAD	Coronary Artery Disease
cm	Centimeter
COXIV	Cytochrome c Oxidase Subunit IV
Deg	Degree
DIGE	Difference Gel Electrophoresis
dL	Deciliter
DM	Diabetes Mellitus
EDP	End Diastolic Pressure
EF	Ejection Fraction
ER	Endoplasmic Reticulum
ETC	Electron Transport Chain
ET-1	Endothelin-1
FAO	Fatty Acid Oxidation

FS	Fractional Shortening
GFP	Green Fluorescent Protein
GLUT2	Glucose Transporter 2
H^+	Hydrogen
H_2O_2	Hydrogen Peroxide
HF	Heart Failure
HRP	Horseradish Peroxidase
HSP	Heat Shock Protein
ICC	Intra-Class Correlation Coefficient
IF	Inferior Free
IFM	Interfibrillar Mitochondria
IL-1	Interleukin-1
IMM	Inner Mitochondrial Membrane
IMS	Intermembrane Space
IPA	Ingenuity Pathway Analysis
I/R	Ischemia/Reperfusion
iTRAQ	Isobaric Tag for Relative and Absolute Quantitation
IVRT	Isovolumetric Relaxation Time
K^+	Potassium
L	Lateral
LAX	Long-Axis
LC	Liquid Chromatography
LS	Longitudinal Strain
LSR	Longitudinal Strain Rate
LV	Left Ventricle
LVID	Left Ventricular Internal Diameter
MAC	Membrane Attack Complex
MALDI	Matrix-Assisted Laser Desorption/Ionization

mg	Milligram
MI	Myocardial Infarction
mRNA	Messenger RNA
miRNA	MicroRNA
mL	Milliliter
mm	millimeter
M-Mode	Motion Mode
MnSOD	Manganese Superoxide Dismutase
MPD	Mevalonate Pyrophosphate Decarboxylase
mPHGPx	Mitochondrial Phospholipid Hydroperoxide Glutatione Peroxidase
MPP	Matrix Processing Peptidases
mPTP	Mitochondrial Permeability Transition Pore
MS	Mass Spectrometry
mtHsp70	Mitochondrial Heat Shock Protein 70
MudPIT	Multidimensional Protein Identification Technology
NADH	Nicotinamide Adenine Dinucleotide
NADPH	Nicotinamide Adenine Dinucleotide Phosphate
ND	Non-diabetic
NOX	NADPH oxidase
Nt	Nucleotide
OMM	Outer Mitochondrial Membrane
OXPHOS	Oxidative Phosphorylation
P	Posterior
PA	Posterior Apex
PAGE	Polyacrylamide Gel Electrophoresis
PAM	Presequence Translocase-Associated Motor
PB	Posterior Base
PCR	Polymerase Chain Reaction

PM	Posterior Mid
PNPase	Polynucleotide Phosphorylase
PS	Posterior Septum
RISC	RNA-Induced Silencing Complex
ROS	Reactive Oxygen Species
rRNA	Ribosomal RNA
RV	Right Ventricle
S	Second
SAX	Short-Axis
SDS	Sodium Dodecyl Sulfate
SEM	Standard Error of the Mean
SR	Strain Rate
SSM	Subsarcolemmal Mitochondria
STZ	Streptozotocin
T1DM	Type 1 Diabetes Mellitus
T2DM	Type 2 Diabetes Mellitus
TCA	Tricarboxylic Acid
Tg	Transgenic
TIM	Translocase of the Inner Membrane
TOF	Time of Flight
TOM	Translocase of the Outer Membrane
tRNA	Transfer RNA
UTR	Untranslated Region
VDAC	Voltage Dependent Anion Channel
WT	Wild-type
1D	One-Dimensional
2D	Two-Dimensional
3D	Three-Dimensional

αMHC	Alpha-Myosin Heavy-Chain
ΔΨm	Membrane Potential
µL	Microliter

TABLE OF CONTENTS

LIST OF FIGURES

Chapter 1

Chapter 2

Chapter 3

Chapter 4

LIST OF TABLES

Chapter 1

Chapter 2

Chapter 3

SPECIFIC AIMS

Approximately 9% of the United States population is diagnosed with diabetes mellitus (DM) and diabetic cardiomyopathy is the leading cause of heart failure in diabetic patients (1). Type 1 diabetes mellitus (T1DM), caused by insufficient insulin production, affects approximately 5% of diabetic patients, while type 2 diabetes mellitus (T2DM) results from insulin resistance and affects 95% of all diabetic patients (2). The mitochondrion has been identified as a central contributor to contractile dysfunction during DM, with echocardiographic speckle-tracking based strain analyses allowing for an early detection of subtle myocardial changes (7, 8, 13). Examination of mitochondrial dysfunction during DM is further complicated by the presence of two distinct mitochondrial subpopulations residing within the cardiomyocyte (11). A pool of mitochondria exists beneath the sarcolemmal membrane, the subsarcolemmal mitochondria (SSM), while another group exists between the myofibrils, the interfibrillar mitochondria (IFM). Approximately 99% of the mitochondrial proteome is composed of nuclear-encoded proteins, which are imported into the mitochondrion via a complicated mechanism coordinating both the outer and inner mitochondrial membranes (3, 12, 14). Proteomic analyses by our laboratory and others reveal decreased abundance of nuclear-encoded mitochondrial proteins, essential for processes such as oxidative phosphorylation, fatty acid oxidation (FAO) and tricarboxylic acid cycle (TCA), during DM (4, 5, 9, 15). Further, our laboratory has shown decreased nuclear-encoded mitochondrial protein import in the T1DM IFM (5). Prior to this dissertation, evaluation of the diabetic heart using speckle-tracking based strain analyses had not been studied to determine if subtle changes occur prior to overt cardiac dysfunction. Additionally, it was unknown if a key constituent in nuclear-encoded mitochondrial protein import would serve as a locus for reversal of the dysfunction seen during the pathology. Finally, this dissertation also provides insight into a

potential constituent involved in the mechanism of import of microRNAs (miRNAs) into the mitochondria.

Our **long-term goal** was to identify mechanisms to alleviate adverse cardiac and mitochondrial effects associated with DM with the intent of providing a mechanism for therapeutic interventions to be designed. The **objectives** of this dissertation were to determine if during DM: (1) echocardiographic speckle-tracking based strain imaging analyses would lead to a greater ability to detect earlier changes in myocardial dysfunction; (2) mitochondrial heat shock protein 70 (mtHsp70) would provide mitochondrial and cardiac contractile protection through increased mitochondrial proteome stability and nuclear-encoded mitochondrial protein import efficiency; (3) increased polynucleotide phosphorylase (PNPase) expression led to an increase in miRNA import into the mitochondrion via an association with the RNA-induced silencing complex (RISC).

The **central hypothesis** of this dissertation was that strain analyses would offer the capability to detect early decrements in left ventricular (LV) myocardial strain resulting from mitochondrial dysfunction associated with a disrupted mitochondrial proteome potentially due to inefficient mitochondrial protein import or increased miRNA within the mitochondrion. Further, we hypothesized that mtHsp70 would rectify inefficiencies in nuclear-encoded mitochondrial protein import, thus restoring the mitochondrial proteome and cardiac contractile function. Notably, these effects would be most pronounced in the IFM during a T1DM insult and the SSM during a T2DM insult. The central hypothesis was based upon preliminary data produced in our laboratory indicating that cardiac contractile dysfunction occurs during DM and that the mitochondrial proteome is disrupted due to inefficient nuclear-encoded mitochondrial protein import or miRNA redistribution during the pathological setting (5, 6, 9, 10). Our **rationale** for the proposed research was based upon the notion that a greater understanding of the mechanisms

involved in mitochondrial dysfunction during DM, along with a non-invasive mechanism to evaluate and detect early myocardial contractile deficiencies, could potentially allow for the identification of key contributors to alleviate mitochondrial dysfunction, aiding in the development of a therapeutic paradigm to help combat cardiac complications in diabetic patients. We tested our central hypothesis by pursuing the following **Specific Aims**:

Specific Aim I: Determine the therapeutic advantage for using speckle-tracking based strain imaging analyses versus conventional echocardiographic measurements in a small animal model of T1DM.

To address Specific Aim I, we utilized the streptozotocin (STZ) T1DM mouse model and performed a time-course study to evaluate our working hypothesis. Our **working hypothesis** was that subtle changes in myocardial strain could be detected earlier using the speckle-tracking based strain imaging analyses prior to the onset of cardiac contractile dysfunction delineated by conventional echocardiographic measurements.

Specific Aim II: Assess the cardioprotective efficacy of mtHsp70 overexpression on nuclear-encoded mitochondrial protein import and mitochondrial proteome stabilization to alleviate cardiac mitochondrial and contractile dysfunction in the diabetic heart.

MtHsp70 is a vital component to the mitochondrial protein import machinery. Located within the mitochondrial matrix, mtHsp70 provides the active motor for import of proteins into the mitochondrial matrix (3). Previous work from our laboratory demonstrated that this essential component of the protein import machinery is reduced during DM, potentially causing decreased efficiency in nuclear-encoded mitochondrial protein import leading to a deranged mitochondrial

proteome (5, 9). Overexpression of mtHsp70 was employed to assess its effect on proteome restoration and nuclear-encoded protein import efficiency during DM. Our **working hypothesis** was that overexpression of a cardiac-specific mtHsp70 during DM would restore nuclear-encoded mitochondrial protein import deficiencies, reverse proteome instability and alleviate cardiac contractile dysfunction. Further, these effects would be shown to occur in the IFM during T1DM and the SSM during T2DM.

Specific Aim III: Elucidate the role of PNPase in the mechanism of miRNA import into the mitochondrion via RNA-induced silencing complex (RISC) association in the diabetic heart.

To address Specific Aim III, we used the db/db mouse model for T2DM and evaluated PNPase protein expression levels, along with miR-378 levels within the mitochondrion. Further, we overexpressed PNPase in the HL1 cardiomyocyte cell line to examine the impact on miR-378 translocation into the mitochondrion. Our **working hypothesis** was that the increased association of PNPase with the RISC would allow for increased miRNA transport into the mitochondrion during T2DM. Further, increased expression of miRNA, such as miR-378, could affect the mitochondrial genome and processes such as ATP production via ATP synthase.

The research generated from this dissertation was innovative because it uses advanced imaging analysis techniques to detect early changes in the myocardium, allowing for early intervention strategies to be employed for DM patients with cardiac contractile abnormalities. Further, this dissertation expanded upon previous work of the laboratory utilizing a novel cardiac-specific transgenic mouse line, which alleviated dysfunctional processes during DM. At the completion of these studies, we were able to utilize a non-invasive approach to detect subtle myocardial changes during T1DM in a small animal model. This type of analyses will allow

researchers to approach treatment of adverse cardiac function in different pathological states in small animal models at the earliest onset of myocardial abnormalities and evaluate the protection afforded by different therapeutic paradigms. Further, by manipulating mtHsp70, the driving force behind nuclear-encoded mitochondrial protein import, we highlighted the novel therapeutic paradigm in which multiple dysfunctional processes are corrected through a single protein target capable of restoring mitochondrial function independent of diabetic type. Finally, the outcomes on our research for PNPase during T2DM, enhanced our understanding of a potential player in the mechanism of miRNA import into the mitochondrion. Altogether, this dissertation research led to the increased understanding of mitochondrial dysfunction during DM and provided insight into potential therapeutic interventions that could be applied to the treatment of DM patients in order to increase their quality of life.

REFERENCES

1. Diabetes Fact Sheet. *World Health Organization*, 2016.
2. The State of Obesity: Better Policies for a Healthier America. 2015.
3. **Baseler WA, Croston TL, and Hollander JM.** Functional Characteristics of Mortalin. In: *Mortalin Biology: Life, Stress and Death*, edited by Kaul SC and Wadhwa R. New York: Springer, 2012, p. 55-80.
4. **Baseler WA, Dabkowski ER, Jagannathan R, Thapa D, Nichols CE, Shepherd DL, Croston TL, Powell M, Razunguzwa TT, Lewis SE, Schnell DM, and Hollander JM.** Reversal of mitochondrial proteomic loss in Type 1 diabetic heart with overexpression of phospholipid hydroperoxide glutathione peroxidase. *Am J Physiol Regul Integr Comp Physiol* 304: R553-565, 2013.
5. **Baseler WA, Dabkowski ER, Williamson CL, Croston TL, Thapa D, Powell MJ, Razunguzwa TT, and Hollander JM.** Proteomic alterations of distinct mitochondrial subpopulations in the type 1 diabetic heart: contribution of protein import dysfunction. *Am J Physiol Regul Integr Comp Physiol* 300: R186-200, 2011.
6. **Baseler WA, Thapa D, Jagannathan R, Dabkowski ER, Croston TL, and Hollander JM.** miR-141 as a regulator of the mitochondrial phosphate carrier (Slc25a3) in the type 1 diabetic heart. *Am J Physiol Cell Physiol* 303: C1244-1251, 2012.
7. **Bauer M, Cheng S, Jain M, Ngoy S, Theodoropoulos C, Trujillo A, Lin FC, and Liao R.** Echocardiographic speckle-tracking based strain imaging for rapid cardiovascular phenotyping in mice. *Circ Res* 108: 908-916, 2011.
8. **Bauer M, Cheng S, Unno K, Lin FC, and Liao R.** Regional cardiac dysfunction and dyssynchrony in a murine model of afterload stress. *PloS one* 8: e59915, 2013.

9. **Dabkowski ER, Baseler WA, Williamson CL, Powell M, Razunguzwa TT, Frisbee JC, and Hollander JM.** Mitochondrial dysfunction in the type 2 diabetic heart is associated with alterations in spatially distinct mitochondrial proteomes. *Am J Physiol Heart Circ Physiol* 299: H529-540, 2010.
10. **Jagannathan R, Thapa D, Nichols CE, Shepherd DL, Stricker JC, Croston TL, Baseler WA, Lewis SE, Martinez I, and Hollander JM.** Translational Regulation of the Mitochondrial Genome Following Redistribution of Mitochondrial MicroRNA in the Diabetic Heart. *Circ Cardiovasc Genet* 8: 785-802, 2015.
11. **Palmer JW, Tandler B, and Hoppel CL.** Biochemical differences between subsarcolemmal and interfibrillar mitochondria from rat cardiac muscle: effects of procedural manipulations. *Arch Biochem Biophys* 236: 691-702, 1985.
12. **Pfanner N and Geissler A.** Versatility of the mitochondrial protein import machinery. *Nat Rev Mol Cell Biol* 2: 339-349, 2001.
13. **Ram R, Mickelsen DM, Theodoropoulos C, and Blaxall BC.** New approaches in small animal echocardiography: imaging the sounds of silence. *Am J Physiol Heart Circ Physiol* 301: H1765-1780, 2011.
14. **Stojanovski D, Pfanner N, and Wiedemann N.** Import of proteins into mitochondria. *Methods in cell biology* 80: 783-806, 2007.
15. **Turko IV and Murad F.** Quantitative protein profiling in heart mitochondria from diabetic rats. *J Biol Chem* 278: 35844-35849, 2003.

Chapter 1:
Literature Review

BACKGROUND AND SIGNIFICANCE

1.1 Diabetes Mellitus

Diabetes mellitus (DM) is a complex pathological condition characterized into two general types. The predominant form of DM is type 2 diabetes mellitus (T2DM), which encompasses approximately 95% of diabetic patients, while type 1 diabetes mellitus (T1DM) accounts for 5% of diabetic cases (353). Chronic hyperglycemia is a characteristic hallmark of DM and oftentimes leads to damage and failure of organs including the heart, eyes, kidneys and blood vessels (2). When left untreated, complications resulting from DM can result in death. Other lesser-known types of DM exist, such as gestational diabetes, which occurs during pregnancy along with DM arising from genetic conditions, surgeries, medications and other pancreatic diseases. A diagnosis for DM is generally associated with a fasting blood glucose level above 126 mg/dL and for type 1 diabetics, insulin levels under 0.50 ng/mL (389).

1.1a. Type 1 diabetes mellitus

Affecting approximately 5% of diabetic patients, T1DM is characterized by a lack of insulin production due to the autoimmune destruction of the pancreatic β-cells, leading to insulin deficiency within the body (185). The presence of autoantigens within pancreatic islet cells, such as islet cell antigen, insulin, pro insulin, glutamic acid decarboxylase and protein tyrosine phosphatase, can promote the destruction of the β-cells (284). Factors such as genetic predisposition can lead to T1DM, but environmental factors including viral infections, parental age, and low birth weight have also been associated with its development (6). T1DM is also referred to as juvenile-onset diabetes, with the majority of T1DM cases occurring in children,

adolescents and young adults (35). Treatment of T1DM includes monitoring the blood glucose levels of patients and injection with insulin prior to the consumption of food, which allows the body to properly transport cellular glucose and utilize it efficiently. During T1DM, severe insulin deficiency leads to increased ketone body production in the liver, which causes a lowering of the pH of the blood, ultimately resulting in diabetic ketoacidosis (72, 435). Multiple organ and systems are affected during T1DM, including complications with the eyes, liver, kidneys, nervous system, skeletal muscle and heart (2). Diseases and issues such as retinal detachment, diabetic nephropathy leading to renal failure, amputations of limbs, periodontal and heart disease are some of the ailments seen coinciding with uncontrolled T1DM (2). The hyperglycemic environment produced during T1DM produces these catastrophic ailments associated with the disease and no known prevention of T1DM exists to date.

1.1b. Type 2 diabetes mellitus

T2DM is the more prevalent form of DM, affecting approximately 95% of diabetic patients. Nine out of 10 individuals with prediabetes, do not know that they are at risk of developing DM, and of that, 15-30% of people with prediabetes will develop T2DM within 5 years (4). T2DM is known as non-insulin dependent diabetes because it is characterized by insulin resistance, reduced insulin sensitivity and occasionally a defect in insulin secretion from the β-cells, ultimately producing the hallmark hyperglycemic environment of DM (353). Obesity oftentimes accompanies T2DM; however, it is not a prerequisite for the disease. With that being said, most T2DM patients display an increased body fat percentage in their abdominal region and unlike T1DM, T2DM patients do not suffer from ketoacidosis (12). Interestingly, T2DM patients may present with normal insulin levels; however, their insulin levels rarely compensate for the elevation

in blood glucose levels, resulting in a deficiency of insulin secretion. Dyslipidemia and an altered lipoprotein pattern including increased triglyceride levels, low levels of high-density lipoprotein cholesterol and small, dense low-density lipoprotein particles, are characteristic during the early stages of T2DM (368). Treatment of T2DM includes monitoring the blood glucose levels of patients and adherence to a strict regimen of diet and exercise in hopes of reducing the body weight of T2DM patients suffering from obesity and increasing the body's ability to properly handle glucose (368, 424). Treatment with insulin or other medications, such as Metformin, which work to increase insulin sensitivity or reduce glucose production are also commonly used in T2DM patients (319).

1.1c. Significance

The leading causes of morbidity and mortality among diabetic patients in the United States are cardiac failure and heart disease (142). DM is the seventh leading cause of death in the United States and the incidence of DM has doubled its rates over the past two decades (3, 4). Current reports suggest that DM affects a staggering 9% of the population worldwide, with 29 million adults in the United States being diagnosed with DM and another 86 million diagnosed with prediabetes (2-4, 12). Both T1DM and T2DM are characterized by hyperglycemia resulting either from deficits in insulin production or resistance, respectively. This chronic hyperglycemic environment can lead to the damage of many organ systems including the kidneys, eyes, nerves, blood vessels and the heart (2, 431). Due to the increasing incidence of DM in the United States and the world, the disease is quickly becoming an epidemic and the evaluation of mechanisms that underlie the cardiac deficits seen during DM need to be studied in order to develop and implement therapeutic strategies to increase the quality of life in diabetic patients.

1.2 Diabetic Cardiomyopathy

DM-associated cardiac dysfunction, termed diabetic cardiomyopathy, occurs independently of vascular dysfunction, such as atherosclerosis, coronary artery disease (CAD) and hypertension and serves as the leading cause of heart failure (HF) in diabetic patients (30, 52). Literature suggests that while CAD and hypertension often occur as comorbidities to diabetic heart disease, diabetic cardiomyopathy has also been shown to be independent of these pathologies in both the clinical and experimental settings (8, 38, 97, 159, 270, 326, 337). Rubler et al. first showed diabetic cardiomyopathy in congestive HF patients with DM; however, it was noted that these patients also lacked the presence of coronary atherosclerosis and hypertension (337). Following this study, Regan et al. showed that diabetic patients without CAD had alterations in left ventricular (LV) end diastolic pressure (EDP), LV compliance and ejection fraction (EF) (326). Experimental models of DM have revealed decreased contractile efficiency while also being resistant to atherosclerosis, indicating the presence of diabetic cardiomyopathy (187, 397). This evidence suggests that diabetic cardiomyopathy leads to LV dysfunction in the absence of vascular disturbance and further has been associated with decreased mitochondrial function and adenosine triphosphate (ATP) production (97, 130, 154, 236, 326, 353, 373, 390).

1.2a. Cardiac contractile dysfunction

Cardiac contractile dysfunction is a common hallmark of DM, leading to HF in diabetic patients due to the effects of the chronic hyperglycemic environment. Diastolic dysfunction occurs during the beginning stages of DM and is characterized by deficits in LV relaxation time and compliance (30, 118, 249, 353, 441). By utilizing tissue Doppler analyses and assessing the flow

of blood across the mitral valve, patients with T1DM revealed decreases in early peak mitral velocity (E wave) and increased late peak mitral velocity (A wave) leading to a decreased E/A ratio, along with a prolonged deceleration time (56, 320, 321, 344). Patients with T2DM also show abnormal LV relaxation and restrictive filling deficiencies (43, 83, 136, 258, 293). Diastolic dysfunction is also evident in experimental animal models of both T1DM and T2DM (43, 141, 303, 352). Dabkowski et al. showed cardiac dysfunction in T1DM mice through decreased rates of contraction, relaxation and developed pressure via Langendorff perfusion (85). Prolonged relaxation time and slowing of relaxation velocity indicated the presence of diastolic deficits in the diabetic rat myocardium (45). Another study in perfused diabetic rat hearts confirmed diastolic dysfunction by an increased isovolumetric relaxation time along with increases in inflow velocity across the mitral valve and LV EDP during T2DM (192). Similar diastolic dysfunction was seen in animal models of T2DM with decreased rates of relaxation and increased LV wall stiffness (83, 84, 258)

Dysfunction of the heart during systole is also present in diabetic patients and experimental T1DM and T2DM animal models. Patients with T2DM show decreased fractional shortening (FS) and changes in LV mass and geometry; however, these data are complicated by the presence of other comorbidities in the patient populations and the medications of these patients (109, 173, 308). T1DM patients also show dimensional alterations to the myocardium (56, 190). While diastolic dysfunction is observed during DM, depending on the population studied, systolic dysfunction varies (133, 265, 320). Animal models of both types of DM show decreased heart rate, systolic blood pressure, EF, FS, along with dimensional and volumetric changes (22, 84, 91, 161, 171, 192, 431).

1.2b. Fibrosis

Structural changes of the heart have been reported in both animal experimental models and humans with DM (181, 221, 282, 378, 384). Fibrosis accounts for the majority of changes in the structure of the heart, consisting of two types, interstitial and perivascular (92, 145, 294, 326, 402). Postmortem evaluation of diabetic patients showed enhanced collagen deposition in the perivascular loci and between myofibers (326). Further, Regan et al. also found enhanced triglyceride and cholesterol concentrations in the diabetic patients as compared to controls in the LV and septum (326). In a different study, myocardial biopsies revealed higher type III collagen, which is specific to cardiac tissue, while type I collagen is more predominant in the myocardium and was unchanged between diabetic and non-diabetic patients (357). During the evaluation of the right ventricle (RV), Nunoda et al. found that the average diameter of the RV myocardial cells was increased and the percentage of fibrosis was significantly higher in mild diabetic patients without hypertension or CAD as compared to controls (294). While fibrosis is present during DM, the mechanisms behind it are not well understood. Widyantoro et al. reported an increase in endothelin-1 (ET-1) in the plasma, which has been associated with increased fibroblast accumulation, providing a potential mechanism for the development of fibrosis (426). Other factors reported to play a role in the development of fibrosis are protein kinase C beta-1 and transforming growth factor beta-1 receptor II, which were enhanced in the diabetic myocardium of streptozotocin (STZ) diabetic mice (14, 420, 425). In the obese diabetic mice with leptin deficiency, the ob/ob mouse model of T2DM showed no LV myocardial fibrosis; however in the db/db model, cardiac fibrosis was evident (151, 208, 398). It is important to gleam from the current research in both experimental animal models of DM and diabetic patients that fibrosis is a critical player in cardiac dysfunction in the diabetic heart (39).

1.2c. Oxidative stress

One of the major contributing factors in the development of diabetic cardiomyopathy is the hyperglycemic environment, leading to an increase in the formation of reactive oxygen species (ROS) and a decrease in antioxidant levels (332). Oxidative stress is classically defined as the imbalance between ROS generation and the antioxidant defense mechanisms. Common examples of ROS include oxygen-derived free radicals such as superoxide and hydroxyl radicals, as well as non-radical derivatives such as hydrogen peroxide (H_2O_2). Literature suggests that the overproduction of superoxide increases the activity of polyl pathway flux, advanced glycation end product formation, hexosamine pathway flux and activation of protein kinase C leading to oxidative stress (46, 99, 291). The mitochondria are the main source of ROS generation within the cardiomyocyte through the leakage of electrons from the electron transport chain (ETC) in the inner mitochondrial membrane (IMM). In the db/db mouse model, Boudina et al. found increased H_2O_2 production, along with increased oxidative damage to lipids (41). Our laboratory found increased ROS production from cardiac mitochondria in the STZ T1DM mouse model (85). Further, oxidative stress has been show to create alterations in myocyte morphology, function, protein content and ion action, ultimately leading to diabetic cardiomyopathy (46). With the overexpression of mitochondrial phospholipid hydroperoxide glutathione peroxidase (mPHGPx), an antioxidant capable of reducing lipid hydroperoxides to alcohols and free H_2O_2, our laboratory found that lipid peroxidation was decreased and mitochondrial function, along with proteome stabilization was maintained during T1DM and following ischemia/reperfusion (I/R) injury (22, 85, 86, 253, 396).

1.3 Cardiac Function Using Echocardiography

Cardiac function is monitored routinely by the use of non-invasive, ultrasound imaging called echocardiography. There are three basic modes to image the heart: two-dimensional (2D) imaging, motion mode (M-mode) imaging, and Doppler imaging (11). Standard 2D echocardiography can be captured in both the long- and short-axes and allows for the viewing of motion in real time in a cross-section of the heart (11). The long-axis of the heart cuts the heart from top to bottom opening it up into left and right sides, while the short-axis cuts the heart into top and bottom halves. Doppler flow allows for the assessment of blood flow across valves within the heart. These measurements provide an efficient, cost-effective and highly accurate way to complete cardiac functional analyses in order to diagnose and manage patients suffering from heart disease. Assessment of cardiac function can also be performed in animal models and is oftentimes used as a measure to determine how a therapeutic treatment is affecting the heart. In both patients and animal models, systolic and diastolic parameters can be assessed through echocardiography and involves the use of all three modes of echocardiography to acquire a thorough evaluation of decrements in cardiac contractile function.

1.3a. Conventional echocardiography

M-mode is one of the earliest forms of cardiac ultrasound and is widely used in the clinical setting, allowing for the assessment of cardiac function via volumetric and diametric changes across multiple cardiac cycles. Using the parasternal short-axis view of the LV, a gate is placed through the 2D image and the motion of the ventricular walls can be measured across one-dimension (1D), increasing the temporal and spatial resolutions (11). Measurements obtained from

LV M-mode images include end-systolic and end-diastolic volumes and diameters, EF, FS, stroke volume (SV) and cardiac output (CO). M-mode has been found to be a reliable assessment of overt cardiac dysfunction; however, some clinicians consider it to be obsolete because of the development of more sensitive indices of cardiac functional assessment, such a speckle-tracking base strain echocardiography (124).

1.3b. Speckle-tracking based strain echocardiography

Another approach for imaging cardiac function is by using highly sensitive speckle-tracking based strain echocardiography. During recent years, speckle-tracking based strain has gained popularity in the clinical setting to allow for the assessment of velocity, displacement and deformation of the myocardium over the course of multiple cardiac cycles. Speckle-tracking based strain echocardiography provides a more comprehensive and reliable echocardiographic assessment through its ability to detect subtle alterations in cardiac motion. 2D echocardiographic cine loops are used in both the parasternal long- and short-axes to fully evaluate the movement of the myocardium throughout the cardiac cycle. Speckle-tracking based strain analyses are completed offline and the algorithms use speckle artefacts in the echo image (33). These speckles are generated at random from refractions, reflections and the scattering of the echo beams and help to assess wall motion and deformation throughout the cardiac cycle (33, 146). Some of the advantages of using speckle-tracking based stain include that it is angle independent because the speckles move in the direction of the wall and not along the ultrasound beam, it does not require as high of frame rates as other techniques and allows for strain measurements in three different dimensions (33, 312).

Speckle-tracking based strain and its relation to conventional echocardiography is not as straightforward as simple cardiac functional parameters. For instance, speckle-tracking based strain uses the parameters of wall motion velocity and displacement, along with the assessment of strain and strain rate from the deformation of the LV during the cardiac cycles (33, 81, 146, 322). Displacement is the distance that the speckle travels between two consecutive frames, while the velocity is the displacement of the speckle per unit time (322). Strain is a dimensionless quantity of myocardial deformation and measures the magnitude of myocardial fiber contraction and relaxation, otherwise known as the thickening and thinning of the myocardial wall in the radial dimension and elongation and shortening of the myocardium in the longitudinal and circumferential dimensions (33, 81, 146). For example, as the heart goes through the cardiac cycle and reaches systole, or contraction, the space inside of the heart gets smaller and the myocardial wall thickens. This allows for the assessment of the radial dimension, which can be evaluated in both the long- and short-axes. During systole, strain in the radial (R) dimension is represented as positive because of the thickening of the wall; however, in diastole, radial strain is a negative number because of the thinning of the wall (Figure 1.1). Longitudinal (L) shortening and circumferential (C) shortening occur during the contraction of the heart leading to negative values resented during systole, while lengthening happens during diastole and is represented by positive values (Figure 1.1).

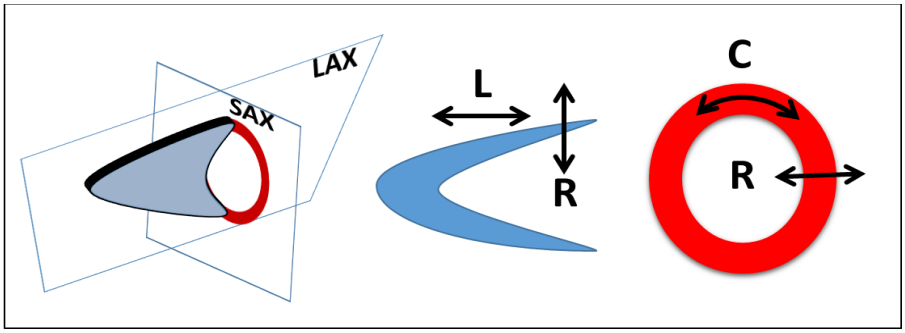

Figure 1.1 Speckle-Tracking Based Strain Echocardiographic Axes

Another important measurement obtained from speckle-tracking based strain analyses is strain rate. Strain rate is the time it takes to reach the peak of deformation or strain during the cardiac cycle (33, 322). Together, speckle-tracking based strain analyses provide adequate measurements for a more thorough evaluation of wall motion during the cardiac cycle.

Strain and strain rate analyses have been performed in the clinical setting in patients suffering from CAD, myocardial infarction (MI), ischemic cardiomyopathy, diastolic HF, Chagas' disease, DM and patients undergoing cardiac resynchronization therapy (13, 17, 34, 62, 96, 112, 160, 243, 410). Speckle-tracking based strain analyses have also been employed in small animal models of disease. Using speckle-tracking based strain analyses, Bauer et al. found that these analyses are capable of detecting subtle changes in myocardial wall function providing high-throughput and sensitive cardiac phenotyping (26). In their study, animals underwent a permanent left anterior descending coronary artery ligation and a portion of the animals received treatment with an angiotensin-converting enzyme inhibitor (ACEi) (26). Bauer et al. found that speckle-tracking based strain analyses were able to detect changes at an earlier time point following MI and the results also predicted the later development of adverse remodeling of the LV (26). Their results also revealed that speckle-tracking based strain analyses were capable of detecting subtle improvement in LV function when MI animals were treated with ACEi (26). Additionally, in the db/db mouse model of T2DM, Li et al. found global radial and circumferential strain values were decreased as compared to controls (241). Speckle-tracking based strain analyses provide an approach to looking at subtle changes in cardiac function in both a clinical and experimental setting.

1.3b.i. Global and regional assessment

When using speckle-tracking based strain analyses, measurements of both global and segmental analyses can be acquired. Global measurements refer to the overall or average data acquired in the LV over multiple cardiac cycles, while segmental analyses are the LV myocardium subdivided into 6 standard anatomic segments (57). For our studies, these measurements are acquired from curvilinear data obtained from the Visual Sonics Vevo2100 speckle-tracking based strain software (Figure 1.2). Using the Vevo2100 speckle-tracking based strain software, segmental analyses can be performed on short-axis images with the LV subdivisions of the following regions: anterior free (AF), lateral (L), posterior (P), inferior free (IF), posterior septum (PS) and anterior septum (AS) (Figure 1.2 Top Panel). The long-axis images subdivide the LV into the anterior base (AB), anterior mid (AM), anterior apex (AA), posterior apex (PA), posterior mid (PM) and posterior base (PB) (Figure 1.2 Bottom Panel).

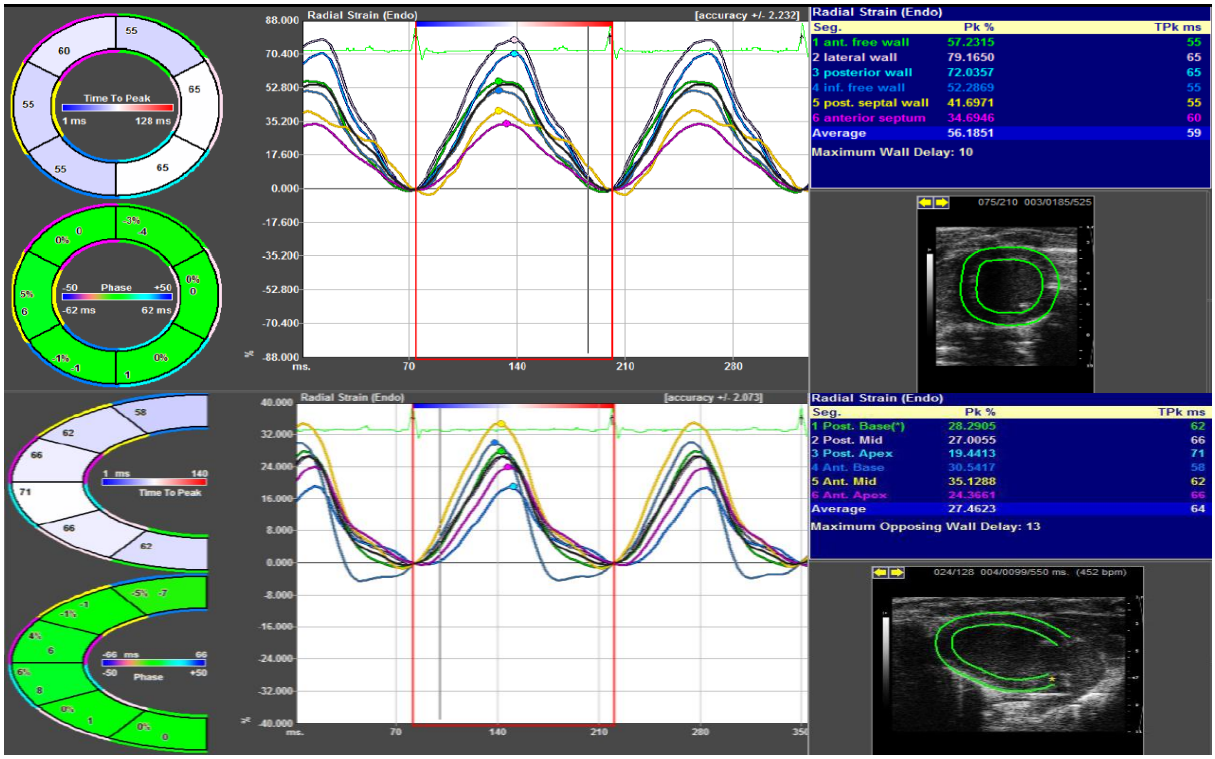

Figure 1.2 Speckle-Tracking Based Strain Global and Regional Assessment

Segmental analyses allow an investigator to find a particular locale within the LV where dysfunction may be occurring. It is imperative in a clinical setting for subtle changes in cardiac function to be detected to allow for intervention before a sudden onset of a cardiac insult. Further, to be able to pinpoint this location of dysfunction via segmental analyses is a powerful tool for therapeutic treatment. Clinical studies have currently shown that speckle-tracking based strain was able to detect subtle changes in LV function and were predictive of future development of cardiovascular disease (77, 112, 113, 117, 119, 239, 276, 283). While conventional measurements are easier to perform in a clinical setting, strain and strain rate imaging have been shown to increase the ability to detect cardiomyopathies in diabetic patients (42, 119, 280). Within the past 5 years, the ability to assess cardiac performance in small animal models was limited; however, speckle-tracking based strain analyses have provided a platform to gain further insight on subtle changes in cardiac function in small animal models. Studies have shown that early global changes in LV function are detected by speckle-tracking based strain analysis prior to changes in conventional measurements in different animal models with cardiac pathologies (26, 27, 211, 432). Further, analyses of particular regions within the LV provide a more accurate picture to pinpoint where the cardiac dysfunction is occurring (26, 33, 167, 322). The ability to obtain a complete picture by using both a global and segmental functional analysis of the LV during a disease state provides the opportunity to evaluate and understand disease progression, as well as potentially develop a therapeutic paradigm to treat a particular locale within the heart.

1.3c. Doppler flow echocardiography

Doppler flow echocardiography is capable of estimating blood flow velocity through the heart and can be measured by using the comparison of the frequency change between the sound

waves that are transmitted and the sound waves that are reflected back (11). The use of Doppler in cardiac ultrasound can be done in three distinct ways: continuous-wave Doppler, pulsed-wave Doppler, and color-flow mapping (11, 325). Continuous-wave Doppler, while sensitive and able to detect high velocities, comes with limitations because the velocity of blood flow is measured along the constant ultrasound beam and not at a specific depth (11). This means that the method is unable to localize the velocity measurements of blood flow (11, 325). Pulsed-wave Doppler was developed because of the limitations in continuous-wave Doppler and overcomes these restrictions by using short bursts of ultrasound with range gating (325). Localized velocity measurements of blood flow can be measured using pulsed-wave Doppler imaging because this technique measures blood flow velocity within a small area at a specific depth (11). Thus, pulsed-wave velocity measurements can be employed to measure blood flow through the valves in the heart; however, because of the intermittent ultrasound bursts, recording high-velocity signals is more difficult (325). Taken together, continuous-wave and pulsed-wave Doppler are complementary and can supply the needed information that is missing from the other mode. Finally, color-flow mapping allows for the superimposition of blood flow imaging on top of "real-time" 2D echocardiographic imaging of blood (11, 164). Color-flow mapping is a pulsed-wave Doppler technique and comes with both the advantages and disadvantages of pulsed-wave Doppler (325). Flow toward the transducer appears as red, while flow away is indicated by blue (11, 325). Shading of these colors also lends information on velocity while these images are being acquired (11). Altogether, Doppler flow echocardiography is a useful non-invasive tool to measure blood flow within the heart.

1.4 Mouse Models of Diabetes Mellitus

Studying both T1DM and T2DM and its associated cardiac abnormalities has been made easier by the development of rodent models, since the mechanisms behind DM and human diabetic cardiomyopathy are only partly understood (49). Using rodent models to study diabetic cardiomyopathy and the mechanisms behind its development is unique in that rodents do not develop atherosclerosis, allowing for the uninhibited study of the diabetic cardiomyopathy without interference from atherosclerotic mechanisms. Many rat and mouse models of T1DM and T2DM exist and specific advantages and disadvantages arise depending on which is used. Common models of T1DM include the STZ, OVE26, and Akita mouse models, while the T2DM models are the ob/ob and db/db mouse models and the Zucker diabetic fatty rat.

1.4a. Streptozotocin mouse model of type 1 diabetes mellitus

The STZ mouse is the most frequently used model of T1DM and is the model that we have chosen to employ in our studies. STZ, a glucosamine-nitrosourea antibiotic with a similar structure to glucose, was first used to destroy cancerous pancreatic β-cells, but now is successfully used to generate a T1DM rodent model (7, 49). Preferentially taken up by the glucose transporter 2 (GLUT2) in the pancreatic β-cells, intraperitoneal injection of STZ results in toxicity and necrosis eventually leading to insulin deficiency (37, 348). Mechanistically, STZ is capable of causing DNA damage through alkylation and with this, activation of poly adenosine disphoasphate (ADP)-ribosylation leads to the depletion of cellular NAD+ and ATP (348). STZ also causes the generation of superoxides and an increase in xanthine oxidase activity through the dephosphorylation of ATP (348). With the increase in ROS within the pancreas, necrosis of the β-cells and decreased insulin production ensue (348). Our laboratory uses the multiple low-dose

intraperitoneal injections (50mg/kg body weight) of STZ in FVB mice for five consecutive days, as suggested by the Animal Models of Diabetic Complications Consortium (AMDCC). Generally, the mice develop hyperglycemia, which our laboratory characterizes as a blood glucose level greater than 250 mg/dL and low levels of insulin at approximately 0.5 ng/mL, within 7 to 14 days after the first STZ injection (49). Mice treated with STZ have been found to have increased serum fatty acid, along with increased triglyceride and cholesterol levels (49). Further, cardiac dysfunction has been found in mice treated with STZ (22, 85, 289, 376, 386, 391). Using a Langendorff setup, we found significantly decreased rates of relaxation and contraction, along with increased developed pressure in STZ-treated mice (85). Further, using the Vevo2100 ultrasound imaging system, we have reported decreased EF, FS, SV and CO in T1DM animals as compared to littermate controls (22, 386). It is important to note that STZ-induced diabetic cardiomyopathy can be reversed through regular treatment with insulin, lending evidence that insulin deficiency and glucose utilization are the cause of cardiac abnormalities in this model (409). Other models of T1DM are the OVE26 and Akita mouse; however, they differ from the STZ model because they are genetically engineered and are T1DM from birth (49). This leads to an important advantage of the STZ model in that DM can be induced at any age and transgenic animals can be made diabetic to evaluate different mechanisms involved in diabetic cardiomyopathy.

1.4b. db/db mouse model of type 2 diabetes mellitus

The db/db mouse model is a model of T2DM, which develops because of a point mutation causing dysfunctional leptin receptors. The normal, long form of the leptin receptor gene is responsible for the action of leptin in the hypothalamus, which regulates appetite and body weight (73). The genetic manipulation by an insertion of a premature stop codon within the db transcript

leads to a short-form isoform of the leptin receptor. Therefore, without the functional form of this leptin receptor, obesity occurs (73). As early as 4 weeks of age, db/db mice begin to show signs of obesity and severe T2DM is developed by 8 weeks (47). Cardiac contractile abnormalities are present in the db/db model, along with hyperinsulinemia, enhanced fatty acid production and increased triglycerides (47). When assessed by echocardiography, db/db mice showed a development of cardiac hypertrophy, decreased FS and velocity of circumferential shortening (352). CO, LV-developed pressure and cardiac power were all decreased in isolated, working db/db hearts (49). Our laboratory and others revealed that in isolated perfused hearts, rates of contraction, relaxation, peak systolic pressure, rate pressure product and developed pressure were significantly decreased in the db/db animals versus controls (29, 84). Diastolic dysfunction also occurs in db/db mice and has been shown through both echocardiography and MRI analyses (375). Further, db/db mice have increased superoxide formation and oxidative damage by-products, which have been linked to cardiac mitochondrial dysfunction (41).

Another model of T2DM is the ob/ob mouse model, which develops DM when the mouse is homozygous for the obese spontaneous mutation (Lep^{ob}), leading to a decrease in leptin and the inability to suppress appetite (134). These mice exhibit obesity, hyperphagia, and diabetes-like syndrome of hyperglycemia, glucose intolerance and elevated plasma insulin levels and are considered T2DM at 15 weeks of age (47). Interestingly, even after the development of T2DM, ob/ob mice develop cardiac hypertrophy, but do not have impaired systolic function (49). Therefore, our laboratory chose to use the db/db mouse model because of our vested interest in cardiac abnormalities and restoration of cardiac pump function during T2DM.

1.5 Mitochondrial Subpopulations

Advanced imaging techniques have allowed for insight into cellular and organellar structure within the cardiomyocyte, leading to the recognition of mitochondria residing within specific locales of the cardiomyocyte. Mitochondrial subpopulations have been found in a number of different mammalian species including mouse, rat, muskrat, guinea pig, hamster, rabbit, dog, pig, monkey, cow and human (86, 137, 166, 237, 267, 272, 356, 358, 370, 392). Two spatially and biochemically distinct mitochondrial subpopulations exist within the cardiomyocyte (306). With the pioneering development of mitochondrial isolation techniques by Palmer et al., distinct mitochondrial subpopulations can be isolated by utilizing both mechanical and enzymatic procedures (306). Evaluation of other non-cardiac cells, such as neurons, revealed that functional heterogeneity between the dendritic, somatic, axonal, and presynaptic segments result from variations in energy demands and calcium (Ca^{2+}) signaling dynamics (199). These differences were associated with structural and biochemical attributes of the mitochondria depending upon their location and demands within a specific neuronal region, leading to particular responses during pathophysiological stress (199). Literature suggests that mitochondrial spatial locale within the myocyte may also be associated with particular responses to physiological and pathological stimuli (157, 193, 217, 266, 384). Within the cardiomyocyte, two spatially distinct mitochondrial subpopulations have been identified through ultrastructure analyses. Further, these mitochondrial subpopulations have also been found to have their own biochemical profile (306). The population of mitochondria that reside beneath the sarcolemmal membrane are termed subsarcolemmal mitochondria (SSM), while those located between the myofibrils are called interfibrillar mitochondria (IFM) (Figure 1.3) (176). Another population of mitochondria, which are isolated with the IFM, reside in the perinuclear region of the cell (176).

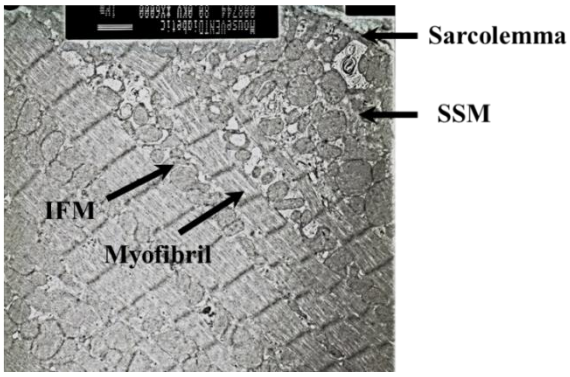

Figure 1.3 Cardiac Mitochondrial Subpopulation Schematic and Electron Micrograph

1.5a. Structural differences

Mitochondria located in distinct subcellular locales have been shown to have different structural appearances. Scanning electron microscopy and transmission electron microscopy revealed distinct mitochondrial populations including perinuclear mitochondria, SSM and IFM in thin sections from the LV tissue of Japanese Monkeys (*Macaca fuscata*) (356). As their name describes, perinuclear mitochondria were clustered at the nuclear poles. These mitochondria maintained a mostly spherical shape, ranging in lengths from 0.8 to 1.4 μm, and contained well-developed, curved cristae with minimal matrix area. Between the myofibrils were situated another pool of mitochondria termed the IFM. These mitochondria occupy the space between the Z-lines of the myofibrils and form longitudinal rows, which are bookended by the junctional sarcoplasmic reticulum (122, 254) (Figure 1.3). IFM typically exist as one mitochondrion per sarcomere, are elongated in shape, and range from 1.5-2.0 μm in length. The cristae structure of the IFM are more complex with curved configurations. Finally, the mitochondrial pool located beneath the sarcolemmal membrane are termed the SSM and are considerably more variable in length ranging from 0.4-3.0 μm. The cristae are typically tightly packed in the SSM. Generally, perinuclear mitochondria are smaller than IFM and possess a rounder shape, while the SSM vary in size and

shape with oval, spherical, polygonal, and horseshoe profiles (254, 356). Similar ultrastructural patterns have been reported in HL-1 cells, a cardiac muscle cell line, using confocal imaging to look at mitochondria clustered around the nucleus (220). Human papillary muscle subjected to en bloc staining revealed differential staining patterns between mitochondrial subpopulations leading to the thought that the SSM, IFM and perinuclear mitochondria may possess differences in chemical makeup and metabolic activities (90). Additionally, flow cytometry analyses using membrane-dependent dyes (MitoTracker Deep Red 633) coupled with size calibration microspheres to determine absolute mitochondrial size and internal complexity in SSM and IFM, indicated differences between mitochondrial subpopulations (80, 84-86, 287, 386, 428). Mitochondrial subcellular distribution has also been studied using probability density analyses via a 3D modeling approach utilized with MitoTracker Deep Red staining (32). This revealed that the IFM maintained a highly organized crystal-like pattern for cristae and were arranged in longitudinal rows between the myofibrils (32). Similar results were found using MitoTracker Deep Red 633 in adult mouse cardiomyocytes (176). Interestingly, cardiomyocytes from rainbow trout (*Oncorhynchus mykiss*) revealed no order of mitochondria when situated beneath the single cylinder-shaped layer of myofibrils underneath the sarcolemma (32). With this finding, it is important to note that differences in mitochondrial spatial patterns may be species specific.

Structural differences in cristae morphology were examined using high resolution scanning election microscopy in rat LV tissue (331). Lamelliform cristae, which are broad and flat, were the predominant pattern in the SSM, while the cristae morphology in the IFM was variable with some mitochondria possessing only tubular cristae or only lamelliform cristae and others possessing a mix of the two cristae forms (331). Riva et al. speculated from this data that individual cristae morphological patterns potentially contribute to functional differences in subpopulations of

mitochondria, including a reduction in the intracristal space of tubular cristae (331). This reduction in intracristal space potentially leads to a higher proton concentration within the structure, enhancing ATP synthase activity, which is consistent with function findings in the IFM compared to SSM (331). Biochemical composition of the cristae morphologies may also be different in lipid or protein content, leading to differences in structural makeup of mitochondrial subpopulations (331). Indeed, Monette et al. found that sphingolipid pools in cardiac SSM and IFM had different ceramide contents, which was shown to be higher in the SSM (277). Altogether, differences in mitochondrial subpopulation structure could be due to their subcellular locale requiring a different biochemical makeup.

1.5b. Communication between mitochondrial subpopulations

It is interesting to note that subpopulations of mitochondria may interact *in vivo*; however, the mechanism by which this occurs is still unclear. Skulachev proposed that intermitochondrial junctions connect the SSM to each other and that the innermost layer of the SSM are connected to the IFM via mitochondrial filaments (363). Using electron microscopy, others have found that the SSM and IFM may be continues in mouse skeletal muscle and network modeling of cardiac mitochondria revealed a communication system across the cell (314). This hypothesis suggests that the interaction between the SSM and IFM allows for the consumption of oxygen by the SSM combined with active respiration to transmit protons by the mitochondrial filaments to the IFM, enabling ATP generation, which can ultimately be used by the contractile apparatus (363). If the proposed hypothesis were true, it would support the IFMs ability to generate ATP despite its locale within the core of the cell with a lower oxygen content (363). With the capability of the IFM to function in a lower oxygen content, ROS may be limited to the periphery of the cell allowing for

the preservation of the cell core from damage (363). With this hypothesis, the SSM may serve as a protective barrier to the cell (220, 363). It is interesting to note that cross talk between the SSM and IFM may occur, which provides a dynamic network across the cell for energy generation and transmission of intracellular signals. Additionally, this hypothesis supports the notion that ATP production from each cardiac mitochondrial subpopulation is likely critical for efficient cardiac contractile function, indicating that both may play a role in preserving cardiac function during pathological states. Further, this interconnected mitochondrial network through the mitochondrial reticulum could provide a pathway for this energy distribution within the cardiomyocyte (149, 364), thus allowing for the restoration of cardiac contractile function if one subpopulation is detrimentally affected during a pathological state, while the other is unaltered such as what is observed in DM.

1.5c. Functional differences

Distinct functional differences between mitochondrial subpopulations have been reported and could be due to their different subcellular locations. While this explanation of differences in function associated with location is not definitive, it aligns with the concept that spatial location reflects the processes in which the particular subpopulation of mitochondria supplies ATP. Perinuclear mitochondria are thought to generate ATP to drive mitochondrial metabolism close to the nucleus, while it is hypothesized that IFM provide the energy needed for contraction and the SSM provide ATP for the active transport of metabolites across the sarcolemmal membrane (279, 306, 334, 356). Biochemical differences between mitochondrial subpopulations support the distinct metabolic roles of the subpopulation within its particular locale of the cell (306). The IFM typically have higher respiratory rates, succinate dehydrogenase and citrate synthase activities, and

higher complex oxidation rates in complexes I, II, III and V when compared to the SSM (24, 79, 85, 305). Similarities between the mitochondrial subpopulations also exist, such as the levels of carnitine palmitoyltransferase and α-glycerophosphate (306). A potential mediator of mitochondrial metabolic and pathological processes is mitochondrial Ca^{2+}, with the Ca^{2+} dynamics being a function of the mitochondria's proximity to constituents of the Ca^{2+}-handling apparatus (176). IFM are located near the junctional sarcoplasmic reticulum, the Ca^{2+} release sites, leading to their central involvement in the process of mitochondrial Ca^{2+} cycling (254). SSM and IFM also possess differences in their ability to accumulate Ca^{2+} and withstand the damage caused by Ca^{2+} overload (307). Further, Kasumov et al. suggest a slower protein synthesis rate in the IFM as compared to the SSM, which potentially contributes to functional differences between the two subpopulations (201). Due to the functional differences within mitochondrial subpopulations based on their subcellular locale, it supports the literature suggesting that mitochondrial subpopulations differentially respond to pathological stimuli.

Table 1.1 Mitochondrial Subpopulations Characteristics (176)

Parameter	SSM	IFM
Location	Beneath Sarcolemma	Between Myofibrils
Organization	Random	Longitudinal Rows
Shape	Oval, spherical, polygonal, horse-shoe	Elongated
Length	0.4-3.0 μm	1.5-2.0 μm
Cristae Structure	Predominantly Lamelliform	Predominantly Tubular
ATP Generated For	Active Sarcolemma Transport	Muscle Contraction
SDH Activity		Higher
CS Activity		Higher
Oxidative Metabolism		
Lipid Substrates		Higher
Non Lipid Substrates		Higher
Oxidative Phosphorylation		
ETC I-V		Higher
Posttranslational Modification	Carbonylation	Nitration
Resistance to Ca^{2+} Overload		Higher

1.6 Mitochondrial Protein Import

With approximately 1500 proteins residing in the human mitochondrion and only 13 of those being transcribed and translated within the organelle itself, nuclear-encoded mitochondrial protein import is critical to maintain a functioning and stable organelle (9, 21, 54, 313). Approximately 99% of proteins that reside within the mitochondrion are imported through a complex mechanism to traverse the two mitochondrial membranes (21, 58). Proteins destined to enter the mitochondria are termed preproteins and are equipped with targeting signals, typically N-terminal presequences that direct the protein to a specific compartment of the mitochondrion (21, 131, 301). For instance, if a protein is targeted to the matrix of the mitochondria, there is a direct interaction between the protein itself, the outer mitochondrial membrane (OMM), the inner mitochondrial membrane (IMM) and the presequence translocase-associated motor (PAM) (21, 60). These interactions make up a "supercomplex" for mitochondrial protein import and provide a pathway for the protein to translocate from the cytosol of the cell, through the mitochondrial membranes and into the mitochondrial matrix (21, 60).

1.6a. Outer membrane protein import

Cytosolic chaperones aid in the transport of preproteins to the OMM. Heat shock cognate 70, heat shock protein 90 and mitochondrial import stimulation factor carry the nuclear-encoded preprotein to the translocase of the outer membrane (TOM) complex, which contains receptors for the recognition of the presequences (110, 440). The TOM complex serves as the gatekeeper to gain entrance into the mitochondrion and once the presequence is recognized, is able to guide the preprotein through the OMM. Tom20 serves as the main receptor and recognizer for the N-terminal presequences on proteins destined for the mitochondrion because of its binding groove that

attaches to the hydrophobic face of the polypeptide presequence, which subsequently allows the protein to bind the cytosolic face of the OMM (21, 434). Another protein, Tom22, possesses a negative charge, which is attracted to the positively charged presequence, and exerts its effects with Tom20 in order to maintain an unfolded state for the translocating protein (21, 434). Finally, Tom40, a large β-barrel protein, along with 3 smaller subunits (Tom5, Tom6 and Tom7) forms the import pore (21, 168). Through this pore, proteins destined to enter the mitochondrion are translocated across the OMM and guided into the intermembrane space (IMS) (Figure 1.4).

1.6b. Inner membrane protein import

After the preprotein successfully translocates across the OMM and into the IMS of the mitochondria, preproteins bind to the IMS domain of Tom22 and translocases of the inner membrane (TIM), Tim50 and Tim21 (59, 286). The binding of the preprotein to Tim50 and Tim21 guides it to the TIM23 complex, which serves as the main mitochondrial import pore, allowing entrance into and through the IMM (59, 286). Tim23 plays a critical role in the translocation of a preprotein to the IMS, IMM and matrix of the mitochondria (59). Membrane potential ($\Delta\Psi m$) is often required for preproteins to translocate through the TIM23 complex, as well as soliciting help from the PAM complex (21). Mitochondrial heat shock protein 70 (mtHsp70) is an essential protein subunit of the PAM complex and through its anchoring to Tim44 within the mitochondrial matrix, which allows it to still associate with the IMM, the protein is able to "trap" and "pull" a translocating preprotein through the IMM in an ATP-dependent manner (411). Matrix processing peptidases (MPP) then cleave the N-terminal presequence upon entrance of the preprotein into the mitochondrial matrix (218). Because the preprotein is translocated in an unfolded state in order to pass through the membranes, the protein has to be refolded into its native confirmation with the

help of co-chaperones hsp60 and hsp10 (156, 361). MtHsp70 is a critical player in the matrix-target nuclear-encoded mitochondrial protein import because it confers unidirectional translocation of the protein and then assists in the refolding once the protein is translocated (261) (Figure 1.4).

1.6c. Pre-sequence translocase-associated motor complex

The essential members of the PAM complex that regulate mtHsp70-driven protein import are Tim44, Pam16 (Tim14), Pam18 (Tim16), GrpE (Mge1) and the non-essential protein Tim17 (21). Tim44 serves as the anchor for mtHsp70 through its attachment to the IMM on the matrix side and has been shown to have multiple functions such as recruitment and coordination of PAM complex constituents increasing the efficiency of protein translocation (347, 395). Interestingly, when Tim44 and mtHsp70 do not interact, protein translocation is decreased significantly. In one study, a mutation to the binding domain of Tim44 where mtHsp70 attaches reduced the mitochondrial translocation activity, while a mutation to the J-related segment of Tim44 in *Saccharomyces cerevisiae* decreased mitochondrial protein import viability (245, 268). Pam16 and Pam18 are a j-like protein and j-protein, respectively, which also regulate mtHsp70 and in turn regulate protein import activity (82, 132). Pam18 stimulates the ATPase activity of mtHsp70 through its j-domain and Pam16 acts as a negative regulator of Pam18 by affecting the formation of the Tim44-mtHsp70 complex (82, 132). In a study that destabilized the Pam16-Pam18 complex, there was decreased mitochondrial protein import, along with decreased yeast cell viability (82, 273). The interactions between Pam17 and other import constituents are influential to the protein import process. For instance, Pam17 and Tim44 interact in a complementary manner to assist in protein import and Pam17 is required for proper Pam16-Pam18 complexing (186, 346, 399).

Interestingly, import and PAM complex formation were only impaired, not abolished, in the absence of Pam17 (399). GrpE is a nucleotide exchange factor in the mitochondrial matrix that promotes the release of ADP from mtHsp70 (95). This is a critical step in the process of protein import because when the ADP is released, the preprotein is subsequently released and allows for ATP to bind to mtHsp70 driving further mitochondrial protein translocation (95). When the eukaryotic homolog to GrpE (Mge1) was mutated, binding efficiency of mtHsp70 to translocating preproteins was decreased, but binding of fully imported preproteins was increased lending insight into the importance of GrpE on the regulation of ADP-ATP binding to mtHsp70 (223). With a complicated network for translocation via mtHsp70 into the matrix of the mitochondria, many proteins are critical to the import process being carried out efficiently. (Figure 1.4).

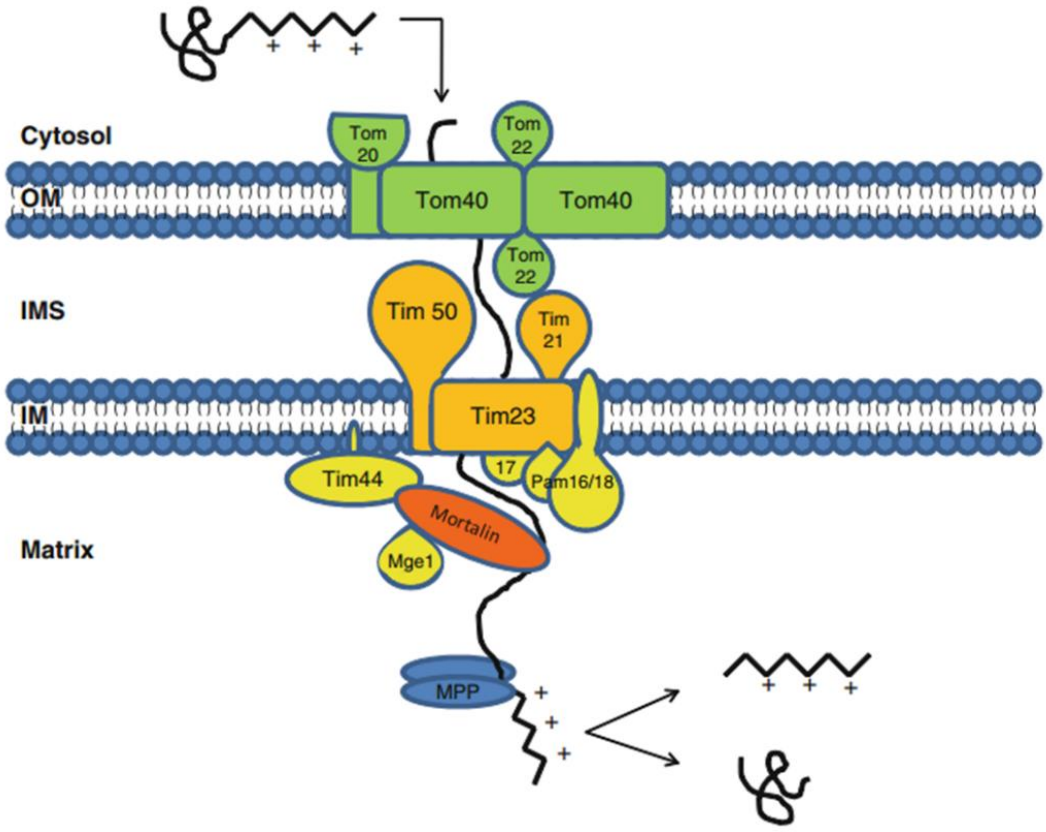

Figure 1.4 Nuclear-encoded Mitochondrial Protein Import Mechanism (21)

1.6d. Brownian ratchet versus power stroke model

While mtHsp70 is known to be critical in the translocation of proteins into the mitochondrial matrix, it remains unclear as to how it exerts its effect upon these proteins. MtHsp70 serves as the ATP-dependent, primary motor subunit for the PAM complex, aiding in the unfolding, transport and refolding of proteins targeted to the mitochondrial matrix, but also playing a role in the import of proteins to the IMM and IMS (21). Examples of proteins using the mtHsp70 import mechanism, but not residing in the matrix are oxidase assembly 1, which is imported into the matrix and then reinserted back into the IMM and cytochrome b_2, which is partially pulled into the matrix, subsequently cleaved, leaving the functional portion of the protein located in the IMS (36, 144).

Two modes of thinking exist for how mtHsp70 exerts effects on translocating proteins: the Brownian ratchet model and the power stroke model (285). In the Brownian ratchet model, the $\Delta\Psi m$ serves as the initial pulling force for the preprotein to get into the matrix (251, 297). Upon entrance into the matrix, the preprotein binds to mtHsp70, ATP hydrolysis occurs causing the release of mtHsp70 from Tim44 and mtHsp70 traps the translocating protein to not allow retrograde movement back into the IMM (251, 297). The binding of additional mtHps70-Tim44 complexes to incoming segments of the polypeptide helps to move the protein into the matrix, where GrpE catalyzes the release of ADP from mtHsp70 allowing for its dissociation from the translocated protein (251, 297).

While the power stroke model begins similarly, the key difference is that mtHsp70 does not dissociate from Tim44. In this model, instead of dissociation, mtHsp70 undergoes a conformational change, actively propelling the protein through the IMM and into the matrix (144). GrpE serves the same function as the nucleotide exchange factor in the matrix, facilitating the

release of mtHsp70 from the translocated protein (297). Because of how this model is set-up, it indicates that multiple molecules of mtHsp70 would be essential for the movement of the protein into the mitochondrial matrix (144). Figure 1.5 depicts the two models side by side in order to visually appreciate their distinct differences.

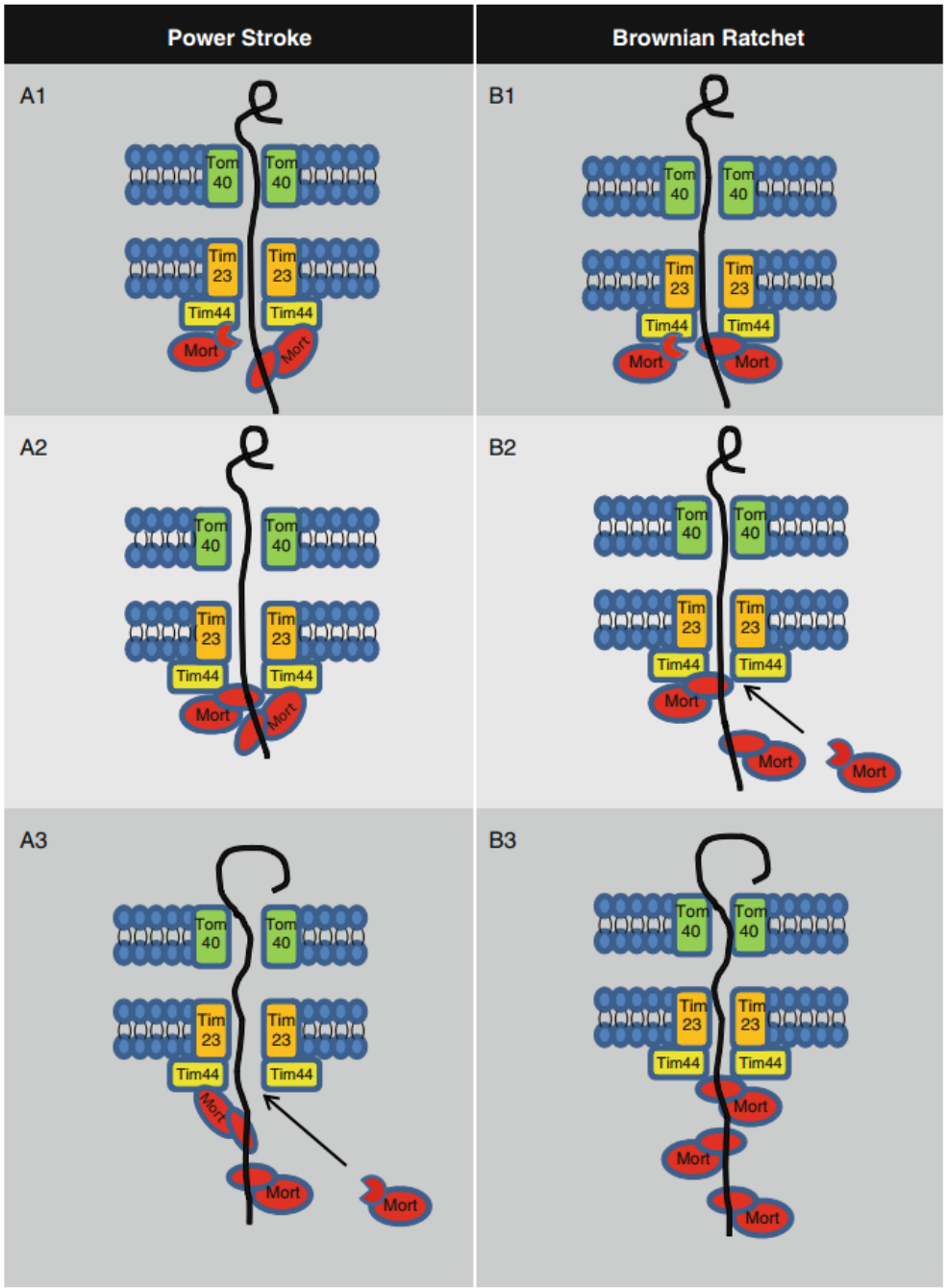

Figure 1.5 Models of Mitochondrial Protein Import (21)

Even though there are two proposed models for mtHsp70-dependent mitochondrial protein import, there may not be a singular method for import, but rather a combined mechanism where both are employed depending on the protein being imported (214). MtHsp70 likely serves as the driving force for the linearization of proteins, since unfolded proteins do not exist at the OMM (411). If the presequence happens to be long enough to span both the OMM and IMM, the unfolding of proteins happens more quickly and likely uses the power stroke model (263, 427). This might occur in the case of a tightly folded protein, which requires a lot of force in order to linearize the protein and maintain its linearization for translocation (263, 427). The contrary occurs with proteins that are not tightly folded and the Brownian ratchet model would be the most efficient mechanism for protein import in this instance (427). In summary, the mechanism by which a protein is transported into the mitochondrial matrix via the mtHsp70-dependent mechanism may depend upon the tightness in the folding of the domain for that particular protein.

1.7 Mitochondrial Heat Shock Protein 70

MtHsp70 is known by many names such as mortalin, peptide binding protein 74 (PBP71) and glucose regulated protein 75 (Grp75). This protein serves as a member of the Hsp70 chaperone family and interestingly, mtHsp70 appears not to be inducible under conditions of heat stress like many members of this family (203). The subcellular localization of mtHsp70 has been studied using microscopy, protein tagging with specific antibodies, cell fractionation and organelle-specific markers revealing a number of locations for the protein including the endoplasmic reticulum (ER), cytoplasmic vesicles, cytosol and the mitochondrion (87, 362, 369); however, the mitochondrion serves as the principle locale of the protein. Because of its many locations within the cell, a multitude of cellular and mitochondrial functions are impacted by this protein. There

are three key regions on mtHsp70: the ATPase domain, the peptide binding domain and the carboxy-terminal segment (216). Each of these segments has been shown to be essential for proper nuclear-encoded mitochondrial protein import because a mutation to a segment has been shown to have detrimental effects on the import process (216).

In response to cellular stress, mtHsp70 has been reported to be responsive during thyroid hormone treatment, glucose deprivation and myocardial I/R (158, 209, 252, 430). Williamson et al. showed that cardiomyocytes from neonatal rats infected with an adenoviral vector expressing mtHsp70 were protected from I/R injury (430). These cardiomyocytes had increased import of nuclear-encoded antioxidant defense proteins, such as manganese superoxide dismutase (MnSOD) (430). When the yeast equivalent to mtHsp70 (Ssc1) was inactivated by a temperature-sensitive mutation, it caused an arrest to the unfolding, translocation and refolding of imported proteins (139, 198). Further, deletion of Ssc1 caused death of the cell lending to the importance of this protein for the import of proteins into the mitochondria, but also for cellular viability (78).

1.7a. Mitochondrial functions

Central to the vitality of the mitochondrion, mtHsp70 provides the active motor for protein import and upon the proteins translocation into the matrix, this protein plays an integral role in the refolding of imported proteins (158, 209, 252). MtHsp70 is fundamental to the mitochondrial protein import process, particularly for the import of matrix, IMS and IMM proteins as described above. During nuclear-encoded mitochondrial protein import, mtHsp70 serves an essential role as the main subunit and motor for the PAM complex. In the mitochondrial matrix, mtHsp70 anchors to Tim44 to trap and pull the preprotein through the IMM in an ATP-dependent manner (411). When mtHsp70 is altered, mitochondrial function is compromised with decrements in nuclear-

encoded mitochondrial protein import, decreased antioxidant defenses, increased misfolding and degradation of proteins, along with increased cellular apoptosis (21). Additionally to protein import, mtHsp70 plays a critical role in protein folding and protein degradation within the mitochondrion. Once the protein is translocated into the mitochondrial matrix, it must be refolded into its active confirmation in order to perform its specific function. Kang et al. used dihydrofolate reductase and a temperature-sensitive mtHsp70 mutant in yeast (Ssc1) to display irreversible binding of mtHsp70 and the translocated preprotein, which resulted in improper protein folding and enhanced degradation mediated by proteinase K (198). MtHsp70 does not act alone in refolding of translocated preproteins, but acts in concert with hsp60, hsp10, GrpE and Mdj1 (259). The current speculation is that mtHsp70, GrpE and Mdj1 form a complex to keep the translocated preprotein in a loosely folded conformation (259). When GrpE-mediated ATP hydrolysis occurs releasing the preprotein from mtHsp70, the preprotein is then transferred to the hsp60-hsp10 complex where it is folded into its native conformation (259). Interestingly, mtHsp70 and Mdj1 also have been shown play a role in mitochondrial protein degradation (342). MtHsp70 has been shown to allow for the stabilization of misfolded or damaged polypeptides into an unfolded conformation so that the protein will be degraded by mitochondrial proteases like m-AAA and PIM1p (343, 414). The process of degradation is critical in the mitochondria because it maintains genome integrity and allows for proper excision of introns in mitochondrially-encoded ETC proteins (400). While mtHsp70 predominantly resides within the mitochondrial matrix, the protein has also been shown to have other processes within the cell.

1.7b. Extra-mitochondrial functions

Though central to mitochondrial viability, mtHsp70 has also been shown to have extra-mitochondrial functions in the cytosol, centrosomes, cellular membranes and the ER (21). MtHsp70 is capable of binding a multitude of proteins leading to a diverse functionality for this multifaceted protein. MtHsp70 has been shown to be important in cellular proliferation, calcium regulation, play a role in the apoptotic cascade pathway, participate in the process of aging, and act as a constituent of the immune system (21). The tumor suppressor protein p53, plays a direct role in DNA repair, cell cycle arrest and cellular apoptotic initiation and mtHsp70 has been shown to bind to this protein in multiple locales such as the cytoplasm, centrosomes and the mitochondrion (224, 257, 260, 274, 275, 412). MtHsp70 binds to p53 and sequesters it from the nucleus to the cytoplasm of the cell, which is important because when bound, this decreases p53 mediated apoptosis (275). MtHsp70 is also known to play a critical role in regulated cell cycle division through its interaction with the centrosomes in late G1, S and G2 phases of the cell cycle (257). Further, literature has revealed that mtHsp70 is able to bind with the receptor for hyaluronan mediated motility during interphase, potentially allowing the protein to play a role in the stabilization of microtubules (219). In addition to all of these capabilities, through its interaction with fibroblast growth factor-1 (FGF-1), mtHsp70 may be involved in the regulation of FGF-1 binding to its receptor, regulating the growth factor's function (269).

As it relates to cellular immunity, the membrane attack complex (MAC) is comprised of C subunits (C5b, C6, C7, C8 and C9) which assemble on the surface of the cell creating a pore, leading to the death of a targeted cell (316). Cancer cells show an increased resistance to complement-dependent cytotoxicity because of the inability for the MAC to form (316). MtHsp70 has been shown to bind to subunits C8 and C9 of the MAC, which Pilzer et al. found to be released

from the cells in membrane vesicles, resulting in decreased MAC formation and increased cellular survival in a cancer cell line (315). Additionally, mtHsp70 has been shown to bind Interleukin-1 (IL-1) receptor, which may play a role in the internalization of the receptor, leading to a regulatory function of mtHsp70 on IL-1 (338).

The ER and mitochondria form a dynamic network among which many processes are controlled such as metabolic flow, protein transport, intracellular Ca^{2+} signaling and cell death (44, 127, 380, 381). MtHsp70 has been shown to link the voltage dependent anion channel (VDAC1) on the OMM of the mitochondrion to the ER Ca^{2+}-release channel inositol 1, 4, 5-triphosphate receptor (IP(3)R) (380). In support of this, when mtHsp70 was knocked down, Ca^{2+} concentration within the mitochondria was shown to be decreased. Finally, the interaction of mtHsp70 with mevalonate pyrophosphate decarboxylase (MPD) indirectly controls proliferation through MPD simulated prenylation of Ras, which inhibits cell growth (413). Altogether, the literature suggests that mtHsp70 is a protein with diverse functional roles both within and outside of the mitochondrion.

1.7c. Pathological influence

Due to the diverse nature of mtHsp70, the protein itself has been shown to be impacted in many different pathological settings leading to its role in both disease initiation and progression. When assessing proteomic alterations, mtHsp70 was affected in cancer, neurological diseases, cardiovascular diseases, aging and DM (21). In a neuroblastoma cell line, the authors found an upregulation of mtHsp70 subsequent to differentiation, which is associated with a high probability of regression, indicating that mtHsp70 is a good prognostic indicator for this disease (182). Conversely, mtHsp70 is thought to be detrimental during different types of cancer and correlated

with increased incidence, progression and poor outcomes for this pathological state. In chronic myeloid leukemia patients, mtHsp70 was increased as compared to controls, demonstrating that mtHsp70 may play a role in mediating the antiapoptotic effects of cancer cells (317). Further, studies of colorectal adenocarcinoma patients, hepatocellular carcinoma-associated hepatitis C virus and human osteosarcoma cell lines all showed increased mtHsp70, suggesting mtHsp70 may be a good predictor of cancer progression and prognosis (107, 290, 382).

In neurological disorders such as Parkinson's disease and Alzheimer's disease, mtHsp70 expression is influenced. MtHsp70 content was found to be decreased in Parkinson's patients as compared to controls in the substantia nigra pars compacta, which could potentially impact nuclear-encoded mitochondrial protein import in the neurons (191). In Alzheimer's disease, Osorio et al. found post-translational modifications, such as phosphorylation and oxidation, of mtHsp70, which could potentially result in diminished binding efficiency and translocation properties for the protein (300). These studies indicate that alterations to mtHsp70 may play a role in the progression of neurological diseases and that this protein could serve as a predictor of neurological disease progression.

During cardiovascular disease, mtHsp70 has been shown to be adversely affected. In the aged heart, mtHsp70 is shown to be decreased through proteomic analyses (89). Additionally, neonatal rat cardiomyocytes treated with ET-1 to stimulate cardiac hypertrophy displayed a decrease in mtHsp70 content, suggesting that mitochondrial impairment may occur during the early development of hypertrophy (5). During MI, mtHsp70 content was shown to be decreased in tissue close to the infarcted area; however, after 5-7 days of recovery, the concentration was higher than other HSP70 family members and returned to normally expressed levels 14-21 days post-infarction (209). Williamson et al. showed that overexpression of mtHsp70 in neonatal rat

cardiomyocytes after hypoxia/reoxygenation insult, preserved both cell viability and mitochondrial function (430). These studies suggest that a therapeutic approach to cardiovascular disease may be through the enhancement of mtHsp70 content.

MtHsp70 is also affected in the heart during both T1DM and T2DM. Interestingly, in rats subjected to STZ, Hamblin et al. studied the proteomic profile, which revealed an increase in mtHsp70, while Turko et al., showed significantly decreased mtHsp70 content, indicating that the protein is affected during T1DM, but literature is unclear as to how the protein is being altered during this pathological insult (158, 393). Our laboratory found that in mice treated with STZ, mtHsp70 is significantly decreased in the mitochondrial proteome of the IFM, potentially leading to the disruption in protein loss coming from nuclear-encoded sources in this particular subpopulation. Since greater than 99% of proteins residing within the mitochondrion are nuclear-encoded and imported from the cytosol to a locale within the organelle, alterations to mtHsp70, a key player in nuclear-encoded mitochondrial protein import, could lead to a deranged mitochondrial proteomic profile for the IFM during T1DM (23). Interestingly, in the db/db mouse model for T2DM, Dabkowski et al. showed decreased mtHsp70 in the SSM subpopulation of mitochondria, with no alterations in the IFM (84). Interestingly, these studies provide evidence that mitochondrial proteomes are differentially affected during the distinct types of DM, leading to mitochondrial dysfunction of a specific mitochondrial subpopulation depending on the type of DM. Overall, these studies suggest that DM detrimentally impacts mtHsp70 in the diabetic heart. Further, studying the alterations to mtHsp70 during pathological settings could lead to the discovery of different therapeutic approaches and interventions within the clinical setting to increase the quality of life for diabetic patients.

1.8 Pathological Influence on Mitochondrial Subpopulations

Cardiovascular disease is associated with a plethora of effects on the mitochondrion, making research efforts regarding pathological influence on mitochondrial subpopulations critical for the treatment of the morbidity and mortality associated with particular disease states. As the mitochondrion continues to be elucidated as a key player in cardiovascular disease, a greater understanding of how to protect this critical organelle during pathology becomes imperative. Pathological insult to the mitochondrion differentially occurs based on its subcellular location (176). During ischemia, the SSM subpopulation is predominantly affected, with significant structural alterations and a decrease in membrane fluidity (358). Further, a study using rabbits subjected to global ischemia showed decreased OXPHOS, along with decreased contents of cytochrome *c* and cardiolipin in the IMM of the SSM (66, 237, 238). Chen et al. showed increased H_2O_2 production from complexes I and III in the SSM, which was associated with ETC damage when global ischemia was induced in rat hearts (66). Oftentimes, an ischemic event is followed by reperfusion of the blood. Studies show that I/R injury influences both mitochondrial subpopulations. In rat hearts, I/R injury decreased OXPHOS rates and ADP/ATP translocase activity in both the SSM and IFM (101, 423). Our laboratory has shown that overexpressing mPHGPx during a global I/R insult affords protection to both mitochondrial subpopulations through preservation of ETC complexes (86). Ischemic preconditioning is a therapeutic approach to protect the heart against damage due to a subsequent ischemic insult (202). Treatments such as phosphatidylcholine, isoflurane, amobarbital and rotenone have shown improved function of the SSM during an ischemic event (63, 64, 67, 104, 229, 318). Preconditioning studies indicate that the SSM is primarily affected, which may be a function of greater sensitivity to the overload of Ca^{2+} during the initial ischemic condition and suggests that this type of approach may be beneficial

in pathologies imparting deleterious effects on the SSM subpopulation. In contrast to preconditioning, cardiac postconditioning can also be used for cardioprotection. Paillard et al. suggest that postconditioning reduces oxidative stress and inhibits mitochondrial permeability transition pore (mPTP) opening (304). Further, studies have shown that postconditioning treatment may also be best considered for pathologies that predominantly affect the SSM (68, 69).

Hypoxia has been shown affect mitochondrial respiration in the cardiomyocyte, leading to cellular dysfunction (175). Heather et al. showed decreases in state 3 respiration rates using fatty acid and pyruvate as substrates in both the SSM and IFM when rats were subjected to chronic hypoxia of 11% oxygen exposure for 14 days (163). When an area of the heart loses the perfusion of blood, that region becomes ischemic, causing irreversible damage to the myocardium. A common model for this MI is coronary artery ligation, which allows for the creation of an ischemic myocardial region (202). Rats subjected to a coronary artery ligation displayed decreased respiration rates, ETC complex III protein contents and activities, decreased mitochondrial cytochrome *c* levels and an increase in H_2O_2 production in both SSM and IFM (162). Further, another study found that coronary artery ligation in rats, along with a high fat feeding protocol led to an increase in fatty acid availability, state 3 respiration rates and ETC complex II and IV activities in SSM and IFM, which improved overall mitochondrial and cardiac contractile function (327-329). During HF, mechanical dysfunction of the myocardium leads to insufficient oxygenated blood delivery to the body in order to meet its metabolic requirements (202, 335). Multiple studies have shown that mitochondrial biogenesis and ETC enzymes are impacted during HF (143, 196, 351). A rodent model of dilated cardiomyopathy that exhibits decreased mitochondrial oxidative capacity, but is responsive to nutritional and metabolic therapies, showed distinct effects to the IFM subpopulation including decreased mitochondrial yield and Ca^{2+}-

induced mPTP opening (137, 138). Hoppel et al. found that cardiomyopathic hamsters have defective OXPHOS in the IFM and suggests that the dysfunction may be due to alterations in IMM transport properties with the ATP synthase (180). Pressure overload using aortic banding revealed a reduced capacity for free radical scavenging in the SSM of mice deficient in apoptosis-inducing factor, while rats undergoing transverse aortic constriction displayed a decrease in state 3 and state 4 respiration rates in the IFM (350, 401). Volume overload, as completed by aortocaval fistula, revealed diminished SSM function through decreased levels of ETC complexes I-V and decreased state 3 respiration rates (148, 394). It is thought that IFM dysfunction may not occur during volume overload due to its ability to lower state 4 respiration thus increasing mitochondrial efficiency and responding to the increased myocardial demand (264, 422). Overall, literature suggests that mitochondrial subpopulations are differentially impacted during HF dependent on the model used. The IFM appear to be predominantly affected during HF and pressure overload, with the exception of volume overload in which the SSM appear to be primarily affected.

Due to its role in the generation of ROS, the mitochondrion has been considered a central player in the development of the aged heart (88). Fannin et al. demonstrated age-related alterations in mitochondrial function in the IFM subpopulation (120). Decreased OXPHOS rates, cytochrome oxidase enzyme activities, enhanced oxidant production, decrease complex IV enzyme activities, increased oxidative stress and antioxidant enzyme activities, along with decreased ETC complex III activities and increased propensity for mPTP opening were shown in the IFM of the aged heart in different species (120, 150, 194, 232, 271, 377). Further, structural changes, such as size and internal complexity, of the IFM were noted by Coleman et al. in an aged mouse model (74). Ultimately, mitochondrial dysfunction associated with aging predominantly affects the IFM. The aged heart is more susceptible to additional cardiac events including I/R and while the IFM are

predominantly affected in the aged heart, both cardiac mitochondrial subpopulation are affected when the aged heart undergoes injury from I/R (69, 231, 233-235).

Exercise has been linked to the prevention of cardiovascular disease and increased mitochondrial biogenesis (169, 177, 311, 387). While exercise has been shown to increase mitochondrial enzyme proteins and activities, it is relatively unexplored what exercise training does to cardiac mitochondrial subpopulations (372, 379). Coleman et al. showed increased IFM hypertrophy and loss of structural internal complexity in aged C57BL/6J mice that underwent a training exercise protocol on the treadmill (74). In contrast, Fischer 344 rats undergoing long-term wheel running showed a reduction in H_2O_2 and lower MnSOD in both cardiac mitochondrial subpopulations (195). Kavazis et al. found that endurance exercise promoted biochemical alterations that helped to resist apoptotic stimuli in both mitochondrial subpopulations and in another study by the same group found that proteomic alterations occurred in both subpopulations as well (205, 206). Rats subjected to an I/R protocol showed increased H_2O_2 production in both subpopulations; however, this increase was prevented by exercise training solely in the SSM (227). This group also found that I/R-induced decrements in state 3 respiration rates were subsequently reversed in the SSM subpopulation when using complex I driven substrates, suggesting that exercise training followed by I/R injury allows for the protection of the SSM subpopulation (227).

Another interesting topic is the effects of pharmacological drugs on cardiac mitochondrial subpopulations. A study using verapamil showed that rat cardiac mitochondrial subpopulations reversed OXPHOS depression in the SSM after the damage was caused by treatment with phosphate (103). Another group indicated that increased H_2O_2 and 8-isoprostane production, leading to increased propensity for mPTP opening in SSM caused by aldosterone/salt treatment, was prevented by cotreatment with Carvedilol and Nebivolol (61). The majority of studies testing

the effects of drugs on cardiac mitochondrial subpopulations found that the SSM were primarily affected. This is potentially due to their location below the sarcolemmal membrane and their closer proximity to the drug, while the IFM is more protected within the cell. Ultimately, literature suggests that mitochondrial subpopulations can be differentially impacted by pathological stimuli, potentially due to their location and particular function within the cell. Table 1.2 provides an overview of the differences in SSM and IFM responses to different cardiac pathologies

Table 1.2 Cardiac Mitochondrial Subpopulation Response to Pathological Stimuli (176)

Stimuli/Factor	Species	Primary Subpopulation Affected	References
Ischemia	Rat, Rabbit, Canine	SSM	(65, 66, 230, 237, 238, 358, 374, 421)
Hypoxia	Rat	SSM	(102, 163)
Myocardial Infarction	Rat, Dog	Both	(162, 296, 327-329, 333, 335)
Ischemia Reperfusion (I/R)	Mouse, Rat, Rabbit, Canine	Both	(86, 106, 230, 423)
Preconditioning	Rat, Rabbit	SSM	(63, 64, 67, 104, 229, 318)
Postconditioning	Rat, Rabbit	SSM	(68-70, 304)
Heart Failure	Rat, Hamster	SSM	(137, 138, 180, 383, 385)
Pressure Overload	Mouse, Rat	IFM	(264, 350, 370, 401)
Volume Overload	Rat	SSM	(148, 264, 394, 422)
Aging	Rat, Canine	IFM	(10, 74, 120, 135, 150, 170, 179, 194, 228, 232, 271, 272, 331, 377)
Aging and I/R	Rat	IFM	(69, 231, 233-235)
Exercise	Mouse, Rat	Both	(74, 195, 204, 206)
Exercise and I/R	Rat	Both	(227)
Pharmacological Interventions	Rat, Hamster	SSM	(61, 103, 105, 178, 359, 407, 408)
Type I Diabetes Mellitus	Mouse	IFM	(22-24, 79, 85, 116, 429)
Type II Diabetes Mellitus	Mouse	SSM	(84)
Hypermetabolism	Rat	IFM	(360)

1.8a. Type 1 diabetes mellitus

DM can be characterized by a lack of insulin production during T1DM or a resistance to insulin during T2DM. Cardiovascular complications, such as diabetic cardiomyopathy, are the leading cause of morbidity and mortality among diabetic patients (142). Mitochondrial dysfunction has been shown to be central to the etiology of cardiac dysfunction associated with DM and dependent upon the type of DM, cardiac mitochondrial subpopulations can differentially influenced.

Swiss-Webster mice that underwent multiple low-dose injections of STZ showed that the IFM subpopulation displayed a decrease in size, internal complexity and ETC complexes I and III function (85). Further, superoxide production and oxidative damage were increased in the T1DM IFM (85). In STZ treated mice, cardiolipin content was shown to be decreased, along with decrements in cardiolipin synthase in the IFM during T1DM (79). Our laboratory has also shown enhanced apoptotic propensity in the IFM during T1DM via increased caspase-3 and -9 activities, mPTP opening, Bax and cyclophilin D protein contents, along with decreases in mitochondrial cytochrome *c* content and Bcl-2 levels (428). The proteomic makeup of the IFM is also disturbed as seen by isobaric tags for relative and absolute quantitation (iTRAQ) and 2D differential in-gel electrophoresis (2D-DIGE) (23). These analyses revealed decreased abundance of fatty acid oxidation (FAO) and ETC proteins in the IFM during T1DM (23). Additionally, nuclear-encoded mitochondrial protein import is compromised in T1DM IFM, which could a mechanism by which proteomic dysregulation is occurring (23). Using a novel transgenic animal overexpressing mPHGPx, our laboratory found that the IFM had restored ETC complex function, as well as the attenuation of H_2O_2 production during T1DM. Furthermore, nuclear-encoded mitochondrial protein import was restored, lessening the proteomic dysregulation observed in the T1DM IFM

(22, 86). Solute carrier family 25 member 3 (Slc25a3), an IMM protein transporter involved in providing the mitochondrial matrix with inorganic phosphate, is decreased in the IFM during T1DM. Further, this decrease in Slc25a3 is associated with decreased ATP synthase activity and ATP production in the T1DM IFM (24). ATP-dependent potassium (K^+) channels have a decrease in Kir6.1, a pore-forming subunit, in both cardiac mitochondrial subpopulations during T1DM; however, SUR1, a diazoxide-sensitive sulphonylurea receptor, was only found to be decreased in the IFM (116). Studies on cardiac mitochondrial subpopulations during T1DM indicate that the IFM is predominantly affected during this type of pathological insult. It is unclear as to why this phenomenon occurs, but it may result from differences in mitochondrial subpopulation function such as higher respiration rates, $\Delta\Psi m$ and protein import rates or the subcellular locale of the IFM subpopulation.

1.8b. Type 2 diabetes mellitus

Interestingly, the evaluation of T2DM cardiac mitochondrial subpopulations reveals substantially different results than T1DM, with the SSM subpopulation being predominantly affected. Our laboratory found the SSM to be detrimentally impacted in the *db/db* mouse model with deficits in mitochondrial size and internal complexity, along with decreased state 3 respiration rates, ETC complex activities, ATP synthase function and $\Delta\Psi m$ (84). Further, there was also increased oxidative damage and a greater loss of SSM proteins shown by proteomic analyses as a result of T2DM (84). It is unclear as to why different cardiac mitochondrial subpopulations are affected during T1DM and T2DM; however, the deleterious effects on the mitochondrion are similar with the only difference being the subpopulation in which they are occurring. One explanation is that the milieu surrounding the distinct mitochondrial subpopulations are somewhat

different, potentially causing the IFM to be affected during T1DM and the SSM to be affected during T2DM. The milieu during T2DM has an enhanced free fatty acid content, which was shown in T2DM patients' vastus lateralis muscles by a 3-fold increase in the lipid volume of the SSM locale without affecting the lipids in the IFM region (288). With the increased lipid content in the SSM region, Nielsen et al. suggests that the lipids may actually interfere with key processes involved in metabolic signaling in the SSM, while the IFM remain unaffected (288). Notably, these authors were working on skeletal muscle, not cardiac tissue in these patients.

1.8c. Commonalities between T1DM and T2DM on the mitochondrion

While striking differences do exist between the impact of T1DM versus T2DM on cardiac mitochondrial subpopulations, with the IFM being predominantly affected during T1DM and the SSM being primarily affected by T2DM, commonalities also exist. For example, loss of proper mitochondrial function correlates with the dysregulation of the proteome, which is observed in the specific mitochondrial subpopulation impacted by that type of DM. Specifically, T1DM IFM show structural damage and functional deficits, which coincide with proteomic dysregulation (22-24, 79, 386). The opposite occurs during T2DM, with the SSM revealing structural damage and decreases in mitochondrial function, which correlate with proteome dysregulation (80, 84). Disturbances to the IMM, which contains proteins involved in OXPHOS and protein import machinery, are shown to be impacted in the IFM during T1DM and the SSM during T2DM, suggestive of the IMM locale being prone to proteomic alterations due to the diabetic insult (174). Nuclear-encoded mitochondrial protein import and protein contents of essential constituents in the import process are impacted in the IFM of T1DM and the SSM of T2DM (22, 23). It is interesting to note that commonalities exist in the mirroring of dysfunction in key processes seen in a specific

subpopulation depending on the type of diabetic insult, allowing each pathology to provide complementary information in order to develop a therapeutic intervention to treat both diabetic phenotypes.

1.9 Mitochondrial Dysfunction during DM

Mitochondria are crucial to the maintenance of homeostasis of many cell types because of their energy producing capacity, along with its oxidative and apoptotic potential. The literature provides evidence that mitochondrial dysfunction plays a role in the etiology of cardiac dysfunction during DM (152, 390, 436). Increased oxidative stress, alterations in mitochondrial Ca^{2+} handling and mitochondrial bioenergetics, inefficient nuclear-encoded mitochondrial protein import and proteomic remodeling all contribute to the mitochondrial dysfunction seen in the diabetic heart.

1.9a. Oxidative stress

The development of cardiovascular disease has been linked to an increase in oxidative stress in cardiomyocytes. The mitochondrion is susceptible to oxidative stress because of the IMM, which serves as the primary source of ROS products via the leakage of electrons from the ETC, particularly from complexes I and III (48, 299). When ROS are generated in excess and the antioxidant defense systems cannot keep up, oxidative stress occurs. Forms of ROS include superoxide radicals, hydroxyl radicals, H_2O_2, nitric oxide and peroxynitrite (48, 431). ROS plays a detrimental role to the mitochondrion and other cellular components through oxidation of DNA and proteins, lipid peroxidations and protein nitrations (48, 416). During DM, cardiac mitochondria have been shown to be detrimentally impacted in animal models of both pathologies,

suggesting that the increased glucose and free fatty acid levels drives the formation of ROS (48, 99, 100, 292, 355, 433). Our laboratory observed increased protein and lipid damage in T1DM IFM; however, overexpression of mPHGPx, an antioxidant located in the IMS of the mitochondrion, provided protection against oxidative damage (22, 85). Shen et al. showed that overexpression of MnSOD during T1DM also afforded protection to mitochondria, while Ye et al. showed catalase to have protective benefits (354, 436). Further, overexpression of metallothionein in STZ-treated mice produced a reduction in nitrosative damage and in OVE26 mice restored levels of oxidized glutathione (52, 437). In T2DM animal models, reduced cardiac efficiency was seen due to enhanced ROS generation and lipid peroxidation by-products, leading to increased oxygen consumption without a subsequent increase in ATP production (41). Yamagishi et al. found increased mitochondrial H_2O_2 production and ROS in conjunction with increased electron delivery from augmented FAO (433). Thus, the development of cardiovascular issues during different pathological states could result from an increased oxidative stress from the mitochondrion.

1.9b. Calcium handling

Mitochondria are intricate sources of ATP for cardiomyocyte contraction, but the mitochondrion is also crucial in its interactions with Ca^{2+} in order to regulate the excitation-contraction coupling and energy metabolism within the heart (188). When high levels of Ca^{2+} occur in the matrix, generation of ROS is increased, which causes the opening of the mPTP disrupting the function of the ETC in the IMM (155). With the opening of the mPTP, ionic homeostasis is disrupted and uncoupling of OXPHOS occurs, triggering an increase in cell death (345). In T1DM, Flarsheim et al. showed decreased mitochondrial Ca^{2+} uptake, while Lagadic-Gossmann et al. showed decreased mitochondrial Ca^{2+} content (130, 222). Additionally, during

T1DM, mitochondria did not retain the Ca^{2+} because of an increased propensity for mPTP opening (298). Our laboratory corroborated these results in our findings of increased mPTP opening and decreased mitochondrial cytochrome *c* content in the IFM of T1DM mice (428). Abnormalities in Ca^{2+} homeostasis may also be a mechanism linking impaired mitochondrial oxidative function to insulin resistance (281, 309, 330). Altogether, these studies indicate an impairment in Ca^{2+} handling during DM, leading to decreased contractility and energy metabolism, while increasing cellular apoptosis via the mitochondria.

1.9c. Mitochondrial energetics

Mitochondrial energetics play a distinct role in the cell and mitochondrial dysfunction has been linked to a wide range of pathological states including metabolic diseases, cancer and aging. Gross et al. showed decreased respiration in STZ-treated rats when assessed with substrates for complexes I and II in skeletal muscle mitochondria, which was corroborated in other rodent studies looking at mitochondrial respiration in the heart and brain (85, 125, 153, 278). In the Akita mouse model for T1DM, mitochondria from the heart displayed decreased state 3 respiration when fueled with complex I substrates along with decreased ATP synthase activity (50). Additionally, cardiac mitochondria and mitochondria isolated from the gastrocnemius of STZ-treated rats also showed a decreased state 3 respiration, ADP/O ratio and ATP synthesis rate (165). In a clinical setting, T1DM patients showed decreased ATP production in skeletal muscle mitochondria as a result of discontinued insulin treatment (200). Altogether, mitochondrial respiration and ATP production are impaired in the T1DM setting. Dysfunction in mitochondrial energetics has also been reported in animal models of T2DM. In the db/db mouse heart, respiration rates were decreased when fueled with glutamate/malate and palmitoyl-carnitine, along with decreased expression of the F_1 α-

subunit of ATP synthase and increased proton leak induced by fatty acids (41). In another study using the db/db model, Boudina et al. found impairments in OXPHOS and increased fatty acid-induced mitochondrial uncoupling (40, 41). Further, in a high-fat feeding model of T2DM, decreases in tricarboxylic acid (TCA) cycle proteins were found in skeletal muscle along with an inability to switch substrate utilization from fat to glucose, suggestive of an incapability to deal with increased fatty acid substrates during T2DM (212). When assessing T2DM patients, decreased NADH oxidoreductase and reduced citrates synthase activity were seen in skeletal muscle mitochondria (207). Other studies have indicated increased lipid deposition, deficits in OXPHOS, decreased ATP synthase and creatine kinase B protein expression in T2DM patients (172, 288, 324). Altogether, these studies indicate decrements in mitochondrial respiration and ATP production during T2DM. Independent of the type of DM, mitochondrial energetics are detrimentally altered.

1.9d. Protein import

Proteomic analyses have revealed that the abundance of nuclear-encoded proteins residing within the mitochondria are decreased during DM, including proteins essential for the mitochondrial protein import process (23, 84, 393). Results from our laboratory revealed that nuclear-encoded mitochondrial protein import is decreased in the T1DM IFM, with no impact on the SSM subpopulation (23). Interestingly, it is thought that the decrease in import efficiency is due to a diminished protein content of mtHsp70 in the IFM as discussed above (23). The overexpression of mPHGPx was able to restore mitochondrial protein import efficiency in the IFM during T1DM (22). While protein content of mtHsp70 has been shown to be downregulated in

SSM during T2DM, to date, nuclear-encoded mitochondrial protein import has not been reported in a T2DM mouse model (84).

1.9e. Proteomic remodeling

Attainment of a broad overview of what proteins are changing in the heart during DM has allowed for an increased understanding of how mitochondria are affected during the disease state. Recently, broad scale proteomics have become prevalent within different types of DM models (23, 51, 84, 158, 355, 393). 2D polyacrylamide gel electrophoresis (2D-PAGE) along with matrix-assisted laser desorption/ionization time of flight mass spectrometry (MALDI-TOF-MS) was performed on mitochondria isolated from STZ-induced T1DM rats (393). Alterations in FAO proteins, OXPHOS complex I subunits, and mitochondrial heat shock proteins were found in the T1DM animals (393). Another group using the same model found increases in FAO proteins and decreases in proteins involved with the antioxidant defense system (158). Using iTRAQ proteomic labeling coupled with multidimensional protein identification technology mass spectrometry (MudPIT MS/MS), cardiac mitochondria from STZ-treated rats were analyzed four months post-diabetic onset (197). In this study, Jullig et al. found increases in long chain fatty acid proteins and decreases in catabolic short chain fatty acid enzymes, potentially providing an explanation for the lipotoxicity seen in the T1DM setting (197). Further, results from another study found that the Akita mouse model of T1DM had increased FAO proteins, decreased TCA proteins and alterations in OXPHOS proteins in mitochondria isolated from the kidney, liver, brain and heart (51). Proteomic evaluations of mitochondrial subpopulations has been performed by our laboratory in the STZ-induced T1DM mouse model using two separate approaches: 2D-difference gel electrophoresis (DIGE) and iTRAQ coupled with MALDI-TOF-MS (23). While similar findings

were found as far as changes in proteomic evaluations, the two mitochondrial subpopulations were differentially affected during T1DM, with the IFM showing the predominant changes during this pathological insult (23). FAO, OXPHOS subunits, TCA cycle intermediates, mitochondrial structural proteins and mitochondrial protein import constituents were significantly decreased in the T1DM IFM (23). Further, MudPIT was used in order to assess the posttranslational modifications of the proteins, which revealed higher oxidation and deamidations to proteins in the T1DM IFM (23). Our laboratory also assessed proteomic alterations and posttranslational modifications in the mitochondrial subpopulations of the db/db T2DM mouse model (84). Dysregulation of proteins in the SSM was more prevalent than that in the IFM of db/db mice when compared to controls with changes in FAO, respiratory chain components, TCA cycle proteins, the antioxidant defense protein peroxiredoxin V and mitochondrial protein import constituents (84). Posttranslational modifications were found on proteins of the SSM and IFM during the T2DM pathology, with proteins of the ETC being affected with alterations such as acetylations, deamidations and oxidations (84). Interestingly, the majority of proteins that were altered were located in the IMM, suggesting that the pathogenesis of the mitochondrial dysfunction may result from alterations to this sub-compartment during T2DM (84). Altogether, this data reveals that the mitochondrial proteome is detrimentally impacted during DM.

1.10 MicroRNA

With their original discovery in *C. elegans*, microRNAs (miRNAs) are regulators of gene expression that are abundant in many species (415). These miRNAs work by targeting mRNAs of protein-coding genes for posttranscriptional regulation and translational repression. miRNAs play a regulatory role in cell physiology and development; however, they have also been

implicated in pathological disease states such as autoimmune diseases, viral infections, cancer and DM (24, 184, 189, 213, 302, 310, 438).

MiRNAs are transcribed by RNA Polymerase II, which produces a pri-miRNA transcript containing a hairpin loop, capped 5' end and a polyadenylated (poly(A)) tail. Drosha, an RNase III enzyme located in the nucleus, serves to cut the pri-miRNA into an intermediate form known as the pre-miRNA (225, 226, 442). This pre-miRNA contains the hairpin loop, but its size is significantly smaller and once trimmed, the pre-miRNA is then actively transported to the cytoplasm from the nucleus by exportin-5 and ran-guanosine triphosphate (256, 439). Dicer, a cytoplasmic protein and RNase III enzyme, cuts the pre-miRNA resulting in the mature, double-stranded miRNA, which now ranges in size from 20-25 base pairs (255). Finally, formation of the RNA-Induced Silencing Complex (RISC) occurs. First, dicer, along with assistance from cofactors transactivating response RNA binding protein and protein activator of interferon induced protein kinase, unravels the miRNA from its complementary sequence, leaving a single-stranded functional miRNA. Then, dicer helps to bring the miRNA to a member of the argonaute family (AGO1-4), completing the formation of the RISC (323). Importantly, AGO family proteins function in miRNA repression through the inhibition of protein synthesis when bound to the mRNA 3' untranslated region (UTR) (129). miRNAs then target the RISC via AGO to a specific mRNA and the seeding region, a particular 2-7 base pair region of the miRNA, can bind directly to the target mRNA. Once bound, translational repression, deadenylation or endonucleolytic cleavage causing mRNA degradation to occur in the RISC (246) (Figure 1.6).

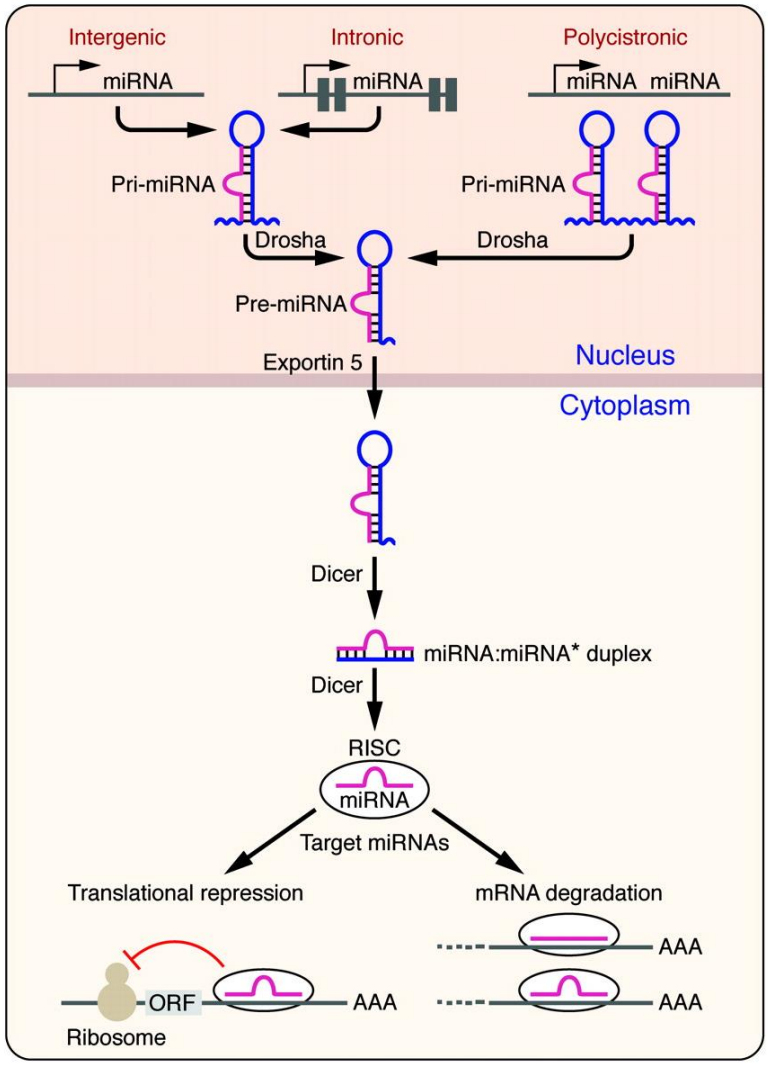

Figure 1.6 miRNA Biogenesis and Function (403)

1.10a. In physiology

miRNAs have been shown to be involved in physiological developmental processes such as regulation of cellular functions including growth, proliferation, differentiation and apoptosis (20). Since miRNAs play a role in differentiation, the expression profiles for miRNA can be used to identify specific cell types, thus leading to the identification of certain tissues (443). Further, miRNAs have been investigated for their role in stem cells, specifically controlling the fate of the

stem cell through differentiation and behavior of the cell (55). When looking at embryonic cell differentiation regulation by miRNA-296 and miRNA-22, miRNA-296 promoted differentiation, while miRNA-22 inhibited differentiation (140). Additional studies revealed that osteogenic differentiation of stem cells is regulated by miR-26a and miRNA-138 through the targeting of transcription factor SMAD1 (114, 140). Interestingly, miRNA networks during development also interact in important processes for the fate of a cell, conferring robustness to certain biological processes and reinforcement of transcriptional programs (108). First, miRNAs oftentimes target a transcriptional regulator and second, with the combination of a feedforward and feedback loop, cells are able to distinguish between whether they should counteract a transient fluctuation or incorporate a permanent change (108, 123). Finally, specific cell type miRNA exist and reinforce the same cell fate decisions for all cells (108, 123). In a study by Cheung et al., the authors found that the miRNA pathway was essential in the maintenance of quiescence in satellite cells (71). Specifically, the authors showed that miR-489 regulates satellite cell quiescence through *Dek* and helps to promote the proliferation of myogenic progenitors (71). The vast majority of literature reveals that miRNA play an unprecedented role in proper and controlled physiological development.

1.10b. In pathologies

Recently, an expanse of research has been performed to elucidate the roles of miRNAs in pathologies such as cancer, cardiovascular disease, DM and pathologies dealing with the immune system (76, 98, 121, 295). miR-15a/16-1 are implicated as tumor suppressors, which have been found to be deleted in chronic lymphocytic leukemia (53). This discovery by Calin et al. set the stage for the role of miRNA in cancer, where miRNAs have been shown to affect all 6 hallmarks

of malignant cells (98). Further, miRNAs have important roles in cardiovascular disease such as MI, hypertrophy and HF (121). In a study of ischemic pre- and post-conditioning, characterization of the miRNA expression levels showed alterations to 18 miRNAs (405). miR-423-5p was highly expressed in the blood of HF patients and elevated plasma levels of the same miRNA are linked with N-terminal prohormone brain natriuretic peptide levels in dilated cardiomyopathy (115, 388). miRNAs exist in all parts of the body and play a role in cellular processes dealing with both physiological and pathological development. It is suggested that miRNA can circulate in the blood during times of stress to target areas within the body, which allows for these circulating miRNAs to be used as clinical markers for disease states (147).

1.10c. Within the heart

MiRNA are present throughout the body; however, within the heart, certain miRNA have been shown to be highly expressed and impact cardiomyocyte differentiation, cardiac development and ventricular hypertrophy (19, 25, 244). Nine miRNAs have been described previously as having important roles in cardiovascular disease and disease progression: miR-1, miR-133a-2, miR-133b, miR-208a, miR-208b, miR-214-3p, miR-146a-5p, miR-155-5p and miR-150-5p (126). miR-1 and miR-133a have been shown to be important in ventricular development, particularly in regulation of cardiomyocyte growth (250, 371). Interestingly, miR-133a, miR-133b, miR208a and miR-208b have been shown to be downregulated in chronic Chagas disease cardiomyopathy when compared to control (126). Further, these authors found that miR-133b, miR-208a and miR-208b were also reduced in diabetic cardiomyopathy samples when compared with controls (126). In physiological, exercise-induced LV hypertrophy, the global analysis of miRNAs revealed that miR-26b, miR-27a and miR-143 were decreased after 7 days of exercise, while miR-150 was increased after 35

days of exercise, potentially alluding to these miRNAs playing a role in the regulation of hypertrophy (262). miR-29 and miR-34a have been suggested to have a role in the development of cardiac fibrosis, while miR-30d plays a role in diabetic cardiomyopathy (183, 242, 404). Literature suggests that miRNAs have been abundantly studied in the heart relating to both physiological and pathophysiological roles, along with their potential use as therapeutic targets and treatments for cardiac diseases.

1.10d. Within the mitochondria

miRNAs exist throughout the body in many different locales, but recently, research has focused on determining the role of particular miRNAs within certain organelles. With the mitochondrion playing a critical role in providing energy for the cell and utilizing proteins generated from the mitochondrial and nuclear genome in order to properly function, it is critical for the role of miRNAs within this organelle be elucidated due to their influence on mRNA and protein expression. Particularly, the study of miRNAs in pathophysiological states is extremely important to determine their regulatory roles. Studies of liver mitochondria revealed the presence of miRNA within this organ and suggested that miRNAs have influenced cellular proliferation, apoptosis and cellular differentiation (31, 215). Further, literature suggests that specific miRNA subpopulations could potentially exist within the mitochondrion (240). The changing concentrations of miRNAs within the mitochondria have shown detrimental impacts on OXPHOS, ATP synthase and FAO during disease states. Interestingly, Bian et al. found that the most highly expressed miRNAs located in liver mitochondria did not show up in the liver fractions (31). Das et al. performed a study looking at miRNA-181c translocation into the mitochondria and its regulation of the mitochondrial genome through the targeting of cytochrome *c* oxidase subunit 1

mRNA (93). In the STZ-induced T1DM mouse model, increased levels of miR-494, miR-202-5p, miR155 and miR-134 were found, while miR-705 and miR122 were decreased in the liver mitochondria and are suggested to target specific mitochondrial genes (31). Looking at isolated cardiac mitochondrial subpopulations, our laboratory found that spatially distinct mitochondrial subpopulations are differentially affected during DM (189). During T1DM, the redistribution of miR-378 in the IFM led to a decrease in the F_0 component of ATP6 in cardiac mitochondria (189). Another study performed in our laboratory showed an increase in miR-141 expression with a subsequent decrease in the IMM phosphate transporter, Slc25a3, in the IFM during T1DM (24). Further investigation of miRNAs within the mitochondria, particularly mitochondrial subpopulations, could lead to and understanding of how mitochondrial processes are dysfunctional during pathological settings.

1.10e. Import into the mitochondria

Import of nuclear-encoded proteins into the mitochondrion is a well-studied mechanism, with the machinery for the process identified; however, the mechanisms behind the import of miRNAs into the mitochondrion and the constituents involved are unknown. Studies using different species indicate that nuclear-encoded RNA is likely imported into the mitochondrion via mechanisms that are ATP-dependent. Schneider showed the import of tRNAs into the mitochondrion through Tom20, Tom40 and VDAC; however, the mechanisms behind the import of non-coding RNAs still need to be elucidated (349). Interestingly, studies looking at 5S rRNA and tRNA targeted to the mitochondrion suggested that the mechanism behind protein import could potentially be the same machinery used for RNA import (15, 111, 210, 366, 367). In addition to the pores used by nuclear-encoded protein import, RNA could be imported into the

mitochondrion initially through porins, which are voltage-dependent anion channels located on the OMM (15, 75, 339).

Argonaute 2 (Ago2) could also serve as a mediator in the localization of miRNAs to the mitochondria and potentially facilitate the miRNAs movement through and into the mitochondrial matrix, indicating that the RISC potentially plays a role in miRNA import (15). Ago2 has been shown to associate with mitochondrial transcripts *mt*-CO3 and *mt*-CO1, along with miR-181c, indicating that Ago2 may play a key role in the association of miRNAs being imported into the mitochondrion (16, 28, 93). Ago2 and its associated miRNA could be delivered to the mitochondrion through a system of vesicles (15). While miRNAs have been shown to exist in microvesicles and exosomes, allowing for the transfer of the miRNA between cells, this process has not been shown to occur on a particular organelle, such as the mitochondrion (128).

Another important protein postulated to be involved in the import of miRNA into the mitochondrion is polynucleotide phosphorylase (PNPase). Utilizing PNPase for RNA import into the mitochondrion requires the presence of a specific stem-loop secondary structure in the target RNA (247, 418). Barrey et al. found that pre-miR-302a and pre-let-7b are predicted to fold into these stem-loop configurations, leading to the assumption that PNPase could be critical for the import of these pre-miRNAs into the mitochondrion (18). While potential machinery and mechanisms of import for miRNA have been postulated, studies still need to be completed in order to confirm these speculations.

1.10e.i. Polynucleotide Phosphorylase

PNPase is located in the IMS of the mitochondrion, potentially situated on the IMM (418, 419). Functioning as a homotrimeric protein, PNPase aids in the import of RNA into the

mitochondrion, editing and degradation of RNA, along with controlling cellular senescence and cell cycle (15, 248, 340, 341, 365, 418). Interestingly, Vedrenne et al. found that a mutation to PNPT1, the gene encoding for PNPase, impairs RNA import into the mitochondrion and causes deficiencies in respiratory chain function (406). PNPase also has the capability to form homo-multimers, providing the protein with a diverse array of interactions with RNA and other small molecules, but also complicating the study of the protein (417). PNPase has been shown to induce degradation of mature miRNA by selectively binding it; however, its role in the import of mature miRNA has been postulated, but not studied (94). PNPase has been established to play an important role in the import of nuclear RNA; however, its involvement in the import of miRNAs needs to be evaluated (336, 349, 418).

1.11 Summary

DM continues to increase in prevalence across the United States and worldwide, with rates of DM doubling in the past two decades (4). The global prevalence of DM is 8.5%, with a staggering 9.3% of people within the United States suffering from the disease (1, 2). Annually, DM costs the United States roughly $245 billion in medical costs and lost productivity (4). Among the leading causes of morbidity and mortality among diabetic patients are cardiovascular complications, such as HF (142). We sought to determine if speckle-tracking based strain echocardiographic analyses were able to detect subtle changes in cardiac function during DM, prior to detection using conventional measurements, thus allowing for earlier detection and treatment of cardiac complications during the progression of the disease. Mitochondrial dysfunction has been suggested as central to the etiology of DM; therefore, it is critical for scientists to study and elucidate the mechanisms behind mitochondrial dysfunction during DM,

ultimately leading to better diagnostic and therapeutic treatment options. Alterations to the mitochondrial proteome during DM could be a leading cause of mitochondrial dysfunction. The goal of the studies presented was to elucidate whether mitochondrial proteome dysregulation resulted from dysfunctional nuclear-encoded mitochondrial protein import efficiency in the SSM during T2DM and the IFM during T1DM. Further, subsequent studies were performed to determine whether overexpression of mtHsp70, a critical subunit of the PAM complex and motor for nuclear-encoded mitochondrial protein import, preserves import efficiency, stabilizing the mitochondrial proteome and ultimately leading to restored mitochondrial and cardiac contractile function. We also assessed the importance of PNPase for the import of miRNA during T2DM in order to help elucidate how the miRNAs are translocating into the mitochondria and regulating the mitochondrial genome with the intent of providing potential targets for therapeutic strategies. Efficient evaluation of cardiac contractile function via echocardiography and examination of nuclear-encoded mitochondrial protein import and import of miRNAs into the mitochondrion during DM could potentially allow for the discovery of therapeutic strategies aimed at helping to alleviate the mitochondrial dysfunction and cardiac contractile deficiencies seen in patients suffering from DM.

REFERENCES

1. Diabetes Fact Sheet. *World Health Organization*, 2016.
2. National Diabetes Fact Sheet, edited by **Prevention CfDCa**, 2012.
3. National Diabetes Statistics Report. *American Diabetes Association*, 2014.
4. The State of Obesity: Better Policies for a Healthier America. 2015.
5. **Agnetti G, Bezstarosti K, Dekkers DH, Verhoeven AJ, Giordano E, Guarnieri C, Caldarera CM, Van Eyk JE, and Lamers JM.** Proteomic profiling of endothelin-1-stimulated hypertrophic cardiomyocytes reveals the increase of four different desmin species and alpha-B-crystallin. *Biochim Biophys Acta* 1784: 1068-1076, 2008.
6. **Akerblom HK, Vaarala O, Hyoty H, Ilonen J, and Knip M.** Environmental factors in the etiology of type 1 diabetes. *Am J Med Genet* 115: 18-29, 2002.
7. **Al-Achi A and Greenwood R.** A brief report on some physiological parameters of streptozocin-diabetic rat. *Drug Dev Ind Pharm* 27: 465-468, 2001.
8. **An D and Rodrigues B.** Role of changes in cardiac metabolism in development of diabetic cardiomyopathy. *Am J Physiol Heart Circ Physiol* 291: H1489-1506, 2006.
9. **Anderson S, Bankier AT, Barrell BG, de Bruijn MH, Coulson AR, Drouin J, Eperon IC, Nierlich DP, Roe BA, Sanger F, Schreier PH, Smith AJ, Staden R, and Young IG.** Sequence and organization of the human mitochondrial genome. *Nature* 290: 457-465, 1981.
10. **Asemu G, O'Connell KA, Cox JW, Dabkowski ER, Xu W, Ribeiro RF, Jr., Shekar KC, Hecker PA, Rastogi S, Sabbah HN, Hoppel CL, and Stanley WC.** Enhanced resistance to permeability transition in interfibrillar cardiac mitochondria in dogs: effects of aging and long-term aldosterone infusion. *Am J Physiol Heart Circ Physiol* 304: H514-528, 2013.

11. **Ashley EA and Niebauer J.** Chapter 4 Understanding the echocardiogram. In: *Cardiology Explained*. London, 2004.

12. **Association AD.** Diagnosis and Classification of Diabetes Mellitus. *Diabetes Care*: S62-S69, 2010.

13. **Baicu CF, Zile MR, Aurigemma GP, and Gaasch WH.** Left ventricular systolic performance, function, and contractility in patients with diastolic heart failure. *Circulation* 111: 2306-2312, 2005.

14. **Ban CR and Twigg SM.** Fibrosis in diabetes complications: pathogenic mechanisms and circulating and urinary markers. *Vasc Health Risk Manag* 4: 575-596, 2008.

15. **Bandiera S, Mategot R, Girard M, Demongeot J, and Henrion-Caude A.** MitomiRs delineating the intracellular localization of microRNAs at mitochondria. *Free Radic Biol Med* 64: 12-19, 2013.

16. **Bandiera S, Ruberg S, Girard M, Cagnard N, Hanein S, Chretien D, Munnich A, Lyonnet S, and Henrion-Caude A.** Nuclear outsourcing of RNA interference components to human mitochondria. *PloS one* 6: e20746, 2011.

17. **Barbosa MM, Costa Rocha MO, Vidigal DF, Bicalho Carneiro Rde C, Araujo RD, Palma MC, Lins de Barros MV, and Nunes MC.** Early detection of left ventricular contractility abnormalities by two-dimensional speckle tracking strain in Chagas' disease. *Echocardiography* 31: 623-630, 2014.

18. **Barrey E, Saint-Auret G, Bonnamy B, Damas D, Boyer O, and Gidrol X.** Pre-microRNA and mature microRNA in human mitochondria. *PloS one* 6: e20220, 2011.

19. **Barringhaus KG and Zamore PD.** MicroRNAs: regulating a change of heart. *Circulation* 119: 2217-2224, 2009.

20. **Bartel DP.** MicroRNAs: genomics, biogenesis, mechanism, and function. *Cell* 116: 281-297, 2004.

21. **Baseler WA, Croston TL, and Hollander JM.** Functional Characteristics of Mortalin. In: *Mortalin Biology: Life, Stress and Death*, edited by Kaul SC and Wadhwa R. New York: Springer, 2012, p. 55-80.

22. **Baseler WA, Dabkowski ER, Jagannathan R, Thapa D, Nichols CE, Shepherd DL, Croston TL, Powell M, Razunguzwa TT, Lewis SE, Schnell DM, and Hollander JM.** Reversal of mitochondrial proteomic loss in Type 1 diabetic heart with overexpression of phospholipid hydroperoxide glutathione peroxidase. *Am J Physiol Regul Integr Comp Physiol* 304: R553-565, 2013.

23. **Baseler WA, Dabkowski ER, Williamson CL, Croston TL, Thapa D, Powell MJ, Razunguzwa TT, and Hollander JM.** Proteomic alterations of distinct mitochondrial subpopulations in the type 1 diabetic heart: contribution of protein import dysfunction. *Am J Physiol Regul Integr Comp Physiol* 300: R186-200, 2011.

24. **Baseler WA, Thapa D, Jagannathan R, Dabkowski ER, Croston TL, and Hollander JM.** miR-141 as a regulator of the mitochondrial phosphate carrier (Slc25a3) in the type 1 diabetic heart. *Am J Physiol Cell Physiol* 303: C1244-1251, 2012.

25. **Baskerville S and Bartel DP.** Microarray profiling of microRNAs reveals frequent coexpression with neighboring miRNAs and host genes. *RNA* 11: 241-247, 2005.

26. **Bauer M, Cheng S, Jain M, Ngoy S, Theodoropoulos C, Trujillo A, Lin FC, and Liao R.** Echocardiographic speckle-tracking based strain imaging for rapid cardiovascular phenotyping in mice. *Circ Res* 108: 908-916, 2011.

27. **Bauer M, Cheng S, Unno K, Lin FC, and Liao R.** Regional cardiac dysfunction and dyssynchrony in a murine model of afterload stress. *PloS one* 8: e59915, 2013.

28. **Beitzinger M, Peters L, Zhu JY, Kremmer E, and Meister G.** Identification of human microRNA targets from isolated argonaute protein complexes. *RNA Biol* 4: 76-84, 2007.

29. **Belke DD, Larsen TS, Gibbs EM, and Severson DL.** Altered metabolism causes cardiac dysfunction in perfused hearts from diabetic (db/db) mice. *Am J Physiol-Endoc M* 279: E1104-E1113, 2000.

30. **Bell DS.** Diabetic cardiomyopathy. *Diabetes Care* 26: 2949-2951, 2003.

31. **Bian Z, Li LM, Tang R, Hou DX, Chen X, Zhang CY, and Zen K.** Identification of mouse liver mitochondria-associated miRNAs and their potential biological functions. *Cell Res* 20: 1076-1078, 2010.

32. **Birkedal R, Shiels HA, and Vendelin M.** Three-dimensional mitochondrial arrangement in ventricular myocytes: from chaos to order. *Am J Physiol Cell Physiol* 291: C1148-1158, 2006.

33. **Blessberger H and Binder T.** Two dimensional speckle tracking echocardiography: clinical applications. *Heart* 96: 2032-2040, 2010.

34. **Blondheim DS, Kazatsker M, Friedman Z, Lysyansky P, Meisel SR, Asif A, Smirin N, and Shotan A.** Effect of medical therapy for heart failure on segmental myocardial function in patients with ischemic cardiomyopathy. *The American journal of cardiology* 99: 1741-1744, 2007.

35. **Bloom A, Hayes TM, and Gamble DR.** Register of newly diagnosed diabetic children. *Br Med J* 3: 580-583, 1975.

36. **Bohnert M, Rehling P, Guiard B, Herrmann JM, Pfanner N, and van der Laan M.** Cooperation of stop-transfer and conservative sorting mechanisms in mitochondrial protein transport. *Curr Biol* 20: 1227-1232, 2010.

37. **Bonnevie-Nielsen V, Steffes MW, and Lernmark A.** A major loss in islet mass and B-cell function precedes hyperglycemia in mice given multiple low doses of streptozotocin. *Diabetes* 30: 424-429, 1981.

38. **Boudina S and Abel ED.** Diabetic cardiomyopathy revisited. *Circulation* 115: 3213-3223, 2007.

39. **Boudina S and Abel ED.** Diabetic cardiomyopathy, causes and effects. *Rev Endocr Metab Disord* 11: 31-39, 2010.

40. **Boudina S and Abel ED.** Mitochondrial uncoupling: a key contributor to reduced cardiac efficiency in diabetes. *Physiology (Bethesda)* 21: 250-258, 2006.

41. **Boudina S, Sena S, Theobald H, Sheng X, Wright JJ, Hu XX, Aziz S, Johnson JI, Bugger H, Zaha VG, and Abel ED.** Mitochondrial energetics in the heart in obesity-related diabetes: direct evidence for increased uncoupled respiration and activation of uncoupling proteins. *Diabetes* 56: 2457-2466, 2007.

42. **Boyer JK, Thanigaraj S, Schechtman KB, and Perez JE.** Prevalence of ventricular diastolic dysfunction in asymptomatic, normotensive patients with diabetes mellitus. *The American journal of cardiology* 93: 870-875, 2004.

43. **Brooks BA, Franjic B, Ban CR, Swaraj K, Yue DK, Celermajer DS, and Twigg SM.** Diastolic dysfunction and abnormalities of the microcirculation in type 2 diabetes. *Diabetes Obes Metab* 10: 739-746, 2008.

44. **Brough D, Schell MJ, and Irvine RF.** Agonist-induced regulation of mitochondrial and endoplasmic reticulum motility. *Biochem J* 392: 291-297, 2005.

45. **Brown RA, Filipovich P, Walsh MF, and Sowers JR.** Influence of sex, diabetes and ethanol on intrinsic contractile performance of isolated rat myocardium. *Basic Res Cardiol* 91: 353-360, 1996.

46. **Brownlee M.** Biochemistry and molecular cell biology of diabetic complications. *Nature* 414: 813-820, 2001.

47. **Buchanan J, Mazumder PK, Hu P, Chakrabarti G, Roberts MW, Yun UJ, Cooksey RC, Litwin SE, and Abel ED.** Reduced cardiac efficiency and altered substrate metabolism precedes the onset of hyperglycemia and contractile dysfunction in two mouse models of insulin resistance and obesity. *Endocrinology* 146: 5341-5349, 2005.

48. **Bugger H and Abel ED.** Mitochondria in the diabetic heart. *Cardiovasc Res* 88: 229-240, 2010.

49. **Bugger H and Abel ED.** Rodent models of diabetic cardiomyopathy. *Dis Model Mech* 2: 454-466, 2009.

50. **Bugger H, Boudina S, Hu XX, Tuinei J, Zaha VG, Theobald HA, Yun UJ, McQueen AP, Wayment B, Litwin SE, and Abel ED.** Type 1 diabetic akita mouse hearts are insulin sensitive but manifest structurally abnormal mitochondria that remain coupled despite increased uncoupling protein 3. *Diabetes* 57: 2924-2932, 2008.

51. **Bugger H, Chen D, Riehle C, Soto J, Theobald HA, Hu XX, Ganesan B, Weimer BC, and Abel ED.** Tissue-specific remodeling of the mitochondrial proteome in type 1 diabetic akita mice. *Diabetes* 58: 1986-1997, 2009.

52. **Cai L, Li W, Wang G, Guo L, Jiang Y, and Kang YJ.** Hyperglycemia-induced apoptosis in mouse myocardium: mitochondrial cytochrome C-mediated caspase-3 activation pathway. *Diabetes* 51: 1938-1948, 2002.

53. **Calin GA, Dumitru CD, Shimizu M, Bichi R, Zupo S, Noch E, Aldler H, Rattan S, Keating M, Rai K, Rassenti L, Kipps T, Negrini M, Bullrich F, and Croce CM.** Frequent deletions and down-regulation of micro- RNA genes miR15 and miR16 at 13q14 in chronic lymphocytic leukemia. *Proc Natl Acad Sci U S A* 99: 15524-15529, 2002.

54. **Calvo S, Jain M, Xie X, Sheth SA, Chang B, Goldberger OA, Spinazzola A, Zeviani M, Carr SA, and Mootha VK.** Systematic identification of human mitochondrial disease genes through integrative genomics. *Nature genetics* 38: 576-582, 2006.

55. **Cao H, Wang J, Li X, Florez S, Huang Z, Venugopalan SR, Elangovan S, Skobe Z, Margolis HC, Martin JF, and Amendt BA.** MicroRNAs play a critical role in tooth development. *J Dent Res* 89: 779-784, 2010.

56. **Carugo S, Giannattasio C, Calchera I, Paleari F, Gorgoglione MG, Grappiolo A, Gamba P, Rovaris G, Failla M, and Mancia G.** Progression of functional and structural cardiac alterations in young normotensive uncomplicated patients with type 1 diabetes mellitus. *J Hypertens* 19: 1675-1680, 2001.

57. **Cerqueira MD, Weissman NJ, Dilsizian V, Jacobs AK, Kaul S, Laskey WK, Pennell DJ, Rumberger JA, Ryan T, Verani MS, American Heart Association Writing Group on Myocardial S, and Registration for Cardiac I.** Standardized myocardial segmentation and nomenclature for tomographic imaging of the heart. A statement for healthcare professionals from the Cardiac Imaging Committee of the Council on Clinical Cardiology of the American Heart Association. *Circulation* 105: 539-542, 2002.

58. **Chacinska A, Koehler CM, Milenkovic D, Lithgow T, and Pfanner N.** Importing mitochondrial proteins: machineries and mechanisms. *Cell* 138: 628-644, 2009.

59. **Chacinska A, Lind M, Frazier AE, Dudek J, Meisinger C, Geissler A, Sickmann A, Meyer HE, Truscott KN, Guiard B, Pfanner N, and Rehling P.** Mitochondrial presequence translocase: switching between TOM tethering and motor recruitment involves Tim21 and Tim17. *Cell* 120: 817-829, 2005.

60. **Chacinska A, Rehling P, Guiard B, Frazier AE, Schulze-Specking A, Pfanner N, Voos W, and Meisinger C.** Mitochondrial translocation contact sites: separation of dynamic and stabilizing elements in formation of a TOM-TIM-preprotein supercomplex. *EMBO J* 22: 5370-5381, 2003.

61. **Cheema Y, Sherrod JN, Zhao W, Zhao T, Ahokas RA, Sun Y, Gerling IC, Bhattacharya SK, and Weber KT.** Mitochondriocentric pathway to cardiomyocyte necrosis in aldosteronism: cardioprotective responses to carvedilol and nebivolol. *Journal of cardiovascular pharmacology* 58: 80-86, 2011.

62. **Chen J, Cao T, Duan Y, Yuan L, and Yang Y.** Velocity vector imaging in assessing the regional systolic function of patients with post myocardial infarction. *Echocardiography* 24: 940-945, 2007.

63. **Chen Q, Hoppel CL, and Lesnefsky EJ.** Blockade of electron transport before cardiac ischemia with the reversible inhibitor amobarbital protects rat heart mitochondria. *J Pharmacol Exp Ther* 316: 200-207, 2006.

64. **Chen Q and Lesnefsky EJ.** Blockade of electron transport during ischemia preserves bcl-2 and inhibits opening of the mitochondrial permeability transition pore. *FEBS Lett* 585: 921-926, 2011.

65. **Chen Q and Lesnefsky EJ.** Depletion of cardiolipin and cytochrome c during ischemia increases hydrogen peroxide production from the electron transport chain. *Free Radic Biol Med* 40: 976-982, 2006.

66. **Chen Q, Moghaddas S, Hoppel CL, and Lesnefsky EJ.** Ischemic defects in the electron transport chain increase the production of reactive oxygen species from isolated rat heart mitochondria. *Am J Physiol Cell Physiol* 294: C460-466, 2008.

67. **Chen Q, Moghaddas S, Hoppel CL, and Lesnefsky EJ.** Reversible blockade of electron transport during ischemia protects mitochondria and decreases myocardial injury following reperfusion. *J Pharmacol Exp Ther* 319: 1405-1412, 2006.

68. **Chen Q, Paillard M, Gomez L, Li H, Hu Y, and Lesnefsky EJ.** Postconditioning modulates ischemia-damaged mitochondria during reperfusion. *Journal of cardiovascular pharmacology* 59: 101-108, 2012.

69. **Chen Q, Ross T, Hu Y, and Lesnefsky EJ.** Blockade of electron transport at the onset of reperfusion decreases cardiac injury in aged hearts by protecting the inner mitochondrial membrane. *J Aging Res* 2012: 753949, 2012.

70. **Chen Q, Yin G, Stewart S, Hu Y, and Lesnefsky EJ.** Isolating the segment of the mitochondrial electron transport chain responsible for mitochondrial damage during cardiac ischemia. *Biochem Biophys Res Commun* 397: 656-660, 2010.

71. **Cheung TH, Quach NL, Charville GW, Liu L, Park L, Edalati A, Yoo B, Hoang P, and Rando TA.** Maintenance of muscle stem-cell quiescence by microRNA-489. *Nature* 482: 524-528, 2012.

72. **Chiasson JL, Aris-Jilwan N, Belanger R, Bertrand S, Beauregard H, Ekoe JM, Fournier H, and Havrankova J.** Diagnosis and treatment of diabetic ketoacidosis and the hyperglycemic hyperosmolar state. *CMAJ* 168: 859-866, 2003.

73. **Coleman DL.** Obese and diabetes: two mutant genes causing diabetes-obesity syndromes in mice. *Diabetologia* 14: 141-148, 1978.

74. **Coleman R, Weiss A, Finkelbrand S, and Silbermann M.** Age and exercise-related changes in myocardial mitochondria in mice. *Acta histochemica* 83: 81-90, 1988.

75. **Colombini M.** Structure and mode of action of a voltage dependent anion-selective channel (VDAC) located in the outer mitochondrial membrane. *Ann N Y Acad Sci* 341: 552-563, 1980.

76. **Condorelli G, Latronico MV, and Cavarretta E.** microRNAs in cardiovascular diseases: current knowledge and the road ahead. *J Am Coll Cardiol* 63: 2177-2187, 2014.

77. **Cottrell C and Kirkpatrick JN.** Echocardiographic strain imaging and its use in the clinical setting. *Expert review of cardiovascular therapy* 8: 93-102, 2010.

78. **Craig EA, Kramer J, and Kosic-Smithers J.** SSC1, a member of the 70-kDa heat shock protein multigene family of Saccharomyces cerevisiae, is essential for growth. *Proc Natl Acad Sci U S A* 84: 4156-4160, 1987.

79. **Croston TL, Shepherd DL, Thapa D, Nichols CE, Lewis SE, Dabkowski ER, Jagannathan R, Baseler WA, and Hollander JM.** Evaluation of the cardiolipin biosynthetic pathway and its interactions in the diabetic heart. *Life sciences* 93: 313-322, 2013.

80. **Croston TL, Thapa D, Holden AA, Tveter KJ, Lewis SE, Shepherd DL, Nichols CE, Long DM, Olfert IM, Jagannathan R, and Hollander JM.** Functional deficiencies of subsarcolemmal mitochondria in the type 2 diabetic human heart. *Am J Physiol Heart Circ Physiol* 307: H54-65, 2014.

81. **D'Hooge J, Heimdal A, Jamal F, Kukulski T, Bijnens B, Rademakers F, Hatle L, Suetens P, and Sutherland GR.** Regional strain and strain rate measurements by cardiac ultrasound: principles, implementation and limitations. *Eur J Echocardiogr* 1: 154-170, 2000.

82. **D'Silva PR, Schilke B, Walter W, and Craig EA.** Role of Pam16's degenerate J domain in protein import across the mitochondrial inner membrane. *Proc Natl Acad Sci U S A* 102: 12419-12424, 2005.

83. **D'Souza A, Howarth FC, Yanni J, Dobryznski H, Boyett MR, Adeghate E, Bidasee KR, and Singh J.** Left ventricle structural remodelling in the prediabetic Goto-Kakizaki rat. *Exp Physiol* 96: 875-888, 2011.

84. **Dabkowski ER, Baseler WA, Williamson CL, Powell M, Razunguzwa TT, Frisbee JC, and Hollander JM.** Mitochondrial dysfunction in the type 2 diabetic heart is associated with alterations in spatially distinct mitochondrial proteomes. *Am J Physiol Heart Circ Physiol* 299: H529-540, 2010.

85. **Dabkowski ER, Williamson CL, Bukowski VC, Chapman RS, Leonard SS, Peer CJ, Callery PS, and Hollander JM.** Diabetic cardiomyopathy-associated dysfunction in spatially distinct mitochondrial subpopulations. *Am J Physiol Heart Circ Physiol* 296: H359-369, 2009.

86. **Dabkowski ER, Williamson CL, and Hollander JM.** Mitochondria-specific transgenic overexpression of phospholipid hydroperoxide glutathione peroxidase (GPx4) attenuates ischemia/reperfusion-associated cardiac dysfunction. *Free Radic Biol Med* 45: 855-865, 2008.

87. **Dahlseid JN, Lill R, Green JM, Xu X, Qiu Y, and Pierce SK.** PBP74, a new member of the mammalian 70-kDa heat shock protein family, is a mitochondrial protein. *Mol Biol Cell* 5: 1265-1275, 1994.

88. **Dai DF, Rabinovitch PS, and Ungvari Z.** Mitochondria and cardiovascular aging. *Circ Res* 110: 1109-1124, 2012.

89. **Dai Q, Escobar GP, Hakala KW, Lambert JM, Weintraub ST, and Lindsey ML.** The left ventricle proteome differentiates middle-aged and old left ventricles in mice. *J Proteome Res* 7: 756-765, 2008.

90. **Dalen H.** An ultrastructural study of the hypertrophied human papillary muscle cell with special emphasis on specific staining patterns, mitochondrial projections and association between mitochondria and SR. *Virchows Arch A Pathol Anat Histopathol* 414: 187-198, 1989.

91. **Daniels A, van Bilsen M, Janssen BJ, Brouns AE, Cleutjens JP, Roemen TH, Schaart G, van der Velden J, van der Vusse GJ, and van Nieuwenhoven FA.** Impaired cardiac functional reserve in type 2 diabetic db/db mice is associated with metabolic, but not structural, remodelling. *Acta Physiol (Oxf)* 200: 11-22, 2010.

92. **Das AK, Das JP, and Chandrasekar S.** Specific heart muscle disease in diabetes mellitus--a functional structural correlation. *International journal of cardiology* 17: 299-302, 1987.

93. **Das S, Ferlito M, Kent OA, Fox-Talbot K, Wang R, Liu D, Raghavachari N, Yang Y, Wheelan SJ, Murphy E, and Steenbergen C.** Nuclear miRNA regulates the mitochondrial genome in the heart. *Circ Res* 110: 1596-1603, 2012.

94. **Das SK, Sokhi UK, Bhutia SK, Azab B, Su ZZ, Sarkar D, and Fisher PB.** Human polynucleotide phosphorylase selectively and preferentially degrades microRNA-221 in human melanoma cells. *Proc Natl Acad Sci U S A* 107: 11948-11953, 2010.

95. **Dekker PJ and Pfanner N.** Role of mitochondrial GrpE and phosphate in the ATPase cycle of matrix Hsp70. *J Mol Biol* 270: 321-327, 1997.

96. **Delgado V, Ypenburg C, van Bommel RJ, Tops LF, Mollema SA, Marsan NA, Bleeker GB, Schalij MJ, and Bax JJ.** Assessment of left ventricular dyssynchrony by speckle tracking strain imaging comparison between longitudinal, circumferential, and radial strain in cardiac resynchronization therapy. *J Am Coll Cardiol* 51: 1944-1952, 2008.

97. **Devereux RB, Roman MJ, Paranicas M, O'Grady MJ, Lee ET, Welty TK, Fabsitz RR, Robbins D, Rhoades ER, and Howard BV.** Impact of diabetes on cardiac structure and function: the strong heart study. *Circulation* 101: 2271-2276, 2000.

98. **Di Leva G, Garofalo M, and Croce CM.** MicroRNAs in cancer. *Annu Rev Pathol* 9: 287-314, 2014.

99. **Du XL, Edelstein D, Rossetti L, Fantus IG, Goldberg H, Ziyadeh F, Wu J, and Brownlee M.** Hyperglycemia-induced mitochondrial superoxide overproduction activates the hexosamine pathway and induces plasminogen activator inhibitor-1 expression by increasing Sp1 glycosylation. *Proc Natl Acad Sci U S A* 97: 12222-12226, 2000.

100. **Du Y, Miller CM, and Kern TS.** Hyperglycemia increases mitochondrial superoxide in retina and retinal cells. *Free Radic Biol Med* 35: 1491-1499, 2003.

101. **Duan J and Karmazyn M.** Relationship between oxidative phosphorylation and adenine nucleotide translocase activity of two populations of cardiac mitochondria and mechanical recovery of ischemic hearts following reperfusion. *Can J Physiol Pharmacol* 67: 704-709, 1989.

102. **Duan JM and Karmazyn M.** Acute effects of hypoxia and phosphate on two populations of heart mitochondria. *Mol Cell Biochem* 90: 47-56, 1989.

103. **Duan JM and Karmazyn M.** Effect of verapamil on phosphate-induced changes in oxidative phosphorylation and atractyloside-sensitive adenine nucleotide translocase activity in two populations of rat heart mitochondria. *Biochem Pharmacol* 38: 3873-3878, 1989.

104. **Duan JM and Karmazyn M.** Protection of the reperfused ischemic isolated rat heart by phosphatidylcholine. *Journal of cardiovascular pharmacology* 15: 163-171, 1990.

105. **Duan JM and Karmazyn M.** Reduction of phosphate-induced dysfunction in rat heart mitochondria by carnitine. *European journal of pharmacology* 189: 163-174, 1990.

106. **Duan JM and Karmazyn M.** Relationship between Oxidative-Phosphorylation and Adenine-Nucleotide Translocase Activity of 2 Populations of Cardiac Mitochondria and Mechanical Recovery of Ischemic Hearts Following Reperfusion. *Canadian Journal of Physiology and Pharmacology* 67: 704-709, 1989.

107. **Dundas SR, Lawrie LC, Rooney PH, and Murray GI.** Mortalin is over-expressed by colorectal adenocarcinomas and correlates with poor survival. *J Pathol* 205: 74-81, 2005.

108. **Ebert MS and Sharp PA.** Roles for microRNAs in conferring robustness to biological processes. *Cell* 149: 515-524, 2012.

109. **Ehl NF, Kuhne M, Brinkert M, Muller-Brand J, and Zellweger MJ.** Diabetes reduces left ventricular ejection fraction--irrespective of presence and extent of coronary artery disease. *Eur J Endocrinol* 165: 945-951, 2011.

110. **Emr SD, Vassarotti A, Garrett J, Geller BL, Takeda M, and Douglas MG.** The amino terminus of the yeast F1-ATPase beta-subunit precursor functions as a mitochondrial import signal. *The Journal of cell biology* 102: 523-533, 1986.

111. **Entelis NS, Kolesnikova OA, Dogan S, Martin RP, and Tarassov IA.** 5 S rRNA and tRNA import into human mitochondria. Comparison of in vitro requirements. *J Biol Chem* 276: 45642-45653, 2001.

112. **Ernande L, Bergerot C, Girerd N, Thibault H, Davidsen ES, Gautier Pignon-Blanc P, Amaz C, Croisille P, De Buyzere ML, Rietzschel ER, Gillebert TC, Moulin P, Altman M, and Derumeaux G.** Longitudinal myocardial strain alteration is associated with left ventricular remodeling in asymptomatic patients with type 2 diabetes mellitus. *J Am Soc Echocardiogr* 27: 479-488, 2014.

113. **Ernande L, Rietzschel ER, Bergerot C, De Buyzere ML, Schnell F, Groisne L, Ovize M, Croisille P, Moulin P, Gillebert TC, and Derumeaux G.** Impaired myocardial radial function in asymptomatic patients with type 2 diabetes mellitus: a speckle-tracking imaging study. *J Am Soc Echocardiogr* 23: 1266-1272, 2010.

114. **Eskildsen T, Taipaleenmaki H, Stenvang J, Abdallah BM, Ditzel N, Nossent AY, Bak M, Kauppinen S, and Kassem M.** MicroRNA-138 regulates osteogenic differentiation of human stromal (mesenchymal) stem cells in vivo. *Proc Natl Acad Sci U S A* 108: 6139-6144, 2011.

115. **Fan KL, Zhang HF, Shen J, Zhang Q, and Li XL.** Circulating microRNAs levels in Chinese heart failure patients caused by dilated cardiomyopathy. *Indian Heart J* 65: 12-16, 2013.

116. **Fancher IS, Dick GM, and Hollander JM.** Diabetes mellitus reduces the function and expression of ATP-dependent K(+) channels in cardiac mitochondria. *Life sciences* 92: 664-668, 2013.

117. **Fang ZY, Leano R, and Marwick TH.** Relationship between longitudinal and radial contractility in subclinical diabetic heart disease. *Clin Sci (Lond)* 106: 53-60, 2004.

118. **Fang ZY, Prins JB, and Marwick TH.** Diabetic cardiomyopathy: evidence, mechanisms, and therapeutic implications. *Endocr Rev* 25: 543-567, 2004.

119. **Fang ZY, Yuda S, Anderson V, Short L, Case C, and Marwick TH.** Echocardiographic detection of early diabetic myocardial disease. *J Am Coll Cardiol* 41: 611-617, 2003.

120. **Fannin SW, Lesnefsky EJ, Slabe TJ, Hassan MO, and Hoppel CL.** Aging selectively decreases oxidative capacity in rat heart interfibrillar mitochondria. *Arch Biochem Biophys* 372: 399-407, 1999.

121. **Faruq O and Vecchione A.** microRNA: Diagnostic Perspective. *Front Med (Lausanne)* 2: 51, 2015.

122. **Fawcett DW and McNutt NS.** The ultrastructure of the cat myocardium. I. Ventricular papillary muscle. *The Journal of cell biology* 42: 1-45, 1969.

123. **Fazi F, Rosa A, Fatica A, Gelmetti V, De Marchis ML, Nervi C, and Bozzoni I.** A minicircuitry comprised of microRNA-223 and transcription factors NFI-A and C/EBPalpha regulates human granulopoiesis. *Cell* 123: 819-831, 2005.

124. **Feigenbaum H.** Role of M-mode technique in today's echocardiography. *J Am Soc Echocardiogr* 23: 240-257; 335-247, 2010.

125. **Ferko M, Gvozdjakova A, Kucharska J, Mujkosova J, Waczulikova I, Styk J, Ravingerova T, Ziegelhoffer-Mihalovicova B, and Ziegelhoffer A.** Functional remodeling of heart mitochondria in acute diabetes: interrelationships between damage, endogenous protection and adaptation. *Gen Physiol Biophys* 25: 397-413, 2006.

126. **Ferreira LR, Frade AF, Santos RH, Teixeira PC, Baron MA, Navarro IC, Benvenuti LA, Fiorelli AI, Bocchi EA, Stolf NA, Chevillard C, Kalil J, and Cunha-Neto E.** MicroRNAs miR-1, miR-133a, miR-133b, miR-208a and miR-208b are dysregulated in

Chronic Chagas disease Cardiomyopathy. *International journal of cardiology* 175: 409-417, 2014.

127. **Ferri KF and Kroemer G.** Organelle-specific initiation of cell death pathways. *Nat Cell Biol* 3: E255-263, 2001.

128. **Fichtlscherer S, Zeiher AM, and Dimmeler S.** Circulating microRNAs: biomarkers or mediators of cardiovascular diseases? *Arterioscler Thromb Vasc Biol* 31: 2383-2390, 2011.

129. **Filipowicz W, Bhattacharyya SN, and Sonenberg N.** Mechanisms of post-transcriptional regulation by microRNAs: are the answers in sight? *Nat Rev Genet* 9: 102-114, 2008.

130. **Flarsheim CE, Grupp IL, and Matlib MA.** Mitochondrial dysfunction accompanies diastolic dysfunction in diabetic rat heart. *Am J Physiol* 271: H192-202, 1996.

131. **Folsch H, Guiard B, Neupert W, and Stuart RA.** Internal targeting signal of the BCS1 protein: a novel mechanism of import into mitochondria. *EMBO J* 15: 479-487, 1996.

132. **Frazier AE, Dudek J, Guiard B, Voos W, Li Y, Lind M, Meisinger C, Geissler A, Sickmann A, Meyer HE, Bilanchone V, Cumsky MG, Truscott KN, Pfanner N, and Rehling P.** Pam16 has an essential role in the mitochondrial protein import motor. *Nat Struct Mol Biol* 11: 226-233, 2004.

133. **Friedman NE, Levitsky LL, Edidin DV, Vitullo DA, Lacina SJ, and Chiemmongkoltip P.** Echocardiographic evidence for impaired myocardial performance in children with type I diabetes mellitus. *Am J Med* 73: 846-850, 1982.

134. **Frustaci A, Kajstura J, Chimenti C, Jakoniuk I, Leri A, Maseri A, Nadal-Ginard B, and Anversa P.** Myocardial cell death in human diabetes. *Circ Res* 87: 1123-1132, 2000.

135. **Fujioka H, Moghaddas S, Murdock DG, Lesnefsky EJ, Tandler B, and Hoppel CL.** Decreased cytochrome c oxidase subunit VIIa in aged rat heart mitochondria: immunocytochemistry. *Anat Rec (Hoboken)* 294: 1825-1833, 2011.

136. **Galderisi M.** Diastolic dysfunction and diabetic cardiomyopathy: evaluation by Doppler echocardiography. *J Am Coll Cardiol* 48: 1548-1551, 2006.

137. **Galvao TF, Brown BH, Hecker PA, O'Connell KA, O'Shea KM, Sabbah HN, Rastogi S, Daneault C, Des Rosiers C, and Stanley WC.** High intake of saturated fat, but not polyunsaturated fat, improves survival in heart failure despite persistent mitochondrial defects. *Cardiovasc Res* 93: 24-32, 2012.

138. **Galvao TF, Khairallah RJ, Dabkowski ER, Brown BH, Hecker PA, O'Connell KA, O'Shea KM, Sabbah HN, Rastogi S, Daneault C, Des Rosiers C, and Stanley WC.** Marine n3 polyunsaturated fatty acids enhance resistance to mitochondrial permeability transition in heart failure but do not improve survival. *Am J Physiol Heart Circ Physiol* 304: H12-21, 2013.

139. **Gambill BD, Voos W, Kang PJ, Miao B, Langer T, Craig EA, and Pfanner N.** A dual role for mitochondrial heat shock protein 70 in membrane translocation of preproteins. *The Journal of cell biology* 123: 109-117, 1993.

140. **Gangaraju VK and Lin H.** MicroRNAs: key regulators of stem cells. *Nat Rev Mol Cell Biol* 10: 116-125, 2009.

141. **Ganguly PK, Thliveris JA, and Mehta A.** Evidence against the involvement of nonenzymatic glycosylation in diabetic cardiomyopathy. *Metabolism: clinical and experimental* 39: 769-773, 1990.

142. **Garcia MJ, McNamara PM, Gordon T, and Kannel WB.** Morbidity and mortality in diabetics in the Framingham population. Sixteen year follow-up study. *Diabetes* 23: 105-111, 1974.

143. **Garnier A, Fortin D, Delomenie C, Momken I, Veksler V, and Ventura-Clapier R.** Depressed mitochondrial transcription factors and oxidative capacity in rat failing cardiac and skeletal muscles. *J Physiol* 551: 491-501, 2003.

144. **Gartner F, Bomer U, Guiard B, and Pfanner N.** The sorting signal of cytochrome b2 promotes early divergence from the general mitochondrial import pathway and restricts the unfoldase activity of matrix Hsp70. *EMBO J* 14: 6043-6057, 1995.

145. **Genda A, Mizuno S, Nunoda S, Nakayama A, Igarashi Y, Sugihara N, Namura M, Takeda R, Bunko H, and Hisada K.** Clinical studies on diabetic myocardial disease using exercise testing with myocardial scintigraphy and endomyocardial biopsy. *Clin Cardiol* 9: 375-382, 1986.

146. **Geyer H, Caracciolo G, Abe H, Wilansky S, Carerj S, Gentile F, Nesser HJ, Khandheria B, Narula J, and Sengupta PP.** Assessment of myocardial mechanics using speckle tracking echocardiography: fundamentals and clinical applications. *J Am Soc Echocardiogr* 23: 351-369; quiz 453-355, 2010.

147. **Gilad S, Meiri E, Yogev Y, Benjamin S, Lebanony D, Yerushalmi N, Benjamin H, Kushnir M, Cholakh H, Melamed N, Bentwich Z, Hod M, Goren Y, and Chajut A.** Serum microRNAs are promising novel biomarkers. *PloS one* 3: e3148, 2008.

148. **Gladden JD, Zelickson BR, Wei CC, Ulasova E, Zheng J, Ahmed MI, Chen Y, Bamman M, Ballinger S, Darley-Usmar V, and Dell'Italia LJ.** Novel insights into interactions

between mitochondria and xanthine oxidase in acute cardiac volume overload. *Free Radic Biol Med* 51: 1975-1984, 2011.

149. **Glancy B, Hartnell LM, Malide D, Yu ZX, Combs CA, Connelly PS, Subramaniam S, and Balaban RS.** Mitochondrial reticulum for cellular energy distribution in muscle. *Nature* 523: 617-620, 2015.
150. **Gomez LA, Heath SH, and Hagen TM.** Acetyl-L-carnitine supplementation reverses the age-related decline in carnitine palmitoyltransferase 1 (CPT1) activity in interfibrillar mitochondria without changing the L-carnitine content in the rat heart. *Mech Ageing Dev* 133: 99-106, 2012.
151. **Gonzalez-Quesada C, Cavalera M, Biernacka A, Kong P, Lee DW, Saxena A, Frunza O, Dobaczewski M, Shinde A, and Frangogiannis NG.** Thrombospondin-1 induction in the diabetic myocardium stabilizes the cardiac matrix in addition to promoting vascular rarefaction through angiopoietin-2 upregulation. *Circ Res* 113: 1331-1344, 2013.
152. **Green K, Brand MD, and Murphy MP.** Prevention of mitochondrial oxidative damage as a therapeutic strategy in diabetes. *Diabetes* 53 Suppl 1: S110-118, 2004.
153. **Gross MD, Harris S, and Beyer RE.** The effect of streptozotocin-induced diabetes on oxidative phosphorylation and related reactions in skeletal muscle mitochondria. *Horm Metab Res* 4: 1-7, 1972.
154. **Grundy SM, Benjamin IJ, Burke GL, Chait A, Eckel RH, Howard BV, Mitch W, Smith SC, Jr., and Sowers JR.** Diabetes and cardiovascular disease: a statement for healthcare professionals from the American Heart Association. *Circulation* 100: 1134-1146, 1999.
155. **Gunter TE, Yule DI, Gunter KK, Eliseev RA, and Salter JD.** Calcium and mitochondria. *FEBS Lett* 567: 96-102, 2004.

156. **Gupta RS.** Evolution of the chaperonin families (Hsp60, Hsp10 and Tcp-1) of proteins and the origin of eukaryotic cells. *Mol Microbiol* 15: 1-11, 1995.

157. **Gustafsson R, Tata JR, Lindberg O, and Ernster L.** The relationship between the structure and activity of rat skeletal muscle mitochondria after thyroidectomy and thyroid hormone treatment. *The Journal of cell biology* 26: 555-578, 1965.

158. **Hamblin M, Friedman DB, Hill S, Caprioli RM, Smith HM, and Hill MF.** Alterations in the diabetic myocardial proteome coupled with increased myocardial oxidative stress underlies diabetic cardiomyopathy. *J Mol Cell Cardiol* 42: 884-895, 2007.

159. **Hamby RI, Zoneraich S, and Sherman L.** Diabetic cardiomyopathy. *JAMA : the journal of the American Medical Association* 229: 1749-1754, 1974.

160. **Hare JL, Brown JK, and Marwick TH.** Association of myocardial strain with left ventricular geometry and progression of hypertensive heart disease. *The American journal of cardiology* 102: 87-91, 2008.

161. **Hayashi K, Okumura K, Matsui H, Murase K, Kamiya H, Saburi Y, Numaguchi Y, Toki Y, and Hayakawa T.** Involvement of 1,2-diacylglycerol in improvement of heart function by etomoxir in diabetic rats. *Life sciences* 68: 1515-1526, 2001.

162. **Heather LC, Carr CA, Stuckey DJ, Pope S, Morten KJ, Carter EE, Edwards LM, and Clarke K.** Critical role of complex III in the early metabolic changes following myocardial infarction. *Cardiovasc Res* 85: 127-136, 2010.

163. **Heather LC, Cole MA, Tan JJ, Ambrose LJ, Pope S, Abd-Jamil AH, Carter EE, Dodd MS, Yeoh KK, Schofield CJ, and Clarke K.** Metabolic adaptation to chronic hypoxia in cardiac mitochondria. *Basic Res Cardiol* 107: 268, 2012.

164. **Helmcke F, Mahan EF, 3rd, Nanda NC, Jain SP, Soto B, Kirklin JK, and Pacifico AD.** Two-dimensional echocardiography and Doppler color flow mapping in the diagnosis and prognosis of ventricular septal rupture. *Circulation* 81: 1775-1783, 1990.

165. **Herlein JA, Fink BD, O'Malley Y, and Sivitz WI.** Superoxide and respiratory coupling in mitochondria of insulin-deficient diabetic rats. *Endocrinology* 150: 46-55, 2009.

166. **Herpin P and Barre H.** Loose-coupled subsarcolemmal mitochondria from muscle Rhomboideus in cold-acclimated piglets. *Comp Biochem Physiol B* 92: 59-65, 1989.

167. **Hiemstra JA, Liu S, Ahlman MA, Schuleri KH, Lardo AC, Baines CP, Dellsperger KC, Bluemke DA, and Emter CA.** A new twist on an old idea: a two-dimensional speckle tracking assessment of cyclosporine as a therapeutic alternative for heart failure with preserved ejection fraction. *Physiological reports* 1: e00174, 2013.

168. **Hill K, Model K, Ryan MT, Dietmeier K, Martin F, Wagner R, and Pfanner N.** Tom40 forms the hydrophilic channel of the mitochondrial import pore for preproteins [see comment]. *Nature* 395: 516-521, 1998.

169. **Hoene M, Lehmann R, Hennige AM, Pohl AK, Haring HU, Schleicher ED, and Weigert C.** Acute regulation of metabolic genes and insulin receptor substrates in the liver of mice by one single bout of treadmill exercise. *J Physiol* 587: 241-252, 2009.

170. **Hofer T, Servais S, Seo AY, Marzetti E, Hiona A, Upadhyay SJ, Wohlgemuth SE, and Leeuwenburgh C.** Bioenergetics and permeability transition pore opening in heart subsarcolemmal and interfibrillar mitochondria: effects of aging and lifelong calorie restriction. *Mech Ageing Dev* 130: 297-307, 2009.

171. **Hoit BD, Castro C, Bultron G, Knight S, and Matlib MA.** Noninvasive evaluation of cardiac dysfunction by echocardiography in streptozotocin-induced diabetic rats. *J Card Fail* 5: 324-333, 1999.

172. **Hojlund K, Wrzesinski K, Larsen PM, Fey SJ, Roepstorff P, Handberg A, Dela F, Vinten J, McCormack JG, Reynet C, and Beck-Nielsen H.** Proteome analysis reveals phosphorylation of ATP synthase beta -subunit in human skeletal muscle and proteins with potential roles in type 2 diabetes. *J Biol Chem* 278: 10436-10442, 2003.

173. **Hoke U, Thijssen J, van Bommel RJ, van Erven L, van der Velde ET, Holman ER, Schalij MJ, Bax JJ, Delgado V, and Marsan NA.** Influence of diabetes on left ventricular systolic and diastolic function and on long-term outcome after cardiac resynchronization therapy. *Diabetes Care* 36: 985-991, 2013.

174. **Hollander JM, Baseler WA, and Dabkowski ER.** Proteomic remodeling of mitochondria in heart failure. *Congestive heart failure* 17: 262-268, 2011.

175. **Hollander JM, Lin KM, Scott BT, and Dillmann WH.** Overexpression of PHGPx and HSP60/10 protects against ischemia/reoxygenation injury. *Free Radic Biol Med* 35: 742-751, 2003.

176. **Hollander JM, Thapa D, and Shepherd DL.** Physiological and structural differences in spatially distinct subpopulations of cardiac mitochondria: influence of cardiac pathologies. *Am J Physiol Heart Circ Physiol* 307: H1-14, 2014.

177. **Holloszy JO.** Biochemical adaptations in muscle. Effects of exercise on mitochondrial oxygen uptake and respiratory enzyme activity in skeletal muscle. *J Biol Chem* 242: 2278-2282, 1967.

178. **Holmuhamedov EL, Oberlin A, Short K, Terzic A, and Jahangir A.** Cardiac subsarcolemmal and interfibrillar mitochondria display distinct responsiveness to protection by diazoxide. *PloS one* 7: e44667, 2012.

179. **Hoppel CL, Moghaddas S, and Lesnefsky EJ.** Interfibrillar cardiac mitochondrial comples III defects in the aging rat heart. *Biogerontology* 3: 41-44, 2002.

180. **Hoppel CL, Tandler B, Parland W, Turkaly JS, and Albers LD.** Hamster cardiomyopathy. A defect in oxidative phosphorylation in the cardiac interfibrillar mitochondria. *J Biol Chem* 257: 1540-1548, 1982.

181. **Howarth FC, Qureshi MA, White E, and Calaghan SC.** Cardiac microtubules are more resistant to chemical depolymerisation in streptozotocin-induced diabetes in the rat. *Pflugers Arch* 444: 432-437, 2002.

182. **Hsu WM, Lee H, Juan HF, Shih YY, Wang BJ, Pan CY, Jeng YM, Chang HH, Lu MY, Lin KH, Lai HS, Chen WJ, Tsay YG, Liao YF, and Hsieh FJ.** Identification of GRP75 as an independent favorable prognostic marker of neuroblastoma by a proteomics analysis. *Clin Cancer Res* 14: 6237-6245, 2008.

183. **Huang Y, Qi Y, Du JQ, and Zhang DF.** MicroRNA-34a regulates cardiac fibrosis after myocardial infarction by targeting Smad4. *Expert Opin Ther Targets* 18: 1355-1365, 2014.

184. **Hui AB, Lenarduzzi M, Krushel T, Waldron L, Pintilie M, Shi W, Perez-Ordonez B, Jurisica I, O'Sullivan B, Waldron J, Gullane P, Cummings B, and Liu FF.** Comprehensive MicroRNA profiling for head and neck squamous cell carcinomas. *Clin Cancer Res* 16: 1129-1139, 2010.

185. **Hummel M, Bonifacio E, Schmid S, Walter M, Knopff A, and Ziegler AG.** Brief communication: early appearance of islet autoantibodies predicts childhood type 1 diabetes in offspring of diabetic parents. *Ann Intern Med* 140: 882-886, 2004.

186. **Hutu DP, Guiard B, Chacinska A, Becker D, Pfanner N, Rehling P, and van der Laan M.** Mitochondrial protein import motor: differential role of Tim44 in the recruitment of Pam17 and J-complex to the presequence translocase. *Mol Biol Cell* 19: 2642-2649, 2008.

187. **Icho T, Ikeda T, Matsumoto Y, Hanaoka F, Kaji K, and Tsuchida N.** A novel human gene that is preferentially transcribed in heart muscle. *Gene* 144: 301-306, 1994.

188. **Isenberg G, Han S, Schiefer A, and Wendt-Gallitelli MF.** Changes in mitochondrial calcium concentration during the cardiac contraction cycle. *Cardiovasc Res* 27: 1800-1809, 1993.

189. **Jagannathan R, Thapa D, Nichols CE, Shepherd DL, Stricker JC, Croston TL, Baseler WA, Lewis SE, Martinez I, and Hollander JM.** Translational Regulation of the Mitochondrial Genome Following Redistribution of Mitochondrial MicroRNA in the Diabetic Heart. *Circ Cardiovasc Genet* 8: 785-802, 2015.

190. **Jedrzejewska I, Krol W, Swiatowiec A, Wilczewska A, Grzywanowska-Laniewska I, Dluzniewski M, and Braksator W.** Left and right ventricular systolic function impairment in type 1 diabetic young adults assessed by 2D speckle tracking echocardiography. *Eur Heart J Cardiovasc Imaging* 17: 438-446, 2016.

191. **Jin J, Hulette C, Wang Y, Zhang T, Pan C, Wadhwa R, and Zhang J.** Proteomic identification of a stress protein, mortalin/mthsp70/GRP75: relevance to Parkinson disease. *Mol Cell Proteomics* 5: 1193-1204, 2006.

192. **Joffe, II, Travers KE, Perreault-Micale CL, Hampton T, Katz SE, Morgan JP, and Douglas PS.** Abnormal cardiac function in the streptozotocin-induced non-insulin-dependent diabetic rat: noninvasive assessment with doppler echocardiography and contribution of the nitric oxide pathway. *J Am Coll Cardiol* 34: 2111-2119, 1999.

193. **Jones M, Ferrans VJ, Morrow AG, and Roberts WC.** Ultrastructure of crista supraventricularis muscle in patients with congenital heart diseases associated with right ventricular outflow tract obstruction. *Circulation* 51: 39-67, 1975.

194. **Judge S, Jang YM, Smith A, Hagen T, and Leeuwenburgh C.** Age-associated increases in oxidative stress and antioxidant enzyme activities in cardiac interfibrillar mitochondria: implications for the mitochondrial theory of aging. *FASEB J* 19: 419-421, 2005.

195. **Judge S, Jang YM, Smith A, Selman C, Phillips T, Speakman JR, Hagen T, and Leeuwenburgh C.** Exercise by lifelong voluntary wheel running reduces subsarcolemmal and interfibrillar mitochondrial hydrogen peroxide production in the heart. *Am J Physiol Regul Integr Comp Physiol* 289: R1564-1572, 2005.

196. **Jullig M, Hickey AJ, Chai CC, Skea GL, Middleditch MJ, Costa S, Choong SY, Philips AR, and Cooper GJ.** Is the failing heart out of fuel or a worn engine running rich? A study of mitochondria in old spontaneously hypertensive rats. *Proteomics* 8: 2556-2572, 2008.

197. **Jullig M, Hickey AJ, Middleditch MJ, Crossman DJ, Lee SC, and Cooper GJ.** Characterization of proteomic changes in cardiac mitochondria in streptozotocin-diabetic rats using iTRAQ isobaric tags. *Proteomics Clin Appl* 1: 565-576, 2007.

198. **Kang PJ, Ostermann J, Shilling J, Neupert W, Craig EA, and Pfanner N.** Requirement for hsp70 in the mitochondrial matrix for translocation and folding of precursor proteins. *Nature* 348: 137-143, 1990.

199. **Kann O and Kovacs R.** Mitochondria and neuronal activity. *Am J Physiol Cell Physiol* 292: C641-657, 2007.

200. **Karakelides H, Asmann YW, Bigelow ML, Short KR, Dhatariya K, Coenen-Schimke J, Kahl J, Mukhopadhyay D, and Nair KS.** Effect of insulin deprivation on muscle mitochondrial ATP production and gene transcript levels in type 1 diabetic subjects. *Diabetes* 56: 2683-2689, 2007.

201. **Kasumov T, Dabkowski ER, Shekar KC, Li L, Ribeiro RF, Jr., Walsh K, Previs SF, Sadygov RG, Willard B, and Stanley WC.** Assessment of cardiac proteome dynamics with heavy water: slower protein synthesis rates in interfibrillar than subsarcolemmal mitochondria. *Am J Physiol Heart Circ Physiol* 304: H1201-1214, 2013.

202. **Katz AM.** *Physiology of the Heart*. Philadelphia: Lippincott, Williams and Wilkins, 2006.

203. **Kaul SC, Taira K, Pereira-Smith OM, and Wadhwa R.** Mortalin: present and prospective. *Exp Gerontol* 37: 1157-1164, 2002.

204. **Kavazis AN, Alvarez S, Talbert E, Lee Y, and Powers SK.** Exercise training induces a cardioprotective phenotype and alterations in cardiac subsarcolemmal and intermyofibrillar mitochondrial proteins. *American Journal of Physiology-Heart and Circulatory Physiology* 297: H144-H152, 2009.

205. **Kavazis AN, Alvarez S, Talbert E, Lee Y, and Powers SK.** Exercise training induces a cardioprotective phenotype and alterations in cardiac subsarcolemmal and intermyofibrillar mitochondrial proteins. *Am J Physiol Heart Circ Physiol* 297: H144-152, 2009.

206. **Kavazis AN, McClung JM, Hood DA, and Powers SK.** Exercise induces a cardiac mitochondrial phenotype that resists apoptotic stimuli. *Am J Physiol Heart Circ Physiol* 294: H928-935, 2008.

207. **Kelley DE, He J, Menshikova EV, and Ritov VB.** Dysfunction of mitochondria in human skeletal muscle in type 2 diabetes. *Diabetes* 51: 2944-2950, 2002.

208. **Khaidar A, Marx M, Lubec B, and Lubec G.** L-arginine reduces heart collagen accumulation in the diabetic db/db mouse. *Circulation* 90: 479-483, 1994.

209. **Kilgore JL, Musch TI, and Ross CR.** Regional distribution of HSP70 proteins after myocardial infarction. *Basic Res Cardiol* 91: 283-288, 1996.

210. **Kolesnikova OA, Entelis NS, Mireau H, Fox TD, Martin RP, and Tarassov IA.** Suppression of mutations in mitochondrial DNA by tRNAs imported from the cytoplasm. *Science* 289: 1931-1933, 2000.

211. **Kovacs A, Olah A, Lux A, Matyas C, Nemeth BT, Kellermayer D, Ruppert M, Torok M, Szabo L, Meltzer A, Assabiny A, Birtalan E, Merkely B, and Radovits T.** Strain and strain rate by speckle-tracking echocardiography correlate with pressure-volume loop-derived contractility indices in a rat model of athlete's heart. *Am J Physiol Heart Circ Physiol* 308: H743-748, 2015.

212. **Koves TR, Ussher JR, Noland RC, Slentz D, Mosedale M, Ilkayeva O, Bain J, Stevens R, Dyck JR, Newgard CB, Lopaschuk GD, and Muoio DM.** Mitochondrial overload and incomplete fatty acid oxidation contribute to skeletal muscle insulin resistance. *Cell Metab* 7: 45-56, 2008.

213. **Kozaki K, Imoto I, Mogi S, Omura K, and Inazawa J.** Exploration of tumor-suppressive microRNAs silenced by DNA hypermethylation in oral cancer. *Cancer Res* 68: 2094-2105, 2008.

214. **Krayl M, Lim JH, Martin F, Guiard B, and Voos W.** A cooperative action of the ATP-dependent import motor complex and the inner membrane potential drives mitochondrial preprotein import. *Mol Cell Biol* 27: 411-425, 2007.

215. **Kren BT, Wong PY, Sarver A, Zhang X, Zeng Y, and Steer CJ.** MicroRNAs identified in highly purified liver-derived mitochondria may play a role in apoptosis. *RNA Biol* 6: 65-72, 2009.

216. **Krimmer T, Rassow J, Kunau WH, Voos W, and Pfanner N.** Mitochondrial protein import motor: the ATPase domain of matrix Hsp70 is crucial for binding to Tim44, while the peptide binding domain and the carboxy-terminal segment play a stimulatory role. *Mol Cell Biol* 20: 5879-5887, 2000.

217. **Kubista V, Kubistova J, and Pette D.** Thyroid hormone induced changes in the enzyme activity pattern of energy-supplying metabolism of fast (white), slow (red), and heart muscle of the rat. *Eur J Biochem* 18: 553-560, 1971.

218. **Kulawiak B, Hopker J, Gebert M, Guiard B, Wiedemann N, and Gebert N.** The mitochondrial protein import machinery has multiple connections to the respiratory chain. *Biochim Biophys Acta* 1827: 612-626, 2013.

219. **Kuwabara H, Yoneda M, Hayasaki H, Nakamura T, and Mori H.** Glucose regulated proteins 78 and 75 bind to the receptor for hyaluronan mediated motility in interphase microtubules. *Biochem Biophys Res Commun* 339: 971-976, 2006.

220. **Kuznetsov AV, Troppmair J, Sucher R, Hermann M, Saks V, and Margreiter R.** Mitochondrial subpopulations and heterogeneity revealed by confocal imaging: possible physiological role? *Biochim Biophys Acta* 1757: 686-691, 2006.

221. **Lababidi ZA and Goldstein DE.** High prevalence of echocardiographic abnormalities in diabetic youths. *Diabetes Care* 6: 18-22, 1983.

222. **Lagadic-Gossmann D, Buckler KJ, Le Prigent K, and Feuvray D.** Altered Ca2+ handling in ventricular myocytes isolated from diabetic rats. *Am J Physiol* 270: H1529-1537, 1996.

223. **Laloraya S, Dekker PJ, Voos W, Craig EA, and Pfanner N.** Mitochondrial GrpE modulates the function of matrix Hsp70 in translocation and maturation of preproteins. *Mol Cell Biol* 15: 7098-7105, 1995.

224. **Lane DP.** Cancer. p53, guardian of the genome. *Nature* 358: 15-16, 1992.

225. **Lee Y, Ahn C, Han J, Choi H, Kim J, Yim J, Lee J, Provost P, Radmark O, Kim S, and Kim VN.** The nuclear RNase III Drosha initiates microRNA processing. *Nature* 425: 415-419, 2003.

226. **Lee Y, Jeon K, Lee JT, Kim S, and Kim VN.** MicroRNA maturation: stepwise processing and subcellular localization. *EMBO J* 21: 4663-4670, 2002.

227. **Lee Y, Min K, Talbert EE, Kavazis AN, Smuder AJ, Willis WT, and Powers SK.** Exercise protects cardiac mitochondria against ischemia-reperfusion injury. *Medicine and science in sports and exercise* 44: 397-405, 2012.

228. **Lemieux H, Vazquez EJ, Fujioka H, and Hoppel CL.** Decrease in mitochondrial function in rat cardiac permeabilized fibers correlates with the aging phenotype. *The journals of gerontology Series A, Biological sciences and medical sciences* 65: 1157-1164, 2010.

229. **Lesnefsky EJ, Chen Q, Moghaddas S, Hassan MO, Tandler B, and Hoppel CL.** Blockade of electron transport during ischemia protects cardiac mitochondria. *J Biol Chem* 279: 47961-47967, 2004.

230. **Lesnefsky EJ, Chen Q, Slabe TJ, Stoll MSK, Minkler PE, Hassan MO, Tandler B, and Hoppel CL.** Ischemia, rather than reperfusion, inhibits respiration through cytochrome oxidase in the isolated, perfused rabbit heart: role of cardiolipin. *American Journal of Physiology-Heart and Circulatory Physiology* 287: H258-H267, 2004.

231. **Lesnefsky EJ, Gudz TI, Migita CT, Ikeda-Saito M, Hassan MO, Turkaly PJ, and Hoppel CL.** Ischemic injury to mitochondrial electron transport in the aging heart: damage to the iron-sulfur protein subunit of electron transport complex III. *Arch Biochem Biophys* 385: 117-128, 2001.

232. **Lesnefsky EJ, Gudz TI, Moghaddas S, Migita CT, Ikeda-Saito M, Turkaly PJ, and Hoppel CL.** Aging decreases electron transport complex III activity in heart interfibrillar mitochondria by alteration of the cytochrome c binding site. *J Mol Cell Cardiol* 33: 37-47, 2001.

233. **Lesnefsky EJ, He D, Moghaddas S, and Hoppel CL.** Reversal of mitochondrial defects before ischemia protects the aged heart. *FASEB J* 20: 1543-1545, 2006.

234. **Lesnefsky EJ and Hoppel CL.** Cardiolipin as an oxidative target in cardiac mitochondria in the aged rat. *Biochim Biophys Acta* 1777: 1020-1027, 2008.

235. **Lesnefsky EJ, Minkler P, and Hoppel CL.** Enhanced modification of cardiolipin during ischemia in the aged heart. *J Mol Cell Cardiol* 46: 1008-1015, 2009.

236. **Lesnefsky EJ, Moghaddas S, Tandler B, Kerner J, and Hoppel CL.** Mitochondrial dysfunction in cardiac disease: ischemia--reperfusion, aging, and heart failure. *J Mol Cell Cardiol* 33: 1065-1089, 2001.

237. **Lesnefsky EJ, Slabe TJ, Stoll MS, Minkler PE, and Hoppel CL.** Myocardial ischemia selectively depletes cardiolipin in rabbit heart subsarcolemmal mitochondria. *Am J Physiol Heart Circ Physiol* 280: H2770-2778, 2001.

238. **Lesnefsky EJ, Tandler B, Ye J, Slabe TJ, Turkaly J, and Hoppel CL.** Myocardial ischemia decreases oxidative phosphorylation through cytochrome oxidase in subsarcolemmal mitochondria. *Am J Physiol* 273: H1544-1554, 1997.

239. **Leung DY and Ng AC.** Emerging clinical role of strain imaging in echocardiography. *Heart, lung & circulation* 19: 161-174, 2010.

240. **Li P, Jiao J, Gao G, and Prabhakar BS.** Control of mitochondrial activity by miRNAs. *J Cell Biochem* 113: 1104-1110, 2012.

241. **Li RJ, Yang J, Yang Y, Ma N, Jiang B, Sun QW, and Li YJ.** Speckle tracking echocardiography in the diagnosis of early left ventricular systolic dysfunction in type II diabetic mice. *BMC Cardiovasc Disord* 14: 141, 2014.

242. **Li X, Du N, Zhang Q, Li J, Chen X, Liu X, Hu Y, Qin W, Shen N, Xu C, Fang Z, Wei Y, Wang R, Du Z, Zhang Y, and Lu Y.** MicroRNA-30d regulates cardiomyocyte pyroptosis by directly targeting foxo3a in diabetic cardiomyopathy. *Cell Death Dis* 5, 2014.

243. **Liang HY, Cauduro S, Pellikka P, Wang J, Urheim S, Yang EH, Rihal C, Belohlavek M, Khandheria B, Miller FA, and Abraham TP.** Usefulness of two-dimensional speckle strain for evaluation of left ventricular diastolic deformation in patients with coronary artery disease. *The American journal of cardiology* 98: 1581-1586, 2006.

244. **Liang Y, Ridzon D, Wong L, and Chen C.** Characterization of microRNA expression profiles in normal human tissues. *BMC Genomics* 8: 166, 2007.

245. **Lim JH, Martin F, Guiard B, Pfanner N, and Voos W.** The mitochondrial Hsp70-dependent import system actively unfolds preproteins and shortens the lag phase of translocation. *EMBO J* 20: 941-950, 2001.

246. **Lim LP, Lau NC, Garrett-Engele P, Grimson A, Schelter JM, Castle J, Bartel DP, Linsley PS, and Johnson JM.** Microarray analysis shows that some microRNAs downregulate large numbers of target mRNAs. *Nature* 433: 769-773, 2005.

247. **Lin CL, Wang YT, Yang WZ, Hsiao YY, and Yuan HS.** Crystal structure of human polynucleotide phosphorylase: insights into its domain function in RNA binding and degradation. *Nucleic Acids Res* 40: 4146-4157, 2012.

248. **Liou GG, Chang HY, Lin CS, and Lin-Chao S.** DEAD box RhlB RNA helicase physically associates with exoribonuclease PNPase to degrade double-stranded RNA independent of the degradosome-assembling region of RNase E. *J Biol Chem* 277: 41157-41162, 2002.

249. **Liu JE, Palmieri V, Roman MJ, Bella JN, Fabsitz R, Howard BV, Welty TK, Lee ET, and Devereux RB.** The impact of diabetes on left ventricular filling pattern in normotensive and hypertensive adults: the Strong Heart Study. *J Am Coll Cardiol* 37: 1943-1949, 2001.

250. **Liu N, Bezprozvannaya S, Williams AH, Qi X, Richardson JA, Bassel-Duby R, and Olson EN.** microRNA-133a regulates cardiomyocyte proliferation and suppresses smooth muscle gene expression in the heart. *Genes Dev* 22: 3242-3254, 2008.

251. **Liu Q, D'Silva P, Walter W, Marszalek J, and Craig EA.** Regulated cycling of mitochondrial Hsp70 at the protein import channel. *Science* 300: 139-141, 2003.

252. **Liu Y, Liu W, Song XD, and Zuo J.** Effect of GRP75/mthsp70/PBP74/mortalin overexpression on intracellular ATP level, mitochondrial membrane potential and ROS

accumulation following glucose deprivation in PC12 cells. *Mol Cell Biochem* 268: 45-51, 2005.

253. **Lu J and Holmgren A.** Selenoproteins. *J Biol Chem* 284: 723-727, 2009.
254. **Lukyanenko V, Chikando A, and Lederer WJ.** Mitochondria in cardiomyocyte Ca2+ signaling. *Int J Biochem Cell Biol* 41: 1957-1971, 2009.
255. **Lund E and Dahlberg JE.** Substrate selectivity of exportin 5 and Dicer in the biogenesis of microRNAs. *Cold Spring Harb Symp Quant Biol* 71: 59-66, 2006.
256. **Lund E, Guttinger S, Calado A, Dahlberg JE, and Kutay U.** Nuclear export of microRNA precursors. *Science* 303: 95-98, 2004.
257. **Ma Z, Izumi H, Kanai M, Kabuyama Y, Ahn NG, and Fukasawa K.** Mortalin controls centrosome duplication via modulating centrosomal localization of p53. *Oncogene* 25: 5377-5390, 2006.
258. **Mandavia CH, Pulakat L, DeMarco V, and Sowers JR.** Over-nutrition and metabolic cardiomyopathy. *Metabolism: clinical and experimental* 61: 1205-1210, 2012.
259. **Manning-Krieg UC, Scherer PE, and Schatz G.** Sequential action of mitochondrial chaperones in protein import into the matrix. *EMBO J* 10: 3273-3280, 1991.
260. **Marchenko ND, Zaika A, and Moll UM.** Death signal-induced localization of p53 protein to mitochondria. A potential role in apoptotic signaling. *J Biol Chem* 275: 16202-16212, 2000.
261. **Martin J.** Molecular chaperones and mitochondrial protein folding. *J Bioenerg Biomembr* 29: 35-43, 1997.
262. **Martinelli NC, Cohen CR, Santos KG, Castro MA, Biolo A, Frick L, Silvello D, Lopes A, Schneider S, Andrades ME, Clausell N, Matte U, and Rohde LE.** An analysis of the global

expression of microRNAs in an experimental model of physiological left ventricular hypertrophy. *PloS one* 9: e93271, 2014.

263. **Matouschek A, Azem A, Ratliff K, Glick BS, Schmid K, and Schatz G.** Active unfolding of precursor proteins during mitochondrial protein import. *EMBO J* 16: 6727-6736, 1997.
264. **Mayer LR, Bonner HW, and Farrar RP.** Myocardial mitochondrial synthesis in response to various workloads. *Research communications in chemical pathology and pharmacology* 34: 157-160, 1981.
265. **Mbanya JC, Sobngwi E, Mbanya DS, and Ngu KB.** Left ventricular mass and systolic function in African diabetic patients: association with microalbuminuria. *Diabetes Metab* 27: 378-382, 2001.
266. **McCallister BD and Brown AL, Jr.** A quantitative study of myocardial mitochondria in experimental cardiac hypertrophy. *Ann N Y Acad Sci* 156: 469-479, 1969.
267. **McKean TA.** Comparison of respiration in rat, guinea pig and muskrat heart mitochondria. *Comp Biochem Physiol B* 97: 109-112, 1990.
268. **Merlin A, Voos W, Maarse AC, Meijer M, Pfanner N, and Rassow J.** The J-related segment of tim44 is essential for cell viability: a mutant Tim44 remains in the mitochondrial import site, but inefficiently recruits mtHsp70 and impairs protein translocation. *The Journal of cell biology* 145: 961-972, 1999.
269. **Mizukoshi E, Suzuki M, Misono T, Loupatov A, Munekata E, Kaul SC, Wadhwa R, and Imamura T.** Cell-cycle dependent tyrosine phosphorylation on mortalin regulates its interaction with fibroblast growth factor-1. *Biochem Biophys Res Commun* 280: 1203-1209, 2001.

270. **Mizushige K, Yao L, Noma T, Kiyomoto H, Yu Y, Hosomi N, Ohmori K, and Matsuo H.** Alteration in left ventricular diastolic filling and accumulation of myocardial collagen at insulin-resistant prediabetic stage of a type II diabetic rat model. *Circulation* 101: 899-907, 2000.

271. **Moghaddas S, Hoppel CL, and Lesnefsky EJ.** Aging defect at the QO site of complex III augments oxyradical production in rat heart interfibrillar mitochondria. *Arch Biochem Biophys* 414: 59-66, 2003.

272. **Moghaddas S, Stoll MS, Minkler PE, Salomon RG, Hoppel CL, and Lesnefsky EJ.** Preservation of cardiolipin content during aging in rat heart interfibrillar mitochondria. *J Gerontol A Biol Sci Med Sci* 57: B22-28, 2002.

273. **Mokranjac D, Bourenkov G, Hell K, Neupert W, and Groll M.** Structure and function of Tim14 and Tim16, the J and J-like components of the mitochondrial protein import motor. *EMBO J* 25: 4675-4685, 2006.

274. **Moll UM, LaQuaglia M, Benard J, and Riou G.** Wild-type p53 protein undergoes cytoplasmic sequestration in undifferentiated neuroblastomas but not in differentiated tumors. *Proc Natl Acad Sci U S A* 92: 4407-4411, 1995.

275. **Moll UM, Riou G, and Levine AJ.** Two distinct mechanisms alter p53 in breast cancer: mutation and nuclear exclusion. *Proc Natl Acad Sci U S A* 89: 7262-7266, 1992.

276. **Mondillo S, Galderisi M, Mele D, Cameli M, Lomoriello VS, Zaca V, Ballo P, D'Andrea A, Muraru D, Losi M, Agricola E, D'Errico A, Buralli S, Sciomer S, Nistri S, Badano L, and Echocardiography Study Group Of The Italian Society Of C.** Speckle-tracking echocardiography: a new technique for assessing myocardial function. *Journal of ultrasound*

in medicine : official journal of the American Institute of Ultrasound in Medicine 30: 71-83, 2011.

277. **Monette JS, Gomez LA, Moreau RF, Bemer BA, Taylor AW, and Hagen TM.** Characteristics of the rat cardiac sphingolipid pool in two mitochondrial subpopulations. *Biochem Biophys Res Commun* 398: 272-277, 2010.
278. **Moreira PI, Rolo AP, Sena C, Seica R, Oliveira CR, and Santos MS.** Insulin attenuates diabetes-related mitochondrial alterations: a comparative study. *Med Chem* 2: 299-308, 2006.
279. **Muller W.** Subsarcolemmal mitochondria and capillarization of soleus muscle fibers in young rats subjected to an endurance training. A morphometric study of semithin sections. *Cell and tissue research* 174: 367-389, 1976.
280. **Muranaka A, Yuda S, Tsuchihashi K, Hashimoto A, Nakata T, Miura T, Tsuzuki M, Wakabayashi C, Watanabe N, and Shimamoto K.** Quantitative assessment of left ventricular and left atrial functions by strain rate imaging in diabetic patients with and without hypertension. *Echocardiography* 26: 262-271, 2009.
281. **Murgia M, Giorgi C, Pinton P, and Rizzuto R.** Controlling metabolism and cell death: at the heart of mitochondrial calcium signalling. *J Mol Cell Cardiol* 46: 781-788, 2009.
282. **Naito J, Koretsune Y, Sakamoto N, Shutta R, Yoshida J, Yasuoka Y, Yoshida S, Chin W, Kusuoka H, and Inoue M.** Transmural heterogeneity of myocardial integrated backscatter in diabetic patients without overt cardiac disease. *Diabetes Res Clin Pract* 52: 11-20, 2001.
283. **Nakai H, Takeuchi M, Nishikage T, Lang RM, and Otsuji Y.** Subclinical left ventricular dysfunction in asymptomatic diabetic patients assessed by two-dimensional speckle tracking echocardiography: correlation with diabetic duration. *Eur J Echocardiogr* 10: 926-932, 2009.

284. **Narendran P, Estella E, and Fourlanos S.** Immunology of type 1 diabetes. *QJM* 98: 547-556, 2005.

285. **Neupert W and Brunner M.** The protein import motor of mitochondria. *Nat Rev Mol Cell Biol* 3: 555-565, 2002.

286. **Neupert W and Herrmann JM.** Translocation of proteins into mitochondria. *Annu Rev Biochem* 76: 723-749, 2007.

287. **Nichols CE, Shepherd DL, Knuckles TL, Thapa D, Stricker JC, Stapleton PA, Minarchick VC, Erdely A, Zeidler-Erdely PC, Alway SE, Nurkiewicz TR, and Hollander JM.** Cardiac and mitochondrial dysfunction following acute pulmonary exposure to mountaintop removal mining particulate matter. *Am J Physiol Heart Circ Physiol* 309: H2017-2030, 2015.

288. **Nielsen J, Mogensen M, Vind BF, Sahlin K, Hojlund K, Schroder HD, and Ortenblad N.** Increased subsarcolemmal lipids in type 2 diabetes: effect of training on localization of lipids, mitochondria, and glycogen in sedentary human skeletal muscle. *Am J Physiol Endocrinol Metab* 298: E706-713, 2010.

289. **Nielsen LB, Bartels ED, and Bollano E.** Overexpression of apolipoprotein B in the heart impedes cardiac triglyceride accumulation and development of cardiac dysfunction in diabetic mice. *J Biol Chem* 277: 27014-27020, 2002.

290. **Niforou KM, Anagnostopoulos AK, Vougas K, Kittas C, Gorgoulis VG, and Tsangaris GT.** The proteome profile of the human osteosarcoma U2OS cell line. *Cancer Genomics Proteomics* 5: 63-78, 2008.

291. **Nishikawa T, Edelstein D, and Brownlee M.** The missing link: a single unifying mechanism for diabetic complications. *Kidney Int Suppl* 77: S26-30, 2000.

292. **Nishikawa T, Edelstein D, Du XL, Yamagishi S, Matsumura T, Kaneda Y, Yorek MA, Beebe D, Oates PJ, Hammes HP, Giardino I, and Brownlee M.** Normalizing mitochondrial superoxide production blocks three pathways of hyperglycaemic damage. *Nature* 404: 787-790, 2000.

293. **Nishimura RA and Tajik AJ.** Evaluation of diastolic filling of left ventricle in health and disease: Doppler echocardiography is the clinician's Rosetta Stone. *J Am Coll Cardiol* 30: 8-18, 1997.

294. **Nunoda S, Genda A, Sugihara N, Nakayama A, Mizuno S, and Takeda R.** Quantitative approach to the histopathology of the biopsied right ventricular myocardium in patients with diabetes mellitus. *Heart Vessels* 1: 43-47, 1985.

295. **O'Connell RM, Rao DS, Chaudhuri AA, and Baltimore D.** Physiological and pathological roles for microRNAs in the immune system. *Nat Rev Immunol* 10: 111-122, 2010.

296. **O'Shea KM, Khairallah RJ, Sparagna GC, Xu W, Hecker PA, Robillard-Frayne I, Des Rosiers C, Kristian T, Murphy RC, Fiskum G, and Stanley WC.** Dietary omega-3 fatty acids alter cardiac mitochondrial phospholipid composition and delay Ca2+-induced permeability transition. *J Mol Cell Cardiol* 47: 819-827, 2009.

297. **Okamoto K, Brinker A, Paschen SA, Moarefi I, Hayer-Hartl M, Neupert W, and Brunner M.** The protein import motor of mitochondria: a targeted molecular ratchet driving unfolding and translocation. *EMBO J* 21: 3659-3671, 2002.

298. **Oliveira PJ, Seica R, Coxito PM, Rolo AP, Palmeira CM, Santos MS, and Moreno AJ.** Enhanced permeability transition explains the reduced calcium uptake in cardiac mitochondria from streptozotocin-induced diabetic rats. *FEBS Lett* 554: 511-514, 2003.

299. **Orrenius S, Gogvadze V, and Zhivotovsky B.** Mitochondrial oxidative stress: implications for cell death. *Annu Rev Pharmacol Toxicol* 47: 143-183, 2007.

300. **Osorio C, Sullivan PM, He DN, Mace BE, Ervin JF, Strittmatter WJ, and Alzate O.** Mortalin is regulated by APOE in hippocampus of AD patients and by human APOE in TR mice. *Neurobiol Aging* 28: 1853-1862, 2007.

301. **Otera H, Taira Y, Horie C, Suzuki Y, Suzuki H, Setoguchi K, Kato H, Oka T, and Mihara K.** A novel insertion pathway of mitochondrial outer membrane proteins with multiple transmembrane segments. *The Journal of cell biology* 179: 1355-1363, 2007.

302. **Ouellet DL, Plante I, Barat C, Tremblay MJ, and Provost P.** Emergence of a complex relationship between HIV-1 and the microRNA pathway. *Methods Mol Biol* 487: 415-433, 2009.

303. **Ozasa N, Furukawa Y, Morimoto T, Tadamura E, Kita T, and Kimura T.** Relation among left ventricular mass, insulin resistance, and hemodynamic parameters in type 2 diabetes. *Hypertens Res* 31: 425-432, 2008.

304. **Paillard M, Gomez L, Augeul L, Loufouat J, Lesnefsky EJ, and Ovize M.** Postconditioning inhibits mPTP opening independent of oxidative phosphorylation and membrane potential. *J Mol Cell Cardiol* 46: 902-909, 2009.

305. **Palmer JW, Tandler B, and Hoppel CL.** Biochemical differences between subsarcolemmal and interfibrillar mitochondria from rat cardiac muscle: effects of procedural manipulations. *Arch Biochem Biophys* 236: 691-702, 1985.

306. **Palmer JW, Tandler B, and Hoppel CL.** Biochemical properties of subsarcolemmal and interfibrillar mitochondria isolated from rat cardiac muscle. *J Biol Chem* 252: 8731-8739, 1977.

307. **Palmer JW, Tandler B, and Hoppel CL.** Heterogeneous response of subsarcolemmal heart mitochondria to calcium. *Am J Physiol* 250: H741-748, 1986.

308. **Palmieri V, Bella JN, Arnett DK, Liu JE, Oberman A, Schuck MY, Kitzman DW, Hopkins PN, Morgan D, Rao DC, and Devereux RB.** Effect of type 2 diabetes mellitus on left ventricular geometry and systolic function in hypertensive subjects: Hypertension Genetic Epidemiology Network (HyperGEN) study. *Circulation* 103: 102-107, 2001.

309. **Patti ME and Corvera S.** The role of mitochondria in the pathogenesis of type 2 diabetes. *Endocr Rev* 31: 364-395, 2010.

310. **Pauley KM, Cha S, and Chan EK.** MicroRNA in autoimmunity and autoimmune diseases. *J Autoimmun* 32: 189-194, 2009.

311. **Pearson TA, Blair SN, Daniels SR, Eckel RH, Fair JM, Fortmann SP, Franklin BA, Goldstein LB, Greenland P, Grundy SM, Hong Y, Miller NH, Lauer RM, Ockene IS, Sacco RL, Sallis JF, Jr., Smith SC, Jr., Stone NJ, and Taubert KA.** AHA Guidelines for Primary Prevention of Cardiovascular Disease and Stroke: 2002 Update: Consensus Panel Guide to Comprehensive Risk Reduction for Adult Patients Without Coronary or Other Atherosclerotic Vascular Diseases. American Heart Association Science Advisory and Coordinating Committee. *Circulation* 106: 388-391, 2002.

312. **Perk G, Tunick PA, and Kronzon I.** Non-Doppler two-dimensional strain imaging by echocardiography--from technical considerations to clinical applications. *J Am Soc Echocardiogr* 20: 234-243, 2007.

313. **Perocchi F, Jensen LJ, Gagneur J, Ahting U, von Mering C, Bork P, Prokisch H, and Steinmetz LM.** Assessing systems properties of yeast mitochondria through an interaction map of the organelle. *PLoS genetics* 2: e170, 2006.

314. **Picard M, White K, and Turnbull DM.** Mitochondrial morphology, topology, and membrane interactions in skeletal muscle: a quantitative three-dimensional electron microscopy study. *J Appl Physiol (1985)* 114: 161-171, 2013.

315. **Pilzer D and Fishelson Z.** Mortalin/GRP75 promotes release of membrane vesicles from immune attacked cells and protection from complement-mediated lysis. *Int Immunol* 17: 1239-1248, 2005.

316. **Pilzer D, Saar M, Koya K, and Fishelson Z.** Mortalin inhibitors sensitize K562 leukemia cells to complement-dependent cytotoxicity. *Int J Cancer* 126: 1428-1435, 2010.

317. **Pizzatti L, Sa LA, de Souza JM, Bisch PM, and Abdelhay E.** Altered protein profile in chronic myeloid leukemia chronic phase identified by a comparative proteomic study. *Biochim Biophys Acta* 1764: 929-942, 2006.

318. **Qian LP, Zhu SS, Cao JL, and Zeng YM.** Isoflurane preconditioning protects against ischemia-reperfusion injury partly by attenuating cytochrome c release from subsarcolemmal mitochondria in isolated rat hearts. *Acta pharmacologica Sinica* 26: 813-820, 2005.

319. **Rabol R, Boushel R, and Dela F.** Mitochondrial oxidative function and type 2 diabetes. *Applied physiology, nutrition, and metabolism = Physiologie appliquee, nutrition et metabolisme* 31: 675-683, 2006.

320. **Raev DC.** Which left ventricular function is impaired earlier in the evolution of diabetic cardiomyopathy? An echocardiographic study of young type I diabetic patients. *Diabetes Care* 17: 633-639, 1994.

321. **Rajan SK and Gokhale SM.** Cardiovascular function in patients with insulin-dependent diabetes mellitus: a study using noninvasive methods. *Ann N Y Acad Sci* 958: 425-430, 2002.

322. **Ram R, Mickelsen DM, Theodoropoulos C, and Blaxall BC.** New approaches in small animal echocardiography: imaging the sounds of silence. *Am J Physiol Heart Circ Physiol* 301: H1765-1780, 2011.

323. **Rana TM.** Illuminating the silence: understanding the structure and function of small RNAs. *Nat Rev Mol Cell Biol* 8: 23-36, 2007.

324. **Razak F and Anand SS.** Impaired mitochondrial activity in the insulin-resistant offspring of patients with type 2 diabetes. Petersen KF, Dufour S, Befroy D, Garcia R, Shulman GI. N Engl J Med 2004; 350: 664-71. *Vasc Med* 9: 223-224, 2004.

325. **Reeder GS, Currie PJ, Hagler DJ, Tajik AJ, and Seward JB.** Use of Doppler techniques (continuous-wave, pulsed-wave, and color flow imaging) in the noninvasive hemodynamic assessment of congenital heart disease. *Mayo Clin Proc* 61: 725-744, 1986.

326. **Regan TJ, Lyons MM, Ahmed SS, Levinson GE, Oldewurtel HA, Ahmad MR, and Haider B.** Evidence for cardiomyopathy in familial diabetes mellitus. *J Clin Invest* 60: 884-899, 1977.

327. **Rennison JH, McElfresh TA, Chen X, Anand VR, Hoit BD, Hoppel CL, and Chandler MP.** Prolonged exposure to high dietary lipids is not associated with lipotoxicity in heart failure. *J Mol Cell Cardiol* 46: 883-890, 2009.

328. **Rennison JH, McElfresh TA, Okere IC, Patel HV, Foster AB, Patel KK, Stoll MS, Minkler PE, Fujioka H, Hoit BD, Young ME, Hoppel CL, and Chandler MP.** Enhanced acyl-CoA dehydrogenase activity is associated with improved mitochondrial and contractile function in heart failure. *Cardiovasc Res* 79: 331-340, 2008.

329. **Rennison JH, McElfresh TA, Okere IC, Vazquez EJ, Patel HV, Foster AB, Patel KK, Chen Q, Hoit BD, Tserng KY, Hassan MO, Hoppel CL, and Chandler MP.** High-fat diet

postinfarction enhances mitochondrial function and does not exacerbate left ventricular dysfunction. *Am J Physiol Heart Circ Physiol* 292: H1498-1506, 2007.

330. **Rimessi A, Giorgi C, Pinton P, and Rizzuto R.** The versatility of mitochondrial calcium signals: from stimulation of cell metabolism to induction of cell death. *Biochim Biophys Acta* 1777: 808-816, 2008.
331. **Riva A, Tandler B, Lesnefsky EJ, Conti G, Loffredo F, Vazquez E, and Hoppel CL.** Structure of cristae in cardiac mitochondria of aged rat. *Mech Ageing Dev* 127: 917-921, 2006.
332. **Rolo AP and Palmeira CM.** Diabetes and mitochondrial function: role of hyperglycemia and oxidative stress. *Toxicol Appl Pharmacol* 212: 167-178, 2006.
333. **Rosca M, Minkler P, and Hoppel CL.** Cardiac mitochondria in heart failure: normal cardiolipin profile and increased threonine phosphorylation of complex IV. *Biochim Biophys Acta* 1807: 1373-1382, 2011.
334. **Rosca MG and Hoppel CL.** Mitochondrial dysfunction in heart failure. *Heart Fail Rev* 18: 607-622, 2013.
335. **Rosca MG, Vazquez EJ, Kerner J, Parland W, Chandler MP, Stanley W, Sabbah HN, and Hoppel CL.** Cardiac mitochondria in heart failure: decrease in respirasomes and oxidative phosphorylation. *Cardiovasc Res* 80: 30-39, 2008.
336. **Rubio MA, Rinehart JJ, Krett B, Duvezin-Caubet S, Reichert AS, Soll D, and Alfonzo JD.** Mammalian mitochondria have the innate ability to import tRNAs by a mechanism distinct from protein import. *Proc Natl Acad Sci U S A* 105: 9186-9191, 2008.

337. **Rubler S, Dlugash J, Yuceoglu YZ, Kumral T, Branwood AW, and Grishman A.** New type of cardiomyopathy associated with diabetic glomerulosclerosis. *The American journal of cardiology* 30: 595-602, 1972.

338. **Sacht G, Brigelius-Flohe R, Kiess M, Sztajer H, and Flohe L.** ATP-sensitive association of mortalin with the IL-1 receptor type I. *Biofactors* 9: 49-60, 1999.

339. **Salinas T, Duchene AM, Delage L, Nilsson S, Glaser E, Zaepfel M, and Marechal-Drouard L.** The voltage-dependent anion channel, a major component of the tRNA import machinery in plant mitochondria. *Proc Natl Acad Sci U S A* 103: 18362-18367, 2006.

340. **Sarkar D, Leszczyniecka M, Kang DC, Lebedeva IV, Valerie K, Dhar S, Pandita TK, and Fisher PB.** Down-regulation of Myc as a potential target for growth arrest induced by human polynucleotide phosphorylase (hPNPaseold-35) in human melanoma cells. *J Biol Chem* 278: 24542-24551, 2003.

341. **Sarkar D, Park ES, Emdad L, Randolph A, Valerie K, and Fisher PB.** Defining the domains of human polynucleotide phosphorylase (hPNPaseOLD-35) mediating cellular senescence. *Mol Cell Biol* 25: 7333-7343, 2005.

342. **Savel'ev AS, Novikova LA, Kovaleva IE, Luzikov VN, Neupert W, and Langer T.** ATP-dependent proteolysis in mitochondria. m-AAA protease and PIM1 protease exert overlapping substrate specificities and cooperate with the mtHsp70 system. *J Biol Chem* 273: 20596-20602, 1998.

343. **Saveliev AS, Kovaleva IE, Novikova LA, Isaeva LV, and Luzikov VN.** Can foreign proteins imported into yeast mitochondria interfere with PIM1p protease and/or chaperone function? *Arch Biochem Biophys* 363: 373-376, 1999.

344. **Schannwell CM, Schneppenheim M, Perings S, Plehn G, and Strauer BE.** Left ventricular diastolic dysfunction as an early manifestation of diabetic cardiomyopathy. *Cardiology* 98: 33-39, 2002.

345. **Scheffler IE.** *Mitochondria. Chapter 5:Mitochondrial electron transport and oxidative phosphorylation*. New York, USA: John Wiley & Sons, Inc., 1999.

346. **Schiller D.** Pam17 and Tim44 act sequentially in protein import into the mitochondrial matrix. *Int J Biochem Cell Biol* 41: 2343-2349, 2009.

347. **Schiller D, Cheng YC, Liu Q, Walter W, and Craig EA.** Residues of Tim44 involved in both association with the translocon of the inner mitochondrial membrane and regulation of mitochondrial Hsp70 tethering. *Mol Cell Biol* 28: 4424-4433, 2008.

348. **Schnedl WJ, Ferber S, Johnson JH, and Newgard CB.** STZ transport and cytotoxicity. Specific enhancement in GLUT2-expressing cells. *Diabetes* 43: 1326-1333, 1994.

349. **Schneider A.** Mitochondrial tRNA import and its consequences for mitochondrial translation. *Annu Rev Biochem* 80: 1033-1053, 2011.

350. **Schwarzer M, Schrepper A, Amorim PA, Osterholt M, and Doenst T.** Pressure overload differentially affects respiratory capacity in interfibrillar and subsarcolemmal mitochondria. *Am J Physiol Heart Circ Physiol* 304: H529-537, 2013.

351. **Sebastiani M, Giordano C, Nediani C, Travaglini C, Borchi E, Zani M, Feccia M, Mancini M, Petrozza V, Cossarizza A, Gallo P, Taylor RW, and d'Amati G.** Induction of mitochondrial biogenesis is a maladaptive mechanism in mitochondrial cardiomyopathies. *J Am Coll Cardiol* 50: 1362-1369, 2007.

352. **Semeniuk LM, Kryski AJ, and Severson DL.** Echocardiographic assessment of cardiac function in diabetic db/db and transgenic db/db-hGLUT4 mice. *Am J Physiol Heart Circ Physiol* 283: H976-982, 2002.

353. **Severson DL.** Diabetic cardiomyopathy: recent evidence from mouse models of type 1 and type 2 diabetes. *Can J Physiol Pharmacol* 82: 813-823, 2004.

354. **Shen X, Zheng S, Metreveli NS, and Epstein PN.** Protection of cardiac mitochondria by overexpression of MnSOD reduces diabetic cardiomyopathy. *Diabetes* 55: 798-805, 2006.

355. **Shen X, Zheng S, Thongboonkerd V, Xu M, Pierce WM, Jr., Klein JB, and Epstein PN.** Cardiac mitochondrial damage and biogenesis in a chronic model of type 1 diabetes. *Am J Physiol Endocrinol Metab* 287: E896-905, 2004.

356. **Shimada T, Horita K, Murakami M, and Ogura R.** Morphological studies of different mitochondrial populations in monkey myocardial cells. *Cell and tissue research* 238: 577-582, 1984.

357. **Shimizu M, Umeda K, Sugihara N, Yoshio H, Ino H, Takeda R, Okada Y, and Nakanishi I.** Collagen remodelling in myocardia of patients with diabetes. *J Clin Pathol* 46: 32-36, 1993.

358. **Shin G, Sugiyama M, Shoji T, Kagiyama A, Sato H, and Ogura R.** Detection of mitochondrial membrane damages in myocardial ischemia with ESR spin labeling technique. *J Mol Cell Cardiol* 21: 1029-1036, 1989.

359. **Siddiq T, Salisbury JR, Richardson PJ, and Preedy VR.** Synthesis of ventricular mitochondrial proteins in vivo: effect of acute ethanol toxicity. *Alcoholism, clinical and experimental research* 17: 894-899, 1993.

360. **Sillau AH, Ernst V, and Reyes N.** Oxidative capacity distribution in the cardiac myocytes of hypermetabolic rats. *Respiration physiology* 79: 279-291, 1990.

361. **Singh B, Patel HV, Ridley RG, Freeman KB, and Gupta RS.** Mitochondrial import of the human chaperonin (HSP60) protein. *Biochem Biophys Res Commun* 169: 391-396, 1990.

362. **Singh B, Soltys BJ, Wu ZC, Patel HV, Freeman KB, and Gupta RS.** Cloning and some novel characteristics of mitochondrial Hsp70 from Chinese hamster cells. *Exp Cell Res* 234: 205-216, 1997.

363. **Skulachev VP.** Mitochondrial filaments and clusters as intracellular power-transmitting cables. *Trends Biochem Sci* 26: 23-29, 2001.

364. **Skulachev VP.** Power transmission along biological membranes. *J Membr Biol* 114: 97-112, 1990.

365. **Slomovic S and Schuster G.** Stable PNPase RNAi silencing: its effect on the processing and adenylation of human mitochondrial RNA. *RNA* 14: 310-323, 2008.

366. **Smirnov A, Comte C, Mager-Heckel AM, Addis V, Krasheninnikov IA, Martin RP, Entelis N, and Tarassov I.** Mitochondrial enzyme rhodanese is essential for 5 S ribosomal RNA import into human mitochondria. *J Biol Chem* 285: 30792-30803, 2010.

367. **Smirnov A, Entelis N, Martin RP, and Tarassov I.** Biological significance of 5S rRNA import into human mitochondria: role of ribosomal protein MRP-L18. *Genes Dev* 25: 1289-1305, 2011.

368. **Solano MP and Goldberg RB.** Management of dyslipidemia in diabetes. *Cardiol Rev* 14: 125-135, 2006.

369. **Soltys BJ and Gupta RS.** Mitochondrial-matrix proteins at unexpected locations: are they exported? *Trends Biochem Sci* 24: 174-177, 1999.

370. **Sparagna GC, Chicco AJ, Murphy RC, Bristow MR, Johnson CA, Rees ML, Maxey ML, McCune SA, and Moore RL.** Loss of cardiac tetralinoleoyl cardiolipin in human and experimental heart failure. *J Lipid Res* 48: 1559-1570, 2007.

371. **Srivastava D and Olson EN.** A genetic blueprint for cardiac development. *Nature* 407: 221-226, 2000.

372. **Stallknecht B, Vinten J, Ploug T, and Galbo H.** Increased activities of mitochondrial enzymes in white adipose tissue in trained rats. *Am J Physiol* 261: E410-414, 1991.

373. **Stanley WC and Hoppel CL.** Mitochondrial dysfunction in heart failure: potential for therapeutic interventions? *Cardiovasc Res* 45: 805-806, 2000.

374. **Stewart S, Lesnefsky EJ, and Chen Q.** Reversible blockade of electron transport with amobarbital at the onset of reperfusion attenuates cardiac injury. *Transl Res* 153: 224-231, 2009.

375. **Stuckey DJ, Carr CA, Tyler DJ, Aasum E, and Clarke K.** Novel MRI method to detect altered left ventricular ejection and filling patterns in rodent models of disease. *Magn Reson Med* 60: 582-587, 2008.

376. **Suarez J, Scott B, and Dillmann WH.** Conditional increase in SERCA2a protein is able to reverse contractile dysfunction and abnormal calcium flux in established diabetic cardiomyopathy. *Am J Physiol Regul Integr Comp Physiol* 295: R1439-1445, 2008.

377. **Suh JH, Heath SH, and Hagen TM.** Two subpopulations of mitochondria in the aging rat heart display heterogenous levels of oxidative stress. *Free Radic Biol Med* 35: 1064-1072, 2003.

378. **Sunni S, Bishop SP, Kent SP, and Geer JC.** Diabetic cardiomyopathy. A morphological study of intramyocardial arteries. *Arch Pathol Lab Med* 110: 375-381, 1986.

379. **Sutherland LN, Bomhof MR, Capozzi LC, Basaraba SA, and Wright DC.** Exercise and adrenaline increase PGC-1{alpha} mRNA expression in rat adipose tissue. *J Physiol* 587: 1607-1617, 2009.

380. **Szabadkai G, Bianchi K, Varnai P, De Stefani D, Wieckowski MR, Cavagna D, Nagy AI, Balla T, and Rizzuto R.** Chaperone-mediated coupling of endoplasmic reticulum and mitochondrial Ca2+ channels. *The Journal of cell biology* 175: 901-911, 2006.

381. **Szabadkai G and Rizzuto R.** Participation of endoplasmic reticulum and mitochondrial calcium handling in apoptosis: more than just neighborhood? *FEBS Lett* 567: 111-115, 2004.

382. **Takashima M, Kuramitsu Y, Yokoyama Y, Iizuka N, Toda T, Sakaida I, Okita K, Oka M, and Nakamura K.** Proteomic profiling of heat shock protein 70 family members as biomarkers for hepatitis C virus-related hepatocellular carcinoma. *Proteomics* 3: 2487-2493, 2003.

383. **Tandler B, Dunlap M, Hoppel CL, and Hassan M.** Giant mitochondria in a cardiomyopathic heart. *Ultrastructural pathology* 26: 177-183, 2002.

384. **Tandler B and Hoppel CL.** Possible division of cardiac mitochondria. *Anat Rec* 173: 309-323, 1972.

385. **Tanne Z, Coleman R, Nahir M, Shomrat D, Finberg JP, and Youdim MB.** Ultrastructural and cytochemical changes in the heart of iron-deficient rats. *Biochem Pharmacol* 47: 1759-1766, 1994.

386. **Thapa D, Nichols CE, Lewis SE, Shepherd DL, Jagannathan R, Croston TL, Tveter KJ, Holden AA, Baseler WA, and Hollander JM.** Transgenic overexpression of mitofilin attenuates diabetes mellitus-associated cardiac and mitochondria dysfunction. *J Mol Cell Cardiol* 79: 212-223, 2015.

387. **Thompson PD, Buchner D, Pina IL, Balady GJ, Williams MA, Marcus BH, Berra K, Blair SN, Costa F, Franklin B, Fletcher GF, Gordon NF, Pate RR, Rodriguez BL, Yancey AK, Wenger NK, American Heart Association Council on Clinical Cardiology Subcommittee on Exercise R, Prevention, American Heart Association Council on Nutrition PA, and Metabolism Subcommittee on Physical A.** Exercise and physical activity in the prevention and treatment of atherosclerotic cardiovascular disease: a statement from the Council on Clinical Cardiology (Subcommittee on Exercise, Rehabilitation, and Prevention) and the Council on Nutrition, Physical Activity, and Metabolism (Subcommittee on Physical Activity). *Circulation* 107: 3109-3116, 2003.

388. **Tijsen AJ, Creemers EE, Moerland PD, de Windt LJ, van der Wal AC, Kok WE, and Pinto YM.** MiR423-5p as a circulating biomarker for heart failure. *Circ Res* 106: 1035-1039, 2010.

389. **Tominaga M.** [Diagnostic criteria for diabetes mellitus]. *Rinsho Byori* 47: 901-908, 1999.

390. **Tomita M, Mukae S, Geshi E, Umetsu K, Nakatani M, and Katagiri T.** Mitochondrial respiratory impairment in streptozotocin-induced diabetic rat heart. *Jpn Circ J* 60: 673-682, 1996.

391. **Trost SU, Belke DD, Bluhm WF, Meyer M, Swanson E, and Dillmann WH.** Overexpression of the sarcoplasmic reticulum Ca(2+)-ATPase improves myocardial contractility in diabetic cardiomyopathy. *Diabetes* 51: 1166-1171, 2002.

392. **Troyer D, Cash W, and Leipold H.** Skeletal muscle of cattle affected with progressive degenerative myeloencephalopathy. *Am J Vet Res* 54: 1084-1087, 1993.

393. **Turko IV and Murad F.** Quantitative protein profiling in heart mitochondria from diabetic rats. *J Biol Chem* 278: 35844-35849, 2003.

394. **Ulasova E, Gladden JD, Chen Y, Zheng J, Pat B, Bradley W, Powell P, Zmijewski JW, Zelickson BR, Ballinger SW, Darley-Usmar V, and Dell'italia LJ.** Loss of interstitial collagen causes structural and functional alterations of cardiomyocyte subsarcolemmal mitochondria in acute volume overload. *J Mol Cell Cardiol* 50: 147-156, 2011.

395. **Ungermann C, Guiard B, Neupert W, and Cyr DM.** The delta psi- and Hsp70/MIM44-dependent reaction cycle driving early steps of protein import into mitochondria. *EMBO J* 15: 735-744, 1996.

396. **Ursini F, Maiorino M, Brigelius-Flohe R, Aumann KD, Roveri A, Schomburg D, and Flohe L.** Diversity of glutathione peroxidases. *Methods Enzymol* 252: 38-53, 1995.

397. **Vadlamudi RV, Rodgers RL, and McNeill JH.** The effect of chronic alloxan- and streptozotocin-induced diabetes on isolated rat heart performance. *Can J Physiol Pharmacol* 60: 902-911, 1982.

398. **Van den Bergh A, Vanderper A, Vangheluwe P, Desjardins F, Nevelsteen I, Verreth W, Wuytack F, Holvoet P, Flameng W, Balligand JL, and Herijgers P.** Dyslipidaemia in type II diabetic mice does not aggravate contractile impairment but increases ventricular stiffness. *Cardiovasc Res* 77: 371-379, 2008.

399. **van der Laan M, Chacinska A, Lind M, Perschil I, Sickmann A, Meyer HE, Guiard B, Meisinger C, Pfanner N, and Rehling P.** Pam17 is required for architecture and translocation activity of the mitochondrial protein import motor. *Mol Cell Biol* 25: 7449-7458, 2005.

400. **van Dyck L, Neupert W, and Langer T.** The ATP-dependent PIM1 protease is required for the expression of intron-containing genes in mitochondria. *Genes Dev* 12: 1515-1524, 1998.

401. **van Empel VP, Bertrand AT, van der Nagel R, Kostin S, Doevendans PA, Crijns HJ, de Wit E, Sluiter W, Ackerman SL, and De Windt LJ.** Downregulation of apoptosis-inducing factor in harlequin mutant mice sensitizes the myocardium to oxidative stress-related cell death and pressure overload-induced decompensation. *Circ Res* 96: e92-e101, 2005.

402. **van Hoeven KH and Factor SM.** A comparison of the pathological spectrum of hypertensive, diabetic, and hypertensive-diabetic heart disease. *Circulation* 82: 848-855, 1990.

403. **van Rooij E.** The art of microRNA research. *Circ Res* 108: 219-234, 2011.

404. **van Rooij E, Sutherland LB, Thatcher JE, DiMaio JM, Naseem RH, Marshall WS, Hill JA, and Olson EN.** Dysregulation of microRNAs after myocardial infarction reveals a role of miR-29 in cardiac fibrosis. *Proc Natl Acad Sci U S A* 105: 13027-13032, 2008.

405. **Varga ZV, Zvara A, Farago N, Kocsis GF, Pipicz M, Gaspar R, Bencsik P, Gorbe A, Csonka C, Puskas LG, Thum T, Csont T, and Ferdinandy P.** MicroRNAs associated with ischemia-reperfusion injury and cardioprotection by ischemic pre- and postconditioning: protectomiRs. *Am J Physiol Heart Circ Physiol* 307: H216-227, 2014.

406. **Vedrenne V, Gowher A, De Lonlay P, Nitschke P, Serre V, Boddaert N, Altuzarra C, Mager-Heckel AM, Chretien F, Entelis N, Munnich A, Tarassov I, and Rotig A.** Mutation in PNPT1, which encodes a polyribonucleotide nucleotidyltransferase, impairs RNA import into mitochondria and causes respiratory-chain deficiency. *Am J Hum Genet* 91: 912-918, 2012.

407. **Vergeade A, Mulder P, Vendeville-Dehaudt C, Estour F, Fortin D, Ventura-Clapier R, Thuillez C, and Monteil C.** Mitochondrial impairment contributes to cocaine-induced

cardiac dysfunction: Prevention by the targeted antioxidant MitoQ. *Free Radic Biol Med* 49: 748-756, 2010.

408. **Vergeade A, Mulder P, Vendeville C, Ventura-Clapier R, Thuillez C, and Monteil C.** Xanthine oxidase contributes to mitochondrial ROS generation in an experimental model of cocaine-induced diastolic dysfunction. *Journal of cardiovascular pharmacology* 60: 538-543, 2012.
409. **Villanueva DS, Poirier P, Standley PR, and Broderick TL.** Prevention of ischemic heart failure by exercise in spontaneously diabetic BB Wor rats subjected to insulin withdrawal. *Metabolism: clinical and experimental* 52: 791-797, 2003.
410. **Voigt JU, Exner B, Schmiedehausen K, Huchzermeyer C, Reulbach U, Nixdorff U, Platsch G, Kuwert T, Daniel WG, and Flachskampf FA.** Strain-rate imaging during dobutamine stress echocardiography provides objective evidence of inducible ischemia. *Circulation* 107: 2120-2126, 2003.
411. **Voos W, Martin H, Krimmer T, and Pfanner N.** Mechanisms of protein translocation into mitochondria. *Biochim Biophys Acta* 1422: 235-254, 1999.
412. **Wadhwa R, Takano S, Kaur K, Deocaris CC, Pereira-Smith OM, Reddel RR, and Kaul SC.** Upregulation of mortalin/mthsp70/Grp75 contributes to human carcinogenesis. *Int J Cancer* 118: 2973-2980, 2006.
413. **Wadhwa R, Yaguchi T, Hasan MK, Taira K, and Kaul SC.** Mortalin-MPD (mevalonate pyrophosphate decarboxylase) interactions and their role in control of cellular proliferation. *Biochem Biophys Res Commun* 302: 735-742, 2003.

414. **Wagner I, van Dyck L, Savel'ev AS, Neupert W, and Langer T.** Autocatalytic processing of the ATP-dependent PIM1 protease: crucial function of a pro-region for sorting to mitochondria. *EMBO J* 16: 7317-7325, 1997.

415. **Walker MD.** Role of MicroRNA in pancreatic beta-cells: where more is less. *Diabetes* 57: 2567-2568, 2008.

416. **Wallace DC.** Mitochondrial genetics: a paradigm for aging and degenerative diseases? *Science* 256: 628-632, 1992.

417. **Wang DD, Shu Z, Lieser SA, Chen PL, and Lee WH.** Human mitochondrial SUV3 and polynucleotide phosphorylase form a 330-kDa heteropentamer to cooperatively degrade double-stranded RNA with a 3'-to-5' directionality. *J Biol Chem* 284: 20812-20821, 2009.

418. **Wang G, Chen HW, Oktay Y, Zhang J, Allen EL, Smith GM, Fan KC, Hong JS, French SW, McCaffery JM, Lightowlers RN, Morse HC, 3rd, Koehler CM, and Teitell MA.** PNPASE regulates RNA import into mitochondria. *Cell* 142: 456-467, 2010.

419. **Wang G, Shimada E, Koehler CM, and Teitell MA.** PNPASE and RNA trafficking into mitochondria. *Biochim Biophys Acta* 1819: 998-1007, 2012.

420. **Way KJ, Isshiki K, Suzuma K, Yokota T, Zvagelsky D, Schoen FJ, Sandusky GE, Pechous PA, Vlahos CJ, Wakasaki H, and King GL.** Expression of connective tissue growth factor is increased in injured myocardium associated with protein kinase C beta2 activation and diabetes. *Diabetes* 51: 2709-2718, 2002.

421. **Weinstein ES, Benson DW, Ratcliffe DJ, Maksem J, and Fry DE.** Experimental myocardial ischemia. Differential injury of mitochondrial subpopulations. *Arch Surg* 120: 332-338, 1985.

422. **Weinstein ES, Hampton WW, Yokum MD, and Fry DE.** Isovolemic hemodilution: correlations of mitochondrial and myocardial performance. *J Trauma* 26: 620-624, 1986.

423. **Weinstein ES, Spector ML, Adams EM, Yokum MD, Humphrey RW, and Fry DE.** Mitochondrial and myocardial performance. Response to ischemia and reperfusion. *Arch Surg* 121: 324-329, 1986.

424. **Weiss JS and Sumpio BE.** Review of prevalence and outcome of vascular disease in patients with diabetes mellitus. *Eur J Vasc Endovasc Surg* 31: 143-150, 2006.

425. **Westermann D, Rutschow S, Jager S, Linderer A, Anker S, Riad A, Unger T, Schultheiss HP, Pauschinger M, and Tschope C.** Contributions of inflammation and cardiac matrix metalloproteinase activity to cardiac failure in diabetic cardiomyopathy: the role of angiotensin type 1 receptor antagonism. *Diabetes* 56: 641-646, 2007.

426. **Widyantoro B, Emoto N, Nakayama K, Anggrahini DW, Adiarto S, Iwasa N, Yagi K, Miyagawa K, Rikitake Y, Suzuki T, Kisanuki YY, Yanagisawa M, and Hirata K.** Endothelial cell-derived endothelin-1 promotes cardiac fibrosis in diabetic hearts through stimulation of endothelial-to-mesenchymal transition. *Circulation* 121: 2407-2418, 2010.

427. **Wilcox AJ, Choy J, Bustamante C, and Matouschek A.** Effect of protein structure on mitochondrial import. *Proc Natl Acad Sci U S A* 102: 15435-15440, 2005.

428. **Williamson CL, Dabkowski ER, Baseler WA, Croston TL, Alway SE, and Hollander JM.** Enhanced apoptotic propensity in diabetic cardiac mitochondria: influence of subcellular spatial location. *Am J Physiol Heart Circ Physiol* 298: H633-642, 2010.

429. **Williamson CL, Dabkowski ER, Baseler WA, Croston TL, Alway SE, and Hollander JM.** Enhanced apoptotic propensity in diabetic cardiac mitochondria: influence of subcellular spatial location. *Am J Physiol Heart Circ Physiol* 298: H633-642, 2009.

430. **Williamson CL, Dabkowski ER, Dillmann WH, and Hollander JM.** Mitochondria protection from hypoxia/reoxygenation injury with mitochondria heat shock protein 70 overexpression. *Am J Physiol Heart Circ Physiol* 294: H249-256, 2008.

431. **Wold LE, Ceylan-Isik AF, and Ren J.** Oxidative stress and stress signaling: menace of diabetic cardiomyopathy. *Acta pharmacologica Sinica* 26: 908-917, 2005.

432. **Yamada S, Arrell DK, Kane GC, Nelson TJ, Perez-Terzic CM, Behfar A, Purushothaman S, Prinzen FW, Auricchio A, and Terzic A.** Mechanical dyssynchrony precedes QRS widening in ATP-sensitive K(+) channel-deficient dilated cardiomyopathy. *J Am Heart Assoc* 2: e000410, 2013.

433. **Yamagishi SI, Edelstein D, Du XL, Kaneda Y, Guzman M, and Brownlee M.** Leptin induces mitochondrial superoxide production and monocyte chemoattractant protein-1 expression in aortic endothelial cells by increasing fatty acid oxidation via protein kinase A. *J Biol Chem* 276: 25096-25100, 2001.

434. **Yano M, Terada K, and Mori M.** Mitochondrial import receptors Tom20 and Tom22 have chaperone-like activity. *J Biol Chem* 279: 10808-10813, 2004.

435. **Yared Z and Chiasson JL.** Ketoacidosis and the hyperosmolar hyperglycemic state in adult diabetic patients. Diagnosis and treatment. *Minerva Med* 94: 409-418, 2003.

436. **Ye G, Metreveli NS, Donthi RV, Xia S, Xu M, Carlson EC, and Epstein PN.** Catalase protects cardiomyocyte function in models of type 1 and type 2 diabetes. *Diabetes* 53: 1336-1343, 2004.

437. **Ye G, Metreveli NS, Ren J, and Epstein PN.** Metallothionein prevents diabetes-induced deficits in cardiomyocytes by inhibiting reactive oxygen species production. *Diabetes* 52: 777-783, 2003.

438. **Yeung ML, Bennasser Y, Myers TG, Jiang G, Benkirane M, and Jeang KT.** Changes in microRNA expression profiles in HIV-1-transfected human cells. *Retrovirology* 2: 81, 2005.

439. **Yi R, Qin Y, Macara IG, and Cullen BR.** Exportin-5 mediates the nuclear export of pre-microRNAs and short hairpin RNAs. *Genes Dev* 17: 3011-3016, 2003.

440. **Young JC, Hoogenraad NJ, and Hartl FU.** Molecular chaperones Hsp90 and Hsp70 deliver preproteins to the mitochondrial import receptor Tom70. *Cell* 112: 41-50, 2003.

441. **Zarich SW and Nesto RW.** Diabetic cardiomyopathy. *American heart journal* 118: 1000-1012, 1989.

442. **Zeng Y, Yi R, and Cullen BR.** MicroRNAs and small interfering RNAs can inhibit mRNA expression by similar mechanisms. *Proc Natl Acad Sci U S A* 100: 9779-9784, 2003.

443. **Zhang C.** MicroRNomics: a newly emerging approach for disease biology. *Physiological genomics* 33: 139-147, 2008.

Chapter 2:

Early Cardiac Dysfunction in the Type 1 Diabetic Heart Using Speckle-Tracking Based Strain Imaging

As published in J Mol Cell Cardiol. 2016 Jan;90:74-83.

Danielle L. Shepherd[a], Cody E. Nichols[a], Tara L. Croston[a], Sarah L. McLaughlin[b], Ashley B. Petrone[c], Sara E. Lewis[a], Dharendra Thapa[a], Dustin M. Long[d], Gregory M. Dick[a], and John M. Hollander[a]

[a]Department of Exercise Physiology, Center for Cardiovascular and Respiratory Sciences, School of Medicine, [b]Department of Cancer Cell Biology, School of Medicine, [c]Department of Neurobiology and Anatomy, School of Medicine, [d]Department of Biostatistics, School of Public Health, Robert C. Byrd Health Sciences Center, West Virginia University, Morgantown, WV, 26505

Running Title: Type I Diabetic Mice Echocardiographic Analysis

Corresponding Author:
John M. Hollander, Ph.D., F.A.H.A.
West Virginia University School of Medicine
Division of Exercise Physiology
Center for Cardiovascular and Respiratory Sciences
1 Medical Center Drive
Morgantown, WV 26506
Tel: (304) 293-3683
Fax: (304) 293-7105
Email: jhollander@hsc.wvu.edu

Abstract

Enhanced sensitivity in echocardiographic analyses may allow for early detection of changes in cardiac function beyond the detection limits of conventional echocardiographic analyses, particularly in a small animal model. The goal of this study was to compare conventional echocardiographic measurements and speckle-tracking based strain imaging analyses in a small animal model of type 1 diabetes mellitus. Conventional analyses revealed differences in ejection fraction, fractional shortening, cardiac output, and stroke volume in diabetic animals relative to controls at 6-weeks post-diabetic onset. In contrast, when assessing short- and long-axis speckle-tracking based strain analyses, diabetic mice showed changes in average systolic radial strain, radial strain rate, radial displacement, and radial velocity, as well as decreased circumferential and longitudinal strain rate, as early as 1-week post-diabetic onset and persisting throughout the diabetic study. Further, we performed regional analyses for the left ventricle and found that the free wall region was affected in both the short- and long-axis when assessing radial dimension parameters. These changes began 1-week post-diabetic onset and remained throughout the progression of the disease. These findings demonstrate the use of speckle-tracking based strain as an approach to elucidate cardiac dysfunction from a global perspective, identifying left ventricular cardiac regions affected during the progression of type 1 diabetes mellitus earlier than contractile changes detected by conventional echocardiographic measurements.

Keywords

Echocardiography; Cardiac Function; Diabetic Cardiomyopathy; Strain Analysis; Speckle-tracking Imaging; Diabetes Mellitus

1.1 Introduction

Cardiac complications, such as diabetic cardiomyopathy, are the leading cause of mortality among diabetic patients [1, 2]. Diabetic cardiomyopathy is characterized by contractile abnormalities in the absence of coronary disease [1, 2]. The ability to assess cardiac performance within a clinical setting has been established in patients with coronary artery disease, myocardial infarction, and ischemic cardiomyopathy by numerous studies providing strain analyses [3-5]. Importantly, however, while this type of imaging and analysis has been utilized in the clinical setting, it is somewhat limited when considering small animal models of cardiovascular diseases [6-9]. Multiple methods for imaging cardiac performance noninvasively are available, but highly sensitive *in vivo* imaging is imperative for the assessment of cardiovascular dysfunction within small animal models. Evaluation of potential therapeutic treatments for diseases in small animal models is difficult without a way to critically assess cardiac function. Some treatments may elicit subtle beneficial or detrimental changes in cardiac function, undetectable with conventional echocardiographic assessment such as ejection fraction, emphasizing the importance of methods capable of detecting minute changes. Sensitive imaging analyses would afford the ability to detect cardiotoxic side effects of potential therapeutic treatments given for systemic pathological diseases. It would also allow investigators to assess the ability of pharmacological treatments for cardiovascular pathological disease states to subtly enhance contractile function. Until recently, the speckle-tracking based strain approach has been unavailable in small animal models because of the lack of highly sensitive imaging probes and software limitations preventing rapid assessment of cardiac performance. Bauer et al. suggested echocardiographic speckle-tracking based strain analyses as a way to quickly and accurately cardiac phenotype using an experimentally-induced myocardial infarction model [6]. Compared with conventional echocardiography, these authors

found that speckle-tracking based strain analyses were capable of detecting subtle changes in myocardial deformation of the left ventricle (LV) [6]. Our current manuscript focuses on a type 1 diabetic mouse model, previously established to exhibit global cardiac dysfunction, which we hypothesize will be detected earlier using speckle-tracking based strain analyses compared to conventional analyses [10, 11]. Moreover, we aim to elucidate whether distinct regions of the LV develop dysfunction throughout the progression of type 1 diabetes mellitus, as well as decrements in global LV cardiac strain measurements, prior to the overt LV changes detected by conventional measurements. We describe the utility of using speckle-tracking based strain analyses to evaluate the progression of cardiac dysfunction in the type 1 diabetic heart. Comparing speckle-tracking based strain to conventional echocardiographic analyses, we found that analysis of strain allowed us to detect subtle changes much earlier during the progression of type 1 diabetes mellitus.

1.2 Research Design and Methods

1.2.1 Experimental Animals and Diabetes Induction

Animal experiments performed in this study conformed to the National Institutes of Health Eighth Edition *Guidelines for the Care and Use of Laboratory Animals* and were approved by the West Virginia University Care and Use Committee. Male FVB mice were obtained from The Jackson Laboratory (Bar Harbor, Maine) at 4 weeks of age, placed on a standard diet, and received free access to water. Animals were housed in the West Virginia University Health Sciences Center animal facility on a 12-hour light/dark cycle in a temperature-controlled room. Type 1 diabetes mellitus was induced in 6-week-old mice using multiple low-dose streptozotocin (STZ) (Sigma, St. Louis, MO) injections. Briefly, mice were injected intraperitoneally after a 6-hour fasting period for 5 consecutive days with STZ at a dose of 50 mg/kg body weight dissolved in sodium citrate buffer (pH 4.5) [12, 13]. Hyperglycemia was confirmed one week post-injection by measuring blood glucose (Contour Blood Glucose test strips; Bayer, Mishawaka, IN), where >250 mg/dL was considered diabetic. One STZ injected animal was removed from the study. Animals were imaged at baseline prior to STZ injection, as well as at weeks 1, 3, and 6 after confirmation of type 1 diabetes mellitus.

1.2.2 Echocardiography

For echocardiographic assessment, each mouse was anesthetized in an induction chamber with inhalant isofluorane at 2.5% in 100% oxygen. When fully anesthetized, the mouse was transferred to dorsal recumbency, placed on a heated imaging platform, and maintained at 1% isofluorane for the duration of the experiment [14]. Electrode gel was applied to the limb leads allowing for an electrocardiogram and the respiration rate to be recorded during ultrasound

imaging. A rectal probe was used to monitor the temperature of the mouse. Ultrasound images were acquired using a 32-55 MHz linear array transducer on the Vevo2100 Imaging System (Visual Sonics, Toronto, Canada). Placing the transducer to the left of the sternum allowed us to obtain images of the aortic outflow tract, the apex of the heart, and LV along its longest axis (i.e., long-axis B-mode images). Once all long-axis B-mode images were attained, the transducer was rotated 90 degrees to acquire short-axis B-mode images at the mid-papillary muscle level. Additionally, M-mode images were taken by placing a gate through the center of the short-axis B-mode images to obtain M-mode recordings of internal parameters of the myocardium. All images were acquired using the highest possible frame rate (233-401 frames/second) depending on the imaging axis to get the best possible image resolution for speckle-tracking based strain analyses. One trained individual in the West Virginia University Animal Models and Imaging Facility acquired all images.

1.2.3 Conventional Echocardiographic M-mode and Doppler Imaging

Conventional echocardiographic assessment was completed on grayscale M-mode parasternal short-axis images at the mid-papillary level of the LV (Figure 2.1A). Measurements obtained from LV M-mode images included end-diastolic and end-systolic diameters and volumes, anterior and posterior wall thickness at both systole and diastole, fractional shortening, ejection fraction, stroke volume, and cardiac output. LV volumes were automatically calculated by the Vevo2100 system when using M-mode imaging (Visual Sonics, Toronto, Canada). LV volume in systole (Volume;systole) was calculated by the program using the equation (7.0 / (2.4 + LVID;s)) x LVID;s^3), while LV volume in diastole (Volume;diastole) was calculated using the equation (7.0 / (2.4 + LVID;d)) x LVID;d^3) (Visual Sonics, Toronto, Canada). To calculate stroke volume for

M-mode images, systolic volume was subtracted from diastolic volume (Visual Sonics, Toronto, Canada). All M-mode image measurements were calculated over three consecutive cardiac cycles and then averaged. As a measure of diastolic function, LV filling was assessed using Doppler echocardiography and measuring the E/A ratio, deceleration time, and Isovolumetric Relaxation Time (IVRT) over three cardiac cycles. The E/A ratio is a ratio of ventricular filling velocities of the early (E) peak to the late (A) peak of transmitral blood flow. Deceleration time of the E peak refers to the deceleration of blood flow through the mitral valve, while IVRT is the time from the closure of the aortic valve to the onset of mitral flow.

To assess reliability of the conventional measurements, each observer scored the parameter three times, and the average of the three observations was used for analysis on a subset of our study population (n=4). To determine intraobserver variability, the average coefficient of variance ((standard deviation/ mean) x 100) was calculated for the observer for each measurement. The average coefficient of variance values for ejection fraction and E/A ratio were 3.4% and 1.3%, respectively. To determine both interobserver and test-retest intraobserver reliability, intra-class correlation (ICC) coefficients were calculated using a two-way mixed model with absolute agreement and reported in Table S2.1. Intraobserver test-retest reliability was calculated using values obtained at two separate time-points by a single rater. All ICC values for conventional measurements were greater than 0.8, indicating a high degree of both interobserver and intraobserver test-retest reliability [15]. When performing interobserver reproducibility measurements, the second observer selected and used the most appropriate image and frames to complete the strain measurements. All reported analyses in the manuscript used the Vevo2100 Imaging analysis software and included measurements from all animals for M-mode analyses (Visual Sonics, Toronto, Canada).

1.2.4 Speckle-tracking-based Strain Imaging Analyses

Based on concepts previously described, strain is defined as the change in the length of a segment divided by the original length of the segment and the strain rate as the rate at which this deformation occurs during a cardiac cycle [16-18]. Using the B-mode videos acquired from the parasternal short- and long-axes (Figure 2.1A), strain and strain rate were calculated for the radial, longitudinal, and circumferential dimensions with the Visual Sonics VevoStrain software (Toronto, Canada) using a speckle-tracking algorithm. Velocity and displacement were also calculated in both the long- and short-axes. Values generated by strain analyses were positive or negative depending on the assessed measurement. A positive value for strain indicates fiber lengthening or thickening, such as in the radial dimension, while a negative value illustrates fiber shortening, in the circumferential or longitudinal dimensions [16, 19]. Briefly, B-mode video loops were chosen based upon image quality and the ability to visualize both the endocardial and epicardial wall borders, with limited interference by artifacts such as the sternum or lungs. Borders of the endocardium and epicardium were traced and checked throughout three cardiac cycles to ensure tracking was sufficient. Both the endocardial and epicardial borders were tracked through the image in a frame-by-frame manner by the software for measurements of strain, strain rate, velocity, and displacement. Strain analyses were performed, giving curvilinear data as output for both global and segmental values. Average peak global strain values were obtained from six independent anatomical segments of the LV. Global dyssynchrony for radial velocity, strain and strain rate were measured by using the standard deviation of time to peak strain, corrected for the RR interval [20, 21]. Further, segmental analyses were performed on short-axis images with the LV being split into the following regions: anterior free (AF), lateral (L), posterior (P), inferior free

(IF), posterior septum (PS), and anterior septum (AS) (Figure 2.1B). Regional analyses were also performed on long-axis images with the LV divided into the following segments: anterior base (AB), anterior mid (AM), anterior apex (AA), posterior apex (PA), posterior mid (PM), and posterior base (PB) (Figure 2.1C). Because type 1 diabetes mellitus presents as a global dysfunction of LV parameters, segments were grouped into septal (AS and PS for short-axis; AA, AM, and AB for long-axis) and free wall (AF, L, P, and IF for short-axis; PA, PM, and PB for long-axis) regions for short- and long-axis in order to assess whether a particular section of the LV is affected during the progression of the disease. All individual regions were utilized during analyses and grouped as previously stated.

High intraobserver reproducibility was demonstrated on a subset of animals (n = 4) using speckle-tracking based strain measurements with a coefficient of variance equal to 6.1%, respectively. To determine both interobserver and test-retest intraobserver reliability, ICC coefficients were calculated using a two-way mixed model with absolute agreement and reported in Table S2.1. Interobserver and test-retest ICC values for strain were greater than 0.8, indicating a high degree of both interobserver and test-retest intraobserver reliability [15]. When performing interobserver reproducibility measurements, the second observer selected and used the most appropriate image and frames to complete the strain measurements. All reported analyses in the manuscript used the Vevo2100 Imaging analysis software (Visual Sonics, Toronto, Canada). One control and diabetic short-axis, along with one control long-axis image were excluded from strain measurements. In the short-axis, only still image pictures were collected and no movie loops; therefore, strain analyses could not be performed. For the excluded long-axis image, landmarks, such as the left atria and outflow track were not present; therefore, the movie loop was not used for strain analysis.

1.2.5 Statistical Analysis

All data are presented as mean ± standard error of the mean (SEM). Comparisons between control and diabetic animals were made within each given week to see whether changes were noted between the two groups using different types of echocardiographic analyses. Data were analyzed using a two-tailed Student's t test to directly compare the type 1 diabetic animals to the controls at a given time. $P < 0.05$ was considered statistically significant. Statistical analyses were performed using GraphPad Prism version 5.00 (GraphPad Software, San Diego, California).

1.3 Results

1.3.1 Conventional Echocardiographic Imaging and Analysis

To assess LV functional changes over time during type 1 diabetes, mice were imaged prior to diabetes induction (baseline) and at weeks 1, 3 and 6 after onset. Table 2.1 represents data collected from M-mode images at baseline and weeks 1, 3, and 6. M-mode images showed decreases in anterior and posterior wall thickness at diastole in diabetic animals as compared to controls 1-week post-diabetic onset (Table 2.1). At 3-weeks post-diabetic onset, decreased anterior and posterior wall thickness at diastole, as well as a decreased heart rate were noted in type 1 diabetic animals (Table 2.1). Six weeks after diabetes induction, overt LV dysfunction was present in the type 1 diabetic animals. Global function, assessed by conventional measures of echocardiography using M-mode images, showed decreased LV function in the type 1 diabetic animals at 6-weeks as compared to controls. Type 1 diabetes induced decreases in stroke volume, cardiac output, ejection fraction, and fractional shortening (Table 2.1). Further, type 1 diabetes caused decreases in diastolic diameter and volume, along with decreases in anterior and posterior wall thickness, indicative of myocardial remodeling (Table 2.1).

Representative Doppler images from control and type 1 diabetic animals illustrate a decreased E/A ratio in type 1 diabetic animals as compared to their controls at 6-weeks post-diabetic onset, with no changes occurring before this time point (Figure 2.2A-B). The decreased E/A ratio is due to the significantly decreased E wave at 6-weeks post-diabetic onset in the type 1 diabetic animals (Figure 2.2C). A decrease in the E wave, or early diastolic filling, could be a reflection of hemodynamic load, heart rate and/or cardiac output given the known dependence of the E/A ratio on these factors [22, 23]. The decreased E wave during type 1 diabetes is potentially due to a decreased ability for LV relaxation, while no changes were seen in the A wave (Figure

2.2D). E wave deceleration, a measure of how blood flow velocity declines during early diastole, was unchanged between control and type 1 diabetic animals throughout the course of our study (Figure 2.2E). IVRT, a measure of the time from the closure of the aortic valve to the onset of mitral flow, is increased in the type 1 diabetic animals 6-weeks post-diabetic onset (Figure 2.2F). Together, the echocardiography data indicate deficient systolic and diastolic LV function during type 1 diabetes mellitus predominantly being observed through conventional measures at 6-weeks post-diabetic onset.

1.3.2 Measures of Global Myocardial Performance During a Type I Diabetic Insult

Using the VevoStrain software to complete functional analyses for the LV, the complex pattern of deformation can be examined in the longitudinal, radial, and circumferential dimensions in both systole and diastole. Speckle-tracking based strain analyses trace the endocardium and epicardium frame-to-frame during the cine loop, providing assessment of the deformation of the tissue by using measurements of strain and strain rate in each of these dimensions. Strain refers to the assessment of myocardial deformation, while strain rate measures the tissue velocity of deformation [16]. Global LV functional analyses, as well as the evaluation of six anatomic segments of the LV providing information on regional function, produce curvilinear data for strain analysis (Figure S2.1). Interestingly, speckle-tracking based strain analyses revealed differences as early as 1-week post-diabetic onset and persisting throughout the remainder of the study. Decreases in short-axis average systolic radial strain, strain rate, velocity, and displacement were noted in the type 1 diabetic animals at week 1 when compared to control animals, along with significantly decreased circumferential strain (Table 2.2). Three weeks post-diabetic onset, average systolic circumferential strain rate, radial strain, strain rate, velocity, and displacement

were all significantly decreased in the diabetic animals as compared to controls (Table 2.2). Finally, at 6-weeks post-diabetic onset, decrements in average systolic circumferential strain rate, radial strain, strain rate, and velocity were noted in the type 1 diabetic animals when compared to controls (Table 2.2). No changes were noted in circumferential rate or displacement (Table 2.2). When assessing global diastolic strain measurements in the short-axis, radial strain was significantly decreased in diabetic animals when compared to controls starting at week 1 and persisting throughout the study (Table 2.2). Further, radial strain rate was decreased at weeks 3 and 6 post-diabetic onset (Table 2.2).

In the long-axis images, diabetic animals had decreased average systolic radial strain, strain rate, and velocity at weeks 1, 3 and 6 as compared to control within a given week (Table 2.3). Radial displacement was decreased at 1-week post-diabetic onset; however, this change was not observed throughout the rest of the study (Table 2.3). Further, longitudinal strain rate was decreased at weeks 3 and 6 post-diabetic onset; however, other longitudinal parameters such as strain, velocity, and displacement were unaltered during the progression of type 1 diabetes (Table 2.3). Average diastolic strain parameters were unchanged between control and diabetic animals in the long-axis (Table 2.3).

Systolic radial velocity, strain, and strain rate parameters, which were globally changing due to type 1 diabetes mellitus, were also analyzed for dyssynchrony in both the short- and long-axes. Type 1 diabetes mellitus was not associated with significant increases in global dyssynchrony for radial velocity, strain, and strain rate at any time point throughout the course of the study (Table S2.2).

Notably, it was discerned that changes in the short-axis, as seen by average myocardial systolic radial strain, strain rate, velocity, and displacement, as well as changes in circumferential

strain rate occurred earlier than changes in LV function for conventional echocardiographic measurements. Further, radial strain and strain rate were also significantly decreased during diastole as early as 1-week post-diabetic onset. Similarly, decrements in average myocardial systolic radial measurements in the long-axis, along with longitudinal strain rate, were noted earlier during the progression of type 1 diabetes mellitus than measurements obtained by conventional echocardiography. This data provides evidence that global speckle-tracking-based strain analyses are capable of detecting early, subtle changes in LV function in the type 1 diabetic STZ mouse model in both systole and diastole.

1.3.3 Measures of Segmental Myocardial Performance During Type I Diabetes

Speckle-tracking based strain allows for the assessment of regional cardiac function by separating the LV into six distinct segments in both the short- and long-axes (Figure S2.1). Regional analyses were performed on short-axis images with the LV divided into the free wall (anterior free, lateral, posterior, and inferior free) and septal wall (posterior septum and anterior septum) regions (Figure 2.1B). Global strain analyses showed decreases in both short- and long-axis radial dimensions by deficient radial velocity, radial strain, and radial strain rate in the type 1 diabetic animals (Tables 2.2 and 2.3). When assessing these parameters using a regional approach in the short-axis, we found that radial velocity in the free wall and septal wall regions was decreased in the type 1 diabetic animals at weeks 1 and 3 (Figure 2.3A-B). Interestingly, only the free wall region of the LV was affected in the type 1 diabetic animals when looking at radial strain beginning at week 1 and remaining throughout the progression of type 1 diabetes, with no changes in the septal wall (Figure 2.3C-D). Finally, radial strain rate was also affected in both the free wall and septal wall regions of the LV (Figure 2.3E-F). Decreases in radial strain rate in the free wall

occurred at week 1 and persisted throughout the study, while the septal wall was affected at weeks 3 and 6 post-diabetic onset (Figure 2.3E-F).

We also performed regional assessment on radial velocity, radial strain, and radial strain rate in the long-axis by separating the LV into free wall (posterior apex, posterior mid, and posterior base) and septal wall (anterior apex, anterior mid, and anterior base) regions (Figure 2.1C). Type 1 diabetic animals showed a decreased radial velocity in the free wall region of LV beginning at week 1 and persisting throughout the study, with only week 3 being affected in the septal wall region (Figure 2.4A-B). Radial strain was decreased in the free wall region of the type 1 diabetic animals at weeks 1, 3, and 6 post-diabetic onset, with no decrements in the septal wall region (Figure 2.4C-D). Finally, radial strain rate was decreased in the type 1 diabetic animals in the free wall region of the LV beginning 1-week post-diabetic onset and continuing throughout the progression of diabetes, while the septal wall region was only affected at week 3 (Figure 2.4E-F). Overall, regional assessment of the LV in the radial dimension showed that the free wall region in the short- and long-axis was predominantly affected during the progression of type 1 diabetes mellitus.

1.4 Discussion

This is the first application of echocardiographic speckle-tracking based strain analyses for cardiac phenotyping during the progression of type 1 diabetes in a mouse model. Here we describe the utility of using noninvasive echocardiographic analyses, such as speckle-tracking based strain, for early detection of LV dysfunction during the progression of type 1 diabetes mellitus.

The goal of this study was to provide a comparison between conventional echocardiographic measurements and speckle-tracking based strain analyses to see if changes in cardiac function would be detected earlier by means of more advanced methods. Further, we aimed to see if a particular region of the LV was predominantly affected during the progression of type 1 diabetes mellitus. The principal finding of this study was that speckle-tracking based strain analyses provided a sensitive approach to detect early global changes in LV function, as compared to changes identified using conventional echocardiography during the development of diabetes mellitus in a type 1 diabetic mouse model. As early as 1-week post-diabetic onset, decreases in average systolic radial strain, radial strain rate, radial velocity, and radial displacement, along with circumferential and longitudinal strain rate at week 3 post-diabetic onset, were observed in short- and long-axis speckle-tracking based strain analyses and persisted throughout the study. Strain and strain rate were both found to be decreased in the radial axis at 1-week post-diabetic onset, indicating that myocardial deformation and the velocity at which that tissue deforms is impaired in this axis during the early stages of type 1 diabetes mellitus. Decreases in these systolic radial measurements are indicative of LV dysfunction allowing for subtle detection of early dysfunction occurring during type 1 diabetes mellitus [24]. Further, we found that the free wall region was predominantly affected in the radial dimension in both the short- and long-axis during type 1 diabetes mellitus. These findings highlight that the LV free wall could potentially be more affected

than the septal wall during the progression of type 1 diabetes mellitus. These outcomes confirm other findings indicating that early changes are detected by speckle-tracking-based strain analysis prior to changes in conventional measurements giving investigators an approach to evaluate cardiac function in a small animal model with a cardiac pathology [6-9]. Additionally, speckle-tracking based strain analyses allow the ability to detect particular regions of the LV that may not be functioning properly. Finally, it provides investigators with the opportunity to assess the therapeutic benefit or detriment of treatment strategies on cardiac contractile function.

It is imperative in a clinical setting to be able to detect subtle changes in LV function and global heart function in order to intervene before the onset of a cardiac insult. Currently, clinical studies have shown that early detection of subtle changes in strain measurements were associated with the future development of cardiovascular disease, while conventional measures of cardiac structure and function were unaltered [25-32]. Though ejection fraction is typically the most prominent clinical measure for systolic dysfunction in the diabetic patient, strain and strain rate imaging have been shown to increase subclinical diabetic cardiomyopathy detection in patients [31, 33, 34]. Consequently, it is imperative that researchers using small animal models are able to detect these subtle and early changes in cardiac function in order to assess different cardiac therapies used to prevent cardiac dysfunction in the disease state. While strain measures have been utilized in clinical studies, experimental studies on small animal models were more complicated to perform due to fast heart rates, imaging equipment, and analysis software. However, advances such as high frame rates allowing for angle-independent measurements have permitted the adoption of strain analyses into an experimental setting, advancing the assessment of cardiac abnormalities and therapeutic approaches in small animal models of cardiovascular disease [27, 35, 36].

Because previous studies indicate that myocardial ischemia is associated with a dyssynchronous profile that undermines appropriate contractile function [9, 20, 21, 37], we assessed global dyssynchrony in a temporal fashion following type 1 diabetes mellitus induction. Our data indicated that the progression of the type 1 diabetic pathology through the initial six weeks was not associated with an increase in dyssynchrony. Our data are in contrast to others who have shown in models of myocardial infarction, impairments in longitudinal and radial strain and strain rate parameters along with a concomitant increase in dyssynchrony [9, 20, 21, 37]. It is not entirely clear why the differences in findings occurred, though it may be a function of the different pathological models being studied. Specifically, these previous studies examined a focal cardiac region of tissue damage resulting from infarct, whereas our study in the diabetic heart reflect global dysfunction at an earlier pathological time point which may not be sufficient to induce an increase in dyssynchrony. Regardless, our current data suggests that dyssynchrony does not play a prominent role in cardiac pump function deficits during the initial progression of type 1 diabetes mellitus.

Speckle-tracking based strain allows for the separation of the LV into six distinct segments, permitting us to investigate regional cardiac dysfunction during the progression of type 1 diabetes mellitus. In this study, we found that the region predominantly affected in the radial dimension was the free wall in the short- and long-axis during the progression of type 1 diabetes mellitus. These findings highlight that the free wall of the LV could potentially be more affected than the septal wall during type 1 diabetes mellitus. This finding corroborates the potential use for regional assessment of the LV in myocardial function during type 1 diabetes, particularly via changes in the average systolic and diastolic radial measurements.

Our findings support the current literature stating that speckle-tracking based strain analysis possesses the potential for the sensitive evaluation of global and regional cardiac function [6, 16, 38, 39]. Studies of patients with acute heart failure and LV dysfunction concluded that strain powerfully predicted adverse cardiac events better than other conventional parameters, such as ejection fraction [40, 41]. In a swine model of heart failure with preserved ejection fraction, Hiemstra et al. showed decreases in systolic apical rotation rate, changes in strain measurements from longitudinal, radial, and circumferential axes, as well as strain rate changes all prior to the onset of increases in LV end diastolic pressure [39]. These results are in agreement with our findings, as this group found that speckle-tracking was capable of detecting early changes prior to the onset of overt LV impairment [39]. Bauer et al. found similar results in their assessment of a small animal model of myocardial infarction with the addition of ACE inhibitors [6]. Their principal findings concluded that speckle-tracking based strain was more sensitive than conventional echocardiographic measurements when assessing both the infarct region and the remote region, while subtle improvements were found in LV function in response to treatment with ACE inhibitors [6]. Additionally, in a recent study by the same group, they determined whether speckle-tracking based strain would provide insight regarding early changes in cardiac performance, prior to LV dysfunction seen by conventional echocardiography, during early stages of compensatory hypertrophic cardiac remodeling due to pressure overload [7]. These authors found regional myocardial dysfunction in a mouse model of pressure overload further illustrating the utility of using speckle-tracking based strain analyses, as well as regional assessment, in the characterization of early cardiac dysfunction that is not detectable by conventional echocardiographic measurements [7].

While standard echocardiographic techniques are useful in the evaluation of cardiac structure and function, they are often insensitive to subtle changes that occur early during the progression of cardiovascular disease preceding overt dysfunction. Previously, our laboratory has reported changes in stroke volume, ejection fraction, fractional shortening and cardiac output due to type 1 diabetes mellitus; however, this current study offers a unique approach into pointing out a particular locale of dysfunction within the LV of the type 1 diabetic heart by implementing speckle-tracking based strain analysis [10, 11]. This study expounds upon current echocardiographic research providing evidence for using speckle-tracking based strain as an echocardiographic analysis software in small animal models of cardiovascular diseases [6, 7, 42-44]. It has been shown that speckle-tracking based strain analyses are highly sensitive compared to conventional measurements in small animal models, suggesting that these analyses could be used for the assessment of different therapeutic treatments for cardiovascular diseases or predisposing risk factors, including diabetes mellitus.

It is widely accepted that conventional measures of echocardiography are used to assess both cardiac structure, as well as function. However, the limitation for these types of measurements lies in the lack of sensitivity, which is overcome by the use of speckle-tracking based strain analyses. Although, limitations to this study exist even when using speckle-tracking based strain analyses and should be taken into consideration. The use of isofluorane, or any other anesthetic, is common in performing echocardiography on animals; however, it should be noted that anesthetics have the potential to alter the measurements recorded, though multiple studies have shown that even under anesthesia, echocardiographic measurements are reliable, particularly using speckle-tracking based strain analyses [45-47]. Although this is a concern because of the risk of causing a decrease in heart rate during image acquisition, heart rates recorded for the duration of this study

remained near a physiological level. Literature notes that speckle tracking is heavily dependent upon 2D image quality, high frame rates, and angle dependency [17, 48]. To prevent variation, a single trained imaging technician acquired all images at the highest possible frame rate and avoided artifacts including the lungs and sternum. Other limitations such as out of plane motion and unknown software algorithms, known as filtering algorithms which calculate strain and strain rate values, are also important to keep in mind [16]. During a cardiac cycle the heart will move, sometimes causing speckles to move out of frame, making it difficult to surmise how the accuracy of speckle-tracking based strain analyses are affected [16]. Further, it is difficult to compare filtering algorithms between different software vendors and between the analyses, inherently posing another limitation [16]. Variability in the assessment of strain has also been addressed within the literature [49, 50]. As in the study performed by Hiemstra et al., we observed variation between our time points, which could potentially be due to the methodology used, but also because of animal maturation and normal physiological growth over the duration of the study [39]. Indeed, we previously reported differences in heart weights, 6 weeks following STZ induction, which may be a function of animal growth and pathology development that may have occurred similarly in the current study [10, 51]. With that being said, it is important to note that the goal of the present study was to determine whether speckle-tracking based strain analyses could identify cardiac dysfunction at a given time point, earlier than conventional measures, as opposed to across time points, limiting concern for serial assessment. Further, it is crucial to do a longer period of study to see if parameters of stress/strain are transient and/or worsen during type 1 diabetes at a longer duration. As others have previously shown, strain is dependent on a number of factors, such as complexity of myocardial fiber orientation, which could potentially include the evaluation of different fiber layers at a diverse number of levels leading to variation in results [6, 39, 52].

Because of this, we decided that the question of interest was to find out if certain echocardiographic parameters were capable of detecting changes in LV function earlier during the progression of type 1 diabetes mellitus. Therefore, we chose to not include the serial change, but instead evaluate different echocardiographic parameters at each time point individually.

One question raised by the current study regards what mechanisms contribute to the observed changes in cardiac strain parameters? Of note are our findings of decreased radial strain during diastole which in combination with reduced early diastolic filling (decreased E), decreased end diastolic volume, and increased IVRT, suggest that impaired filling may be involved in the decreased stroke volume observed and ultimately, reduced cardiac output following diabetic insult. Since reduced E and IVRT typically reflect early filling, impaired energetics leading to increased time to reuptake calcium or trouble breaking cross-bridges during early diastole may be mechanistic contributors to changes in strain parameters. Because these processes are ATP-dependent, any bioenergetic compromise in the mitochondrion's ability to provide an adequate supply of ATP could have an effect on strain dynamics. Indeed, we have previously reported compromised mitochondrial function and ATP-generating capacity during type 1 diabetes mellitus [10, 51, 53]. Taken together, mitochondrial dysfunction in the face of type 1 diabetes mellitus may provide a mechanistic link between altered bioenergetic function and changes cardiac strain dynamics.

During normal LV function the heart deforms to show myocardial thickening and thinning via the radial axis, as well as shortening and lengthening in the longitudinal and circumferential axes, depending on whether the heart is in systole or diastole [16]. Alterations in the deformation of the myocardium, revealed by strain measurements, are the earliest noninvasive indicators for the development of cardiac dysfunction [54, 55]. We demonstrate the advantage of using speckle-

tracking based strain analyses to detect changes in LV function earlier than conventional echocardiographic measurements. While the correlation between contractile complications and diabetic cardiomyopathy have been well established, the results presented in this study reveal how early detection via strain measurements has the potential to play a critical role in evaluating therapeutic treatments for contractile dysfunction in the diabetic heart.

Acknowledgements and Grants

The authors would like to thank the WVU Animal Models and Imaging Facility for all of the echocardiographic images, which has been supported by the Mary Babb Randolph Cancer Center and NIH grants P20 RR016440, P30 GM103488 and S10 RR026378. This work was supported by NIH DP2DK083095 (J.M.H.), NIH T32HL090610 (T.L.C., D.L.S.), AHA-14PRE19890020 (D.L.S.), AHA-13PRE16850066 (C.E.N.), DGE-1144676 (C.E.N.) and WVU CTSI (NIH U54GM104942).

Author Contributions

D.L.S., T.L.C., C.E.N., S.E.L., S.L.M. researched data. D.L.S., T.L.C., A.B.P., G.M.D., J.M.H. performed statistical analyses. D.L.S. wrote the manuscript. D.L.S., C.E.N., D.T., G.M.D., T.L.C., S.L.M., A.B.P., S.E.L., J.M.H. reviewed/edited manuscript. D.L.S., C.E.N., D.T., J.M.H. contributed to discussion.

Disclosures

None

References

[1] W.B. Kannel, D.L. McGee, Diabetes and cardiovascular disease. The Framingham study, JAMA : the journal of the American Medical Association 241(19) (1979) 2035-8.

[2] S.W. Zarich, R.W. Nesto, Diabetic cardiomyopathy, American heart journal 118(5 Pt 1) (1989) 1000-12.

[3] D.S. Blondheim, M. Kazatsker, Z. Friedman, P. Lysyansky, S.R. Meisel, A. Asif, N. Smirin, A. Shotan, Effect of medical therapy for heart failure on segmental myocardial function in patients with ischemic cardiomyopathy, The American journal of cardiology 99(12) (2007) 1741-4.

[4] J. Chen, T. Cao, Y. Duan, L. Yuan, Y. Yang, Velocity vector imaging in assessing the regional systolic function of patients with post myocardial infarction, Echocardiography 24(9) (2007) 940-5.

[5] H.Y. Liang, S. Cauduro, P. Pellikka, J. Wang, S. Urheim, E.H. Yang, C. Rihal, M. Belohlavek, B. Khandheria, F.A. Miller, T.P. Abraham, Usefulness of two-dimensional speckle strain for evaluation of left ventricular diastolic deformation in patients with coronary artery disease, The American journal of cardiology 98(12) (2006) 1581-6.

[6] M. Bauer, S. Cheng, M. Jain, S. Ngoy, C. Theodoropoulos, A. Trujillo, F.C. Lin, R. Liao, Echocardiographic speckle-tracking based strain imaging for rapid cardiovascular phenotyping in mice, Circ Res 108(8) (2011) 908-16.

[7] M. Bauer, S. Cheng, K. Unno, F.C. Lin, R. Liao, Regional cardiac dysfunction and dyssynchrony in a murine model of afterload stress, PloS one 8(4) (2013) e59915.

[8] A. Kovacs, A. Olah, A. Lux, C. Matyas, B.T. Nemeth, D. Kellermayer, M. Ruppert, M. Torok, L. Szabo, A. Meltzer, A. Assabiny, E. Birtalan, B. Merkely, T. Radovits, Strain and strain

rate by speckle-tracking echocardiography correlate with pressure-volume loop-derived contractility indices in a rat model of athlete's heart, Am J Physiol Heart Circ Physiol 308(7) (2015) H743-8.

[9] S. Yamada, D.K. Arrell, G.C. Kane, T.J. Nelson, C.M. Perez-Terzic, A. Behfar, S. Purushothaman, F.W. Prinzen, A. Auricchio, A. Terzic, Mechanical dyssynchrony precedes QRS widening in ATP-sensitive K(+) channel-deficient dilated cardiomyopathy, J Am Heart Assoc 2(6) (2013) e000410.

[10] W.A. Baseler, E.R. Dabkowski, R. Jagannathan, D. Thapa, C.E. Nichols, D.L. Shepherd, T.L. Croston, M. Powell, T.T. Razunguzwa, S.E. Lewis, D.M. Schnell, J.M. Hollander, Reversal of mitochondrial proteomic loss in Type 1 diabetic heart with overexpression of phospholipid hydroperoxide glutathione peroxidase, Am J Physiol Regul Integr Comp Physiol 304(7) (2013) R553-65.

[11] D. Thapa, C.E. Nichols, S.E. Lewis, D.L. Shepherd, R. Jagannathan, T.L. Croston, K.J. Tveter, A.A. Holden, W.A. Baseler, J.M. Hollander, Transgenic overexpression of mitofilin attenuates diabetes mellitus-associated cardiac and mitochondria dysfunction, J Mol Cell Cardiol 79 (2015) 212-23.

[12] A. Inada, H. Kanamori, H. Arai, T. Akashi, M. Araki, G.C. Weir, A. Fukatsu, A model for diabetic nephropathy: advantages of the inducible cAMP early repressor transgenic mouse over the streptozotocin-induced diabetic mouse, Journal of cellular physiology 215(2) (2008) 383-91.

[13] E. Kim, S. Sohn, M. Lee, J. Jung, R.D. Kineman, S. Park, Differential responses of the growth hormone axis in two rat models of streptozotocin-induced insulinopenic diabetes, The Journal of endocrinology 188(2) (2006) 263-70.

[14] J.F. James, T.E. Hewett, J. Robbins, Cardiac physiology in transgenic mice, Circ Res 82(4) (1998) 407-15.

[15] D.G. Altman, Practical Statistics for Medical Research, Chapman and Hall, London, 1991.

[16] H. Blessberger, T. Binder, Two dimensional speckle tracking echocardiography: clinical applications, Heart 96(24) (2010) 2032-40.

[17] J. D'Hooge, A. Heimdal, F. Jamal, T. Kukulski, B. Bijnens, F. Rademakers, L. Hatle, P. Suetens, G.R. Sutherland, Regional strain and strain rate measurements by cardiac ultrasound: principles, implementation and limitations, Eur J Echocardiogr 1(3) (2000) 154-70.

[18] H. Pavlopoulos, P. Nihoyannopoulos, Strain and strain rate deformation parameters: from tissue Doppler to 2D speckle tracking, The international journal of cardiovascular imaging 24(5) (2008) 479-91.

[19] T.H. Marwick, Measurement of strain and strain rate by echocardiography: ready for prime time?, J Am Coll Cardiol 47(7) (2006) 1313-27.

[20] A. Bhan, A. Sirker, J. Zhang, A. Protti, N. Catibog, W. Driver, R. Botnar, M.J. Monaghan, A.M. Shah, High-frequency speckle tracking echocardiography in the assessment of left ventricular function and remodeling after murine myocardial infarction, Am J Physiol Heart Circ Physiol 306(9) (2014) H1371-83.

[21] C.M. Yu, J. Gorcsan, 3rd, G.B. Bleeker, Q. Zhang, M.J. Schalij, M.S. Suffoletto, J.W. Fung, D. Schwartzman, Y.S. Chan, M. Tanabe, J.J. Bax, Usefulness of tissue Doppler velocity and strain dyssynchrony for predicting left ventricular reverse remodeling response after cardiac resynchronization therapy, The American journal of cardiology 100(8) (2007) 1263-70.

[22] J.C. Hill, R.A. Palma, Doppler tissue imaging for the assessment of left ventricular diastolic function: a systematic approach for the sonographer, J Am Soc Echocardiogr 18(1) (2005) 80-8; quiz 89.

[23] S.F. Nagueh, C.P. Appleton, T.C. Gillebert, P.N. Marino, J.K. Oh, O.A. Smiseth, A.D. Waggoner, F.A. Flachskampf, P.A. Pellikka, A. Evangelista, Recommendations for the evaluation of left ventricular diastolic function by echocardiography, J Am Soc Echocardiogr 22(2) (2009) 107-33.

[24] I. Hashimoto, X. Li, A. Hejmadi Bhat, M. Jones, A.D. Zetts, D.J. Sahn, Myocardial strain rate is a superior method for evaluation of left ventricular subendocardial function compared with tissue Doppler imaging, J Am Coll Cardiol 42(9) (2003) 1574-83.

[25] C. Cottrell, J.N. Kirkpatrick, Echocardiographic strain imaging and its use in the clinical setting, Expert review of cardiovascular therapy 8(1) (2010) 93-102.

[26] S. Mondillo, M. Galderisi, D. Mele, M. Cameli, V.S. Lomoriello, V. Zaca, P. Ballo, A. D'Andrea, D. Muraru, M. Losi, E. Agricola, A. D'Errico, S. Buralli, S. Sciomer, S. Nistri, L. Badano, C. Echocardiography Study Group Of The Italian Society Of, Speckle-tracking echocardiography: a new technique for assessing myocardial function, Journal of ultrasound in medicine : official journal of the American Institute of Ultrasound in Medicine 30(1) (2011) 71-83.

[27] D.Y. Leung, A.C. Ng, Emerging clinical role of strain imaging in echocardiography, Heart, lung & circulation 19(3) (2010) 161-74.

[28] L. Ernande, C. Bergerot, N. Girerd, H. Thibault, E.S. Davidsen, P. Gautier Pignon-Blanc, C. Amaz, P. Croisille, M.L. De Buyzere, E.R. Rietzschel, T.C. Gillebert, P. Moulin, M. Altman, G. Derumeaux, Longitudinal myocardial strain alteration is associated with left ventricular

remodeling in asymptomatic patients with type 2 diabetes mellitus, J Am Soc Echocardiogr 27(5) (2014) 479-88.

[29] L. Ernande, E.R. Rietzschel, C. Bergerot, M.L. De Buyzere, F. Schnell, L. Groisne, M. Ovize, P. Croisille, P. Moulin, T.C. Gillebert, G. Derumeaux, Impaired myocardial radial function in asymptomatic patients with type 2 diabetes mellitus: a speckle-tracking imaging study, J Am Soc Echocardiogr 23(12) (2010) 1266-72.

[30] Z.Y. Fang, R. Leano, T.H. Marwick, Relationship between longitudinal and radial contractility in subclinical diabetic heart disease, Clin Sci (Lond) 106(1) (2004) 53-60.

[31] Z.Y. Fang, S. Yuda, V. Anderson, L. Short, C. Case, T.H. Marwick, Echocardiographic detection of early diabetic myocardial disease, J Am Coll Cardiol 41(4) (2003) 611-7.

[32] H. Nakai, M. Takeuchi, T. Nishikage, R.M. Lang, Y. Otsuji, Subclinical left ventricular dysfunction in asymptomatic diabetic patients assessed by two-dimensional speckle tracking echocardiography: correlation with diabetic duration, Eur J Echocardiogr 10(8) (2009) 926-32.

[33] J.K. Boyer, S. Thanigaraj, K.B. Schechtman, J.E. Perez, Prevalence of ventricular diastolic dysfunction in asymptomatic, normotensive patients with diabetes mellitus, The American journal of cardiology 93(7) (2004) 870-5.

[34] A. Muranaka, S. Yuda, K. Tsuchihashi, A. Hashimoto, T. Nakata, T. Miura, M. Tsuzuki, C. Wakabayashi, N. Watanabe, K. Shimamoto, Quantitative assessment of left ventricular and left atrial functions by strain rate imaging in diabetic patients with and without hypertension, Echocardiography 26(3) (2009) 262-71.

[35] Y. Peng, Z.B. Popovic, N. Sopko, J. Drinko, Z. Zhang, J.D. Thomas, M.S. Penn, Speckle tracking echocardiography in the assessment of mouse models of cardiac dysfunction, Am J Physiol Heart Circ Physiol 297(2) (2009) H811-20.

[36] V. Mor-Avi, R.M. Lang, L.P. Badano, M. Belohlavek, N.M. Cardim, G. Derumeaux, M. Galderisi, T. Marwick, S.F. Nagueh, P.P. Sengupta, R. Sicari, O.A. Smiseth, B. Smulevitz, M. Takeuchi, J.D. Thomas, M. Vannan, J.U. Voigt, J.L. Zamorano, Current and evolving echocardiographic techniques for the quantitative evaluation of cardiac mechanics: ASE/EAE consensus statement on methodology and indications endorsed by the Japanese Society of Echocardiography, J Am Soc Echocardiogr 24(3) (2011) 277-313.

[37] S. Yamada, T.J. Nelson, G.C. Kane, A. Martinez-Fernandez, R.J. Crespo-Diaz, Y. Ikeda, C. Perez-Terzic, A. Terzic, Induced pluripotent stem cell intervention rescues ventricular wall motion disparity, achieving biological cardiac resynchronization post-infarction, J Physiol 591(Pt 17) (2013) 4335-49.

[38] R. Ram, D.M. Mickelsen, C. Theodoropoulos, B.C. Blaxall, New approaches in small animal echocardiography: imaging the sounds of silence, Am J Physiol Heart Circ Physiol 301(5) (2011) H1765-80.

[39] J.A. Hiemstra, S. Liu, M.A. Ahlman, K.H. Schuleri, A.C. Lardo, C.P. Baines, K.C. Dellsperger, D.A. Bluemke, C.A. Emter, A new twist on an old idea: a two-dimensional speckle tracking assessment of cyclosporine as a therapeutic alternative for heart failure with preserved ejection fraction, Physiological reports 1(7) (2013) e00174.

[40] G.Y. Cho, T.H. Marwick, H.S. Kim, M.K. Kim, K.S. Hong, D.J. Oh, Global 2-dimensional strain as a new prognosticator in patients with heart failure, J Am Coll Cardiol 54(7) (2009) 618-24.

[41] A. Mignot, E. Donal, A. Zaroui, P. Reant, A. Salem, C. Hamon, S. Monzy, R. Roudaut, G. Habib, S. Lafitte, Global longitudinal strain as a major predictor of cardiac events in patients

with depressed left ventricular function: a multicenter study, J Am Soc Echocardiogr 23(10) (2010) 1019-24.

[42] Z.B. Popovic, C. Benejam, J. Bian, N. Mal, J. Drinko, K. Lee, F. Forudi, R. Reeg, N.L. Greenberg, J.D. Thomas, M.S. Penn, Speckle-tracking echocardiography correctly identifies segmental left ventricular dysfunction induced by scarring in a rat model of myocardial infarction, Am J Physiol Heart Circ Physiol 292(6) (2007) H2809-16.

[43] H. Thibault, L. Gomez, E. Donal, L. Augeul, M. Scherrer-Crosbie, M. Ovize, G. Derumeaux, Regional myocardial function after myocardial infarction in mice: a follow-up study by strain rate imaging, J Am Soc Echocardiogr 22(2) (2009) 198-205.

[44] H. Thibault, L. Gomez, E. Donal, G. Pontier, M. Scherrer-Crosbie, M. Ovize, G. Derumeaux, Acute myocardial infarction in mice: assessment of transmurality by strain rate imaging, Am J Physiol Heart Circ Physiol 293(1) (2007) H496-502.

[45] J.N. Rottman, G. Ni, M. Brown, Echocardiographic evaluation of ventricular function in mice, Echocardiography 24(1) (2007) 83-9.

[46] D.M. Roth, J.S. Swaney, N.D. Dalton, E.A. Gilpin, J. Ross, Jr., Impact of anesthesia on cardiac function during echocardiography in mice, Am J Physiol Heart Circ Physiol 282(6) (2002) H2134-40.

[47] J. Wu, L. Bu, H. Gong, G. Jiang, L. Li, H. Ma, N. Zhou, L. Lin, Z. Chen, Y. Ye, Y. Niu, A. Sun, J. Ge, Y. Zou, Effects of heart rate and anesthetic timing on high-resolution echocardiographic assessment under isoflurane anesthesia in mice, Journal of ultrasound in medicine : official journal of the American Institute of Ultrasound in Medicine 29(12) (2010) 1771-8.

[48] H. Geyer, G. Caracciolo, H. Abe, S. Wilansky, S. Carerj, F. Gentile, H.J. Nesser, B. Khandheria, J. Narula, P.P. Sengupta, Assessment of myocardial mechanics using speckle tracking echocardiography: fundamentals and clinical applications, J Am Soc Echocardiogr 23(4) (2010) 351-69; quiz 453-5.

[49] T.H. Marwick, Will standardization make strain a standard measurement?, J Am Soc Echocardiogr 25(11) (2012) 1204-6.

[50] D. Oxborough, K. George, K.M. Birch, Intraobserver reliability of two-dimensional ultrasound derived strain imaging in the assessment of the left ventricle, right ventricle, and left atrium of healthy human hearts, Echocardiography 29(7) (2012) 793-802.

[51] E.R. Dabkowski, C.L. Williamson, V.C. Bukowski, R.S. Chapman, S.S. Leonard, C.J. Peer, P.S. Callery, J.M. Hollander, Diabetic cardiomyopathy-associated dysfunction in spatially distinct mitochondrial subpopulations, Am J Physiol Heart Circ Physiol 296(2) (2009) H359-69.

[52] N. Risum, S. Ali, N.T. Olsen, C. Jons, M.G. Khouri, T.K. Lauridsen, Z. Samad, E.J. Velazquez, P. Sogaard, J. Kisslo, Variability of global left ventricular deformation analysis using vendor dependent and independent two-dimensional speckle-tracking software in adults, J Am Soc Echocardiogr 25(11) (2012) 1195-203.

[53] E.R. Dabkowski, C.L. Williamson, J.M. Hollander, Mitochondria-specific transgenic overexpression of phospholipid hydroperoxide glutathione peroxidase (GPx4) attenuates ischemia/reperfusion-associated cardiac dysfunction, Free Radic Biol Med 45(6) (2008) 855-65.

[54] Y. Mizuguchi, Y. Oishi, H. Miyoshi, A. Iuchi, N. Nagase, T. Oki, The functional role of longitudinal, circumferential, and radial myocardial deformation for regulating the early impairment of left ventricular contraction and relaxation in patients with cardiovascular risk

factors: a study with two-dimensional strain imaging, J Am Soc Echocardiogr 21(10) (2008) 1138-44.

[55] J. Wang, D.S. Khoury, Y. Yue, G. Torre-Amione, S.F. Nagueh, Preserved left ventricular twist and circumferential deformation, but depressed longitudinal and radial deformation in patients with diastolic heart failure, Eur Heart J 29(10) (2008) 1283-9.

Figure 2.1

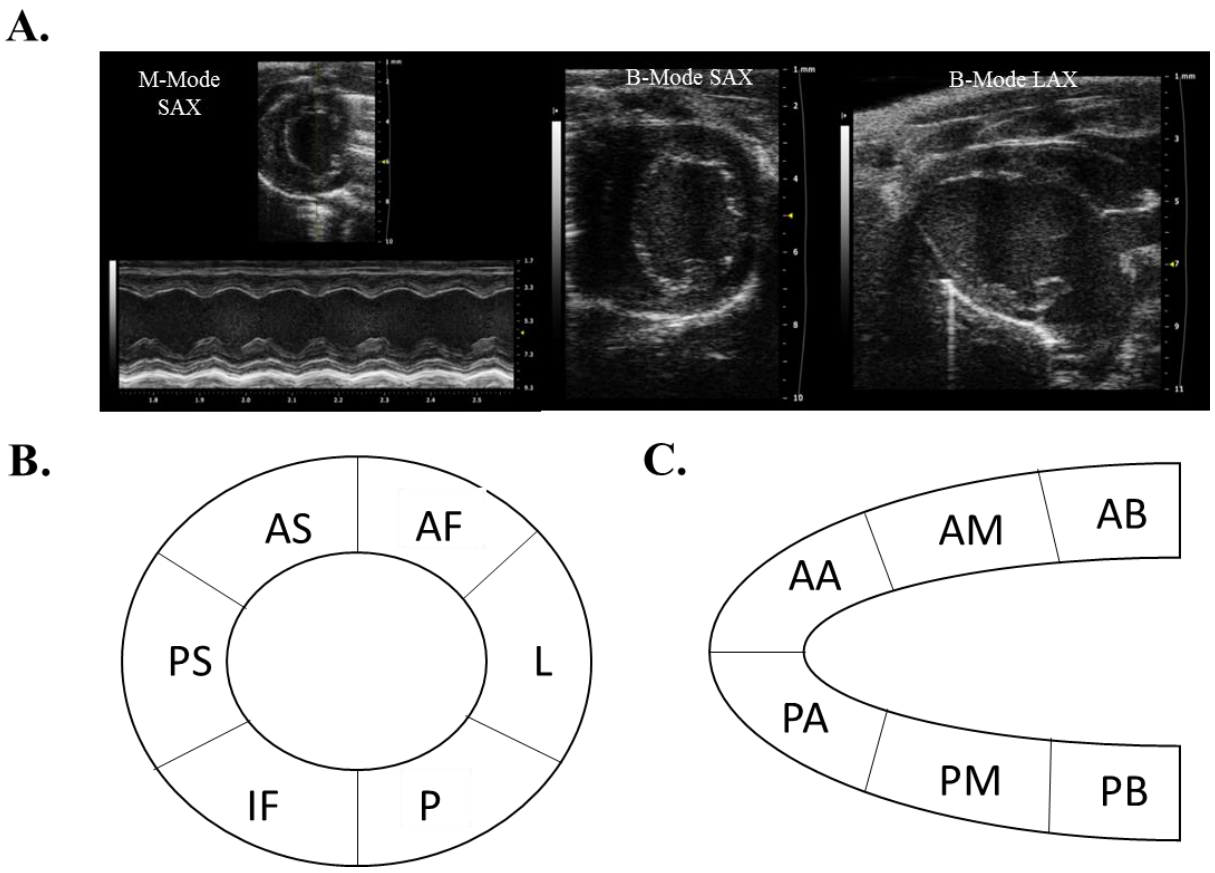

Figure 2.1. Echocardiography and speckle-tracking-based strain. Representative M-mode and B-mode control mouse echocardiographic images from which conventional analyses and speckle-tracking-based strain analyses were performed (**A**). A schematic of myocardial regions identified form the parasternal short-axis view (**B**) and long-axis view (**C**). SAX indicates short-axis; AF, anterior free; L, lateral; P, posterior; IF, inferior free (AF, L, P, and IF considered the free wall region); PS, posterior septum; AS, anterior septum (PS and AS considered the septal wall region). LAX indicates long-axis; AB, anterior base; AM, anterior mid; AA, anterior apex (AB, AM, and AA considered the septal wall region); PA, posterior apex; PM, posterior mid; PB, posterior base (PA, PM, and PB considered the free wall region).

Figure 2.2

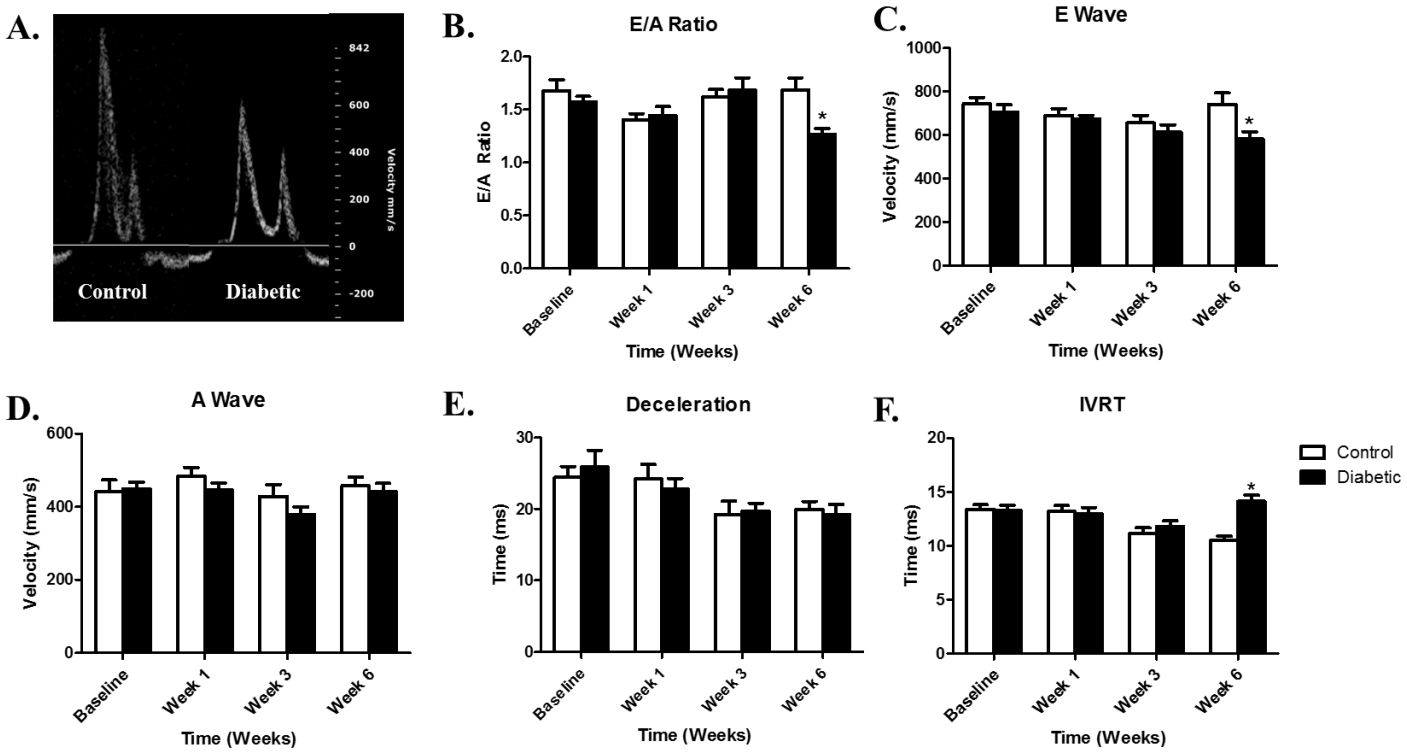
A.
842
600
400
200
0
-200
Velocity mm/s
Control
Diabetic
B.
E/A Ratio
E/A Ratio
2.0
1.5
1.0
0.5
0.0
*
Baseline
Week 1
Week 3
Week 6
Time (Weeks)
C.
E Wave
Velocity (mm/s)
1000
800
600
400
200
0
*
Baseline
Week 1
Week 3
Week 6
Time (Weeks)
D.
A Wave
Velocity (mm/s)
600
400
200
0
Baseline
Week 1
Week 3
Week 6
Time (Weeks)
E.
Deceleration
Time (ms)
30
20
10
0
Baseline
Week 1
Week 3
Week 6
Time (Weeks)
F.
IVRT
Time (ms)
20
15
10
5
0
*
Baseline
Week 1
Week 3
Week 6
Time (Weeks)
Control
Diabetic

Figure 2.2. Color Doppler Imaging for Diastolic Function. Comparative color Doppler images between control (left) and diabetic (right) mice 6-weeks post-diabetic onset **(A)**. E/A ratio data during type 1 diabetes mellitus progression **(B)**. E wave velocity over time during type 1 diabetes mellitus (**C**). A wave velocity over time during type 1 diabetes mellitus (**D**). Deceleration time (**E**) and Isovolumetric Relaxation Time (IVRT) during the progression of type 1 diabetes mellitus (**F**). Values are means ± SEM. $*P < 0.05$ as compared to control at a given time. Open bars = Control animals, $n = 8$; Closed bars = Diabetic animals, $n = 8$.

Figure 2.3

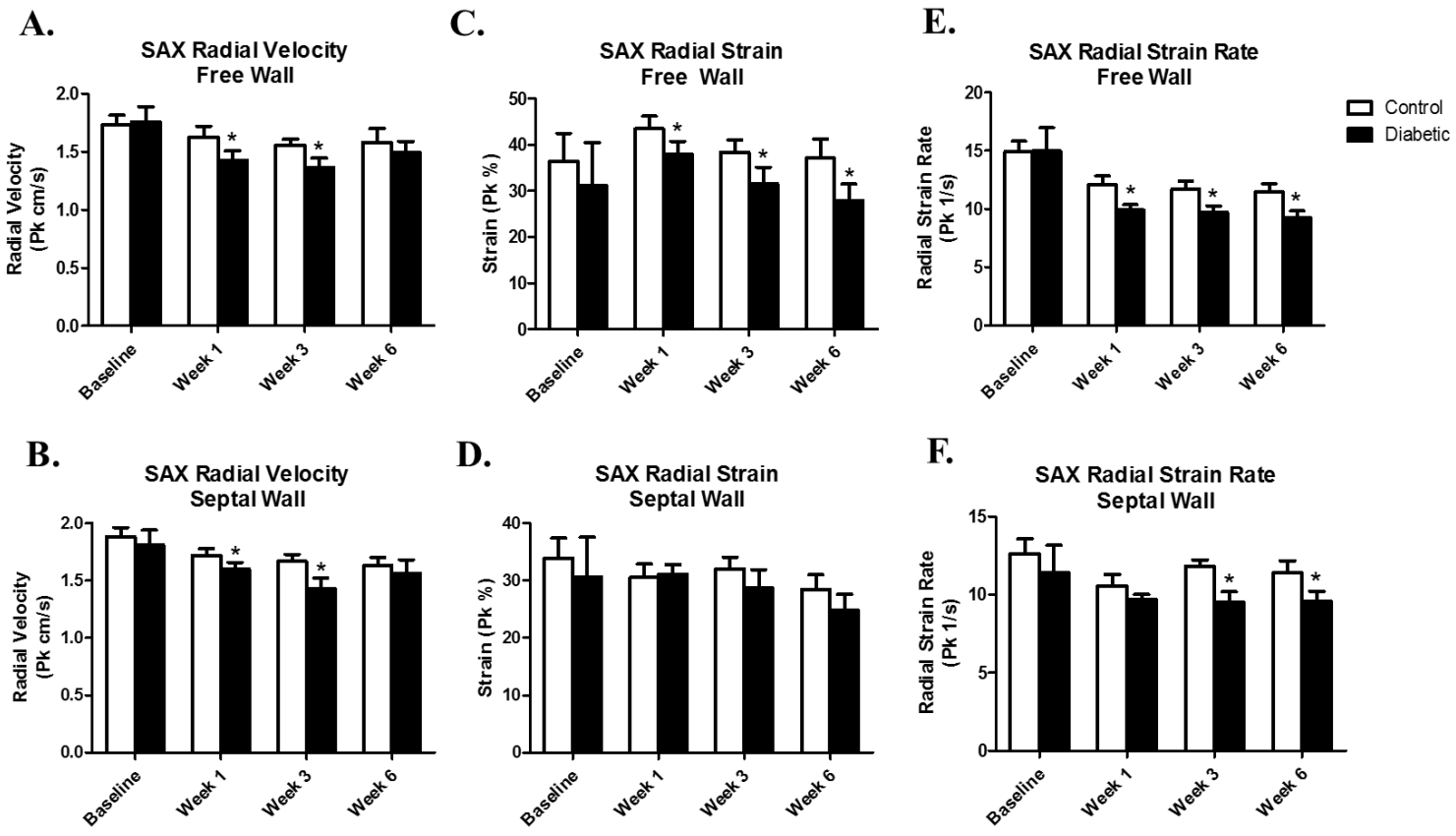
A.
SAX Radial Velocity
Free Wall
Radial Velocity
(Pk cm/s)
2.0
1.5
1.0
0.5
0.0
Baseline
Week 1
Week 3
Week 6
C.
SAX Radial Strain
Free Wall
Strain (Pk %)
50
40
30
20
10
0
E.
SAX Radial Strain Rate
Free Wall
Radial Strain Rate
(Pk 1/s)
20
15
10
5
0
Control
Diabetic
B.
SAX Radial Velocity
Septal Wall
D.
SAX Radial Strain
Septal Wall
F.
SAX Radial Strain Rate
Septal Wall

Figure 2.3. Regional assessment of systolic radial velocity, radial strain, and radial strain rate via speckle-tracking based strain analysis in the short-axis. Comparison of control and type 1 diabetic animals assessing systolic radial velocity, radial strain, and radial strain rate between free wall and septal wall segments of the LV within a given week **(A-F)**. Values are means ± SEM; *$P < 0.05$ as compared to control within a given week. Open bars = Control animals, $n = 8$; Closed bars = Diabetic animals, $n = 8$. Free wall segments include the anterior free wall, lateral, posterior, and inferior free wall. Septal wall segments include the anterior septum and posterior septum.

Figure 2.4

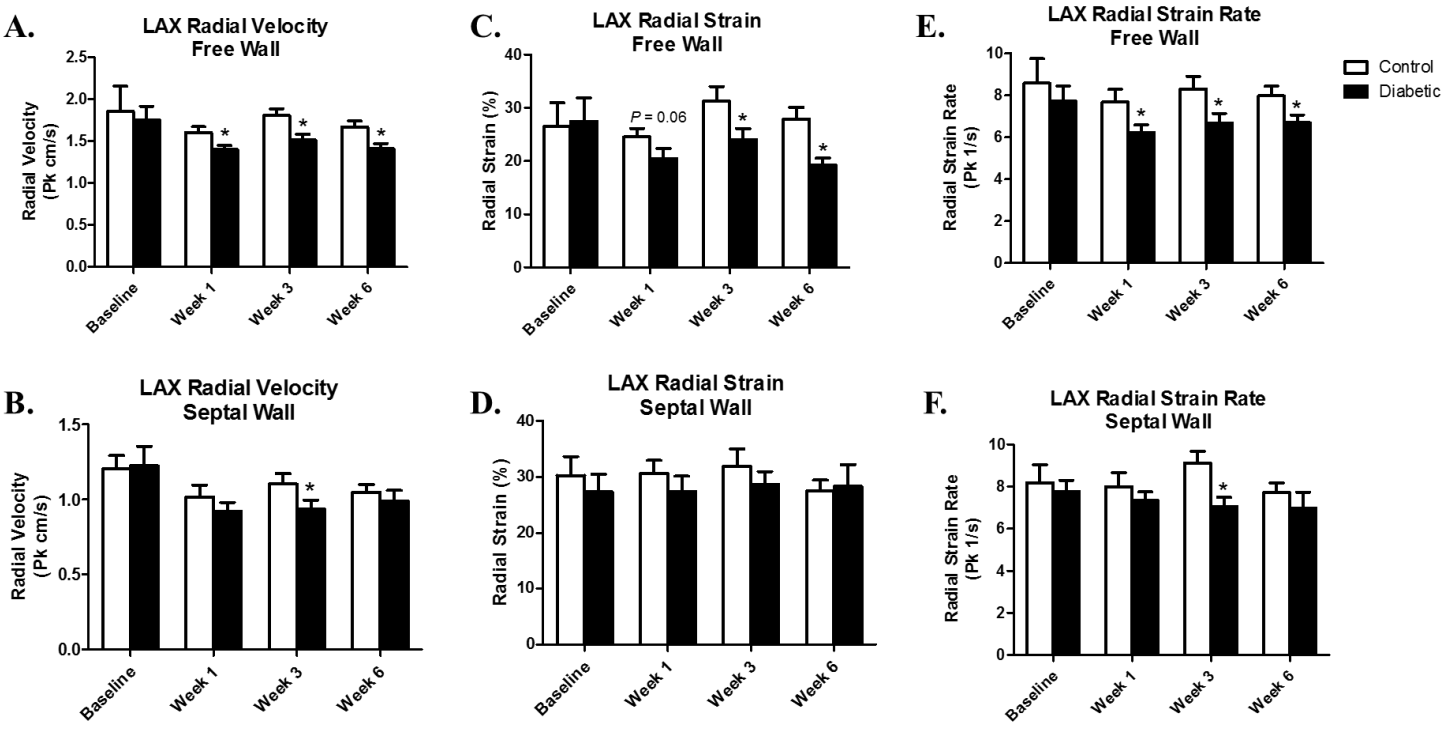
A.
LAX Radial Velocity
Free Wall
Radial Velocity (Pk cm/s)
C.
LAX Radial Strain
Free Wall
Radial Strain (%)
P = 0.06
E.
LAX Radial Strain Rate
Free Wall
Radial Strain Rate (Pk 1/s)
Control
Diabetic
B.
LAX Radial Velocity
Septal Wall
D.
LAX Radial Strain
Septal Wall
F.
LAX Radial Strain Rate
Septal Wall
Baseline
Week 1
Week 3
Week 6

Figure 2.4. Regional assessment of systolic radial velocity, radial strain, and radial strain rate via speckle-tracking-based strain analysis in the long-axis. Comparison of control and type 1 diabetic animals assessing systolic radial velocity, radial strain, and radial strain rate between free wall and septal wall segments of the LV within a given week **(A-F)**. Values are means ± SEM; $*P < 0.05$ as compared to control within a given week. Open bars = Control animals, $n = 8$; Closed bars = Diabetic animals, $n = 8$. Septal wall segments include the anterior base, anterior mid, and anterior apex. Free wall segments include the posterior base, posterior mid, and posterior apex.

Figure S2.1

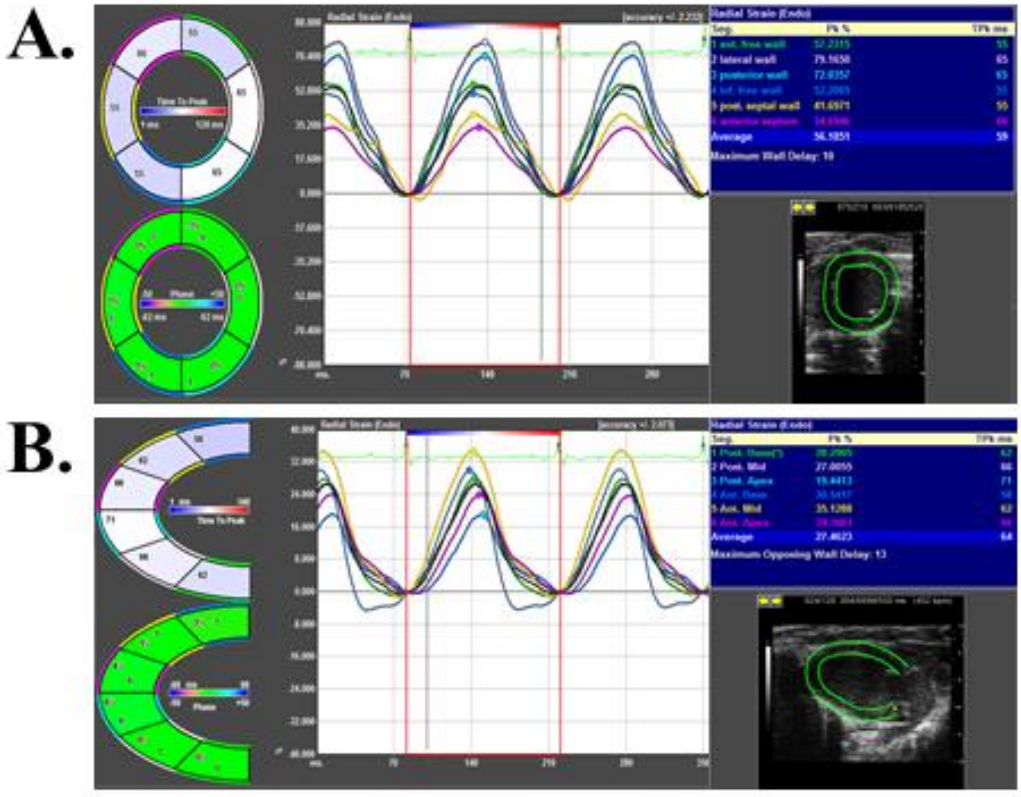

Figure S2.1 Representative Short- and Long-Axis Speckle-Tracking Based Strain Analyses. Curvilinear data is generated for the global (average) strain of the heart, as is denoted by the black line. Strain curves are also generated for each of the 6 anatomical segments of the heart. Speckle-tracking based strain analyses also give curvilinear data and phase circles to indicate the rate at which all segments of the heart are moving. Representative images depicting radial strain measurements in a control animal for the short- (A) and long-axes (B).

Table 2.1. Conventional Echocardiographic Characteristics

	Baseline		Week 1		Week 3		Week 6	
M-mode	Control	Diabetic	Control	Diabetic	Control	Diabetic	Control	Diabetic
Heart Rate (bpm)	418.4 ± 20.9	431.3 ± 14.8	484.0 ± 21.0	457.2 ± 11.9	503.2 ± 11.5	448.4 ± 17.5*	498.5 ± 12.1	494.5 ± 12.1
Stroke Volume (µL)	33.6 ± 2.5	33.0 ± 2.0	30.6 ± 2.4	29.6 ± 1.6	26.7 ± 1.2	25.8 ± 2.5	30.0 ± 1.9	21.0 ± 1.8*
Ejection Fraction (%)	75.3 ± 0.9	74.4 ± 1.4	72.3 ± 1.5	68.6 ± 1.5	71.2 ± 1.3	68.2 ± 3.0	70.9 ± 1.8	65.0 ± 1.7*
Fractional Shortening (%)	42.3 ± 1.0	42.3 ± 1.3	40.5 ± 1.3	37.5 ± 1.1	39.6 ± 1.2	37.4 ± 2.3	39.5 ± 1.7	34.4 ± 1.3*
Cardiac Output (mL/min)	14.0 ± 1.0	13.7 ± 1.3	14.9 ± 1.5	13.4 ± 0.7	13.2 ± 0.6	11.4 ± 1.1	14.9 ± 0.7	10.3 ± 1.0*
Diameter;systole (mm)	1.8 ± 0.1	1.7 ± 0.1	1.9 ± 0.1	2.1 ±0.1	1.8 ± 0.06	1.9 ± 0.2	2.0 ± 0.1	1.9 ± 0.1
Diameter;diastole (mm)	3.3 ± 0.1	3.2 ± 0.1	3.2 ± 0.1	3.3 ± 0.1	3.0 ± 0.05	3.1 ± 0.2	3.2 ± 0.1	2.9 ± 0.1*
Volume;systole (µL)	9.4 ± 0.1	10.6 ± 1.0	12.1 ± 1.2	15.3 ± 1.4	10.4 ± 0.8	13.7 ± 2.9	12.6 ± 1.5	11.5 ± 1.4
Volume;diastole (µL)	43.0 ± 3.4	40.4 ± 2.8	42.7 ± 3.3	44.9 ± 2.7	35.6 ± 1.4	39.5 ± 5.1	42.6 ± 3.2	32.5 ± 3.0*
Anterior Wall Thickness;systole (mm)	1.7 ± 0.07	1.5 ± 0.09	1.4 ± 0.07	1.4 ± 0.03	1.5 ± 0.05	1.4 ± 0.04	1.5 ± 0.04	1.5 ± 0.03
Anterior Wall Thickness;diastole (mm)	1.1 ± 0.05	1.1 ± 0.1	1.2 ± 0.04	1.0 ± 0.05*	1.2 ± 0.06	1.0 ± 0.06*	1.0 ± 0.03	0.9 ± 0.03*
Posterior Wall Thickness;systole (mm)	1.1 ± 0.05	1.1 ± 0.08	1.1 ± 0.04	1.2 ± 0.05	1.3 ± 0.06	1.2 ± 0.05	1.4 ± 0.1	1.3 ± 0.05
Posterior Wall Thickness;diastole (mm)	0.8 ± 0.03	0.9 ± .0.4	1.1 ± 0.06	0.8 ± 0.05*	1.0 ± 0.03	0.8 ± 0.05*	1.0 ± 0.04	0.8 ± 0.03*

Values are shown as means±SEM. *P<0.05 Control versus Diabetic in a given week. 2-tailed Student's t test. Control n=8, Diabetic n=8.

Table 2.1. M-Mode Echocardiography Measurements. Values are shown as means±SEM. *P<0.05 Control versus Diabetic in a given week. 2-tailed Student's t test. Control n=8, Diabetic n=8.

Table 2.2. Average Short-Axis (SAX) Systolic and Diastolic Strain Echocardiographic Characteristics								
	Baseline		Week 1		Week 3		Week 6	
SAX Strain Measurements at Systole	Control	Diabetic	Control	Diabetic	Control	Diabetic	Control	Diabetic
Circumferential Strain (%)	-32.9 ± 1.4	-33.6 ± 1.8	-31.2 ± 1.1	-28.5 ± 0.5*	-29.0 ± 0.9	-27.8 ± 1.4	-29.4 ± 1.5	-26.8 ± 1.8
Circumferential SR (1/s)	-13.7 ± 1.0	-13.8 ± 1.1	-12.8 ± 0.6	-11.6 ± 0.9	-13.3 ± 0.5	-10.9 ± 0.8*	-12.1 ± 0.4	-11.6 ± 1.5*
Circumferential Rotation Rate (deg/s)	340.3 ± 27.5	342.7 ± 34.6	280.4 ± 18.6	270.2 ± 15.7	320.2 ± 33.5	321.9 ± 24.2	318.9 ± 37.6	347.4 ± 31.0
Circumferential Displacement (deg)	4.0 ± 0.5	3.6 ± 0.7	3.2 ± 0.4	3.3 ± 0.3	4.4 ± 0.8	4.7 ± 0.5	4.1 ± 0.6	4.5 ± 0.7
Radial Strain (%)	35.8 ± 2.0	35.1 ± 2.9	37.4 ± 0.8	34.0 ± 1.3*	35.5 ± 0.9	30.5 ± 2.1*	33.7 ± 0.8	25.7 ± 1.8*
Radial SR (1/s)	12.8 ± 0.5	12.8 ± 1.0	11.8 ± 0.6	10.1 ± 0.4*	11.8 ± 0.3	10.0 ± 0.4*	11.3 ± 0.6	9.8 ± 0.4*
Radial Velocity (cm/s)	1.7 ± 0.07	1.8 ± 0.1	1.6 ± 0.06	1.5 ± 0.05*	1.6 ± 0.04	1.4 ± 0.07*	1.6 ± 0.08	1.4 ± 0.09*
Radial Displacement (mm)	0.57 ± 0.01	0.61 ± 0.05	0.55 ± 0.02	0.48 ± 0.02*	0.53 ± 0.01	0.44 ± 0.01*	0.52 ± 0.02	0.48 ± 0.04
SAX Strain Measurements at Diastole								
Circumferential Strain (%)	1.5 ± 0.8	2.0 ± 0.5	1.5 ± 0.2	1.4 ± 0.3	2.0 ± 0.4	2.1 ± 0.3	1.9 ± 0.4	2.2 ± 0.2
Circumferential SR (1/s)	24.3 ± 1.6	22.9 ± 2.3	16.4 ± 0.6	17.5 ± 0.8	15.4 ± 0.4	16.2 ± 1.1	17.4 ± 1.2	17.3 ± 1.2
Circumferential Rotation Rate (deg/s)	-391.5 ± 32.0	-408.3 ± 43.8	-362.7 ± 20.0	-382.4 ± 24.7	-401.5 ± 26.3	-421.5 ± 32.6	361.0 ± 33.5	-395.5 ± 28.9
Circumferential Displacement (deg)	-3.8 ± 0.7	-3.8 ± 0.5	-3.8 ± 0.7	-2.5 ± 0.3	-2.1 ± 0.5	-2.4 ± 0.4	-2.8 ± 0.6	-3.0 ± 0.4
Radial Strain (%)	-2.4 ± 0.4	-3.9 ± 0.9	-2.3 ± 0.2	-1.6 ± 0.3*	-3.7 ± 0.5	-2.0 ± 0.4*	-3.8 ± 0.7	-2.0 ± 0.5*
Radial SR (1/s)	-15.8 ± 0.9	-16.6 ± 2.1	-13.3 ± 0.9	-12.5 ± 0.5	-13.1 ± 0.3	-11.2 ± 0.5*	-13.7 ± 0.7	-11.1 ± 0.9*
Radial Velocity (cm/s)	-2.7 ± 0.2	-2.4 ± 0.3	-1.9 ± 0.08	-1.9 ± 0.1	-1.8 ± 0.07	-1.7 ± 0.1	-2.0 ± 0.1	-1.7 ± 0.2
Radial Displacement (mm)	-0.007 ± 0.002	-0.008 ± 0.002	-0.01 ± 0.003	-0.02 ± 0.3	-0.02 ± 0.005	-0.02 ± 0.003	-0.02 ± 0.006	-0.02 ± 0.002
Values are shown as means±SEM. SR=Strain Rate. *P<0.05 Control versus Diabetic in a given week. 2-tailed Student's t test. Control n=8, Diabetic n=8.								

Table 2.2. Global Short-axis Systolic and Diastolic Strain Measurements. Values are shown as means±SEM. SR=Strain Rate. *P<0.05 Control versus Diabetic in a given week. 2-tailed Student's t test. Control n=8, Diabetic n=8.

Table 2.3. Average Long-Axis (LAX) Systolic and Diastolic Strain Echocardiographic Characteristics								
	Baseline		Week 1		Week 3		Week 6	
LAX Strain Measurements in Systole	Control	Diabetic	Control	Diabetic	Control	Diabetic	Control	Diabetic
Longitudinal Strain (%)	-20.2 ± 0.9	-21.4 ± 2.6	-17.9 ± 0.6	-16.7 ± 0.9	-19.3 ± 1.0	-18.5 ± 0.3	-18.4 ± 1.2	-18.7 ± 1.0
Longitudinal SR (1/s)	-8.3 ± 0.6	-7.5 ± 0.3	-7.1 ± 0.3	-6.7 ± 0.2	-8.3 ± 0.3	-6.8 ± 0.1*	-8.5 ± 0.6	-6.8 ± 0.4*
Longitudinal Velocity (cm/s)	0.9 ± 0.06	0.9 ± 0.08	0.8 ± 0.04	0.9 ± 0.03	1.0 ± 0.05	0.9 ± 0.01	0.9 ± 0.05	0.9 ± 0.05
Longitudinal Displacement (mm)	0.2 ± 0.02	0.2 ± 0.03	0.2 ± 0.01	0.2 ± 0.01	0.2 ± 0.02	0.2 ± 0.01	0.2 ± 0.02	0.2 ± 0.03
Radial Strain (%)	28.8 ± 2.4	26.9 ± 3.0	27.8 ± 1.2	22.0 ± 1.1*	30.1 ± 2.0	24.7 ± 1.0*	27.7 ± 2.0	22.0 ± 0.6*
Radial SR (1/s)	8.6 ± 0.8	8.1 ± 0.4	8.1 ± 0.2	6.7 ± 0.2*	8.6 ± 0.4	6.9 ± 0.3*	7.6 ± 0.2	6.3 ± 0.3*
Radial Velocity (cm/s)	1.5 ± 0.09	1.5 ± 0.1	1.3 ± 0.04	1.1 ± 0.04*	1.5 ± 0.08	1.2 ± 0.05*	1.4 ± 0.01	1.2 ± 0.05*
Radial Displacement (mm)	0.5 ± 0.02	0.5 ± 0.04	0.5 ± 0.01	0.4 ± 0.01*	0.5 ± 0.02	0.5 ± 0.01	0.5 ± 0.01	0.4 ± 0.02
Long-Axis Strain Measurements in Diastole								
Longitudinal Strain (%)	2.3 ± 0.4	2.4 ± 1.0	1.3 ± .02	1.3 ± 0.3	1.1 ± 0.2	1.6 ± 0.3	1.1 ± 0.2	0.9 ± 0.1
Longitudinal SR (1/s)	11.4 ± 0.7	11.5 ± 1.0	7.3 ± 0.2	7.9 ± 0.6	8.9 ± 0.6	9.8 ± 0.6	8.8 ± 0.6	10.0 ± 1.0
Longitudinal Velocity (cm/s)	-1.0 ± 0.08	-1.1 ± 0.05	-0.9 ± 0.01	-1.0 ± 0.06	-1.0 ± 0.05	-0.9 ± 0.08	-0.9 ± 0.06	-1.0 ± 0.05
Longitudinal Displacement (mm)	-0.03 ± 0.01	-0.04 ± 0.008	-0.03 ± 0.004	-0.04 ± 0.008	-0.02 ± 0.005	-0.04 ± 0.005	-0.02 ± 0.006	-0.04 ± 0.008
Radial Strain (%)	-2.8 ± 0.4	-2.4 ± 0.5	-1.6 ± 0.1	-2.1 ± 0.3	-1.6 ± 0.3	-2.0 ± 0.3	-2.1 ± 0.6	-1.9 ± 0.4
Radial SR (1/s)	-10.9 ± 1.1	-10.5 ± 0.5	-9.9 ± 0.6	-9.1 ± 0.7	-10.2 ± 0.6	-10.2 ± 0.6	-10.0 ± 0.4	-10.3 ± 0.5
Radial Velocity (cm/s)	-2.0 ± 0.1	-2.0 ± 0.1	-1.5 ± 0.04	-1.4 ± 0.08	-1.6 ± 0.1	-1.6 ± 0.1	-1.6 ± 0.05	-1.6 ± 0.09
Radial Displacement (mm)	-0.01 ± 0.002	-0.008 ± 0.002	-0.01 ± 0.001	-0.01 ± 0.002	-0.02 ± 0.003	-0.01 ± 0.003	-0.02 ± 0.004	-0.02 ± 0.003
Values are shown as means±SEM. SR=Strain Rate. *P<0.05 Control versus Diabetic in a given week. 2-tailed Student's t test. Control n=8, Diabetic n=8.								

Table 2.3. Global Long-Axis Systolic and Diastolic Strain Measurements. Values are shown as means±SEM. SR=Strain Rate. *P<0.05 Control versus Diabetic in a given week. 2-tailed Student's t test. Control n=8, Diabetic n=8.

Table S2.1	Strain		EA Ratio		Ejection Fraction	
	Interobserver	Intraobserver Test-Retest	Interobserver	Intraobserver Test-Retest	Interobserver	Intraobserver Test-Retest
ICC	0.88	0.82	0.89	0.99	0.87	0.85
95% confidence interval	(-0.19-0.99)	(-0.11-0.99)	(0.23-0.99)	(0.97-1.0)	(0.19-0.99)	(0.19-0.99)
***P* value**	.037	.038	0.14	.000	.026	.081

Table S2.1. Interobserver and Intraobserver Test-Retest Reliability. Reliability tests for Strain, EA Ratio and Ejection Fraction measurements. ICC = Intra-class Correlation Coefficient.

Table S2.2. Average Short-Axis (SAX) and Long-Axis (LAX) Systolic Dyssynchrony								
	Baseline		Week 1		Week 3		Week 6	
LAX Dyssynchrony	Control	Diabetic	Control	Diabetic	Control	Diabetic	Control	Diabetic
Dyssynchrony (%) - Radial Velocity	0.3 ± 0.03	0.3 ± 0.03	0.4 ± 0.04	0.3 ± 0.02	0.4 ± 0.03	0.3 ± 0.03	0.4 ± 0.02	0.3 ± 0.03*
Dyssynchrony (%) - Radial Strain	8.9 ± 1.1	7.6 ± 1.3	7.9 ± 0.8	9.0 ± 0.8	8.2 ± 0.9	7.4 ± 0.8	8.5 ± 1.3	8.6 ± 1.3
Dyssynchrony (%) - Radial Strain Rate	1.6 ± 0.3	1.0 ± 0.1	2.0 ± 0.3	1.2 ± 0.1*	1.5 ± 0.2	1.2 ± 0.1	1.4 ± 0.1	1.5 ± 0.2
SAX Dyssynchrony								
Dyssynchrony (%) - Radial Velocity	0.2 ± 0.02	0.2 ± 0.03	0.2 ± 0.02	0.2 ± 0.02	0.2 ± 0.01	0.1 ± 0.02	0.2 ± 0.03	0.2 ± 0.03
Dyssynchrony (%) - Radial Strain	9.4 ± 1.3	12.3 ± 1.9	11.8 ± 2.4	8.7 ± 0.9	11.9 ± 1.2	12.1 ± 1.05	14.2 ± 2.4	10.9 ± 0.9
Dyssynchrony (%) - Radial Strain Rate	2.0 ± 0.2	3.0 ± 0.6	2.8 ± 0.5	1.6 ± 0.2*	2.8 ± 0.2	2.3 ± 0.3	3.1 ± 0.5	2.6 ± 0.3
Values are shown as means±SEM. *P<0.05 Control versus Diabetic in a given week. 2-tailed Student's t test. Control n=8, Diabetic n=8.								

Table S2.2. Average Short-Axis (SAX) and Long-Axis (LAX) Systolic Dyssynchrony								
	Baseline		Week 1		Week 3		Week 6	
LAX Dyssynchrony	Control	Diabetic	Control	Diabetic	Control	Diabetic	Control	Diabetic
Dyssynchrony (%) - Radial Velocity	0.3 ± 0.03	0.3 ± 0.03	0.4 ± 0.04	0.3 ± 0.02	0.4 ± 0.03	0.3 ± 0.03	0.4 ± 0.02	0.3 ± 0.03*
Dyssynchrony (%) - Radial Strain	8.9 ± 1.1	7.6 ± 1.3	7.9 ± 0.8	9.0 ± 0.8	8.2 ± 0.9	7.4 ± 0.8	8.5 ± 1.3	8.6 ± 1.3
Dyssynchrony (%) - Radial Strain Rate	1.6 ± 0.3	1.0 ± 0.1	2.0 ± 0.3	1.2 ± 0.1*	1.5 ± 0.2	1.2 ± 0.1	1.4 ± 0.1	1.5 ± 0.2
SAX Dyssynchrony								
Dyssynchrony (%) - Radial Velocity	0.2 ± 0.02	0.2 ± 0.03	0.2 ± 0.02	0.2 ± 0.02	0.2 ± 0.01	0.1 ± 0.02	0.2 ± 0.03	0.2 ± 0.03
Dyssynchrony (%) - Radial Strain	9.4 ± 1.3	12.3 ± 1.9	11.8 ± 2.4	8.7 ± 0.9	11.9 ± 1.2	12.1 ± 1.05	14.2 ± 2.4	10.9 ± 0.9
Dyssynchrony (%) - Radial Strain Rate	2.0 ± 0.2	3.0 ± 0.6	2.8 ± 0.5	1.6 ± 0.2*	2.8 ± 0.2	2.3 ± 0.3	3.1 ± 0.5	2.6 ± 0.3
Values are shown as means±SEM. *P<0.05 Control versus Diabetic in a given week. 2-tailed Student's t test. Control n=8, Diabetic n=8.								

Table S2.2. Global Short-Axis and Long-Axis Systolic Dyssynchrony. Values are shown as means±SEM. *P<0.05 Control versus Diabetic in a given week. 2-tailed Student's t test. Control n=8, Diabetic n=8.

Chapter 3:

Mitochondrial Proteome Disruption in the Diabetic Heart: A Central Role for Mitochondrial Heat Shock Protein 70 (mtHsp70) in Proteome Restoration

As submitted to the Journal of Diabetes; November 21, 2016

Danielle L. Shepherd, Quincy A. Hathaway, Cody E. Nichols, Kristen M. Hughes, Mark V. Pinti, Seth M. Stine and John M. Hollander

Division of Exercise Physiology; Mitochondrial, Metabolism and Bioenergetics Working Group; West Virginia University School of Medicine, Morgantown, WV, 26505

Running Title: Proteome restoration with mtHsp70

Corresponding Author:
John M. Hollander
Division of Exercise Physiology
West Virginia University School of Medicine
PO Box 9227
1 Medical Center Drive
Morgantown, WV 26506
Tel: 1-(304) 293-3683
Fax: 1-(304) 293-7105
Email: jhollander@hsc.wvu.edu

Abstract

Disruption of mitochondrial proteomic signature following diabetic insult is correlated with inefficiency in the import of nuclear-encoded mitochondrial proteins that constitute greater than 99% of the organelle's proteome. This disruptive dynamic manifests in a spatially-dependent, subcellular manner such that subsarcolemmal mitochondria display greater dysfunction and proteome disruption during type 2 diabetes mellitus (T2DM), while interfibrillar mitochondria display greater dysfunction and proteome disruption during type 1 diabetes mellitus (T1DM). The goal of this study was to determine whether manipulation of the mitochondrial protein import process through targeted restoration of a central constituent of its active motor, mitochondrial heat shock protein 70 (mtHsp70), which displays loss in content that is correlated with the mitochondrial subpopulation most impacted by a given diabetic phenotype, could rectify proteome signature. Novel lines of cardiac-specific mtHsp70 transgenic mice were examined in T1DM and T2DM models. MtHsp70 overexpression restored cardiac function in both diabetic models. MtHsp70 overexpression restored deficiencies in nuclear-encoded mitochondrial protein import in a subpopulation-specific manner leading to beneficial impact on proteome signature. Our results suggest that restoration of a key import constituent of the active motor, mtHsp70, provides therapeutic benefit to mitochondrial proteome disruption in both T1DM and T2DM leading to attenuation of contractile dysfunction.

Keywords

Diabetes Mellitus; Cardiac Function; Mitochondrial Function, Proteomics, Protein Import

Introduction

Cardiovascular complications are the leading cause of mortality among diabetic patients, with the mitochondrion having a central role in the etiology of the dysfunction seen in the diabetic heart (1-13). Proteomic evaluations have enabled an in-depth survey of potential contributors involved in mitochondrial dysfunction associated with diabetes mellitus (DM) (1; 2; 8; 14-17). Our laboratory has observed differential impacts on spatially-distinct mitochondrial subpopulations during DM with cardiac interfibrillar mitochondria (IFM) being most impacted during type 1 diabetes mellitus (T1DM) and subsarcolemmal mitochondria (SSM) being more impacted during type 2 diabetes mellitus (T2DM) (1-5; 9; 10; 18-20).

Approximately 1500 proteins reside in the human mitochondrion, with 13 transcribed from the mitochondrial genome and the remaining proteins encoded by the nuclear genome, requiring significant contribution from extramitochondrial sources for the maintenance of a stable organelle (21-24). Nuclear-encoded mitochondrial proteins require input from a coordinated import process which includes mitochondrial heat shock protein 70 (mtHsp70) (21). Located in the mitochondrial matrix, mtHsp70 is a central subunit of the presequence translocase-associated motor (PAM) complex (21). Anchored to Tim44, mtHsp70 attaches to a translocating preprotein trapping and pulling it through the inner mitochondrial membrane (IMM) in an ATP-dependent manner (25). When mtHsp70 is altered, mitochondrial function is compromised with decrements noted in nuclear-encoded mitochondrial protein import, decreased antioxidant defenses, increased misfolding and degradation of proteins, along with increased cellular apoptosis (21). Neonatal rat cardiomyocytes infected with an adenoviral vector expressing mtHsp70 were protected from ischemia/reperfusion injury, potentially from an increase in nuclear-encoded antioxidant defense proteins (26). MtHsp70 is dysregulated in the diabetic heart, with proteomic analyses showing decreased mtHsp70 in the IFM during T1DM and the SSM during T2DM, suggesting that

proteome disruption may be the result of loss from nuclear-encoded sources (2; 4). These observations suggests that mtHsp70 loss may represent a central node of dysfunction precipitating mitochondrial proteome disruption and linking DM-induced mitochondrial dysfunction across both DM phenotypes. The goal of the current study was to determine whether mtHsp70 overexpression could restore nuclear-encoded mitochondrial protein import efficiency, leading to preservation of the mitochondrial proteome in the T1DM IFM and T2DM SSM, and alleviate cardiac contractile dysfunction.

Research Design and Methods

MtHsp70 Transgenic Mouse Development

Animal experiments in this study conformed to the National Institutes of Health Eighth Edition *Guidelines for the Care and Use of Laboratory Animals* and were approved by the West Virginia University Care and Use committee. Cardiac-specific mtHsp70 transgenic mouse lines were generated using a chimeric transgene consisting of the human HSPA9 gene (mtHsp70) inserted into the plasmid pJG/Alpha MHC vector containing an alpha-myosin heavy-chain (αMHC) promoter (a kind gift from Dr. Jeffrey Robbins) (27) (**Figure 3.2A**). The HSPA9 gene consists of a 5' mitochondrial targeting sequence (ATG) and the human mtHsp70 cDNA, which was inserted into the Sal1 cloning site of the pJG/Alpha MHC vector via sticky-end and blunt-end ligation of Xho1 and HindIII, as a fragment of approximately 3001 bp (**Figure 3.2A**). The chimeric transgene was cut out of the plasmid by Not1 digestion, purified, and used to generate transgenic mice by the Mouse Transgenic and Gene Targeting Core at Emory University as described previously (1; 9; 19). All control and transgenic mice were generated using an FVB background, and experimental procedures were performed on animals of approximately 12-15-weeks-old for T1DM and 20-22-weeks-old for T2DM.

MtHsp70 Transgenic Mouse Screening

To verify the chimeric transgene presence in the genome, DNA from 3-week-old mice was isolated from tail clips using Allele-In-One Mouse Tail Direct Lysis Buffer (Allele Biotechnology, San Diego, CA) per manufacturer's instructions and screened as previously described (1; 9; 19). Four transgenic mouse lines were generated, with two high expressing transgenic lines (20-22 cycle number) and two low expressing transgenic lines (26-28 cycle number). All experimentation was performed on line 1 (**Figure 3.2B**).

T1DM Induction

Four groups were utilized for the type 1 studies: control, mtHsp70, T1DM, and mtHsp70 T1DM. T1DM was induced in 6-week-old, mixed sex control and mtHsp70 mice using multiple low-dose streptozotocin (Sigma, St. Louis, MO) injections as previously described (1; 2; 5; 9; 18-20; 28). Confirmation of hyperglycemia was performed by measuring blood glucose (Contour Blood Glucose test strips; Bayer, Mishawaka, IN) one week post-injection, with levels >250 mg/dL considered diabetic. Animals were maintained for 6 weeks in a hyperglycemic state, echocardiography performed and then euthanized for experimentation.

Ovarian Transplantation Procedure

A db/db, mtHsp70 transgenic mouse line was generated using an ovarian transplantation procedure developed in our laboratory. Because homozygous db/db mice are unable to breed, generation of db/db, transgenic mice is cumbersome due to the need for extensive breeding with unfavorable Mendelian genetics. Briefly, a db/db donor mouse was euthanized by cervical dislocation, an incision made in the abdominal wall, followed by the exteriorization of the ovarian fat pad where the ovaries were removed for future implantation into recipient mice.

The recipient mouse was maintained under a surgical plane of anesthesia, an incision made in the abdominal cavity and the ovarian fat pad exteriorized. The ovarian bursa was incised cranially at the junction of the bursa and the fat pad to enable access to the ovary. The donor ovary was placed on top of the ovarian blood vessels and the bursa retracted into its original position. The fat pad and ovary were returned into the abdominal cavity and the incision in the abdominal wall closed. Removal of the contralateral ovary was performed after a successful ovarian transplantation.

MtHsp70 db/db Transgenic Mouse Screening

The developmental strategy for ovarian transplantation and breeding can be seen in **Figure 3.2E**. Briefly, ovaries from a homozygous db/db female mouse were excised and then implanted into an immunohistocompatible recipient mouse. This recipient mouse was bred with a mouse heterozygous for both the db/db and mtHsp70 genotype, increasing the probability that the offspring would have the homozygous db/db mutation and the mtHsp70 transgene. MtHsp70 genotyping was completed as described above (**Figure 3.2E**). To determine whether the offspring possessed the db/db mutation, DNA was amplified via PCR for the $Lepr^{db}$ locus followed by allelic discrimination analysis to identify $Lepr^{db/db}$ homozygous (db/db), $Lepr^{db/-}$ heterozygous (db/-) or control (-/-) offspring (**Figure 3.2E**). Fluorometric probes designed by our laboratory were used to detect the db/db point mutation via allelic discrimination. The sequence containing the mutation was tagged with FAM, while the normal sequence was tagged with HEX enabling assessment of whether the animals DNA contained 2 HEX tags (-/-), a HEX tag and a FAM tag (db/-), or 2 FAM tags (db/db) (**Figure 3.2E**). DNA from known db/db, db/-, and -/- mice obtained from and validated by Jackson Laboratory (Bar Harbor, ME) were included as internal controls. Once appropriate genotypes were obtained, animals were aged to 20-22-weeks-old, echocardiography performed and euthanized for experimentation.

Echocardiography

Echocardiography and speckle-tracking based strain imaging analyses were performed as previously described using the Vevo 2100 Imaging analysis software (Visual Sonics, Toronto, Canada) (1; 9; 28; 29).

Preparation of Individual Mitochondrial Subpopulations

Cardiac mitochondrial subpopulations were isolated as previously described following the methods of Palmer et al. (30) with minor modifications by our laboratory (1; 2; 4; 5; 9; 18; 19; 29). Mitochondrial pellets were resuspended in the appropriate buffer depending upon assay. Protein concentrations were determined by the Bradford method with bovine serum albumin as a standard (31), while mitochondrial number was determined by flow cytometry.

Determination of Mitochondrial Number by Flow Cytometry

Mitochondrial number was determined using Sphero AccuCount Blank Particles, 2.0 µm (Spherotech Inc., Lake Forest, IL). An aliquot of mitochondria were diluted in sucrose buffer (1:2,500) and subsequently stained with Mitotracker Deep Red 633 (Invitrogen, Carlsbad, CA), resulting in event rates below 1,000 events/s using FACSDiva 8.0 software (BD Biosciences, San Jose CA) on an LSRFortessa equipped with a FSC PMT (BD Biosciences) in the WVU Flow Cytometry and Single Cell Core Facility. Events were determined as mitochondria by thresholding on Mitotracker Deep Red 633 and each sample was run for 1 minute at low speed. Fifty µL of Sphero AccuCount blank particles were added to 450 µL of sucrose and run on the flow cytometer for 1 minute to obtain the number of events. Mitochondrial number was calculated per manufacturer's instructions.

iTRAQ Labeling and Mass Spectrometry Analyses

Pooled IFM (n = 8) from T1DM and mtHsp70 T1DM mice, as well as pooled SSM (n = 8) from T2DM and mtHsp70 T2DM mice were prepared as previously described (1; 2; 4). Samples were labeled with iTRAQ reagents following the manufacturer's protocol (Applied Biosystems, Foster City, CA) and combined to create a 400 µg pooled protein digest with equal fractions of

labeled samples. The fractions were submitted for LC-MALDI TOF/TOF mass spectral analysis for protein identification, characterization, and differential expression analysis as previously described (2; 4) with slight modifications. Briefly, a Q Exactive MS (Thermo Scientific, San Jose, CA) was utilized with Xcalibur 3.0 software. The resulting spectra were analyzed using ABI ProteinPilot software 4.0 (Applied Biosystems, Foster City, CA).

Ingenuity Pathway Analyses

Proteomic data was integrated into the Ingenuity Pathway Analysis (IPA) software to establish associations between changing mitochondrial protein constituents and upstream/downstream effects on cellular pathways. The "Mitochondrial Dysfunction Metabolic Pathway" was generated through the use of QIAGEN's IPA (www.qiagen.com/ingenuity) and used as the basic model for protein associations. Changes in protein expression are presented for two separate mitochondrial populations: 1) mtHsp70 T2DM SSM in relation to T2DM SSM and 2) mtHsp70 T1DM IFM in relation to T1DM IFM. All changes are depicted as increasing, decreasing, or sustained proteomic expression in the mtHsp70 diabetic mice compared to DM.

Mitochondrial Protein Import

The fusion protein pAcGFP1-Mito (Clonetech Laboratories, Mountain View, CA) containing the precursor subunit VIII of human cytochrome *c* oxidase and the green fluorescent protein (GFP) from Aequorea coerulescens (AcGFP1) were cloned into pIVEX2.3d (Roche Applied Science, Indianapolis, IN) as previously described (1; 2). Using the S30 T7 protein expression system (Promega, Madison, WI) *in vitro* transcription/translation of mitoGFP1 was performed per manufacturer's instructions (1; 2). The mitoGFP1 lysate was used to assess the protein import process and mitochondrial protein import performed as described (32) with

modifications by our laboratory (1; 2). Briefly, mitochondria were counted by flow cytometry, MitoGFP1 lysate added to the samples and protein import performed and assessed at time intervals of 30 s, 1 and 2 mins at 25°C (1; 2).

Human Patient Samples

The West Virginia University Institutional Review Board and Institutional Biosafety Committee approved all protocols. Patient demographics have been described and characterized as non-diabetic, T1DM or T2DM based on a previous diagnosis of DM (3; 9).

Western Blot Analyses

SDS-PAGE was run on 4-12% gradient gels, as previously described (1; 2; 4; 9; 10; 29; 33). For assessment of protein content overexpression and mitochondrial protein import, 100 million intact mitochondria were loaded as determined by flow cytometry. For assessment of protein content in human samples and tissue homogenates, equal amounts of protein were loaded as determined above by the Bradford method (31). Further, assessment of protein loading control was done by utilizing a COXIV antibody and Ponceau S solution (Sigma, St. Louis, MO). Relative amounts of mtHsp70 and COXIV were assessed using the following primary antibodies: anti-mtHsp70 (Stressgen, Ann Arbor, MI) and anti-COXIV (Cell Signaling Technology, Danvers, MA). The secondary antibodies used in the analyses were goat anti-mouse IgG horseradish peroxidase (HRP) conjugate (Pierce Biotechnology, Rockford, IL) for mtHsp70 and goat anti-rabbit IgG HRP conjugate (Cayman Chemical, Ann Arbor, MI) for COXIV. Nuclear-encoded mitochondrial protein import blots were probed with the primary anti-GFP mouse monoclonal antibody (Clonetech Laboratories, Mountain View, CA) followed by the secondary antibody anti-

mouse IgG horseradish peroxidase conjugate (Pierce Biotechnology, Rockford, IL). Densitometry analyses using Image J software, were performed as previously described (1; 2; 9; 19; 20; 29).

Statistics

All data are presented as mean±standard error of the mean (SEM). Data were analyzed using a One-Way Analysis of Variance (ANOVA) with the Bonferroni post-hoc test to determine significant differences between groups (GraphPad Prism 5 Software, La Jolla, CA). When differences in variability between groups was noted by Bartlett's test for equal variances, a Kruskal-Wallis analysis was utilized with the Dunn's multiple comparison tests to assess differences between groups. When appropriate, a Student's *t*-test was used. In all instances, $P \leq 0.05$ was considered significant.

Results

Evaluation of Human Patient Samples

MtHsp70 was assessed in isolated mitochondrial subpopulations from atrial appendage tissue from non-diabetic, T1DM and T2DM patients. Our data revealed decreased mtHsp70 protein content in the IFM of T1DM patients as compared to the non-diabetic patients; however, it did not reach significance ($P = 0.1$) (**Figure 3.1B**). No changes in protein expression level were found in the SSM (**Figure 3.1A**). Conversely, the T2DM SSM showed decreased mtHsp70, with no changes noted in the IFM (**Figure 3.1C-D**).

MtHsp70 Transgenic Mice Characterization

Tissue homogenates were tested for mtHsp70 protein expression. MtHsp70 transgenic mice possessed higher levels of mtHsp70 protein solely in cardiac tissue, with no changes in any other tissue type (**Figure 3.2C**). To determine whether mtHsp70 expression was increased in the mitochondrion, we assessed mtHsp70 protein levels in cardiac mitochondrial subpopulations and observed a significant increase in its expression in both the SSM and IFM (**Figure 3.2D**).

Impact of T1DM and T2DM on mtHsp70

T1DM IFM displayed decreased expression of mtHsp70; however, overexpression of mtHsp70 restored the protein expression (**Figure 3.3B**). SSM were not altered as a result of T1DM (**Figure 3.3A**). In the T2DM heart, mtHsp70 protein levels were decreased in the SSM, and mtHsp70 overexpression was able to restore these levels, while the IFM were not impacted (**Figure 3.3C-D**).

Cardiac Contractile Function

Ejection fraction (EF), fractional shortening (FS) and cardiac output were significantly decreased in T1DM mice as compared to controls, but mtHsp70 restored these decrements (**Table 3.1**). Speckle-tracking based strain echocardiography provided an additional measure of left ventricular (LV) function, specifically longitudinal strain (LS) and longitudinal strain rate (LSR) (34; 35). In agreement with our previous study, we found no changes in LS in the T1DM mice as compared to the controls (**Table 3.1**) (28). Decrements in the T1DM LSR measurement was observed and subsequently restored with mtHsp70 overexpression (**Table 3.1**) (28). Further, in the LSR measure, we assessed the impact of T1DM on the six segments that make up the LV: Posterior Apex (PA), Posterior Mid (PM), Posterior Base (PB), Anterior Apex (AA), Anterior Mid (AM) and Anterior Base (AB). We found a significant decrease in the PA and AA regions of the T1DM animals as compared to controls, with the PA regional function showing a trending (P=0.06) restoration with mtHsp70 overexpression (**Table 3.1**).

Heart rate, EF and FS were significantly decreased in db/db mice versus control; however, mtHsp70 restored these measures (**Table 3.2**). Further, diametric and volumetric changes in the LV during systole were increased during T2DM, which were attenuated with mtHsp70 overexpression (**Table 3.2**). LS and LSR were significantly decreased in the db/db animals as compared to their controls and mtHsp70 overexpression led to the restoration of these measurements in the face of T2DM (**Table 3.2**). In the LS regional measurements, the PB, PA and AM regions were detrimentally impacted in the db/db animals, with mtHsp70 overexpression providing restoration to the PB and PA regions (**Table 3.2**). LSR regional analyses revealed decreased function in the PA, PB, AB, AM, and AA regions in the db/db animals, with mtHsp70 overexpression preserving function in the PB, PA, and AM regions (**Table 3.2**).

Mitochondrial Protein Import

Analyses of protein import efficiency in the T1DM SSM revealed no differences between any of the groups at 30s, 1 min and 2 min time points (**Figure 3.4A**). In contrast, T1DM IFM displayed a significant decrease in protein import efficiency at 2 mins, which was restored with mtHsp70 overexpression (**Figure 3.4B**). Conversely, in the T2DM SSM, protein import efficiency at 30s, 1 min and 2 min were decreased relative to control (**Figure 3.4C**). MtHsp70 overexpression restored protein import efficiency in the T2DM SSM back to that of control levels, while T2DM IFM displayed no import deficiencies (**Figure 3.4C-D**).

MtHsp70 T1DM Proteomic Changes in IFM

During T1DM, overexpression of mtHsp70 impacted protein expression of the ETC differentially. The majority of proteins were increased in complexes I, III, IV and the F_0 component of complex V, while the F_1 complex was decreased (**Figure 3.5A**). Proteins involved in fatty acid oxidation were decreased in mtHsp70 T1DM animals, while glucose oxidation components were increased. These data suggest that proteins involved in glucose oxidation may have been increased in response to the enhanced glycemic milieu present during T1DM, despite an inability to utilize glucose reliably in this model (**Figure 3.5A**). Assessment of the percentage of proteomic alterations within each subcompartment of the mitochondria during T1DM revealed alterations in IFM proteins residing within the IMM (46%) and the mitochondrial matrix (40%) (**Figure 3.5B**). Of the proteins that were increased because of mtHsp70 overexpression, we found approximately 47% located in the IMM and 40% in the mitochondrial matrix (**Figure 3.5C**).

MtHsp70 T2DM Proteomic Changes in SSM

During T2DM, proteins involved in the ETC were increased in complexes I, III, IV, and V (F_0 and F_1 complexes) with mtHsp70 overexpression (**Figure 3.6A**). Enzymes involved in the phosphorylation of glucose and initiation of glucose metabolism pathways were decreased, while proteins essential in fatty acid metabolism were increased in the SSM of mtHsp70 db/db animals suggesting utilization of the substrates available in abundance (fatty acids) (**Figure 3.6A**). Assessment of the percentage of proteomic alterations within each subcompartment of the mitochondria during T2DM revealed alterations in SSM proteins residing within the IMM (46%) and the mitochondrial matrix (45%). Of the proteins that were increased via mtHsp70 overexpression, 53% were located in the IMM, while 47% were in the matrix (**Figure 3.6C**).

Discussion

Mitochondrial dysfunction is central to the etiology of cardiovascular complications observed in diabetic patients (1-13). Our laboratory has reported that mitochondrial subpopulations are differentially affected based on the type of DM, with the SSM being more negatively impacted during T2DM and the IFM being more substantially impacted during T1DM (1-5; 9; 10; 18). The mitochondria are essential for a variety of cellular processes including energy metabolism, oxidative phosphorylation, and ATP synthesis, all of which depend on nuclear-encoded proteins. Thus, the process of nuclear-encoded mitochondrial protein import is critical to the overall function of the mitochondrion. Since the nucleus encodes for the vast majority of proteins in the mitochondrion (>99%), a complex mechanism of translocation through the mitochondrial membranes occurs in order for proteins to enter a particular mitochondrial subcompartment and perform their specific functions, ultimately allowing for a properly functioning mitochondrion (36). Previous studies from our laboratory revealed a decrease in nuclear-encoded mitochondrial protein import efficiency in the T1DM IFM (1; 2).

We speculated that decrements in nuclear-encoded mitochondrial protein import was due to decreased mtHsp70 content, which was found during proteomic analyses (2; 4). As a result, the current study was designed to test the hypothesis that overexpression of mtHsp70 would increase the efficiency of nuclear-encoded mitochondrial protein import. MtHsp70 is an essential component of the PAM complex, anchored to Tim44 within the mitochondrial matrix and serves to “trap” and “pull” the translocating preprotein through the IMM in an ATP-dependent manner (25). Our results revealed decrements at the 2 min time point in the T1DM IFM, with no changes noted at 30s and 1 min; however, the T2DM SSM displayed changes at all time points. These differences may be a function of the distinct etiology and duration of the pathologies. The db/db animals become obese and show elevated plasma insulin at approximately 3-weeks-old, with

hyperglycemia occurring as early as 4-weeks-old (37), thus these animals endure the diabetic milieu throughout the course of the 16-week study, while T1DM is induced by pancreatic β-cell destruction and manifested in the animal for 6 weeks. While it has been shown that mitochondrial subpopulations are differentially impacted by these distinct pathologies, it is unknown how aging and exposure to the diabetic environment for differing times impacts mitochondrial subpopulations. In either case, we observed that overexpression of mtHsp70 allowed for the restoration of the mitochondrial import process in the T1DM IFM and T2DM SSM regardless of the differences in pathology etiology or disease duration.

An important implication for nuclear-encoded mitochondrial protein import is its impact on the mitochondrial proteome. During DM, proteomic analyses have revealed alterations in mitochondrial functional processes such as oxidative phosphorylation and ATP synthesis, which could result from decrements in nuclear-encoded mitochondrial protein import (1; 2; 8; 14-16). Interestingly, during DM, mtHsp70 was affected with decreases in the T2DM SSM and T1DM IFM, which is consistent in both animal and human patient models (2-4). MtHsp70 overexpression increased proteins involved in ETC complexes, along with the transporter protein Slc25a3, independent of diabetic type and mitochondrial subpopulation. Proteomic analyses revealed a differential impact on β-oxidation with mtHsp70 overexpression during T1DM and T2DM, with fatty acid metabolism being decreased in the mtHsp70 T1DM IFM, while showing increases in the mtHsp70 T2DM SSM. These findings suggest that during T1DM and T2DM, mtHsp70 overexpression preserves the import of proteins that are required for processing the substrates that are most abundant despite an inability to do so. Proteomic surveys suggest that approximately 67% of mitochondrial proteins reside in the mitochondrial matrix, followed by 21% located within the IMM, and 6% and 4% residing in the IMS and OMM, respectively (38; 39). Independent of diabetic type and mitochondrial subpopulation, the IMM and matrix were the most predominantly

affected mitochondrial subcompartments for proteomic alterations, with mtHsp70 overexpression revealing targeted restoration within the locations. This was particularly relevant for the IMM which displayed the largest benefit in terms of protein restoration from mtHsp70 overexpression, which may be a function of the greater number of proteins lost in this region during diabetic insult.

Without properly functioning mitochondria and ample ATP production, cardiac contractile dysfunction can occur (1; 2; 4; 5; 37). In the current study, we observed decreases in LV pump function as reflected by changes in EF and FS, along with volume and diametric changes during systole in both the T1DM and T2DM hearts. Overexpression of mtHsp70 restored these measures back to that of control. Analyses using the speckle-tracking based strain software to evaluate global and regional LS and LSR were performed to provide a more complete picture for the deficits noted in the LV. Literature suggests that LS provides a good correlation to LVEF, a measure that is decreased during both T1DM and T2DM (4; 28; 35; 40). Decrements in LS and LSR during both T1DM and T2DM provide complementary evidence of LV systolic dysfunction with subsequent restoration via mtHsp70 overexpression. Evaluation of regional differences revealed commonalities between LSR in T1DM and T2DM with decrements in the apex regions, in which mtHsp70 overexpression was able to restore the PA region independent of DM type. Further, mtHsp70 overexpression provided more regional benefit during T2DM. This restoration potentially occurred due to a positive impact on mitochondrial functionality through increased efficiency of nuclear-encoded mitochondrial proteins, which would be critical for stabilization of the mitochondrial proteome in the face of pathological insult. It is interesting to note that ATP production from each subpopulation is likely critical for efficient cardiac contractile function, indicating that both may play a role in preserving cardiac function during pathological states. Further, an interconnected mitochondrial network through the mitochondrial reticulum could provide a pathway for energy distribution within the cardiomyocyte (41; 42), thus allowing for the

restoration of cardiac contractile function by mtHsp70, despite different mitochondrial subpopulations being affected.

In conclusion our data reveal for the first time, several key findings: 1) disruption of mitochondrial proteomic signature in the spatially-distinct subpopulation most impacted by a given diabetic phenotype is linked to an inability to efficiently import nuclear-encoded mitochondrial proteins; 2) overexpression of mtHsp70 levels provides restoration of protein import efficiency and ultimately proteomic signature in the spatially-distinct subpopulation most impacted by a given diabetic phenotype; 3) overexpression of mtHsp70 provides cardiac contractile benefit in both T1DM and T2DM. Taken together, these findings suggest that restoration of a key import constituent of the active protein import motor provides therapeutic benefit to mitochondrial proteome signature, highlighting the critical role of this mitochondrial process.

Acknowledgements and Grants

This work was supported by the National Institutes of Health from the National Heart, Lung and Blood Institute grant R56 HL128485 and the WVU CTSI grant U54GM104942 awarded to JMH. This work was supported by a National Science Foundation IGERT: Research and Education in Nanotoxicology at West Virginia University Fellowship grant 1144676 awarded to QAH. This work was supported by an American Heart Association Predoctoral Fellowship grant AHA 14PRE19890020 awarded to DLS. This work was supported by an American Heart Association Predoctoral Fellowship grant AHA 13PRE16850066 awarded to CEN. Small animal imaging were performed in the WVU Animal Models & Imaging Facility and supported by S10 RR026378. Flow Cytometry analyses were performed by the WVU Flow Cytometry & Single Cell Core and supported by P30 GM103488 and S10 OD016165. Ingenuity Pathway Analyses were supported by WV INBRE Grant P20 GM103434. Proteomic analyses were performed in conjunction with Protea Biosciences.

Author Contributions

D.L.S., Q.A.H., C.E.N., K.M.H., M.V.P., S.M.S. researched data. D.L.S., Q.A.H., J.M.H. performed statistical analyses. D.L.S. and Q.A.H. wrote the manuscript. D.L.S., Q.A.H., C.E.N., K.M.H., M.V.P., S.M.S., J.M.H. reviewed/edited manuscript. D.L.S., Q.A.H., J.M.H. contributed to discussion.

Disclosures

None

References

1. Baseler WA, Dabkowski ER, Jagannathan R, Thapa D, Nichols CE, Shepherd DL, Croston TL, Powell M, Razunguzwa TT, Lewis SE, Schnell DM, Hollander JM: Reversal of mitochondrial proteomic loss in Type 1 diabetic heart with overexpression of phospholipid hydroperoxide glutathione peroxidase. *Am J Physiol Regul Integr Comp Physiol* 2013;304:R553-565

2. Baseler WA, Dabkowski ER, Williamson CL, Croston TL, Thapa D, Powell MJ, Razunguzwa TT, Hollander JM: Proteomic alterations of distinct mitochondrial subpopulations in the type 1 diabetic heart: contribution of protein import dysfunction. *Am J Physiol Regul Integr Comp Physiol* 2011;300:R186-200

3. Croston TL, Thapa D, Holden AA, Tveter KJ, Lewis SE, Shepherd DL, Nichols CE, Long DM, Olfert IM, Jagannathan R, Hollander JM: Functional deficiencies of subsarcolemmal mitochondria in the type 2 diabetic human heart. *Am J Physiol Heart Circ Physiol* 2014;307:H54-65

4. Dabkowski ER, Baseler WA, Williamson CL, Powell M, Razunguzwa TT, Frisbee JC, Hollander JM: Mitochondrial dysfunction in the type 2 diabetic heart is associated with alterations in spatially distinct mitochondrial proteomes. *Am J Physiol Heart Circ Physiol* 2010;299:H529-540

5. Dabkowski ER, Williamson CL, Bukowski VC, Chapman RS, Leonard SS, Peer CJ, Callery PS, Hollander JM: Diabetic cardiomyopathy-associated dysfunction in spatially distinct mitochondrial subpopulations. *Am J Physiol Heart Circ Physiol* 2009;296:H359-369

6. Flarsheim CE, Grupp IL, Matlib MA: Mitochondrial dysfunction accompanies diastolic dysfunction in diabetic rat heart. *Am J Physiol* 1996;271:H192-202

7. Rolo AP, Palmeira CM: Diabetes and mitochondrial function: role of hyperglycemia and oxidative stress. *Toxicol Appl Pharmacol* 2006;212:167-178

8. Shen X, Zheng S, Thongboonkerd V, Xu M, Pierce WM, Jr., Klein JB, Epstein PN: Cardiac mitochondrial damage and biogenesis in a chronic model of type 1 diabetes. *Am J Physiol Endocrinol Metab* 2004;287:E896-905

9. Thapa D, Nichols CE, Lewis SE, Shepherd DL, Jagannathan R, Croston TL, Tveter KJ, Holden AA, Baseler WA, Hollander JM: Transgenic overexpression of mitofilin attenuates diabetes mellitus-associated cardiac and mitochondria dysfunction. *J Mol Cell Cardiol* 2015;79:212-223

10. Williamson CL, Dabkowski ER, Baseler WA, Croston TL, Alway SE, Hollander JM: Enhanced apoptotic propensity in diabetic cardiac mitochondria: influence of subcellular spatial location. *Am J Physiol Heart Circ Physiol* 2010;298:H633-642

11. Bugger H, Abel ED: Mitochondria in the diabetic heart. *Cardiovasc Res* 2010;88:229-240

12. Boudina S, Abel ED: Diabetic cardiomyopathy revisited. *Circulation* 2007;115:3213-3223

13. Boudina S, Abel ED: Diabetic cardiomyopathy, causes and effects. *Rev Endocr Metab Disord* 2010;11:31-39

14. Bugger H, Chen D, Riehle C, Soto J, Theobald HA, Hu XX, Ganesan B, Weimer BC, Abel ED: Tissue-specific remodeling of the mitochondrial proteome in type 1 diabetic akita mice. *Diabetes* 2009;58:1986-1997

15. Hamblin M, Friedman DB, Hill S, Caprioli RM, Smith HM, Hill MF: Alterations in the diabetic myocardial proteome coupled with increased myocardial oxidative stress underlies diabetic cardiomyopathy. *J Mol Cell Cardiol* 2007;42:884-895

16. Turko IV, Murad F: Quantitative protein profiling in heart mitochondria from diabetic rats. *J Biol Chem* 2003;278:35844-35849

17. Bugger H, Boudina S, Hu XX, Tuinei J, Zaha VG, Theobald HA, Yun UJ, McQueen AP, Wayment B, Litwin SE, Abel ED: Type 1 diabetic akita mouse hearts are insulin sensitive but

manifest structurally abnormal mitochondria that remain coupled despite increased uncoupling protein 3. *Diabetes* 2008;57:2924-2932

18. Croston TL, Shepherd DL, Thapa D, Nichols CE, Lewis SE, Dabkowski ER, Jagannathan R, Baseler WA, Hollander JM: Evaluation of the cardiolipin biosynthetic pathway and its interactions in the diabetic heart. *Life sciences* 2013;93:313-322

19. Dabkowski ER, Williamson CL, Hollander JM: Mitochondria-specific transgenic overexpression of phospholipid hydroperoxide glutathione peroxidase (GPx4) attenuates ischemia/reperfusion-associated cardiac dysfunction. *Free Radic Biol Med* 2008;45:855-865

20. Jagannathan R, Thapa D, Nichols CE, Shepherd DL, Stricker JC, Croston TL, Baseler WA, Lewis SE, Martinez I, Hollander JM: Translational Regulation of the Mitochondrial Genome Following Redistribution of Mitochondrial MicroRNA in the Diabetic Heart. *Circ Cardiovasc Genet* 2015;8:785-802

21. Baseler WA, Croston TL, Hollander JM: Functional Characteristics of Mortalin. In *Mortalin Biology: Life, Stress and Death* Kaul SC, Wadhwa R, Eds. New York, Springer, 2012, p. 55-80

22. Calvo S, Jain M, Xie X, Sheth SA, Chang B, Goldberger OA, Spinazzola A, Zeviani M, Carr SA, Mootha VK: Systematic identification of human mitochondrial disease genes through integrative genomics. *Nature genetics* 2006;38:576-582

23. Perocchi F, Jensen LJ, Gagneur J, Ahting U, von Mering C, Bork P, Prokisch H, Steinmetz LM: Assessing systems properties of yeast mitochondria through an interaction map of the organelle. *PLoS genetics* 2006;2:e170

24. Anderson S, Bankier AT, Barrell BG, de Bruijn MH, Coulson AR, Drouin J, Eperon IC, Nierlich DP, Roe BA, Sanger F, Schreier PH, Smith AJ, Staden R, Young IG: Sequence and organization of the human mitochondrial genome. *Nature* 1981;290:457-465

25. Voos W, Martin H, Krimmer T, Pfanner N: Mechanisms of protein translocation into mitochondria. *Biochim Biophys Acta* 1999;1422:235-254

26. Williamson CL, Dabkowski ER, Dillmann WH, Hollander JM: Mitochondria protection from hypoxia/reoxygenation injury with mitochondria heat shock protein 70 overexpression. *Am J Physiol Heart Circ Physiol* 2008;294:H249-256

27. Gulick J, Subramaniam A, Neumann J, Robbins J: Isolation and characterization of the mouse cardiac myosin heavy chain genes. *J Biol Chem* 1991;266:9180-9185

28. Shepherd DL, Nichols CE, Croston TL, McLaughlin SL, Petrone AB, Lewis SE, Thapa D, Long DM, Dick GM, Hollander JM: Early detection of cardiac dysfunction in the type 1 diabetic heart using speckle-tracking based strain imaging. *J Mol Cell Cardiol* 2016;90:74-83

29. Nichols CE, Shepherd DL, Knuckles TL, Thapa D, Stricker JC, Stapleton PA, Minarchick VC, Erdely A, Zeidler-Erdely PC, Alway SE, Nurkiewicz TR, Hollander JM: Cardiac and mitochondrial dysfunction following acute pulmonary exposure to mountaintop removal mining particulate matter. *Am J Physiol Heart Circ Physiol* 2015;309:H2017-2030

30. Palmer JW, Tandler B, Hoppel CL: Biochemical properties of subsarcolemmal and interfibrillar mitochondria isolated from rat cardiac muscle. *J Biol Chem* 1977;252:8731-8739

31. Bradford MM: A rapid and sensitive method for the quantitation of microgram quantities of protein utilizing the principle of protein-dye binding. *Anal Biochem* 1976;72:248-254

32. Stojanovski D, Pfanner N, Wiedemann N: Import of proteins into mitochondria. *Methods in cell biology* 2007;80:783-806

33. Laemmli UK: Cleavage of structural proteins during the assembly of the head of bacteriophage T4. *Nature* 1970;227:680-685

34. Marwick TH: Measurement of strain and strain rate by echocardiography: ready for prime time? *J Am Coll Cardiol* 2006;47:1313-1327

35. Brown J, Jenkins C, Marwick TH: Use of myocardial strain to assess global left ventricular function: a comparison with cardiac magnetic resonance and 3-dimensional echocardiography. *American heart journal* 2009;157:102 e101-105

36. Chacinska A, Koehler CM, Milenkovic D, Lithgow T, Pfanner N: Importing mitochondrial proteins: machineries and mechanisms. *Cell* 2009;138:628-644

37. Buchanan J, Mazumder PK, Hu P, Chakrabarti G, Roberts MW, Yun UJ, Cooksey RC, Litwin SE, Abel ED: Reduced cardiac efficiency and altered substrate metabolism precedes the onset of hyperglycemia and contractile dysfunction in two mouse models of insulin resistance and obesity. *Endocrinology* 2005;146:5341-5349

38. Distler AM, Kerner J, Hoppel CL: Proteomics of mitochondrial inner and outer membranes. *Proteomics* 2008;8:4066-4082

39. Schnaitman C, Greenawalt JW: Enzymatic properties of the inner and outer membranes of rat liver mitochondria. *The Journal of cell biology* 1968;38:158-175

40. Choi JO, Shin DH, Cho SW, Song YB, Kim JH, Kim YG, Lee SC, Park SW: Effect of preload on left ventricular longitudinal strain by 2D speckle tracking. *Echocardiography* 2008;25:873-879

41. Glancy B, Hartnell LM, Malide D, Yu ZX, Combs CA, Connelly PS, Subramaniam S, Balaban RS: Mitochondrial reticulum for cellular energy distribution in muscle. *Nature* 2015;523:617-620

42. Skulachev VP: Power transmission along biological membranes. *J Membr Biol* 1990;114:97-112

Figure 3.1

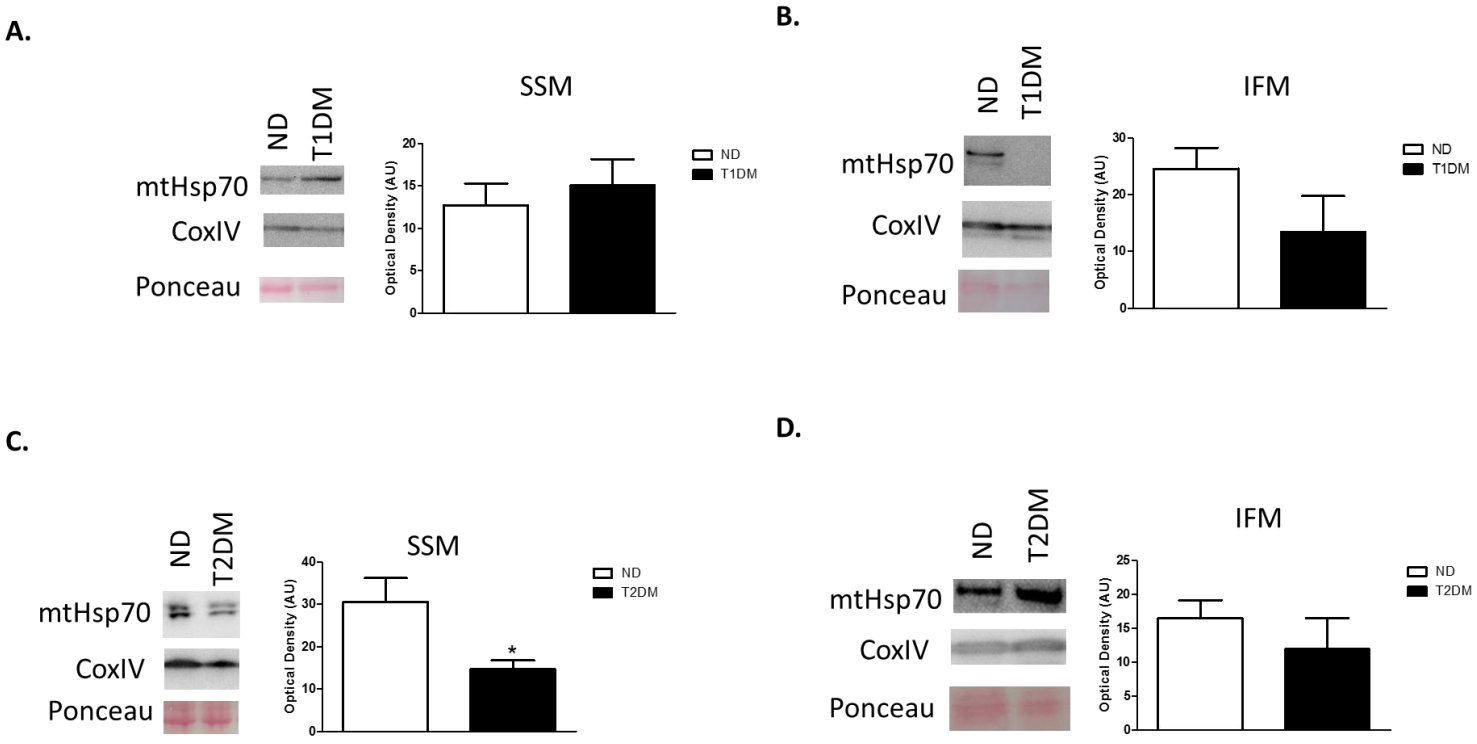
A.
ND
T1DM
mtHsp70
CoxIV
Ponceau
SSM
Optical Density (AU)
ND
T1DM
B.
ND
T1DM
mtHsp70
CoxIV
Ponceau
IFM
Optical Density (AU)
ND
T1DM
C.
ND
T2DM
mtHsp70
CoxIV
Ponceau
SSM
Optical Density (AU)
*
ND
T2DM
D.
ND
T2DM
mtHsp70
CoxIV
Ponceau
IFM
Optical Density (AU)
ND
T2DM

Figure 3.1. Mitochondrial heat shock protein 70 (mtHsp70) levels in human atrial appendage. (A) Representative Western blot analysis and quantification of SSM and (B) IFM in cardiac mitochondria isolated from human atrial appendage in ND and T1DM patients. CoxIV and Ponceau staining were used as loading controls. (C) Representative Western blot analysis and quantification of SSM and (D) IFM in cardiac mitochondria isolated from human atrial appendage in ND and T2DM patients. CoxIV and Ponceau staining were used as loading controls. Values are expressed as means ± SEM. $*P \leq 0.05$ for ND vs DM.

Figure 3.2

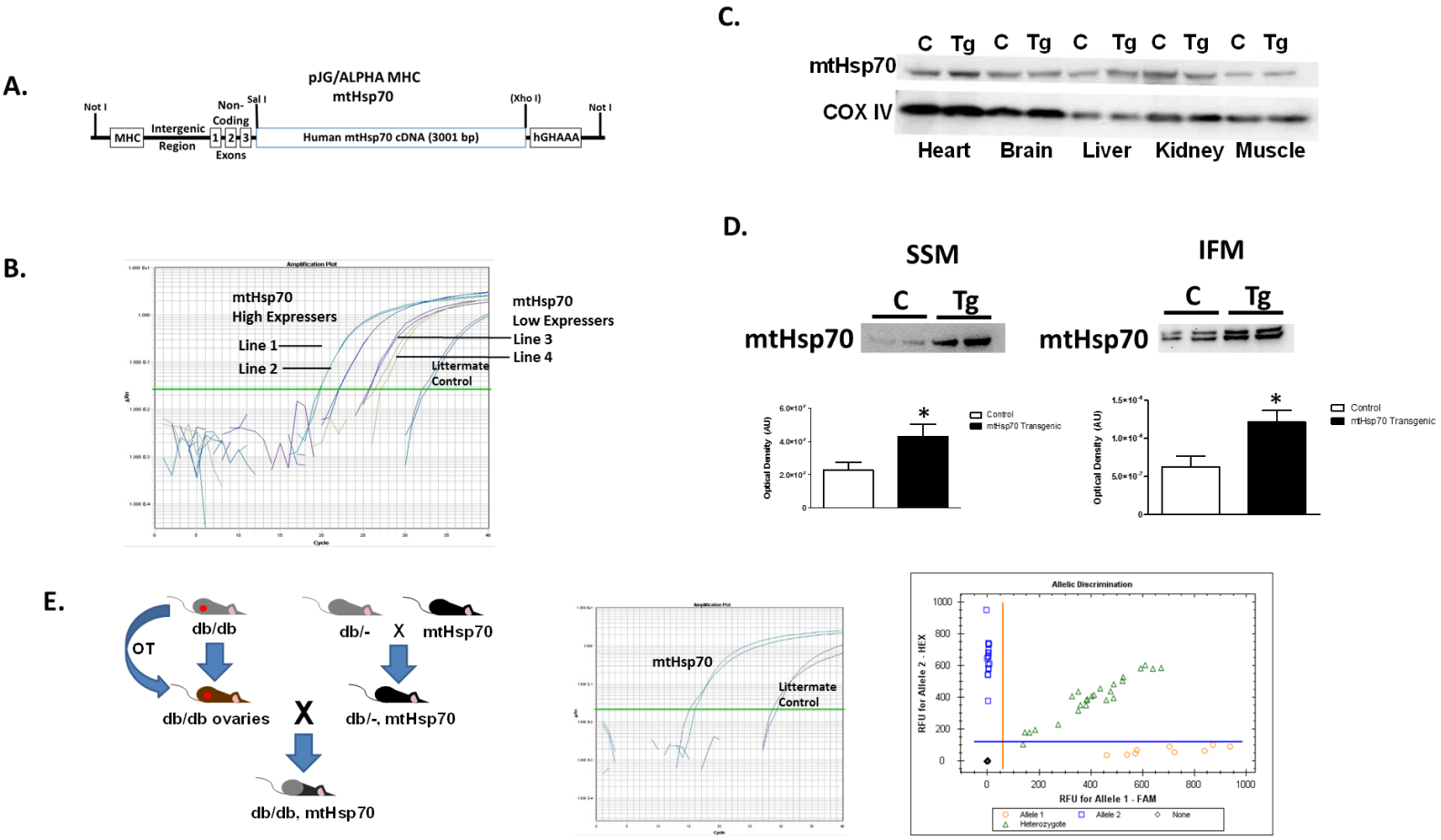
A.
pJG/ALPHA MHC
mtHsp70
Not I
Intergenic Region
MHC
Non-Coding Exons
1
2
3
Sal I
Human mtHsp70 cDNA (3001 bp)
(Xho I)
hGHAAA
Not I
B.
mtHsp70 High Expressers
Line 1
Line 2
mtHsp70 Low Expressers
Line 3
Line 4
Littermate Control
C.
C Tg C Tg C Tg C Tg C Tg
mtHsp70
COX IV
Heart Brain Liver Kidney Muscle
D.
SSM
IFM
C Tg
mtHsp70
Optical Density (AU)
Control
mtHsp70 Transgenic
E.
db/db
OT
db/db ovaries
X
db/-
mtHsp70
db/-, mtHsp70
db/db, mtHsp70
mtHsp70
Littermate Control
Allelic Discrimination
RFU for Allele 2 - HEX
RFU for Allele 1 - FAM
Allele 1
Allele 2
None
Heterozygote

Figure 3.2. MtHsp70 transgenic mouse construction. (A) Schematic of the generation of mtHsp70 transgenic mice. (B) Verification of transgene presence using real-time PCR. (C) Representative Western blot analysis of mtHsp70 protein expression in isolated tissues from control and mtHsp70 transgenic mice. CoxIV was used a loading control. (D) Representative Western blot analysis and quantification of cardiac mitochondrial subpopulations from control and mtHsp70 transgenic mice loaded per mitochondria. (E) Schematic representation of breeding strategy for mtHsp70 db/db mice, verification of transgene presence using real-time PCR and allelic discrimination screening. C = control; Tg = transgenic. Values are expressed as means ± SEM. *$P \leq 0.05$ for control vs. transgenic.

Figure 3.3

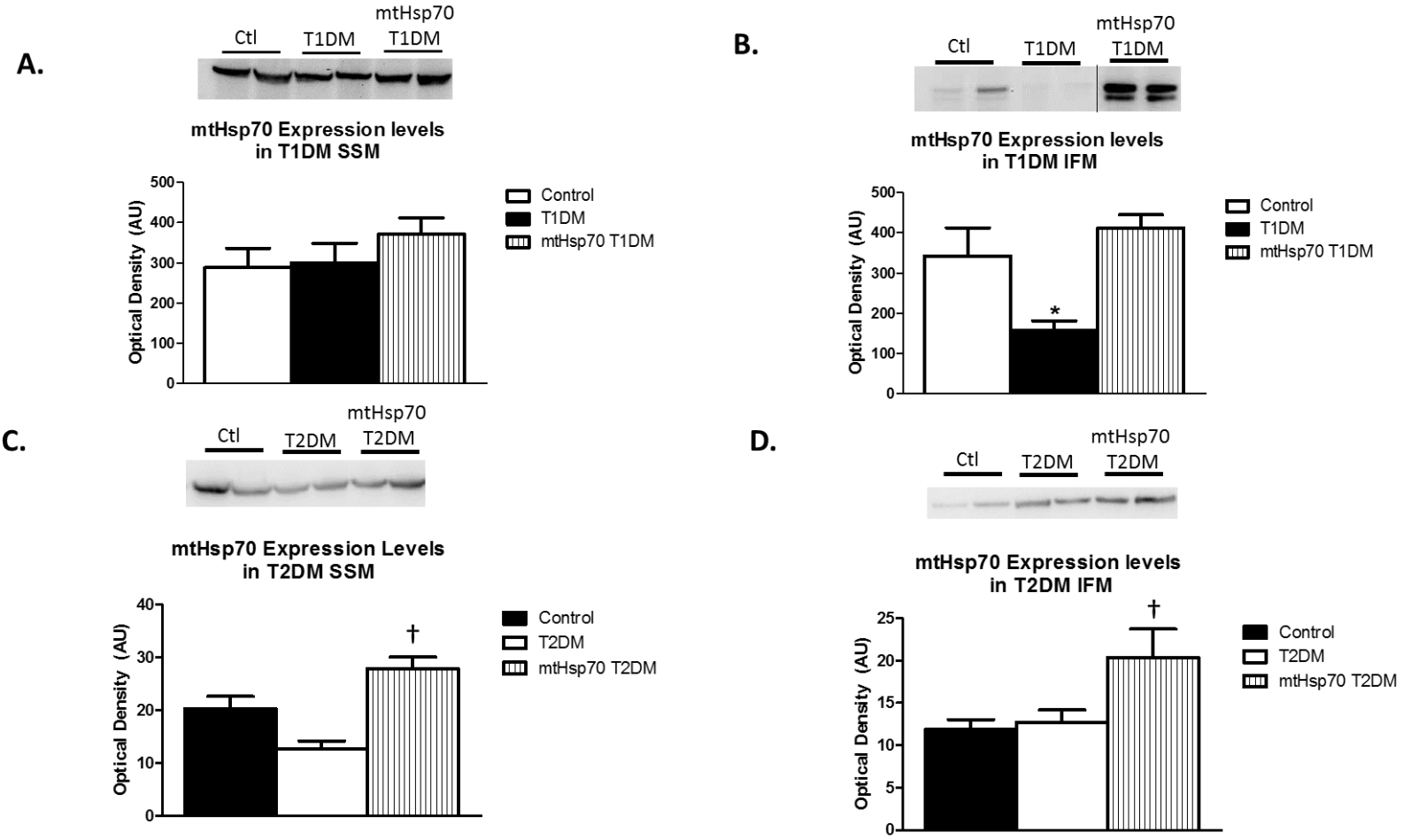
A.
Ctl
T1DM
mtHsp70 T1DM
mtHsp70 Expression levels in T1DM SSM
Optical Density (AU)
500
400
300
200
100
0
Control
T1DM
mtHsp70 T1DM
B.
Ctl
T1DM
mtHsp70 T1DM
mtHsp70 Expression levels in T1DM IFM
*
C.
Ctl
T2DM
mtHsp70 T2DM
mtHsp70 Expression Levels in T2DM SSM
40
30
20
10
0
†
Control
T2DM
mtHsp70 T2DM
D.
mtHsp70 Expression levels in T2DM IFM
25
20
15
10
5

Figure 3.3. MtHsp70 expression during DM. (A) Representative Western blot analysis and quantification of mtHsp70 protein expression in SSM of control, T1DM, and mtHsp70 T1DM mice loaded per mitochondria. (B) Representative Western blot analysis and quantification of mtHsp70 protein expression in IFM of wild-type, T1DM, and mtHsp70 T1DM mice loaded per mitochondria. (C) Representative Western blot analysis and quantification of mtHsp70 protein expression in SSM of wild-type, T2DM, and mtHsp70 T2DM mice loaded per mitochondria. (D) Representative Western blot analysis and quantification of mtHsp70 protein expression in IFM of wild-type, T2DM, and mtHsp70 T2DM mice loaded per mitochondria. Ctl = control; DM = diabetes mellitus; Tg = transgenic; T1DM = type 1 diabetes mellitus; T2DM = type 2 diabetes mellitus. Values are expressed as means ± SEM. *$P \leq 0.05$ for T1DM vs other groups; †$P \leq 0.05$ for mtHsp70 T2DM vs other groups.

Figure 3.4

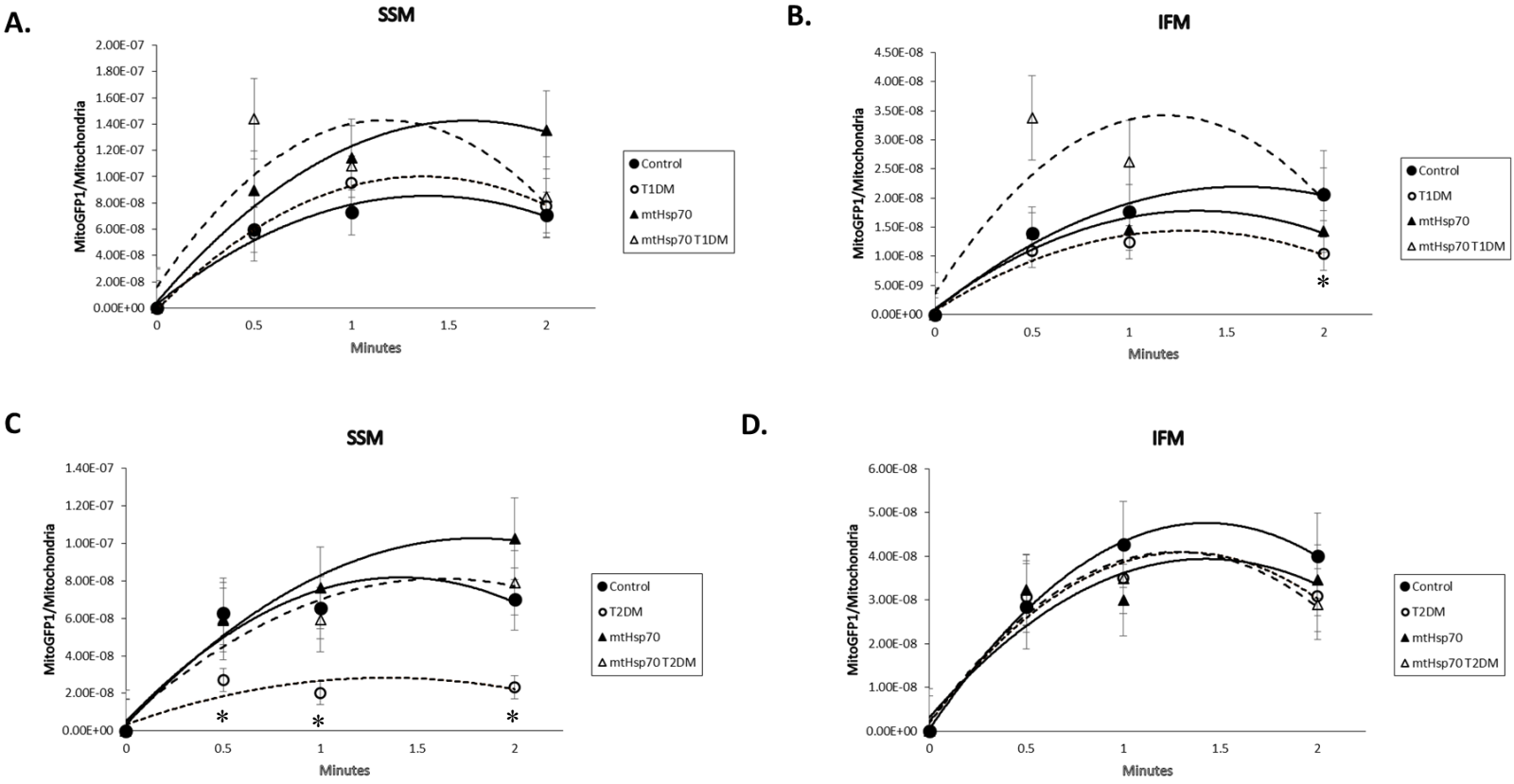
A.
SSM
MitoGFP1/Mitochondria
Minutes
Control
T1DM
mtHsp70
mtHsp70 T1DM
B.
IFM
MitoGFP1/Mitochondria
Minutes
Control
T1DM
mtHsp70
mtHsp70 T1DM
C
SSM
MitoGFP1/Mitochondria
Minutes
Control
T2DM
mtHsp70
mtHsp70 T2DM
D.
IFM
MitoGFP1/Mitochondria
Minutes
Control
T2DM
mtHsp70
mtHsp70 T2DM

Figure 3.4. Mitochondrial protein import during DM. (A) Effect of T1DM and mtHsp70 overexpression on MitoGFP1 import into the SSM and (B) IFM at 30 seconds, 1 minute and 2 minutes. (C) Effect of T2DM and mtHsp70 overexpression on MitoGFP1 import into the SSM and (D) IFM at 30 seconds, 1 minute and 2 minutes. T1DM = type 1 diabetes mellitus; T2DM = type 2 diabetes mellitus. Values are expressed as means ± SEM. *$P \leq 0.05$ for control vs. diabetes mellitus.

Figure 3.5

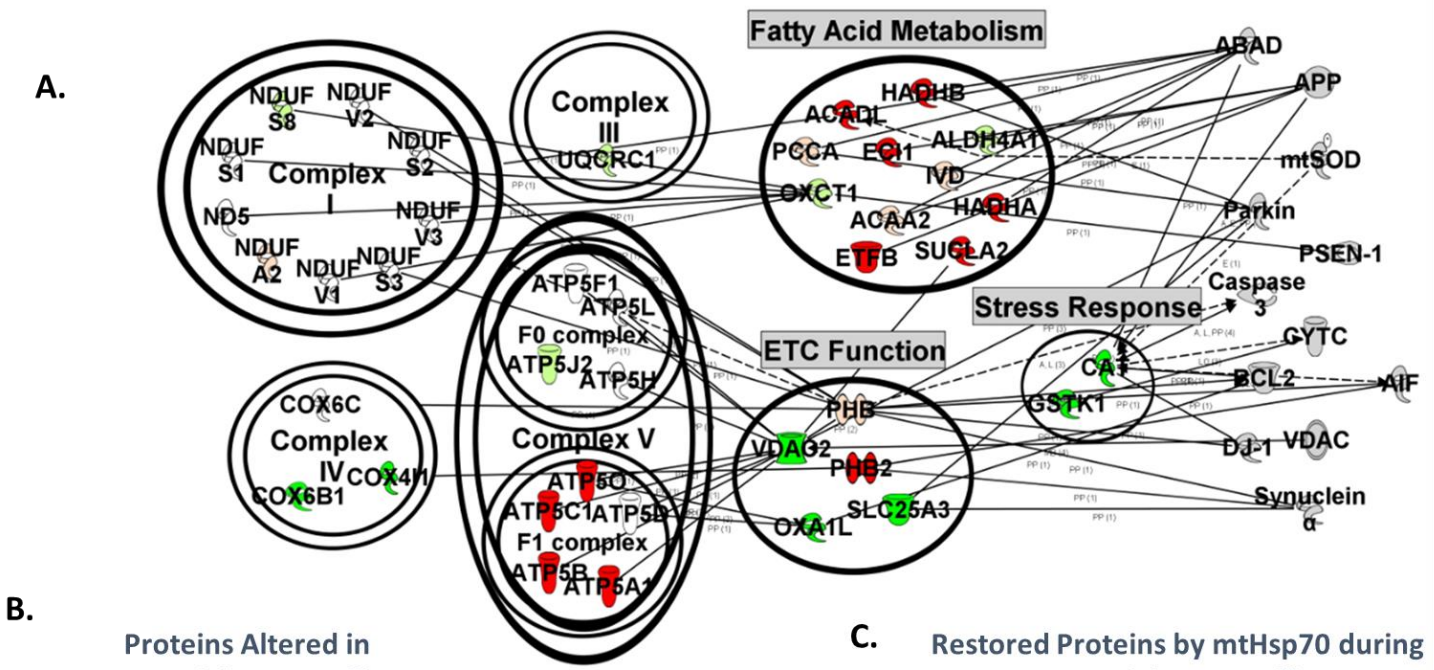
A.
Fatty Acid Metabolism
ABAD
APP
HADHB
ACAT1
ALDH4A1
PCCA
ECI1
IVD
mtSOD
OXCT1
Parkin
ACAA2
HADHA
ETFB
SUCLA2
PSEN-1
Caspase
3
Stress Response
GYTC
ETC Function
CAT
BCL2
AIF
GSTK1
PHB
DJ-1
VDAC
VDAG2
PHB2
Synuclein
α
SLC25A3
OXA1L
NDUF S8
NDUF V2
NDUF S1
Complex I
NDUF S2
ND5
NDUF V3
NDUF A2
NDUF V1
NDUF S3
Complex III
UQCRC1
ATP5F1
ATP5L
F0 complex
ATP5J2
ATP5H
COX6C
Complex IV
COX4I1
COX6B1
Complex V
ATP5O
ATP5C1
ATP5D
F1 complex
ATP5B
ATP5A1

B.

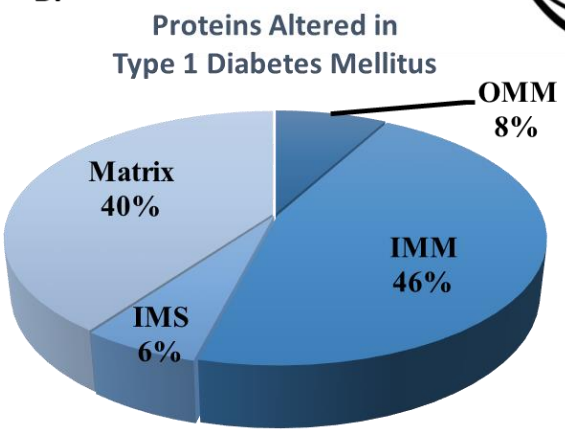
Proteins Altered in
Type 1 Diabetes Mellitus
OMM
8%
Matrix
40%
IMM
46%
IMS
6%

C.

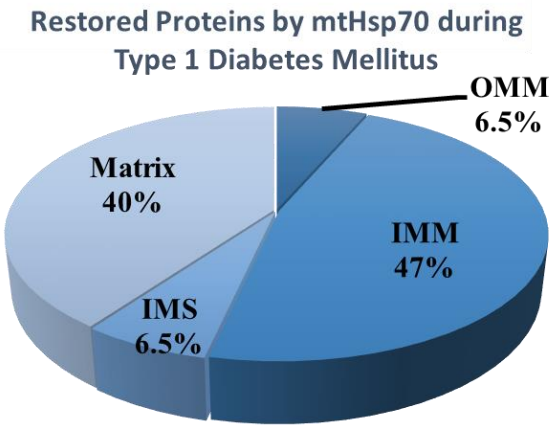
Restored Proteins by mtHsp70 during
Type 1 Diabetes Mellitus
OMM
6.5%
Matrix
40%
IMM
47%
IMS
6.5%

Figure 3.5. Mitochondrial proteome changes during T1DM with mtHsp70 overexpression. (A) IFM from mtHsp70 T1DM mice and T1DM mice representative network connections constructed from the Ingenuity Pathway Analysis (IPA) software database. Arrow heads indicate proteins acting on/being acted upon within a specific pathway. Coloring is indicative of increasing or decreasing protein concentration in the mtHsp70 T1DM mouse model compared to the T1DM mice. Color key: light green = trending increase in expression, dark green = significant increase in expression, light red = trending decrease in expression, dark red = significant decrease in expression, gray = protein constituents not changing in the proteomic analysis. (B) Approximate percentages of protein contents altered and their locales between the T1DM IFM vs. mtHsp70 T1DM IFM. (C) Approximate percentages of proteins restored and their locales with overexpression of mtHsp70 during T1DM. ETC = electron transport chain; OMM = outer mitochondrial membrane; IMS = intermembrane space; IMM = inner mitochondrial membrane.

Figure 3.6

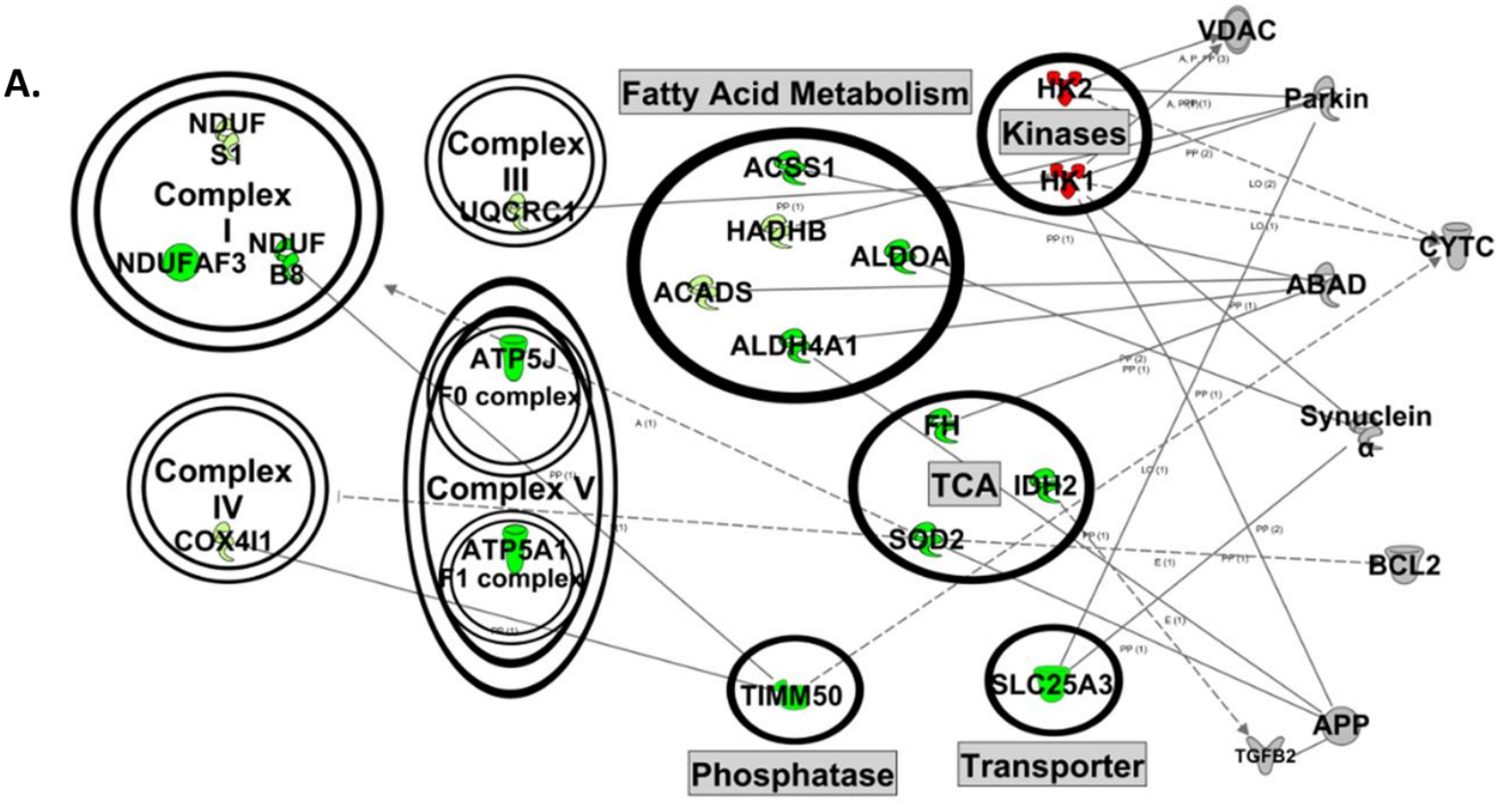
A.
NDUF S1
Complex I
NDUFAF3
NDUF B8
Complex III
UQCRC1
Fatty Acid Metabolism
ACSS1
HADHB
ALDOA
ACADS
ALDH4A1
ATP5J
F0 complex
Complex V
ATP5A1
F1 complex
Complex IV
COX4I1
FH
TCA
IDH2
SOD2
TIMM50
Phosphatase
SLC25A3
Transporter
HK2
Kinases
HK1
VDAC
Parkin
CYTC
ABAD
Synuclein α
BCL2
APP
TGFB2

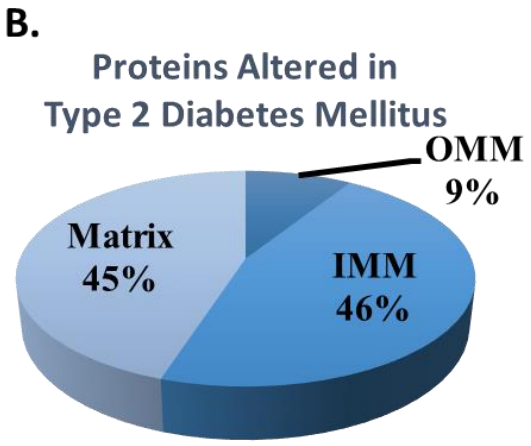
B.
Proteins Altered in
Type 2 Diabetes Mellitus
OMM
9%
Matrix
45%
IMM
46%

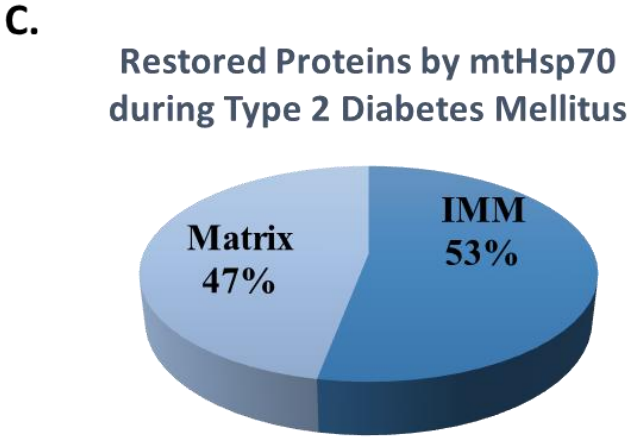
C.
Restored Proteins by mtHsp70
during Type 2 Diabetes Mellitus
Matrix
47%
IMM
53%

Figure 3.6. Mitochondrial proteome changes during T2DM with mtHsp70 overexpression. (A) SSM from mtHsp70 db/db and db/db mice representative network connections constructed from the Ingenuity Pathway Analysis (IPA) software database. Arrow heads indicate proteins acting on/being acted upon within a specific pathway. Coloring is indicative of increasing or decreasing protein concentration in the mtHsp70 db/db mouse model compared to db/db mice. Color key: light green = trending increase in expression, dark green = significant increase in expression, light red = trending decrease in expression, dark red = significant decrease in expression, gray = protein constituents not changing in the proteomic analysis. (B) Approximate percentages of protein contents altered and their locales between the db/db SSM vs. mtHsp70 db/db SSM. (C) Approximate percentages of proteins restored and their locales with overexpression of mtHsp70 during T2DM. TCA = tricarboxylic acid cycle; OMM = outer mitochondrial membrane; IMM = inner mitochondrial membrane.

Table 3.1. T1DM Echocardiographic Measurements

Conventional Echocardiographic Assessment

	Control	T1DM	mtHsp70	mtHsp70 T1DM
Heart Rate (bpm)	531.2 ± 39.5	465.2 ± 19.5	526.6 ± 18.7	430.6 ± 19.7$^{\#}$
Stroke Volume (µL)	34.3 ± 3.9	26.2 ± 1.3	33.4 ± 3.6	35.6 ± 1.8
Ejection Fraction (%)	76.6 ± 2.2	64.5 ± 1.9*$^{\dagger ¥}$	78.2 ± 2.2	76.0 ± 1.7
Fractional Shortening (%)	44.4 ± 1.9	34.4 ± 1.4*$^{\dagger ¥}$	46.5 ± 2.2	44.1 ± 1.7
Cardiac Output (mL/min)	28.6 ± 3.5	13.5 ± 1.0*$^{¥}$	20.7 ± 2.9	26.3 ± 3.0
Diameter;systole (mm)	1.8 ± 0.2	2.1 ± 0.1†	1.7 ± 0.1	1.9 ± 0.1
Diameter;diastole (mm)	3.2 ± 0.2	3.2 ± 0.1	3.1 ± 0.2	3.4 ± 0.1
Volume;systole (µL)	11.0 ± 1.7	15.4 ± 1.5†	9.2 ± 1.4	12.0 ± 1.4
Volume;diastole (µL)	41.9 ± 3.7	42.5 ± 2.7	36.1 ± 3.0	48.2 ± 3.0$^{\#}$
Speckle-tracking Based Strain Echocardiographic Assessment				
Longitudinal Strain (%)	-16.4 ± 1.0	-15.43 ± 0.8$^{¥}$	-18.26 ± 1.3	-18.24 ± 0.9
Longitudinal Strain Rate (1/s)	-6.0 ± 0.3	-5.12 ± 0.2*$^{\dagger ¥}$	-6.98 ± 0.5	-6.50 ± 0.3
Posterior Base (1/s)	-10.5 ± 1.3	-11.1 ± 0.7$^{¥}$	-9.9 ± 1.4	-8.3 ± 1.0
Posterior Mid (1/s)	-7.9 ± 1.0	-8.6 ± 0.7	-8.1 ± 0.6	-8.5 ± 0.7
Posterior Apex (1/s)	-13.8 ± 0.9	-9.38 ± 0.7*†	-14.0 ± 1.1	-12.60 ± 1.3
Anterior Base (1/s)	-9.1 ± 1.3	-9.4 ± 1.1	-11.5 ± 1.8	-10.0 ± 1.0
Anterior Mid (1/s)	-10.3 ± 1.6	-9.2 ± 0.6	-8.7 ± 0.7	-8.5 ± 0.6
Anterior Apex (1/s)	-13.3 ± 1.6	-8.8 ± 0.4*†	-11.6 ± 0.8	-9.5 ± 0.9

Values are shown as means±SEM. *P<0.05 Control versus T1DM animals; $^{\dagger}P$<0.05 T1DM versus mtHsp70 animals; $^{\#}P$<0.05 mtHsp70 T1DM versus mtHsp70 animals; $^{¥}P$<0.05 T1DM versus mtHsp70 T1DM animals. 1-way ANOVA with Bonferroni's Multiple Comparison Post-hoc Test.

Table 3.1. Conventional and Speckle-Tracking Based Strain Echocardiographic Measurements During T1DM. Values are shown as means±SEM. *P<0.05 Control versus T1DM animals; $^{\dagger}P$<0.05 T1DM versus mtHsp70 animals; $^{\#}P$<0.05 mtHsp70 T1DM versus mtHsp70 animals; $^{¥}P$<0.05 T1DM versus mtHsp70 T1DM animals. 1-way ANOVA with Bonferroni's Multiple Comparison Post-hoc Test.

Table 3.2. T2DM Echocardiographic Measurements				
Conventional Echocardiographic Assessment				
	Control	T2DM	mtHsp70	mtHsp70 T2DM
Heart Rate (bpm)	523.3 ± 16.5	430.3 ± 16.6*	500.3 ± 9.3	459.9 ± 38.8
Stroke Volume (µL)	27.3 ± 3.7	28.3 ± 2.8	27.9 ± 1.8	35.3 ± 4.7
Ejection Fraction (%)	77.6 ± 1.7	65.4 ± 1.7*† ¥	82.7 ± 1.5	82.9 ± 2.3
Fractional Shortening (%)	42.3 ± 1.6	35.0 ± 1.3*† ¥	50.4 ± 1.7	50.9 ± 2.4
Cardiac Output (mL/min)	13.7 ± 1.5	12.0 ± 1.2	13.9 ± 0.8	16.0 ± 2.0
Diameter;systole (mm)	1.6 ± 0.1	2.1 ± 0.1†	1.5 ± 0.1	1.6 ± 0.2
Diameter;diastole (mm)	3.0 ± 0.2	3.3 ± 0.2	2.9 ± 0.1	3.2 ± 0.2
Volume;systole (µL)	6.7 ± 1.5	15.7 ± 2.3*†	5.9 ± 0.7	8.0 ± 2.3
Volume;diastole (µL)	30.8 ± 5.4	44.0 ± 4.9	33.8 ± 2.3	43.3 ± 7.0
Speckle-tracking Based Strain Echocardiographic Assessment				
Longitudinal Strain (%)	-18.2 ± 0.8	-13.97 ± 1.0*¥	-17.69 ± 1.6	-17.68 ± 1.0
Posterior Base (%)	-18.4 ± 2.4	-10.5 ± 1.8*¥	-14.4 ± 3.5	-19.5 ± 3.1
Posterior Mid (%)	-13.8 ± 1.8	-19.0 ± 1.6	-20.0 ± 4.3	-15.8 ± 2.4
Posterior Apex (%)	-33.3 ± 2.5	-22.6 ± 3.0*¥	-28.4 ± 3.4	-34.4 ± 2.2
Anterior Base (%)	-20.0 ± 2.7	-18.2 ± 3.0	-19.0 ± 2.3	-20.5 ± 4.6
Anterior Mid (%)	-16.6 ± 1.0	-12.3 ± 1.5*†	-17.9 ± 2.0	-15.6 ± 2.0
Anterior Apex (%)	-23.0 ± 1.9	-20.1 ± 1.2	-24.8 ± 3.3	-17.8 ± 1.4
Longitudinal Strain Rate (1/s)	-7.2 ± 0.7	-4.77 ± 0.3*†¥	-6.43 ± 0.6	-6.79 ± 0.6
Posterior Base (1/s)	-10.0 ± 1.2	-7.1 ± 0.6*†¥	-10.4 ± 1.5	-11.8 ± 1.1
Posterior Mid (1/s)	-7.1 ± 0.7	-8.3 ± 0.7	-10.0 ± 1.7	-7.7 ± 0.5
Posterior Apex (1/s)	-15.5 ± 2.1	-8.2 ± 0.7*¥	-12.1 ± 1.9	-14.0 ± 1.7
Anterior Base (1/s)	-13.8 ± 1.9	-7.4 ± 1.0*†	-12.5 ± 1.6	-9.3 ± 0.7
Anterior Mid (1/s)	-9.3 ± 0.6	-5.4 ± 0.6*†¥	-9.8 ± 0.9	-8.0 ± 0.7
Anterior Apex (1/s)	-10.8 ± 1.0	-7.7 ± 0.7*	-9.3 ± 1.3	-8.5 ± 0.4

Values are shown as means±SEM. *P<0.05 Control versus T2DM animals; †P<0.05 T2DM versus mtHsp70 animals; ¥P<0.05 T2DM versus mtHsp70 T2DM animals. 1-way ANOVA with Bonferroni's Multiple Comparison Post-hoc Test.

Table 3.2. Conventional and Speckle-Tracking Based Strain Echocardiographic Measurements During T2DM. Values are shown as means±SEM. *P<0.05 Control versus T2DM animals; †P<0.05 T2DM versus mtHsp70 animals; ¥P<0.05 T2DM versus mtHsp70 T2DM animals. 1-way ANOVA with Bonferroni's Multiple Comparison Post-hoc Test.

Chapter 4:

The Unique Association of Argonaute 2 and Polynucleotide Phosphorylase: A pathway into the mitochondrion?

Danielle L. Shepherd, Quincy A. Hathaway, Mark V. Pinti, Cody E. Nichols, Shruthi Sreekumar,

Kristen M. Hughes and John M. Hollander

Department of Exercise Physiology, Center for Cardiovascular and Respiratory Sciences, School

of Medicine, West Virginia University, Morgantown, WV, 26505

Running Title: Argonaute 2 and polynucleotide phosphorylase association

Corresponding Author: John M. Hollander
Department of Exercise Physiology
West Virginia University School of Medicine
PO Box 9227
1 Medical Center Drive
Morgantown, WV 26506
Tel: 1-(304) 293-3683
Fax: 1-(304) 293-7105
Email: jhollander@hsc.wvu.edu

Abstract

Cardiac complications and heart failure are the leading cause of death in diabetic patients. The mitochondrion has been implicated in the etiology of the diabetic pathology. Two distinct mitochondrial subpopulations exist within the cardiomyocyte. The subsarcolemmal mitochondria (SSM) are located beneath the sarcolemmal membrane and the interfibrillar mitochondria (IFM) are located between the myofibrils. Proteomic, transcriptomic and epigenomic remodeling occurs during diabetes mellitus in the attempt to adapt to the pathological insult. MicroRNAs (miRNAs) play a vital role in the regulation of gene expression though degradation of target messenger RNAs (mRNAs) or translational repression and have been shown to be present within the mitochondrion; however, the mechanism by which miRNAs traverse the mitochondrial membranes remains unknown. The goal of this study was to elucidate whether polynucleotide phosphorylase (PNPase), an intermembrane space protein potentially anchored to the inner mitochondrial membrane, plays a role in the complicated mechanism of miRNA translocation during type 2 diabetes mellitus. We found an increase in PNPase protein expression in the SSM of the type 2 diabetic human atrial appendage and db/db mouse model. Further, we discovered the novel association of PNPase with Argonaute 2 (Ago2) in both cardiac mitochondrial subpopulations that was subsequently increased in the SSM during the type 2 diabetic insult. In the SSM of the db/db mice, we found an increased level of miR-378, which was associated with a corresponding decrease in ATP6 protein content. Finally, in the HL-1 cardiomyocyte cell line, overexpression of PNPase led to increased miR-378 levels in the mitochondria and a decrease in ATP synthase activity. Altogether, PNPase may potentially be a constituent in the import mechanism of miRNAs via association with Ago2 into cardiac mitochondria.

Keywords

Diabetes Mellitus; MicroRNA; Mitochondria; Polynucleotide Phosphorylase, Argonaute, RNA-Induced Silencing Complex; Import

Introduction

Type 2 diabetes mellitus (T2DM) currently affects 29 million Americans, with an inordinate cost to society of $245 billion in medical bills and missed work (1, 33). Further, T2DM serves as a major risk factor for cardiovascular disease as the heart needs a constant nutrient supply in order to produce the proper amount of energy, which does not always occur in the diabetic pathology (33). During T2DM, when cardiac tissue becomes insulin resistant, a proteomic, transcriptomic and epigenomic remodeling occurs as an adaptive mechanism to the pathological insult (2, 34, 36). Our laboratory and others have shown that the assault to the transcript can occur in both the cytosol and mitochondria within the cardiomyocyte (34, 37). Cardiac mitochondrial subpopluations have been previously shown by our laboratory to be differentially affected during diabetic insult, with the interfibrillar mitochondria (IFM) being negatively influenced during type 1 diabetes mellitus and the subsarcolemmal mitochondria (SSM) predominantly being affected during T2DM (7-9, 17-20, 37, 66).

The mechanism of protein import into the mitochondria consists of the unfolded protein in the cytoplasm being threaded through the translocase of the outer membrane, TOM40, and the translocase of the inner membrane, TIM23, followed by the action of mitochondrial heat shock protein 70 (mtHsp70) “pulling” the polypeptide into the mitochondrial matrix via an ATP-dependent manner (6, 27). Not only are proteins transported into the mitochondria, which is critical due to the vast majority of mitochondrial proteins being encoded by the nuclear genome, but ribosomal RNA (rRNA) and transfer RNA (tRNA) have also been shown to traverse the mitochondrial membranes (3). Polynucleotide phosphorylase (PNPase) situated in the inner mitochondrial membrane and extending into the intermembrane space, has been found to facilitate the transport of rRNA and tRNA based on their hairpin-loop structure (3, 69, 70). This protein also

functions to edit and degrade RNA, as well as plays a role in controlling cellular senescence and cell cycle (44, 56, 57, 60). Interestingly, a major determining factor between RNA degradation or transport by PNPase seems to be the length of the RNA species' 3' overhang. Wang et al. showed that an 8 nucleotide (nt) 3' overhang of a messenger RNA (mRNA) species resulted in degradation, while a 0-2 nt 3' overhang led to transport (43, 64). Various other studies suggested that the machinery facilitating protein import could contribute to RNA import as well (3, 28, 40, 55, 58, 61, 62).

Emerging research is likely to discover how the mitochondrial genome is being regulated to influence both disease initiation and progression. MicroRNAs (miRNAs) are a type of noncoding RNA that have been shown to play a vital role in the regulation of gene expression though degradation of target mRNAs or translational repression (45). MiRNAs exert their influence through binding to the 3'-untranslated region of the target mRNAs (45). The association of miRNA with the RNA-induced silencing complex (RISC) has been shown in the cytoplasm, with the argonaute (AGO) family proteins functioning to help in miRNA repression through the inhibition of protein synthesis when bound to the 3'-untranslated region of the mRNA (5, 30). The miRNA-mediated regulatory potential of the mitochondrial genome is especially precise as the genome itself is comprised of only 37 genes, 13 of which code for protein subunits involved in oxidative phosphorylation and the remaining genes coding for 22 tRNAs and 2 rRNAs (46).

Data from a variety of groups, including our own, has elucidated the presence of miRNA in the mitochondria (3, 4, 11-13, 22, 23, 37, 41, 63-65, 67, 73). Even more exciting has been the validation of miRNA species targeting mRNA transcripts produced by the mitochondrial genome in the mitochondria to control mRNA stability and degradation (22, 23, 26). Since fatty acid oxidation, the citric acid cycle, the electron transport chain and ATP synthase are housed in the

mitochondrial matrix and inner mitochondrial membrane, the differential expression of miRNA in the mitochondria targeting any of these components is consequential to the overall functionality of the organelle. PNPase has been established to play an important role in the import of nuclear RNA; however, its involvement in the import of miRNAs into the mitochondrion needs to be evaluated (55, 58, 69). Our current manuscript focuses on a key player in the mechanism of miRNA import into the mitochondrion. We aim to elucidate whether PNPase in association with Ago2 plays a role in the complicated mechanism of miRNA translocation, influencing the function of SSM during the type 2 diabetic insult.

Research Design and Methods

Human Tissues

The West Virginia University Institutional Review Board and Institutional Biosafety Committee approved all protocols. Patients undergoing cardiac valve replacement or coronary artery bypass graft surgery at Ruby Memorial Hospital in Morgantown, West Virginia, allowed the release of the right atrial appendage tissue to the West Virginia University School of Medicine. Patients were characterized as non-diabetic or type 2 diabetic based on a previous diagnosis of diabetes mellitus by a medical doctor. Pericardial fat was trimmed from right atrial appendage samples and mitochondria isolated as previously described (7, 8, 17-21, 48, 49, 66, 72).

Experimental Animals

The animal experiments performed in this study conform with the National Institutes of Health Eighth Edition Guidelines for the Care and Use of Laboratory Animals and were approved by the West Virginia University Care and Use Committee. Mixed gender *db/db* mice (strain FVB.BKS(D)-Lepr^{db}/ChuaJ) and wild-type (WT) littermate controls (Jackson Laboratories, Bar Harbor, ME) were housed and bred in the West Virginia University Health Sciences Centers animal facility. Microisolator cages were used to maintain animals with *ad libitum* access to food and water and housed on a 12 hour light/dark cycle in a temperature-controlled room. All mice were aged to approximately 20 weeks old and then euthanized for experimentation.

Preparation of Individual Mitochondrial Subpopulations

At approximately 20-22 weeks of age, db/db mice and littermate controls were euthanized, hearts excised and cardiac mitochondrial subpopulations were isolated for analyses as previously

described following the methods of Palmer et al. (49) with minor modifications by our laboratory (7, 8, 17, 19-21, 48, 66). Beneath the sarcolemmal membrane resides a pool of mitochondria termed subsarcolemmal mitochondria (SSM), while the mitochondria that exist between the myofibrils are called interfibrillar mitochondria (IFM). Our laboratory has previously reported SSM dysfunction during the type 2 diabetic pathology, with the IFM being relatively unaffected (19). After isolation of cardiac mitochondrial subpopulations was completed, SSM and IFM were further purified by percoll gradient (23%, 15%, 10% and 3% percoll solution) in the case of the db/db and littermate control animals. The samples were centrifuged in a Beckman Optima MAX-XP Ultracentrifuge (Beckman Coulter, Fullerton, CA) at 32,000 x g for 8 minutes. Mitochondrial subpopulation pellets were resuspended in the appropriate buffer for each assay. Protein concentrations were determined by using the Bradford method with bovine serum albumin as a standard (14).

Cell Culture

For cell culture experiments, the mouse cardiomyocyte cell line (HL-1), which maintains a cardiac-specific phenotype following repeated passages was used as previously described (9, 16, 37). The miR-378 HL-1 overexpressing cell line generated by our laboratory was also used as previously described (37). Cells were grown up in a humidified atmosphere of 5% CO_2/95% air and maintained at 37°C in Claycomb media (Sigma Aldrich, St. Louis, MO) with 10% fetal bovine serum and other supplements as previously described (9).

Overexpression of PNPase

Cells were seeded and transfected at 60% to 70% confluence. RNA importer, PNPase was transfected into the HL-1 cell line to determine if increased overexpression of PNPase leads to increased transport of miRNA into the mitochondrion. Briefly, FuGENE 6 Transfection Reagent (Promega, Madison, WI) was used per manufacturer's instructions. Forty-eight hours post-transfection, cells were washed with PBS and harvested. Sample number was determined by the number of independent transfections performed, accounting for variation of plasmid uptake in cells. Mitochondria were isolated using a mitochondrial isolation kit (Biovision, Milpitas, CA) for protein, qPCR, and enzymatic analyses.

qPCR Analyses

First, total RNA was isolated from HL-1 and HL-1 378 overexpression cell lines and converted to cDNA using the miRNA First Strand cDNA synthesis kit (Origene, Rockville, MD) per the manufacturer's protocol. The cDNA was used with SYBR Green components in a total sample volume of 25µL: 12.5µL 2X SYBER Green I qPCR Master Mix (Origene, Rockville, MD), 9.5µL RNAse/Nuclease free H_2O, 1µL of primer for the control (U6) or experimental group (MP300294 – miR-378, Origene, Rockville, MD), and 2µL of cDNA (~500ng/µL). Data is expressed as fold change relative to the difference in C_t expression of the miR-378 to U6 log expression. All samples were run in duplicate for both the miR-378 and U6 primers. Standard deviation values in either primer pair exceeding a C_t value of 0.5 were excluded from the study. 7900HT Fast Real-Time PCR System (Applied Biosystems, Foster City, CA) was used for analysis, with reaction conditions optimized to Origene's qSTAR miRNA qPCR Detection System instructions.

Immunoprecipitation Analyses

Dynabeads® protein G (Life Technologies, Grand Island, NY) were used to determine protein associations between Ago2 and PNPase per the manufacturer's instructions. Briefly, 50uL of Dynabeads® protein G were incubated with either anti-PNPT1 (PNPase; OriGene, Rockville, MD) or anti-Ago2 (Abcam, Cambridge, MA) primary antibody overnight. The beads were subsequently washed in NP-40 buffer and 150ug of mitochondrial protein, as determined by the Bradford method, was resuspended with beads and NP-40 wash/binding buffer and incubated overnight. Finally, beads were washed and loading dye added to the samples and Western blots performed on the eluted protein and subsequently probed with the protein of interest to examine the associations.

Western Blot Analyses

SDS-PAGE was run on 4-12% gradient gels, as previously described (7, 8, 19, 42, 48, 66, 72) with modifications. For assessment of protein content, equal amounts of protein were loaded as determined by the Bradford method using bovine serum albumin as a standard as previously described (14). Further, assessment of protein loading control was done by utilizing the COXIV antibody and Ponceau S solution (Sigma, St. Louis, MO). Relative amounts of PNPase, Ago2, ATP6, GAPDH, and COXIV were assessed using the following primary antibodies: anti-PNPT1 (PNPase; OriGene, Rockville, MD); anti-Ago2 (Abcam, Cambridge, MA); anti-ATP6 (Abcam, Cambridge, MA); anti-GAPDH (Abcam, Cambridge, MA); and anti-COXIV (Cell Signaling Technology, Danvers, MA). The secondary antibodies used in the analyses were goat anti-mouse IgG horseradish peroxidase (HRP) conjugate (Pierce Biotechnology, Rockford, IL) for Ago2 and

GAPDH and goat anti-rabbit IgG HRP conjugate (Cayman Chemical, Ann Arbor, MI) for the PNPase, ATP6 and CoxIV primary antibodies. Pierce Enhanced Chemiluminescence Western Blotting substrate (Pierce Biotechnology; Rockford, IL) was used to detect signal per manufacturer's instructions. A G:Box Bioimaging system (Syngene, Frederick, MD) was used to detect signals and data were captured using GeneSnap/GeneTools software (Syngene, Frederick, MD). Densitometry was analyzed using Image J Software (National Institutes of Health, Bethesda, MD) and expressed as arbitrary optical density units.

Complex Activities

Electron transport chain complexes I, III, and IV were measured in mitochondria isolated from the cells spectrophotometrically as previously described (19-21, 68). Briefly, by measuring NADH oxidation at 340 nm, complex I activity was determined. Complex III activity was measured by assessing the reduction of cytochrome *c* at 550 nm in the presence of 50 µM of reduced decylubiquinone, while complex IV activity evaluated cytochrome *c* oxidation at 550 nm. Further, ATP synthase activity was measured as oligomycin-sensitive ATPase activity using an assay coupled with pyruvate kinase, which converts ADP to ATP and produces pyruvate from phosphoenolpyruvate as described previously (19, 29, 52, 53). Values for complex activities were expressed as nanomoles substrate converted/min/mg of protein.

Statistics

Means ± SEMs were calculated for all data sets. Data were analyzed with two-tailed Student's t-test to compare differences between groups (GraphPad Software, La Jolla, CA) where a $P \leq 0.05$ was considered significant.

Results

PNPase and Ago2 in Cytosolic Fractions in Non-diabetic and Type 2 Diabetic Settings

PNPase and Ago2 protein expression were assessed in non-diabetic and type 2 diabetic patients. Cytosolic fractions were isolated from atrial appendage tissue and revealed a faint band for PNPase in the cytosolic fraction with no significant alterations in Ago2 in the type 2 diabetic patients (**Figure 4.1A**). A similar phenomenon was noted in the db/db animal model for type 2 diabetes mellitus with no PNPase showing up in the cytosolic fraction and Ago2 remaining unchanged during the pathological setting (**Figure 4.1B**). As a result of our findings, we decided to assess the protein content of Ago2 and PNPase in mitochondrial subpopulations.

Impact of Type 2 Diabetes Mellitus on PNPase and Ago2 in Cardiac Mitochondrial Subpopulations

When assessing the Ago2 protein content in human non-diabetic and type 2 diabetic patients, there was no change noted in either cardiac mitochondrial subpopulations (**Figure 4.2A-B**). Further, in the db/db model, SSM and IFM showed no alterations in Ago2 protein expression levels (**Figure 4.2C-D**). Interestingly, in the type 2 diabetic SSM from atrial appendage tissue from patients, PNPase protein content was increased (**Figure 4.3A**); however, in the IFM, no changes were noted in PNPase protein expression levels (**Figure 4.3B**). A similar story was found in the db/db model, with significantly increased PNPase protein expression levels in the SSM (**Figure 4.3C**), with no changes noted in the IFM subpopulation (**Figure 4.3D**).

Ago2 and PNPase Associate within the Cardiac Mitochondria

Due to our results of finding a conventional cytosolic RISC component in the mitochondrial fraction, we speculate that Ago2 may serve as facilitator for transport of miRNA from the cytosol into the mitochondria. We immunoprecipitated Ago2 from the mitochondrial pellet and found that PNPase was co-immunoprecipitated in both the SSM and IFM subpopulations (**Figure 4.4A-B**). Interestingly, the SSM showed an increased association of immunoprecipitated Ago2 with PNPase (**Figure 4.4A**), while the IFM revealed no difference in the association of these proteins (**Figure 4.4B**). We then performed the reciprocal immunoprecipitation with PNPase, immunoprecipitating with PNPase and looking to see if Ago2 coimmuniprecipitated with this protein. We again found the association between the 2 proteins **(Figure 4.4C-D**). Interestingly, we found a trending increase in association between PNPase and Ago2 in the SSM of the type 2 diabetic animals as compared to their controls (**Figure 4.4C**). Again, we found an association between PNPase and Ago2 in the IFM; however, no differences exist between the control and type 2 diabetic pathology (**Figure 4.4D**).

miR-378 in Cardiac Mitochondria

To assess whether micro-RNAs within the mitochondria are affected in the type 2 diabetic setting, we used qPCR to determine whether miR-378 showed an alteration in expression levels during the diabetic pathology. We found an increase in miR-378 expression level in SSM isolated from db/db cardiac tissue (**Figure 4.5A**), with no changes noted in the IFM (**Figure 4.5A**). Since miR-378 is predicted to target ATP6 within the mitochondrion, we assessed ATP6 protein levels in the SSM and IFM from control and db/db mice (**Figure 4.5B**). Corroborating our miR-378 increased expression levels in the type 2 diabetic SSM, we found decreased ATP6 protein

expression levels in the type 2 diabetic SSM (**Figure 4.5B**). Further, we found no changes in the IFM subpopulation for ATP6 expression levels (**Figure 4.5B**).

Impact of PNPase Overexpression in HL-1 Cardiomyocte Cells

Our laboratory has established and previously published on a HL-1 miR-378 stable overexpression cell line (37). We have elucidated that miR-378 is overexpressed in the mitochondria isolated from this cell line and found that both ATP6 mRNA and ATP6 protein expression levels were down with miR-378 overexpression (37). In the HL-1 cardiomyocyte cell line, we transfected the cells with a plasmid encoding for PNPase and found increased expression levels of PNPase in mitochondria isolated from these cells (**Figure 4.6A**). Further, to determine whether the overexpression of PNPase increased the presence of miR-378 in the mitochondria of Hl-1 cells, we conducted qPCR. We found that overexpression of PNPase significantly increased the miR-378 detected in mitochondria isolated from the HL-1 cells (**Figure 4.6B**). Further, we found that overexpression of miR-378 decreased the ATP synthase activity in isolated mitochondria (**Figure 4.6C**). Interestingly, overexpression of PNPase in the HL-1 cell line also revealed decreased ATP synthase activity. Taken together, these data provide complementary evidence that in a model with PNPase overexpression, miR-378 expression is enhanced within the mitochondria leading to decreased ATP synthase activity, potentially due to an increased mechanism for miRNA transport into the mitochondrion.

Discussion

Mitochondrial dysfunction is central to the etiology of cardiovascular complications seen in diabetic patients (7, 8, 18-20, 31, 54, 59, 66, 72). Within the mitochondria, complex, functional processes occur, such as oxidative phosphorylation and ATP synthesis, which are critical in an appropriately functioning organelle. The mechanisms behind nuclear-encoded mitochondrial protein import and mechanisms of miRNA intercellular transport via exosomes and intracellular transport into the nucleus have been elucidated; however, the process of miRNA import into the mitochondria has proven elusive (6, 24, 27, 71). Nuclear translocation of miRNA involves the co-localization of the Ago2/miRNA complex with Importin 8 on the nuclear membrane followed by transport of the complex into the nucleus (71). Here we have shown a similar co-localization of Ago2 with PNPase in the cardiac mitochondria and this association was increased in the T2DM pathological setting as compared to control mice. While this is not suggestive of an absolute mechanism of miRNA transport into the mitochondrion, with other constituents within the mitochondrion potentially playing a role in import, this work contributes to the validation of specific protein components (PNPase and AGO2) involved in the mechanism of miRNA transport. PNPase upregulation in human T2DM and db/db mice is further complicated by its influence on the transport or degradation of a multitude of RNA species, along with its regulation of other functions.

The decreased activity of ATP synthase in HL-1 PNPase overexpressing cells compared to control HL-1 cells could be a result of a variety of changes downstream of the PNPase protein. One of these changes that may be occurring because of the increase in PNPase is the transport of many miRNA sequences into the mitochondrion, resulting in targeting and negatively regulating transcripts of the electron transport chain or ATP synthase subunits. Further, the decreased activity of ATP synthase in HL-1 miRNA-378 overexpressing cells compared to controls provides a more

causal picture, as miRNA-378 has been shown to directly target and repress the ATP6 subunit of ATP synthase. This corroborates our findings in the T2DM mouse model, where miRNA-378 is upregulated and ATP6 protein expression is downregulated. These changes coincide with an increase in PNPase protein levels within the db/db animals, as well as increased association of PNPase with Ago2. While we have shown that PNPase protein expression level is increased in the T2DM atrial appendages from patient samples as compared to non-diabetic patients, it would be of great interest to determine if the patients also have an association of PNPase and Ago2 within the mitochondrion and further, to see if this association is increased during the diabetic pathology.

MiRNAs localized to the mitochondrion have been found to directly target essential processes such as energy metabolism and apoptosis (22, 23, 37, 41, 50). For example, Das et al. found an increase in miRNA-181c in cardiomyocyte mitochondria during heart failure, which targets and represses mtCOX1, an important component of the respiratory complex IV (22, 23, 25). Further, the role of miR-378 in regulating metabolic processes in multiple organs in the body has been previously noted, with targets include Med13 and Cret in the liver and IGF-1 and ATP6 in the heart (15, 37, 39). Our laboratory previously found an increase in miR-378 in cardiac mitochondria during the type 1 diabetic pathology, which resulted in decreased ATP6 protein content in the IFM and a decreased ATP synthase activity (37). In this study, we have shown an increase in miR-378 and a decrease in ATP6 protein in the SSM during a type 2 diabetic setting, demonstrating that mitochondrial subpopulations are differentially impacted depending on the type of diabetic insult. The systemic pathological environment and accompanying stimuli of the diabetic state undoubtedly provide the impetus for a multitude of proteomic, transcriptomic, and epigenomic adaptations or maladaptations. While this is indeed a complex and interconnected phenomenon of which we have only elucidated a potential component in the process, we present

that differential miRNA expression in the mitochondria of the diabetic heart, particularly miR-378, leads to a decrease in ATP synthase complex activity and potentially contributes to the cardiac dysfunction implicated in T2DM.

The recent characterization of miRNA localization to various organelles within the cell and changes in miRNA species and levels during pathological states suggests a role in miRNA-mediated pathologic phenotypes (3, 32, 51). Further, the introduction of miRNA mimics to increase miRNA species levels that have been downregulated or supplementation with antimiRs to decrease miRNA species levels that have been upregulated, may have the potential to attenuate or reverse decrements due to the pathological state. This strategy is currently being used in the clinic to treat hepatitis C virus, with clinical trials of miRNA mimics and antimiRs underway (38). A variety of miRNA-based therapies to address T2DM and heart disease are in the preclinical trial stage, providing the need for comprehensive study on miRNA effects on different cellular organelles. One such biologic is antimiR-208a, which has been shown to increase systemic metabolism, display a lean phenotype when provided a high-fat diet, and improve overall cardiac function (10, 35, 47). It will be of interest to determine in subsequent studies whether inhibition of miRNA-378 using an antimiR during T2DM will provide benefits to cardiac mitochondrial function and cardiac contractile function. Furthermore, the prospect of elucidating the complicated mechanism for miRNA import into the mitochondrion during T2DM and modulating PNPase expression/activity and its potential role in miRNA import, could lead to a therapeutic paradigm to alleviate mitochondrial and cardiac dysfunction during T2DM.

Our data reveal the following key findings: 1) PNPase protein expression is increased in the type 2 diabetic SSM in both human patient atrial appendage samples and the db/db mouse model; 2) PNPase is associated with Ago2 as shown via immunoprecipitation and this association

is increased in the SSM during T2DM; 3) db/db SSM have an increased level of miR-378, corresponding to a decrease in ATP6 protein content in the SSM; 4) overexpression of PNPase in the mouse cardiomyocyte HL-1 cell line significantly increases miR-378 levels, corresponding to a decrease in ATP synthase activity. These findings suggest that during T2DM, PNPase may be a potential constituent in the import mechanism of miRNAs into cardiac mitochondria.

Acknowledgements and Grants

This work was supported by the National Institutes of Health from the National Heart, Lung and Blood Institute grant R56 HL128485 and the WVU CTSI grant U54GM104942 awarded to JMH. This work was supported by an American Heart Association Predoctoral Fellowship grant AHA 14PRE19890020 awarded to DLS. This work was supported by a National Science Foundation IGERT: Research and Education in Nanotoxicology at West Virginia University Fellowship grant 1144676 awarded to QAH. This work was supported by an American Heart Association Predoctoral Fellowship grant AHA 13PRE16850066 awarded to CEN. This work was supported by a NIH Grant P20GM103434 to the West Virginia IDeA Network for Biomedical Research Excellence awarded to SS.

Author Contributions

D.L.S., Q.A.H., C.E.N., K.M.H., M.V.P., S.S. researched data. D.L.S., Q.A.H. performed statistical analyses. D.L.S., Q.A.H., M.V.P. wrote the manuscript. D.L.S., Q.A.H., C.E.N., K.M.H., M.V.P., S.S., J.M.H. reviewed/edited manuscript. D.L.S., Q.A.H., M.V.P., J.M.H. contributed to discussion.

Disclosures

None

References

1. National Diabetes Statistics Report: Estimates of Diabetes and Its Burden in the United States, edited by Prevention CfDCa, 2014.
2. **Asrih M and Steffens S.** Emerging role of epigenetics and miRNA in diabetic cardiomyopathy. *Cardiovasc Pathol* 22: 117-125, 2013.
3. **Bandiera S, Mategot R, Girard M, Demongeot J, and Henrion-Caude A.** MitomiRs delineating the intracellular localization of microRNAs at mitochondria. *Free Radic Biol Med* 64: 12-19, 2013.
4. **Barrey E, Saint-Auret G, Bonnamy B, Damas D, Boyer O, and Gidrol X.** Pre-microRNA and mature microRNA in human mitochondria. *PloS one* 6: e20220, 2011.
5. **Bartel DP.** MicroRNAs: genomics, biogenesis, mechanism, and function. *Cell* 116: 281-297, 2004.
6. **Baseler WA, Croston TL, and Hollander JM.** Functional Characteristics of Mortalin. In: *Mortalin Biology: Life, Stress and Death*, edited by Kaul SC and Wadhwa R. New York: Springer, 2012, p. 55-80.
7. **Baseler WA, Dabkowski ER, Jagannathan R, Thapa D, Nichols CE, Shepherd DL, Croston TL, Powell M, Razunguzwa TT, Lewis SE, Schnell DM, and Hollander JM.** Reversal of mitochondrial proteomic loss in Type 1 diabetic heart with overexpression of phospholipid hydroperoxide glutathione peroxidase. *Am J Physiol Regul Integr Comp Physiol* 304: R553-565, 2013.
8. **Baseler WA, Dabkowski ER, Williamson CL, Croston TL, Thapa D, Powell MJ, Razunguzwa TT, and Hollander JM.** Proteomic alterations of distinct mitochondrial

subpopulations in the type 1 diabetic heart: contribution of protein import dysfunction. *Am J Physiol Regul Integr Comp Physiol* 300: R186-200, 2011.

9. **Baseler WA, Thapa D, Jagannathan R, Dabkowski ER, Croston TL, and Hollander JM.** miR-141 as a regulator of the mitochondrial phosphate carrier (Slc25a3) in the type 1 diabetic heart. *Am J Physiol Cell Physiol* 303: C1244-1251, 2012.
10. **Baskin KK, Grueter CE, Kusminski CM, Holland WL, Bookout AL, Satapati S, Kong YM, Burgess SC, Malloy CR, Scherer PE, Newgard CB, Bassel-Duby R, and Olson EN.** MED13-dependent signaling from the heart confers leanness by enhancing metabolism in adipose tissue and liver. *EMBO Mol Med* 6: 1610-1621, 2014.
11. **Bienertova-Vasku J, Sana J, and Slaby O.** The role of microRNAs in mitochondria in cancer. *Cancer Lett* 336: 1-7, 2013.
12. **Borralho PM, Rodrigues CM, and Steer CJ.** microRNAs in Mitochondria: An Unexplored Niche. *Adv Exp Med Biol* 887: 31-51, 2015.
13. **Borralho PM, Rodrigues CMP, and Steer CJ.** Mitochondrial MicroRNAs and Their Potential Role in Cell Function. *Current Pathobiology Reports* 2: 123-132, 2014.
14. **Bradford MM.** A rapid and sensitive method for the quantitation of microgram quantities of protein utilizing the principle of protein-dye binding. *Anal Biochem* 72: 248-254, 1976.
15. **Carrer M, Liu N, Grueter CE, Williams AH, Frisard MI, Hulver MW, Bassel-Duby R, and Olson EN.** Control of mitochondrial metabolism and systemic energy homeostasis by microRNAs 378 and 378*. *Proc Natl Acad Sci U S A* 109: 15330-15335, 2012.
16. **Claycomb WC, Lanson NA, Jr., Stallworth BS, Egeland DB, Delcarpio JB, Bahinski A, and Izzo NJ, Jr.** HL-1 cells: a cardiac muscle cell line that contracts and retains phenotypic characteristics of the adult cardiomyocyte. *Proc Natl Acad Sci U S A* 95: 2979-2984, 1998.

17. **Croston TL, Shepherd DL, Thapa D, Nichols CE, Lewis SE, Dabkowski ER, Jagannathan R, Baseler WA, and Hollander JM.** Evaluation of the cardiolipin biosynthetic pathway and its interactions in the diabetic heart. *Life sciences* 93: 313-322, 2013.
18. **Croston TL, Thapa D, Holden AA, Tveter KJ, Lewis SE, Shepherd DL, Nichols CE, Long DM, Olfert IM, Jagannathan R, and Hollander JM.** Functional deficiencies of subsarcolemmal mitochondria in the type 2 diabetic human heart. *Am J Physiol Heart Circ Physiol* 307: H54-65, 2014.
19. **Dabkowski ER, Baseler WA, Williamson CL, Powell M, Razunguzwa TT, Frisbee JC, and Hollander JM.** Mitochondrial dysfunction in the type 2 diabetic heart is associated with alterations in spatially distinct mitochondrial proteomes. *Am J Physiol Heart Circ Physiol* 299: H529-540, 2010.
20. **Dabkowski ER, Williamson CL, Bukowski VC, Chapman RS, Leonard SS, Peer CJ, Callery PS, and Hollander JM.** Diabetic cardiomyopathy-associated dysfunction in spatially distinct mitochondrial subpopulations. *Am J Physiol Heart Circ Physiol* 296: H359-369, 2009.
21. **Dabkowski ER, Williamson CL, and Hollander JM.** Mitochondria-specific transgenic overexpression of phospholipid hydroperoxide glutathione peroxidase (GPx4) attenuates ischemia/reperfusion-associated cardiac dysfunction. *Free Radic Biol Med* 45: 855-865, 2008.
22. **Das S, Bedja D, Campbell N, Dunkerly B, Chenna V, Maitra A, and Steenbergen C.** miR-181c regulates the mitochondrial genome, bioenergetics, and propensity for heart failure in vivo. *PloS one* 9: e96820, 2014.
23. **Das S, Ferlito M, Kent OA, Fox-Talbot K, Wang R, Liu D, Raghavachari N, Yang Y, Wheelan SJ, Murphy E, and Steenbergen C.** Nuclear miRNA regulates the mitochondrial genome in the heart. *Circ Res* 110: 1596-1603, 2012.

24. **Das S and Halushka MK.** Extracellular vesicle microRNA transfer in cardiovascular disease. *Cardiovasc Pathol* 24: 199-206, 2015.

25. **Dennerlein S and Rehling P.** Human mitochondrial COX1 assembly into cytochrome c oxidase at a glance. *J Cell Sci* 128: 833-837, 2015.

26. **Duarte FV, Palmeira CM, and Rolo AP.** The Role of microRNAs in Mitochondria: Small Players Acting Wide. *Genes-Basel* 5: 865-886, 2014.

27. **Dudek J, Rehling P, and van der Laan M.** Mitochondrial protein import: common principles and physiological networks. *Biochim Biophys Acta* 1833: 274-285, 2013.

28. **Entelis NS, Kolesnikova OA, Dogan S, Martin RP, and Tarassov IA.** 5 S rRNA and tRNA import into human mitochondria. Comparison of in vitro requirements. *J Biol Chem* 276: 45642-45653, 2001.

29. **Feniouk BA, Suzuki T, and Yoshida M.** Regulatory interplay between proton motive force, ADP, phosphate, and subunit epsilon in bacterial ATP synthase. *J Biol Chem* 282: 764-772, 2007.

30. **Filipowicz W, Bhattacharyya SN, and Sonenberg N.** Mechanisms of post-transcriptional regulation by microRNAs: are the answers in sight? *Nat Rev Genet* 9: 102-114, 2008.

31. **Flarsheim CE, Grupp IL, and Matlib MA.** Mitochondrial dysfunction accompanies diastolic dysfunction in diabetic rat heart. *Am J Physiol* 271: H192-202, 1996.

32. **Foldes-Papp Z, Konig K, Studier H, Buckle R, Breunig HG, Uchugonova A, and Kostner GM.** Trafficking of mature miRNA-122 into the nucleus of live liver cells. *Curr Pharm Biotechnol* 10: 569-578, 2009.

33. **Goldberg RB.** Type 2 Diabetes. In: *Comprehensive Management of High Risk Cardiovascular Patients*, edited by Gotto AMaTPP. Boca Raton, FL: Taylor & Francis Group, 2007.

34. **Greco S, Fasanaro P, Castelvecchio S, D'Alessandra Y, Arcelli D, Di Donato M, Malavazos A, Capogrossi MC, Menicanti L, and Martelli F.** MicroRNA dysregulation in diabetic ischemic heart failure patients. *Diabetes* 61: 1633-1641, 2012.

35. **Grueter CE, van Rooij E, Johnson BA, DeLeon SM, Sutherland LB, Qi X, Gautron L, Elmquist JK, Bassel-Duby R, and Olson EN.** A cardiac microRNA governs systemic energy homeostasis by regulation of MED13. *Cell* 149: 671-683, 2012.

36. **Hamblin M, Friedman DB, Hill S, Caprioli RM, Smith HM, and Hill MF.** Alterations in the diabetic myocardial proteome coupled with increased myocardial oxidative stress underlies diabetic cardiomyopathy. *J Mol Cell Cardiol* 42: 884-895, 2007.

37. **Jagannathan R, Thapa D, Nichols CE, Shepherd DL, Stricker JC, Croston TL, Baseler WA, Lewis SE, Martinez I, and Hollander JM.** Translational Regulation of the Mitochondrial Genome Following Redistribution of Mitochondrial MicroRNA in the Diabetic Heart. *Circ Cardiovasc Genet* 8: 785-802, 2015.

38. **Janssen HL, Reesink HW, Lawitz EJ, Zeuzem S, Rodriguez-Torres M, Patel K, van der Meer AJ, Patick AK, Chen A, Zhou Y, Persson R, King BD, Kauppinen S, Levin AA, and Hodges MR.** Treatment of HCV infection by targeting microRNA. *N Engl J Med* 368: 1685-1694, 2013.

39. **Knezevic I, Patel A, Sundaresan NR, Gupta MP, Solaro RJ, Nagalingam RS, and Gupta M.** A novel cardiomyocyte-enriched microRNA, miR-378, targets insulin-like growth factor 1 receptor: implications in postnatal cardiac remodeling and cell survival. *J Biol Chem* 287: 12913-12926, 2012.

40. **Kolesnikova OA, Entelis NS, Mireau H, Fox TD, Martin RP, and Tarassov IA.** Suppression of mutations in mitochondrial DNA by tRNAs imported from the cytoplasm. *Science* 289: 1931-1933, 2000.
41. **Kren BT, Wong PY, Sarver A, Zhang X, Zeng Y, and Steer CJ.** MicroRNAs identified in highly purified liver-derived mitochondria may play a role in apoptosis. *RNA Biol* 6: 65-72, 2009.
42. **Laemmli UK.** Cleavage of structural proteins during the assembly of the head of bacteriophage T4. *Nature* 227: 680-685, 1970.
43. **Lin CL, Wang YT, Yang WZ, Hsiao YY, and Yuan HS.** Crystal structure of human polynucleotide phosphorylase: insights into its domain function in RNA binding and degradation. *Nucleic Acids Res* 40: 4146-4157, 2012.
44. **Liou GG, Chang HY, Lin CS, and Lin-Chao S.** DEAD box RhlB RNA helicase physically associates with exoribonuclease PNPase to degrade double-stranded RNA independent of the degradosome-assembling region of RNase E. *J Biol Chem* 277: 41157-41162, 2002.
45. **Macfarlane LA and Murphy PR.** MicroRNA: Biogenesis, Function and Role in Cancer. *Curr Genomics* 11: 537-561, 2010.
46. **Maechler P and Wollheim CB.** Mitochondrial function in normal and diabetic beta-cells. *Nature* 414: 807-812, 2001.
47. **Montgomery RL, Hullinger TG, Semus HM, Dickinson BA, Seto AG, Lynch JM, Stack C, Latimer PA, Olson EN, and van Rooij E.** Therapeutic inhibition of miR-208a improves cardiac function and survival during heart failure. *Circulation* 124: 1537-1547, 2011.
48. **Nichols CE, Shepherd DL, Knuckles TL, Thapa D, Stricker JC, Stapleton PA, Minarchick VC, Erdely A, Zeidler-Erdely PC, Alway SE, Nurkiewicz TR, and Hollander**

JM. Cardiac and mitochondrial dysfunction following acute pulmonary exposure to mountaintop removal mining particulate matter. *Am J Physiol Heart Circ Physiol* 309: H2017-2030, 2015.

49. **Palmer JW, Tandler B, and Hoppel CL.** Biochemical properties of subsarcolemmal and interfibrillar mitochondria isolated from rat cardiac muscle. *J Biol Chem* 252: 8731-8739, 1977.
50. **Pinti MV, Hathaway QA, and Hollander JM.** Role of MicroRNA in Metabolic Shift During Heart Failure. *Am J Physiol Heart Circ Physiol*: ajpheart 00341 02016, 2016.
51. **Politz JC, Zhang F, and Pederson T.** MicroRNA-206 colocalizes with ribosome-rich regions in both the nucleolus and cytoplasm of rat myogenic cells. *Proc Natl Acad Sci U S A* 103: 18957-18962, 2006.
52. **Pullman ME, Penefsky HS, Datta A, and Racker E.** Partial resolution of the enzymes catalyzing oxidative phosphorylation. I. Purification and properties of soluble dinitrophenol-stimulated adenosine triphosphatase. *J Biol Chem* 235: 3322-3329, 1960.
53. **Ritov VB, Menshikova EV, He J, Ferrell RE, Goodpaster BH, and Kelley DE.** Deficiency of subsarcolemmal mitochondria in obesity and type 2 diabetes. *Diabetes* 54: 8-14, 2005.
54. **Rolo AP and Palmeira CM.** Diabetes and mitochondrial function: role of hyperglycemia and oxidative stress. *Toxicol Appl Pharmacol* 212: 167-178, 2006.
55. **Rubio MA, Rinehart JJ, Krett B, Duvezin-Caubet S, Reichert AS, Soll D, and Alfonzo JD.** Mammalian mitochondria have the innate ability to import tRNAs by a mechanism distinct from protein import. *Proc Natl Acad Sci U S A* 105: 9186-9191, 2008.
56. **Sarkar D, Leszczyniecka M, Kang DC, Lebedeva IV, Valerie K, Dhar S, Pandita TK, and Fisher PB.** Down-regulation of Myc as a potential target for growth arrest induced by human

polynucleotide phosphorylase (hPNPaseold-35) in human melanoma cells. *J Biol Chem* 278: 24542-24551, 2003.

57. **Sarkar D, Park ES, Emdad L, Randolph A, Valerie K, and Fisher PB.** Defining the domains of human polynucleotide phosphorylase (hPNPaseOLD-35) mediating cellular senescence. *Mol Cell Biol* 25: 7333-7343, 2005.
58. **Schneider A.** Mitochondrial tRNA import and its consequences for mitochondrial translation. *Annu Rev Biochem* 80: 1033-1053, 2011.
59. **Shen X, Zheng S, Thongboonkerd V, Xu M, Pierce WM, Jr., Klein JB, and Epstein PN.** Cardiac mitochondrial damage and biogenesis in a chronic model of type 1 diabetes. *Am J Physiol Endocrinol Metab* 287: E896-905, 2004.
60. **Slomovic S and Schuster G.** Stable PNPase RNAi silencing: its effect on the processing and adenylation of human mitochondrial RNA. *RNA* 14: 310-323, 2008.
61. **Smirnov A, Comte C, Mager-Heckel AM, Addis V, Krasheninnikov IA, Martin RP, Entelis N, and Tarassov I.** Mitochondrial enzyme rhodanese is essential for 5 S ribosomal RNA import into human mitochondria. *J Biol Chem* 285: 30792-30803, 2010.
62. **Smirnov A, Entelis N, Martin RP, and Tarassov I.** Biological significance of 5S rRNA import into human mitochondria: role of ribosomal protein MRP-L18. *Genes Dev* 25: 1289-1305, 2011.
63. **Srinivasan H and Das S.** Mitochondrial miRNA (MitomiR): a new player in cardiovascular health. *Can J Physiol Pharm* 93: 855-861, 2015.
64. **Sripada L, Tomar D, Prajapati P, Singh R, Singh AK, and Singh R.** Systematic analysis of small RNAs associated with human mitochondria by deep sequencing: detailed analysis of mitochondrial associated miRNA. *PloS one* 7: e44873, 2012.

65. **Sripada L, Tomar D, and Singh R.** Mitochondria: one of the destinations of miRNAs. *Mitochondrion* 12: 593-599, 2012.

66. **Thapa D, Nichols CE, Lewis SE, Shepherd DL, Jagannathan R, Croston TL, Tveter KJ, Holden AA, Baseler WA, and Hollander JM.** Transgenic overexpression of mitofilin attenuates diabetes mellitus-associated cardiac and mitochondria dysfunction. *J Mol Cell Cardiol* 79: 212-223, 2015.

67. **Towheed A, Markantone DM, Crain AT, Celotto AM, and Palladino MJ.** Small mitochondrial-targeted RNAs modulate endogenous mitochondrial protein expression in vivo. *Neurobiol Dis* 69: 15-22, 2014.

68. **Trounce IA, Kim YL, Jun AS, and Wallace DC.** Assessment of mitochondrial oxidative phosphorylation in patient muscle biopsies, lymphoblasts, and transmitochondrial cell lines. *Methods in enzymology* 264: 484-509, 1996.

69. **Wang G, Chen HW, Oktay Y, Zhang J, Allen EL, Smith GM, Fan KC, Hong JS, French SW, McCaffery JM, Lightowlers RN, Morse HC, 3rd, Koehler CM, and Teitell MA.** PNPASE regulates RNA import into mitochondria. *Cell* 142: 456-467, 2010.

70. **Wang G, Shimada E, Koehler CM, and Teitell MA.** PNPASE and RNA trafficking into mitochondria. *Biochim Biophys Acta* 1819: 998-1007, 2012.

71. **Wei Y, Li L, Wang D, Zhang CY, and Zen K.** Importin 8 regulates the transport of mature microRNAs into the cell nucleus. *J Biol Chem* 289: 10270-10275, 2014.

72. **Williamson CL, Dabkowski ER, Baseler WA, Croston TL, Alway SE, and Hollander JM.** Enhanced apoptotic propensity in diabetic cardiac mitochondria: influence of subcellular spatial location. *Am J Physiol Heart Circ Physiol* 298: H633-642, 2010.

73. **Zhang X, Zuo X, Yang B, Li Z, Xue Y, Zhou Y, Huang J, Zhao X, Zhou J, Yan Y, Zhang H, Guo P, Sun H, Guo L, Zhang Y, and Fu XD.** MicroRNA directly enhances mitochondrial translation during muscle differentiation. *Cell* 158: 607-619, 2014.

Figure 4.1

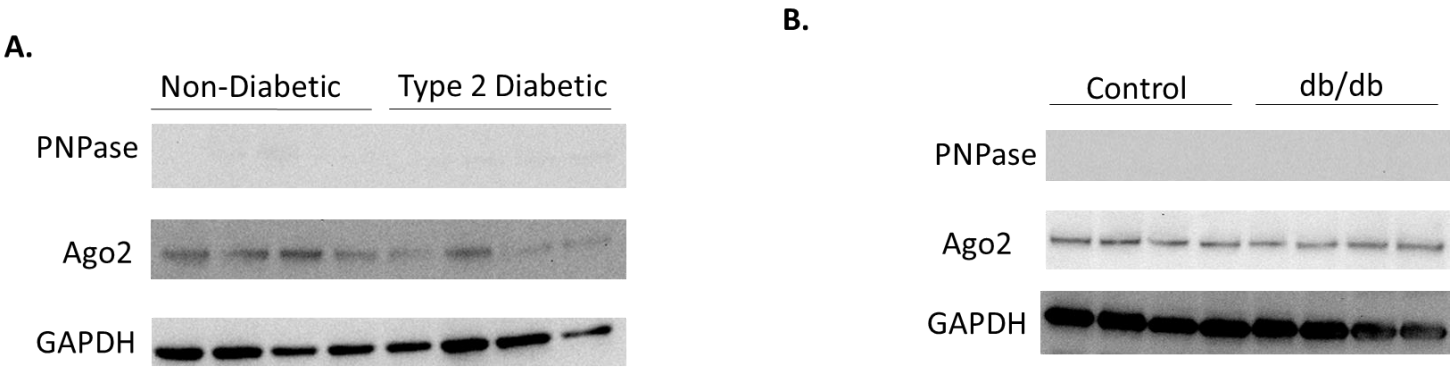
A.
Non-Diabetic
Type 2 Diabetic
PNPase
Ago2
GAPDH
B.
Control
db/db
PNPase
Ago2
GAPDH

Figure 4.1. Expression levels of PNPase and Ago2 in cytoplasm. (A) Representative Western blot analysis of PNPase and Ago2 protein expression levels in the cytoplasm of human atrial appendage from non-diabetic and type 2 diabetic patients. GAPDH was used as a loading control. (B) Representative Western blot analysis of PNPase and Ago2 protein expression levels in the cytoplasm of wild-type and db/db mice. GAPDH was used as a loading control.

Figure 4.2

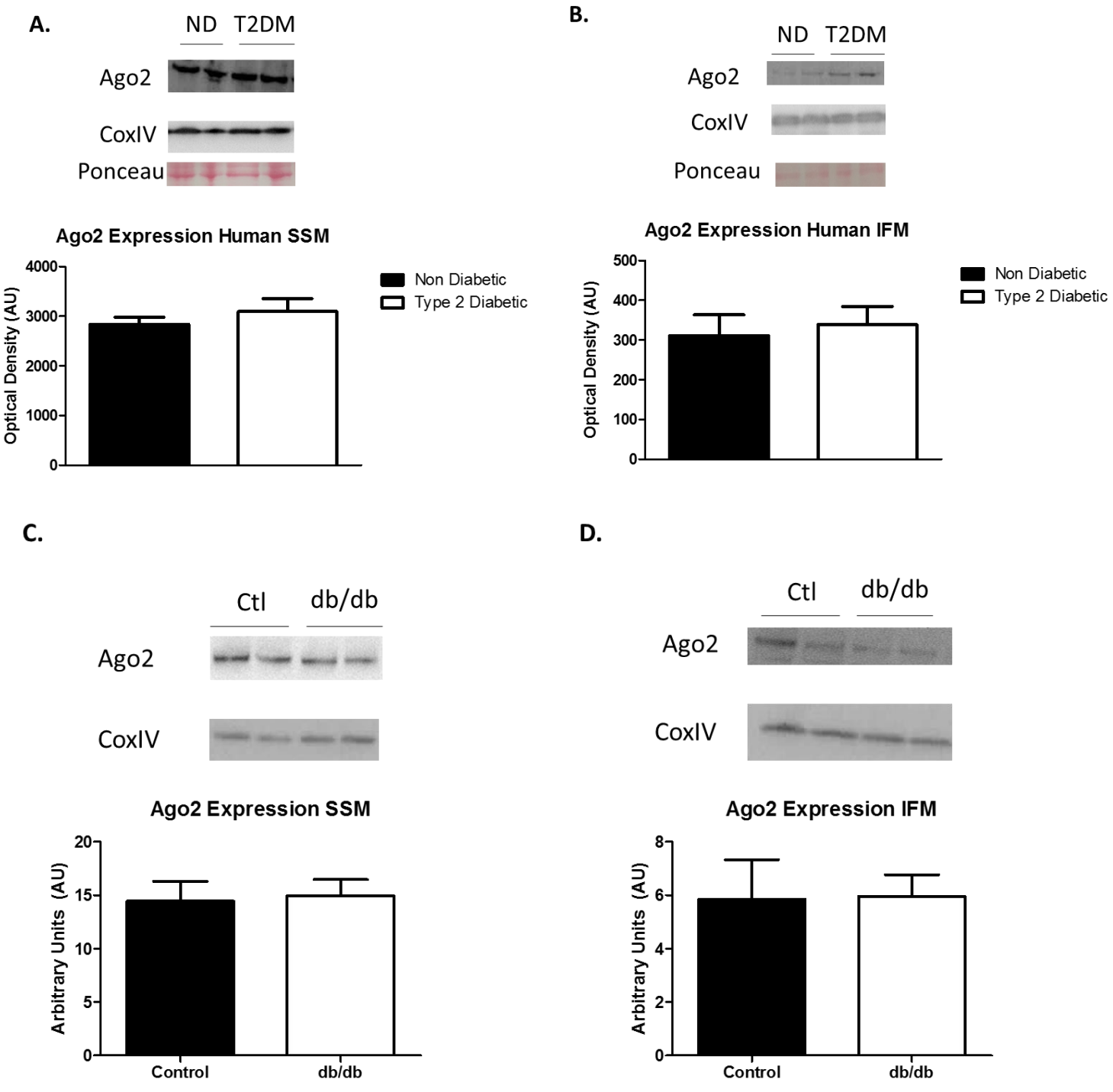
A.
ND T2DM
Ago2
CoxIV
Ponceau
Ago2 Expression Human SSM
Optical Density (AU)
4000
3000
2000
1000
0
Non Diabetic
Type 2 Diabetic
B.
ND T2DM
Ago2
CoxIV
Ponceau
Ago2 Expression Human IFM
Optical Density (AU)
500
400
300
200
100
0
Non Diabetic
Type 2 Diabetic
C.
Ctl db/db
Ago2
CoxIV
Ago2 Expression SSM
Arbitrary Units (AU)
20
15
10
5
0
Control
db/db
D.
Ctl db/db
Ago2
CoxIV
Ago2 Expression IFM
Arbitrary Units (AU)
8
6
4
2
0
Control
db/db

Figure 4.2. Expression levels of Ago2 in cardiac mitochondrial subpopulations. (A) Representative Western blot analysis and quantification of Ago2 protein expression levels in the SSM of human atrial appendage from non-diabetic and type 2 diabetic patients. CoxIV and Ponceau staining were used as loading controls. (B) Representative Western blot analysis and quantification of Ago2 protein expression levels in the IFM of human atrial appendage from non-diabetic and type 2 diabetic patients. CoxIV and Ponceau staining were used as loading controls. (C) Representative Western blot analysis and quantification of Ago2 protein expression levels in the SSM of wild-type and db/db mice. CoxIV was used as loading controls. (D) Representative Western blot analysis and quantification of Ago2 protein expression levels in the IFM of wild-type and db/db mice. CoxIV was used as loading controls. Values are expressed as means ± SEM.

Figure 4.3

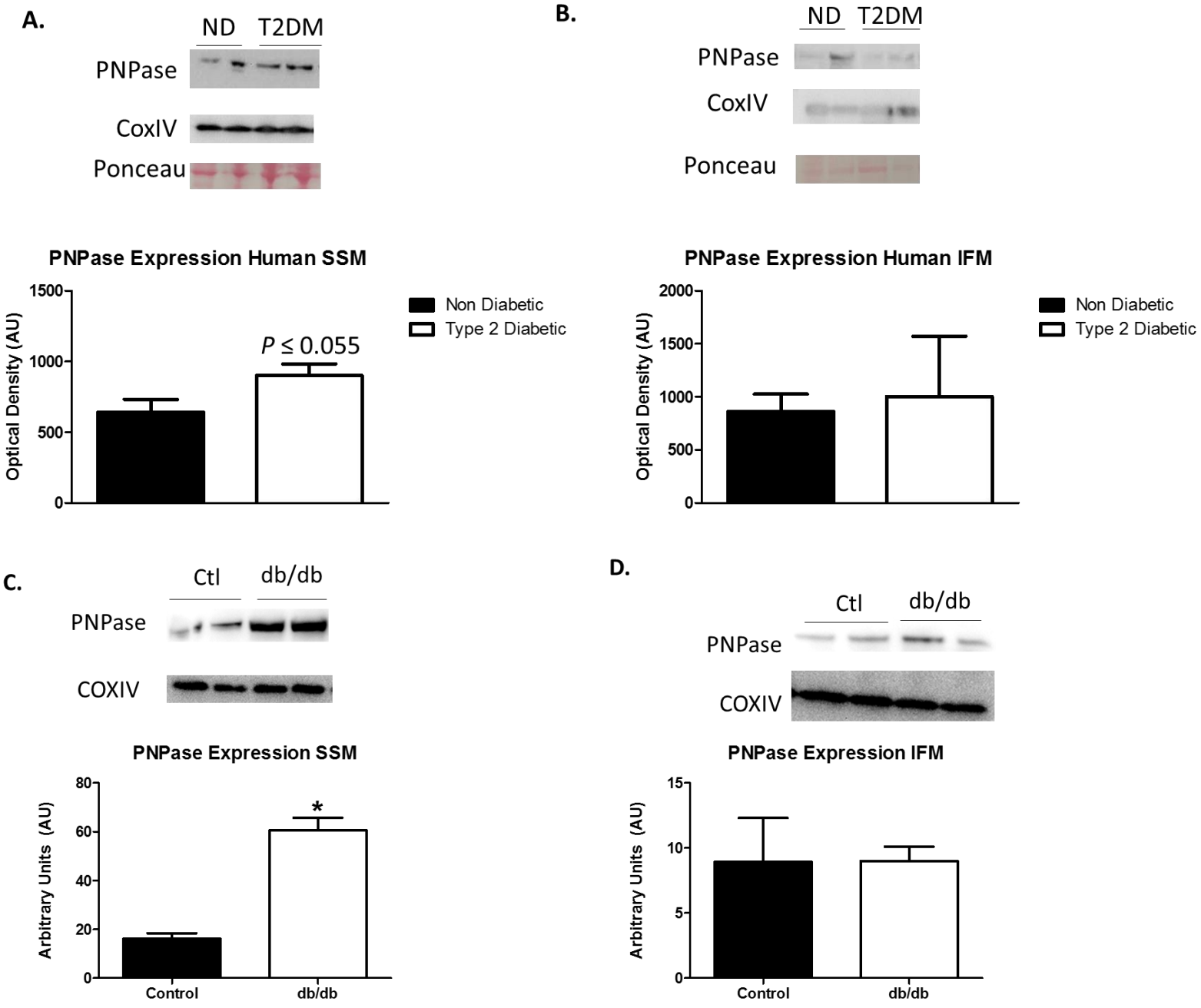
A.
ND
T2DM
PNPase
CoxIV
Ponceau
B.
ND
T2DM
PNPase
CoxIV
Ponceau
PNPase Expression Human SSM
Optical Density (AU)
1500
1000
500
0
P ≤ 0.055
Non Diabetic
Type 2 Diabetic
PNPase Expression Human IFM
Optical Density (AU)
2000
1500
1000
500
0
Non Diabetic
Type 2 Diabetic
C.
Ctl
db/db
PNPase
COXIV
PNPase Expression SSM
Arbitrary Units (AU)
80
60
40
20
0
*
Control
db/db
D.
Ctl
db/db
PNPase
COXIV
PNPase Expression IFM
Arbitrary Units (AU)
15
10
5
0
Control
db/db

Figure 4.3. Expression levels of PNPase in cardiac mitochondrial subpopulations. (A) Representative Western blot analysis and quantification of PNPase protein expression levels in the SSM of human atrial appendage from non-diabetic and type 2 diabetic patients. CoxIV and Ponceau staining were used as loading controls. (B) Representative Western blot analysis and quantification of PNPase protein expression levels in the IFM of human atrial appendage from non-diabetic and type 2 diabetic patients. CoxIV and Ponceau staining were used as loading controls. (C) Representative Western blot analysis and quantification of Ago2 protein expression levels in the SSM of wild-type and db/db mice. CoxIV was used as loading controls. (D) Representative Western blot analysis and quantification of Ago2 protein expression levels in the IFM of wild-type and db/db mice. CoxIV was used as loading controls. Values are expressed as means ± SEM. *$P \leq 0.05$ for control vs. type 2 diabetic.

Figure 4.4

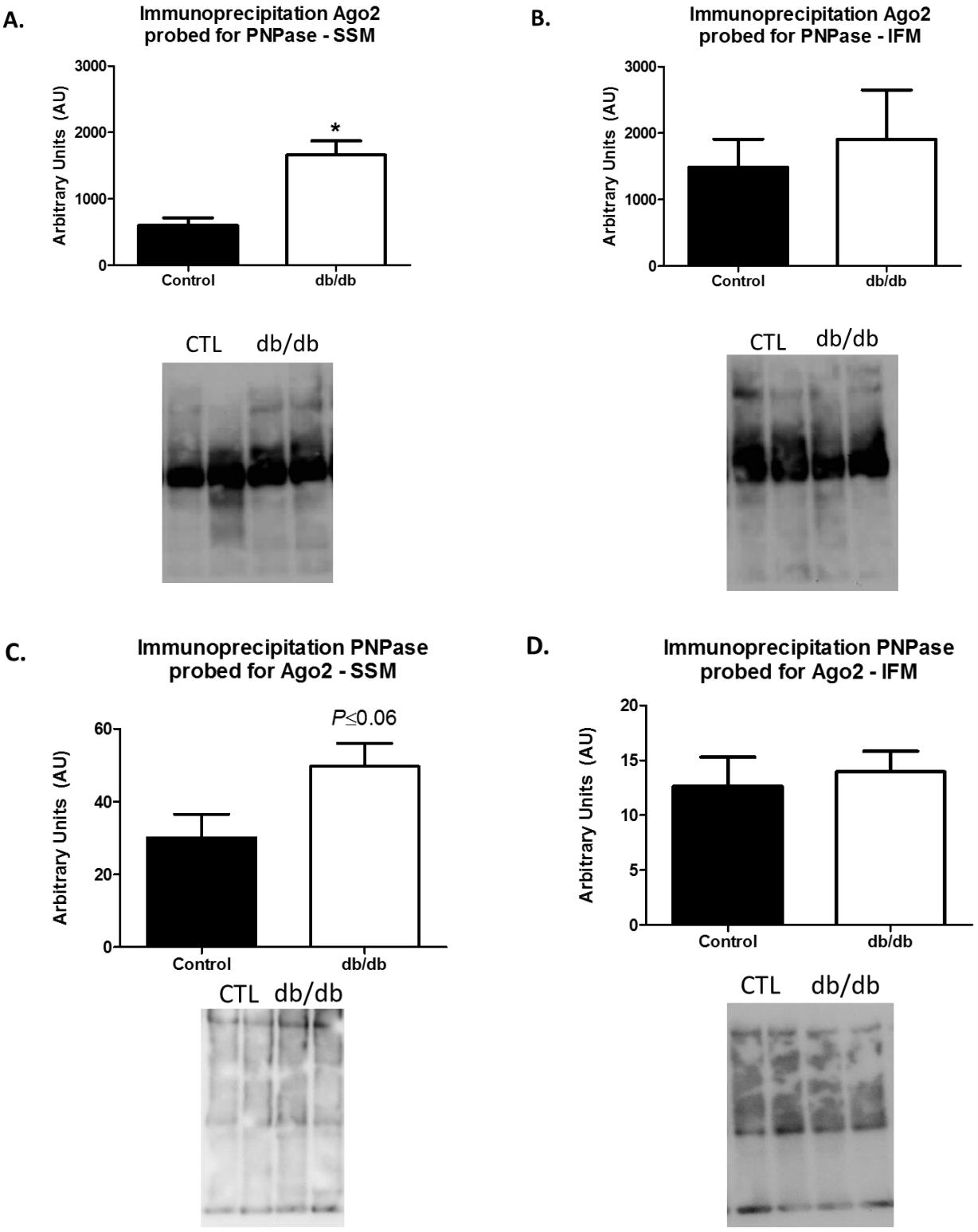
A.
Immunoprecipitation Ago2
probed for PNPase - SSM
Arbitrary Units (AU)
3000
2000
1000
0
*
Control
db/db
CTL
db/db
B.
Immunoprecipitation Ago2
probed for PNPase - IFM
Arbitrary Units (AU)
3000
2000
1000
0
Control
db/db
CTL
db/db
C.
Immunoprecipitation PNPase
probed for Ago2 - SSM
P≤0.06
Arbitrary Units (AU)
60
40
20
0
Control
db/db
CTL
db/db
D.
Immunoprecipitation PNPase
probed for Ago2 - IFM
Arbitrary Units (AU)
20
15
10
5
0
Control
db/db
CTL
db/db

Figure 4.4. Association of Ago2 and PNPase. (A) Representative co-immunopreciptation and quantification with a pulldown of Ago2 and probed with PNPase in control and db/db SSM. (B) Representative co-immunopreciptation and quantification with a pulldown of Ago2 and probed with PNPase in control and db/db IFM. (C) Representative co-immunopreciptation and quantification with a pulldown of PNPase and probed with Ago2 in control and db/db SSM. (D) Representative co-immunopreciptation and quantification with a pulldown of PNPase and probed with Ago2 in control and db/db IFM. Values are expressed as means ± SEM. *$P \leq 0.05$ for control vs. db/db.

Figure 4.5

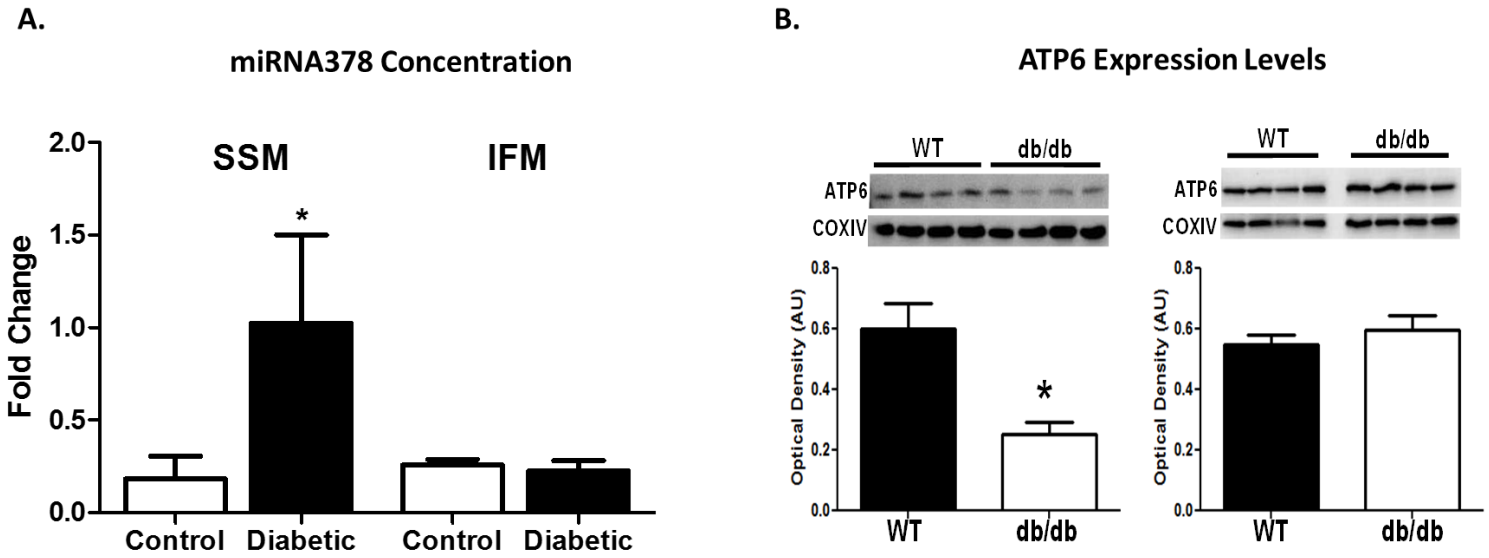
A.
miRNA378 Concentration
SSM
IFM
Fold Change
2.0
1.5
1.0
0.5
0.0
*
Control
Diabetic
Control
Diabetic
B.
ATP6 Expression Levels
WT
db/db
ATP6
COXIV
Optical Density (AU)
0.8
0.6
0.4
0.2
0.0
*
WT
db/db
WT
db/db
ATP6
COXIV
Optical Density (AU)
0.8
0.6
0.4
0.2
0.0
WT
db/db

Figure 4.5. **MicroRNA-378 Concentration and ATP6 Expression levels.** (A) qPCR of mir-378 concentration in control line (n = 3) and db/db (n =3) mice for both the subsarcolemmal mitochondria (SSM) and interfibrillar mitochondria (IFM).. Replicates were determined as individual transfections. (B) Representative Western blot analysis and quantification of ATP6 protein expression levels in the SSM (Left) and IFM (Right) of control and db/db mice. CoxIV was used as a loading control. Values are expressed as means ± SEM. $*P \leq 0.05$ for control vs. db/db.

Figure 4.6

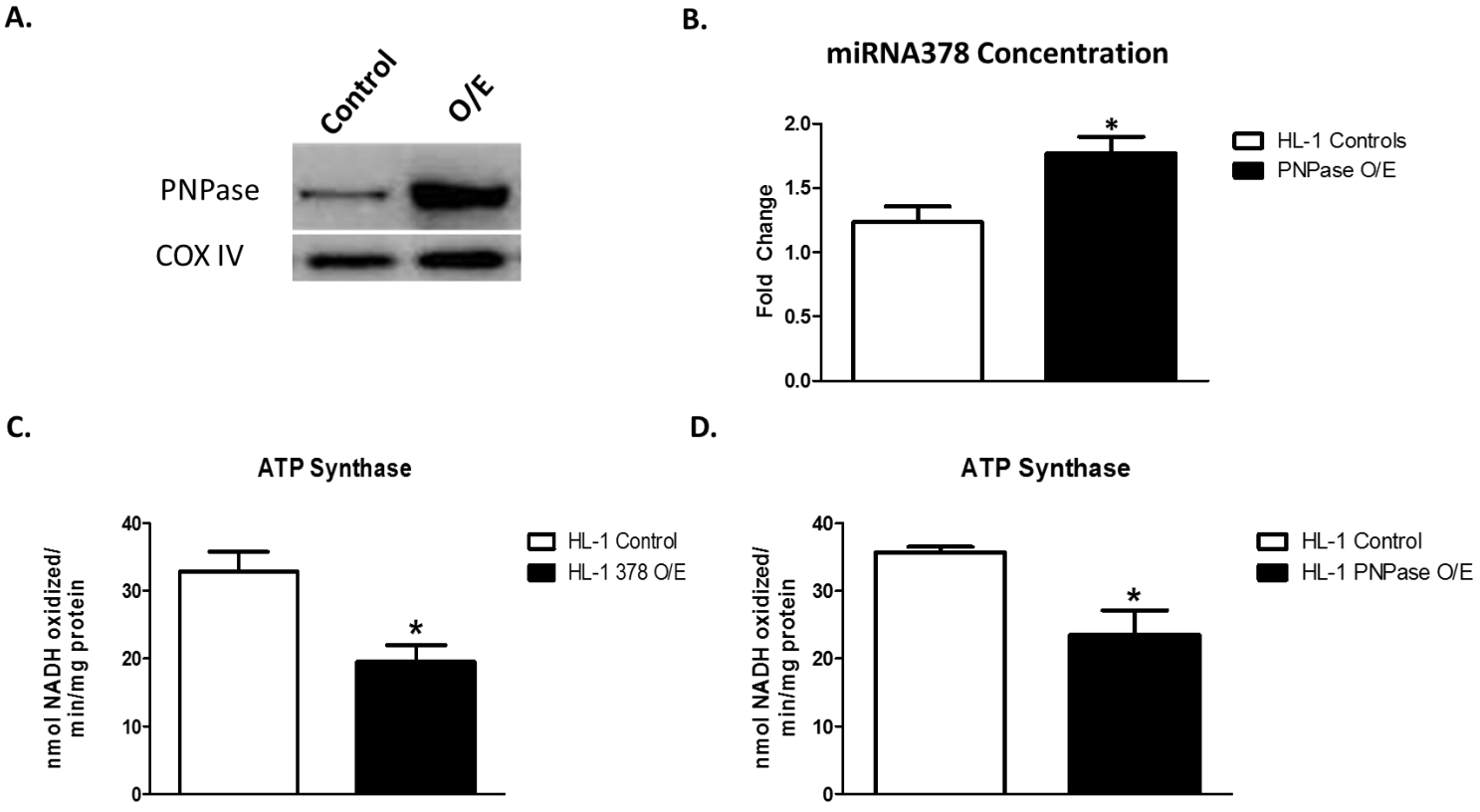
A.
Control
O/E
PNPase
COX IV
B.
miRNA378 Concentration
Fold Change
2.0
1.5
1.0
0.5
0.0
*
HL-1 Controls
PNPase O/E
C.
ATP Synthase
nmol NADH oxidized/ min/mg protein
40
30
20
10
0
*
HL-1 Control
HL-1 378 O/E
D.
ATP Synthase
nmol NADH oxidized/ min/mg protein
40
30
20
10
0
*
HL-1 Control
HL-1 PNPase O/E

Figure 4.6. Overexpression of PNPase in HL-1 Cardiomyocyte Cells. (A) Representative Western blot analysis of PNPase overexpression in the HL-1 Cell line. (B) qPCR of mir-378 concentration in HL-1 cells (n = 3) compared to HL-1 cells overexpressing PNPase (n =3). Replicates were determined as individual transfections. (C) ATP synthase activity in HL-1 control and HL-1 378 overexpression cell lines. (D) ATP synthase activity in HL-1 control and HL-1 PNPase overexpression cell lines. Values are expressed as means ± SEM. $*P \leq 0.05$ for control vs. overexpression cell line.

GENERAL DISCUSSION

The overall objective of this dissertation was to evaluate a new imaging technique for myocardial function and to assess the mechanisms leading to mitochondrial proteome dysregulation and miRNA import into the mitochondrion. Specifically, we wanted to determine if during DM: (1) echocardiographic speckle-tracking based strain imaging analyses would lead to a greater ability to detect earlier changes in myocardial dysfunction; (2) mtHsp70 would provide mitochondrial and cardiac contractile protection via restored nuclear-encoded mitochondrial protein import and mitochondrial proteome stability; (3) increased PNPase expression would lead to an increase in miRNA import into the mitochondrion via an association with the RISC. Our **long-term goal** was to identify mechanisms to alleviate adverse cardiac and mitochondrial effects associated with DM with the intent of providing a mechanism for therapeutic interventions to be designed. The **central hypothesis** of this dissertation was that strain analyses would offer the capability to detect early decrements in myocardial strain resulting from mitochondrial proteome derangement associated with inefficient mitochondrial protein import and mitochondrial dysfunction, all rectified by manipulation of mtHsp70. Further, the increased expression of miRNAs inside of the mitochondrion could potentially be due to an increased association of PNPase with the RISC. Our **rationale** for the proposed research was based upon the notion that a greater understanding of the mechanisms involved in mitochondrial dysfunction during DM, along with a non-invasive mechanism to evaluate and detect early myocardial contractile deficiencies, could potentially allow for the identification of key contributors to alleviate mitochondrial dysfunction, aiding in the development of a therapeutic paradigm to help combat cardiac complications in diabetic patients.

Roughly 9.3% of the United States population is diagnosed with DM and the rate of incidence is increasing at an alarming frequency (1, 3). T1DM, caused by insufficient insulin

production, accounts for approximately 5% of diabetic patients, while T2DM results from insulin resistance and affects 95% of all diabetic patients (3). The cardiovascular complications resulting from DM are the leading cause of morbidity and mortality among diabetic patients (25). The mitochondria within the cardiomyocyte have been linked to the cardiac dysfunction seen during DM with abnormalities associated with altered substrate utilization, increased production of ROS, enhanced susceptibility for apoptosis, altered mitochondrial structure, increased adverse effects due to miRNA, decreased nuclear-encoded mitochondrial protein import efficiency and a dysregulated mitochondrial proteome (11-13, 19-22, 39, 56, 59, 65, 70-72, 81). Further complicating the study of cardiac mitochondria, is the presence of two spatially and biochemically distinct mitochondrial subpopulations within the cardiomyocyte, which respond differentially to physiological stimuli and pathological insults (4, 11-13, 19-22, 40, 41, 45-47, 51, 53-55, 58, 72, 81, 82). A review published by our laboratory highlights the differential impact of distinct pathological insults on cardiac mitochondrial subpopulations including ischemia, hypoxia, myocardial infarction, I/R, preconditioning/postconditioning, HF, aging, exercise, DM and hypermetabolism (33). Previous research from our laboratory demonstrates that T1DM differentially influences mitochondrial subpopulations, with the IFM being predominantly disturbed during this pathological insult, while SSM are detrimentally affected during T2DM (2, 11-13, 19-22, 72, 81). Increased ROS production and damage, along with decreased size and internal complexity were shown in the IFM of the T1DM heart (22). In 18-week-old db/db mice, our laboratory previously reported oxidative damage via lipid peroxidation byproducts and nitrotyrosine residues in the SSM isolated from cardiomyocytes (21). Further, db/db animals revealed decreased mitochondrial size, internal complexity, and $\Delta\Psi m$ in the SSM, with no changes in the IFM (21). A study in skeletal muscle from T2DM patients revealed decreased mitochondrial

size and SSM abundance (43). Interestingly, when fueled with glutamate and malate, decrements in mitochondrial state 3 respiration rates in the SSM subpopulation were observed; however, when fueled with palmitoylcarnitine, fatty acid-stimulated state 3 and state 4 respiration were significantly decreased in the SSM, with no alterations to the IFM (21). This is interesting due to the milieu created during the T2DM setting, with a gross overabundance of lipids present within the environment. Additionally, mitochondrial function was assessed via ETC complex activities, which revealed deficits in complexes I, III and IV, as well as the ATP synthase for the SSM subpopulations, without having an effect on the IFM (21). These studies reveal that cardiac mitochondrial subpopulations are differentially impacted depending on the type of DM.

It is interesting to note that T1DM and T2DM affect cardiac mitochondrial subpopulations differentially; however, it is unknown as to why this occurs. Our speculation to the differential impact on cardiac mitochondrial subpopulations during the distinct types of DM arises from the differences in the phenotypes elicited by the pathologies. While similar deleterious effects are noted in the cardiac mitochondrial subpopulations, the milieu resulting from the pathology are somewhat different. The T1DM condition creates a milieu of starvation and deprivation while the glucose remains in the bloodstream instead of being utilized by the cells, leading to the cells being starved of this energy source. Conversely, in the T2DM condition, the cells are still facing starvation; however, this is in the face of excess. In our particular DM models, the IFM could potentially be more susceptible to damage from the STZ during T1DM because of their innately higher respiratory rates and subsequent oxidative environment caused by the pathology. Our laboratory has previously shown in the db/db model of T2DM that lipid profiles are significantly increased compared to the T1DM condition (21, 22). Further, db/db mice have higher circulating fatty acids and triglycerides than STZ mice, which is likely due to the phenotype elicited by the

pathological insult of T2DM (21, 22). With a greater propensity for lipid accumulation and the proximity of the SSM to the sarcolemmal membrane, the SSM are likely subjected to an environment high in lipid content, which was found by Nielson et al. in T2DM skeletal muscle (52). As the circulating free fatty acids and lipid deposition to the subsarcolemmal region during T2DM increases, the SSM are likely at a larger susceptibility for damage as they are located at the cell periphery, than the IFM located between myofibrils (52). This leads to the speculation that as lipid accumulation occurs in the SSM region, processes involved in metabolic signaling including insulin signaling, may be more readily affected (52). While the two primary cardiac mitochondrial subpopulations are differentially impacted during DM, commonalities in the dysfunction exist. For instance, loss of function and proteomic dysregulation in a specific mitochondrial subpopulation during DM insult is noted depending on the subpopulation predominantly impacted (12, 21). Key processes such as nuclear-encoded mitochondrial protein import and ETC function, along with the loss of mtHsp70 protein expression results in dysfunctional IFM during T1DM and SSM during T2DM (12, 21), indicating that the most negatively impacted mitochondrial subpopulation incurs similar deleterious effects to key mitochondrial processes. In Chapter 3, overexpression of mtHsp70 allowed for restoration of these impacted mitochondrial processes in the mitochondrial subpopulation most impacted by the type of DM. Within our transgenic model, mtHsp70 overexpression is not specific to a single mitochondrial subpopulation and should be expressed at equivalent levels within the cardiac mitochondrial subpopulations, thus imparting protection to the subpopulation detrimentally impacted by the disease state. It is important to note that overexpression of mtHsp70 in the subpopulation that appears to be unaltered during the type of DM does not preclude a positive benefit to the mitochondria within that locale and could potentially allow for the mitochondria to function more efficiently; however, our data indicate that

an elevated level of mtHsp70 in the unaffected mitochondrial subpopulation during DM does not necessarily provide an extra positive benefit (Chapter 3). As a result, both pathologies are capable of providing complementary information in order to delineate potential therapeutic interventions that could treat cardiac mitochondrial dysfunction in both diabetic phenotypes.

Interestingly, in both the T1DM and T2DM diabetic pathologies, mtHsp70 was shown to be decreased in the subpopulation predominantly impacted by the disease, revealing the T2DM SSM and the T1DM IFM to have altered mtHsp70 (12, 21). Since greater than 99% of proteins within the mitochondria are imported to the organelle, alterations to mtHsp70, a key player in nuclear-encoded mitochondrial protein import, could lead to a deranged mitochondrial proteomic profile during DM (12). In addition to mtHsp70 being shown to have an essential role in matrix-targeted mitochondrial protein import, mtHsp70 can also play a role in protein import into the IMM and IMS (10). When mtHsp70 is altered, mitochondrial function is compromised with decrements noted in processes including nuclear-encoded mitochondrial protein import, decreased antioxidant defenses, increased misfolding and degradation of proteins, along with increased cellular apoptosis (10). In the aged heart, mtHsp70 is shown to be decreased through proteomic analyses (23). Additionally, neonatal rat cardiomyocytes treated with ET-1 to stimulate cardiac hypertrophy displayed a decrease in mtHsp70 content, suggesting that mitochondrial impairment may occur during the early development of hypertrophy (5). Williamson et al. showed that cardiac myocytes from neonatal rats infected with an adenoviral vector expressing mtHsp70 were protected from I/R injury (82). These cardiomyocytes had increased import of nuclear-encoded antioxidant defense proteins, such as MnSOD (82). In the current work, overexpression of mtHsp70 could lead to a greater efficiency of the nuclear-encoded mitochondrial protein import process.

With mtHsp70 being the key player in powering the mitochondrial import process, along with consistently being altered during both types of DM in our proteomic data, we sought to understand the role of mtHsp70 overexpression during both T1DM and T2DM in Chapter 3. As an integral member of the PAM complex, mtHsp70 is anchored to Tim44 within the mitochondrial matrix and serves as the protein that "traps" and "pulls" the translocating preprotein through the IMM in an ATP-dependent manner (77). Previously our laboratory has shown that during T1DM insult, import of mitochondrial matrix import protein (MitoGFP1) is decreased in the IFM subpopulation, with no changes in the SSM (12). Further, overexpression of mPHGPx, provided protection to processes in the IMM and proteomic restoration likely due to its antioxidant defense system and its restoration of mtHsp70 (11). In the current work, we overexpressed mtHsp70 in order to evaluate its impact on nuclear-encoded mitochondrial protein import during DM. In agreeance with previous work, we saw decrements in MitoGFP1 protein import efficiency at 2 minutes in the T1DM IFM and as early as 30 seconds in the T2DM SSM (Chapter 3). We found that overexpression of mtHsp70 allowed for the restoration of nuclear-encoded mitochondrial protein import in the IFM during T1DM and the SSM during T2DM (Chapter 3).

While decrements in mtHsp70 is one mechanism for nuclear-encoded mitochondrial protein import deficiencies in the heart, other potential mechanisms may include alterations to $\Delta\Psi m$ or structural stability of the mitochondria during a pathological state. Interestingly, previous work from our laboratory shows that during T1DM and T2DM, IFM and SSM have a reduced $\Delta\Psi m$, respectively, which could be involved in decrements to protein import processes, as this is a critical force required for proper protein translocation (12, 21, 35). The currently proposed methods for nuclear-encoded mitochondrial protein import through mtHsp70 both require an active $\Delta\Psi m$, as it is essential for opening the Tim23 channel within the IMM and allowing the pre-

protein to enter into the matrix (14, 73). The Brownian ratchet model for nuclear-encoded mitochondrial protein import relies on the ΔΨm electrophoretic force to move the protein across the IMM, with mtHsp70 trapping the protein and not allowing it to slide backward into the IMS (10). Further, ΔΨm can also help to promote unfolding of protein domains; however, this mechanism is still relatively unexplored (34).

Secondly, alterations to other proteins involved in the import process could be occurring. While our lab has previously assessed major import constituents such as Tom20, Tom40, Tim23 and Tim44 and found no changes during T1DM (12), these protein contents have not been assessed during T2DM. Differences in the pathological conditions, as well as subcellular locale of the mitochondrial subpopulations predominantly affected during the disease, could lead to a differential impact on other import constituents and should be evaluated. Further, while Tim44 may not be decreased in expression level, as was previously shown by our laboratory in the T1DM IFM (12), if the dissociation of mtHsp70 from Tim44 is impaired in the power stroke model, this could potentially lead to an inefficient import process. In regards to structure, proteins involved in mitochondrial protein import, such as mtHsp70, were shown to be associated with mitofilin, an IMM structural protein known to maintain cristae morphology and structure (72). While this likely does not represent a direct association between mitofilin and mtHsp70, it will be important to further investigate the role of maintaining cristae morphology during DM and its effects on nuclear-encoded mitochondrial protein import efficiency.

Mitofilin may also play a critical role in the import of miRNA into the mitochondrion, particularly during DM. While mitofilin has been shown to be directly related to mitochondrial proteins involved in the import of nuclear-encoded proteins, it would be interesting to see if mitofilin is also associated with PNPase, a potential player for the import of miRNA. PNPase is

located in the IMS of the mitochondrion; however, it is speculated to be situated on the IMM (79, 80). If an interaction between PNPase and mitofilin existed, this could be one explanation for how PNPase is tethered to the IMM to allow for the import of miRNA. Our laboratory has previously reported that mitofilin is decreased in the IFM during T1DM, altering the morphology of the mitochondrion and disrupting the proteomic makeup (12, 72). Overexpression of mitofilin during DM could potentially allow for maintained associations between PNPase and unknown miRNA import constituents to the IMM. Preserving the structural stability of the mitochondrion during DM could sustain the functionality of the organelle; however, this might also allow the influx of miRNA into the mitochondrion through PNPase, which could serve a beneficial or detrimental role during DM. Our data revealed that PNPase is upregulated in the T2DM SSM, with an increased association between PNPase and Ago 2, an integral member of the RISC (Chapter 4). It is unknown whether the upregulation of PNPase is detrimental or a compensatory mechanism for miRNA import during a pathological insult. On the one hand, harmful miRNAs targeting important proteins involved in the ETC could be imported through the upregulated PNPase during DM, thus decreasing the ability for the mitochondrion to function properly. Conversely, PNPase expression could be increased in the diabetic setting to allow the entry of miRNAs targeting ROS, which are present due to the diabetic environment. The oxidative environment generated by the induction of the NADPH oxidase (NOX) protein family during different pathological states, could be due to the downregulation of miRNAs targeting these proteins (57). For example, the loss of NOX2 prevents oxidative stress in a pressure overload model of HF, with miRNA-34 and miRNA-17 showing capability of targeting this protein and miRNA-17 being downregulated during HF (27, 36, 38, 48). It would be interesting to utilize the mPHGPx transgenic animal to decrease oxidative stress during DM and evaluate the impact this antioxidant overexpression could have on PNPase

protein expression levels and miRNA import into the mitochondrion. This could potentially allow for scavenging of ROS, thus increasing the functionality of the mitochondrion and decreasing PNPase expression levels during DM, thus in turn influencing miRNA influx into the mitochondrion. Further, while mtHsp70 overexpression has been shown to decrease the accumulation of intracellular ROS when overexpressed in cells subjected to glucose deprivation (49), we did not study ROS levels in our novel transgenic line to determine whether this could also play a role in the association with PNPase and miRNA import into the mitochondrion. MtHsp70 overexpression could potentially serve as a mechanism to protect the mitochondrion from ROS damage during DM, thus allowing for better functionality of the organelle. Additionally, overexpression of mtHsp70 may also play a role in decreasing PNPase levels during DM and influencing the import of miRNA into the mitochondrion. Further research needs to be done to elucidate the mechanism of and the constituents involved in miRNA import into the mitochondrion, particularly within the context of a pathological insult. Moreover, it will be important to determine whether the upregulation of PNPase is due and contributing to the detrimental impact of the pathological insult or is a compensatory mechanism to counteract this insult.

While the different diabetic pathologies reveal influences on mitochondrial processes, our laboratory previously analyzed the impact of DM on the mitochondrial proteome (11, 12, 21). Proteomic profile analyses revealed differential alterations between the mitochondrial subpopulations affected depending on type of DM, with the IFM proteome showing more changes as a result of T1DM, while the SSM proteome showed increased detriment during T2DM (12, 21). We have previously shown in the T1DM and T2DM pathological conditions, alterations to proteins of the mitochondrial respiratory chain, TCA cycle, FAO components, along with transport and

structural proteins (12, 21). Studies from our laboratory indicate that during T1DM, FAO proteins were significantly decreased in the IFM as compared to control (12). In contrast, proteomic analyses from other STZ models of T1DM, displayed increased FAO protein concentrations as compared to controls (31, 74). It is important to note that the protocols for STZ injections, duration of DM and animal backgrounds were different from our previous study, as well as the analysis on total mitochondria not individual mitochondrial subpopulations. Interestingly, overexpression of mtHsp70 during T1DM revealed further decrements in FAO proteins in the IFM when compared to the T1DM mice, whereas in the T2DM SSM, proteins involved in fatty acid metabolism were significantly increased (Chapter 3). During T1DM, the manifestation of the pathology does not possess a gross hyperlipidemia as seen during T2DM, yet our proteomic analyses for the mtHsp70 T1DM mice revealed a down regulation of proteins involved in FAO, indicating that the alternate fuel source is not in use during T1DM. This is contrary to what would be expected because during T1DM while the heart does not utilize glucose efficiently, it would be assumed another fuel source, such as β-oxidation would be increased to allow for proper mitochondrial function. Further, the overexpression of mtHsp70 could be showing decreases in fatty acid metabolism due to the decrease in ETFB, an essential protein for the shuttling of protons to initiate the process (Chapter 3). Our study also found GSTK1 to be significantly increased in the mtHsp70 T1DM IFM, which would allow for a greater insulin sensitivity through adiponectin in these animals, providing evidence that mtHsp70 is utilizing the fuel source most available during the pathological insult (Chapter 3). During T2DM insult, enzymes involved in the phosphorylation of glucose and initiation of glucose metabolism pathways, HK1 and HK2, were decreased in the T2DM SSM, while FAO proteins were increased, thus in line with the milieu that is present during this pathological condition (Chapter 3). Overall, our mitochondrial proteomic evaluation reveals that

in the T1DM IFM and T2DM SSM, mtHsp70 overexpression is responsive to the most abundant fuel source.

Additionally, our laboratory has previously shown alterations to complexes I, IV and V in the IFM during a T1DM insult and the SSM during T2DM (12, 21). Overexpression of mtHsp70 during T1DM led to an increase in proteins involved in complexes I, III, IV and the F_0 complex of complex V as compared to the T1DM mice (Chapter 3). Interestingly, decrements in four subunits of the F_1 complex of complex V were further decreased with the overexpression of mtHsp70 in the T1DM setting (Chapter 3). The F_1 complex contains the extramembraneous core responsible for catalysis, while the F_0 complex forms the membrane channel for protons to travel through (37). As complex V is situated in the IMM and uses the energy of the H^+ electrochemical gradient, which is generated by the movement of electrons through the ETC, the movement of this proton from the IMS to the matrix is coupled with the generation of ATP (29). While it is puzzling as to why the F_1 complex would show increasing decrements with mtHsp70 overexpression during T1DM, mtHsp70 utilizes ATP for the process of nuclear-encoded mitochondrial protein import potentially altering the ATP levels within the mitochondrion. Mechanisms that change the F_1 subunit protein expression levels, however, are difficult to elucidate. Previously, our laboratory has shown decrements in essential proteins in the mitochondrial respiratory chain during T2DM, particularly in the SSM (21). During T2DM, proteins from complexes III, IV and both the F_0 and F_1 of complex V, were increased in the SSM with mtHsp70 overexpression (Chapter 3). Thus, our proteomic data reveal that constituents in the ETC, as well as those involved with ATP production, were preserved with mtHsp70 overexpression in the SSM during T2DM (Chapter 3).

The mitochondrial proteome could be altered via mechanisms of miRNA regulation, as miRNAs play a role in nuclear gene transcription and translation and proteins encoded by the

nuclear genome are key players in normal mitochondrial function. Gene silencing and regulation occurs via the 18-24 nucleotide miRNA binding to the target mRNA (9, 18, 24). Interestingly, miRNAs are capable of getting into the mitochondrion and regulating mitochondrial gene expression (6-8, 13, 16, 39, 44, 57, 68, 69); however, the mechanism of translocation is currently unknown. With literature suggesting a key role for miRNAs in pathological disease states, it is essential to understand their role in cardiovascular diseases, particularly the role within the mitochondrion. While the underlying mechanism for miRNA import into the mitochondria is unknown, evidence suggests that Ago2 plays a pivotal role in the transportation of miRNAs into and out of the mitochondrion (15, 24, 32, 50, 84). While the recent thinking of miRNA transport into the mitochondrion utilizes import constituents from the protein import process (TOM and TIM) (67), we suggest that PNPase may also contribute to this complex import mechanism for miRNA transport across the mitochondrial membranes (Chapter 4). Our research has shown a unique association between Ago2 and PNPase within the mitochondria, which was increased in the SSM during T2DM (Chapter 4). It is currently unknown whether other players in the protein import process play a role in miRNA import; however, it would be important to investigate if PNPase or Ago2 associate directly with TOM or TIM proteins. It would also be interesting to note that if TIM proteins, such as Tim44, played a role in miRNA import into the mitochondrion, whether mtHsp70 would also influence this import process. In addition, it has been postulated that different sequences within the miRNA are capable of targeting the miRNA into the nucleus (67), which could potentially be another mechanism that miRNA are translocating into the mitochondrion. Our laboratory revealed that of the mitomiRs identified in the mitoRISCome by next generation sequencing and microarray analyses, sequences enriched in the nucleotide motifs

AGG and UGG were present (39), potentially supporting the hypothesis that a sequence within the miRNA may target the miRNA to its particular location, such as the mitochondrion.

Another complicating factor in miRNA translocation into the mitochondrion is the differential impact a pathological state can have on mitochondrial subpopulations. Our laboratory has previously shown alterations to miR-141 within the IFM during T1DM (13). MiR-141 regulates IMM phosphate transporter, Slc25a3, which provides inorganic phosphate to the mitochondrial matrix, an essential component for ATP production (13). In addition to miR-141, our laboratory has found a redistribution of miR-378 in the IFM of the T1DM heart, which coincided with a decrease in ATP6 protein expression levels and ATP synthase function (39). Interestingly, alterations to the SSM were uncommon indicating that miRNA can translationally regulate mitochondrially encoded proteins in spatially distinct mitochondrial subpopulations during DM (13, 39). In the current work, we found that overexpression of PNPase in the HL-1 cardiomyocyte cell line resulted in the accumulation of miR-378 within the mitochondrion (Chapter 4). This accumulation corresponded with the decrease in ATP6 protein expression levels and ATP synthase activity (Chapter 4). Further, in the T2DM db/db mouse model we found increased expression of PNPase in the SSM, the mitochondrial subpopulation predominantly affected by T2DM, along with an increase in the association of PNPase with Ago2, providing evidence that PNPase may play a role in the translocation of miRNAs into the mitochondria (Chapter 4). Further studies including PNPase knockdown or knockout would help to clarify our current results and support our claim of PNPases role in miRNA translocation. While we suggest that PNPase may be a player in mitochondrial miRNA import, other constituents playing a role in this translocation mechanism still need to be elucidated.

Within the mitochondrion, proteins are not evenly distributed to the different subcompartments: OMM, IMS, IMM and matrix. Proteomic surveys suggest that approximately 67% of mitochondrial proteins reside in the mitochondrial matrix, followed by 21% located within the IMM, and 6% and 4% residing in the IMS and OMM, respectively (26, 63). Independent of diabetic type and mitochondrial subpopulation, our laboratory has previously shown the IMM and matrix as the most predominantly affected mitochondrial subcompartments for proteomic alterations (12, 21). Of the 21% of total proteins residing within the IMM, approximately 50% of them are altered in the respective subpopulation during DM insult (12, 21). Importantly, the IMM houses the complexes of the ETC, which are imperative for sufficient ATP production and properly functioning mitochondria; therefore, we aimed to restore the proper proteomic makeup for the IMM through overexpression of mtHsp70 during DM. Interestingly, in Chapter 3 we note that both the T1DM IFM and T2DM SSM revealed proteomic alterations in the IMM and mitochondrial matrix, with mtHsp70 allowing for restoration in both subcompartments, thus suggesting that mtHsp70 overexpression allowed for targeted restoration particularly within these locales. MtHsp70 is known to play a role in matrix-targeted mitochondrial protein import, but mtHsp70 has also been demonstrated to play a role in proteins targeted to the IMM and IMS (10). Work by Bohnert et al., revealed that oxidase assembly 1 (oxa1), an IMM translocase, is imported into the matrix via mtHsp70 and reinserted back into the IMM (17). This provides evidence for the assumption that overexpression of mtHsp70 could lead to an increase in nuclear-encoded mitochondrial protein import efficiency into the IMM and help provide stability to the mitochondrial proteome during DM.

In addition to mtHsp70 helping to restore the mitochondrial proteome via increased efficiency in nuclear-encoded mitochondrial protein import, mtHsp70 has been shown to play a

critical role in mitochondrial stability via protein degradation (60). During environmental stress, such as a pathological insult, proteins are at an increased susceptibility for inactivation through misfolding or aggregation (28). Literature suggests that mtHsp70 is capable of stabilizing misfolded or damaged proteins in their unfolded state in order to make them more susceptible to proteolytic degradation from m-AAA and PIM1, which was decreased when mtHsp70 was inactive (60, 61, 78). During DM, mtHsp70 expression levels are decreased, thus leading to the assumption that proteolytic degradation of proteins could be impaired during this pathological insult. With impaired PIM1 proteolysis activity, mitochondrial genomic integrity and proper intron excision of mitochondrially-encoded ETC proteins could be disturbed (75, 76), which may be the case during DM. Further investigation into mtHsp70s role in protein degradation during a pathological influence is warranted due to the effects this could have on the mitochondrial proteome.

Cardiac complications are the leading cause of morbidity and mortality among diabetic patients (42, 83). It is imperative for physicians to be able to detect changes in cardiac function through either conventional measures or using the highly sensitive speckle-tracking based strain analysis software. In Chapter 2, we discussed the efficiency of using speckle-tracking based strain analyses in detecting subtle changes of LV function prior to conventional changes during the progression of T1DM. Conventional measures revealed changes at 6-weeks in the T1DM heart (Chapter 2). In Chapter 3, we highlight that LV pump function is decreased in the type 1 and type 2 diabetic animals as seen by conventional measures, such as EF and FS. We found that overexpression of mtHsp70 restored conventional measurements back to that of control level, likely due to the restored functionality of the mitochondria through increased efficiency of nuclear-encoded mitochondrial protein import, leading to a stabilized mitochondrial proteome despite the pathological influence of DM (Chapter 3). Further, analyses using the speckle-tracking based

strain software to evaluate global and regional strain were performed to provide a more complete picture for the deficits noted in the LV. When using speckle-tracking based strain analyses, we found changes as early as 1-week post-T1DM onset, mainly in the radial dimension (Chapter 2). Further, assessment of regional changes within the LV were performed during T1DM, with the detriments predominantly in the free wall region (Chapter 2). This brings into question, why the free wall region was affected by T1DM, but few decrements were seen in the septal wall region. We speculate that the IFM, which are predominantly affected during T1DM, are dysfunctional particularly within the free wall region of the LV. The LV myocardial wall becomes activated in the septal and anterior free wall regions through the Purkinje system, with this activation traveling from the apex to the base of the LV (62, 64). Interestingly, the LV activation sequence through this system is relatively similar between the septal and free wall regions (62, 64), thus it would be interesting to evaluate each region of the LV and determine if mitochondrial function is decreased within the particular locale coinciding with the strain and strain rate dysfunction during T1DM. Further, it would also be interesting to evaluate subpopulations within each LV region to determine if deficits during T1DM is due to decreased IFM function. Without properly functioning mitochondria and ample production of ATP, cardiac contractile dysfunction is oftentimes disrupted (11, 12, 21, 22). In Chapter 3, our studies using speckle-tracking based strain analyses provide evidence that this technique is capable of detecting subtle changes in myocardial performance during both types of DM; however, these mice already demonstrated decreased LV function through conventional measures. Decrements in longitudinal strain and longitudinal strain rate during both T1DM and T2DM provide complementary evidence of LV systolic dysfunction with subsequent restoration via mtHsp70 overexpression (Chapter 3). Evaluation of regional differences revealed commonalities between longitudinal strain rate in T1DM and T2DM with

decrements in the apex regions, in which mtHsp70 overexpression was able to restore the posterior apex region independent of DM type. Interestingly, mtHsp70 overexpression appeared to provide more regional benefit during T2DM than T1DM. It is noteworthy to evaluate why mtHsp70 overexpression appears to provide protection to certain regions and not others of the LV when the αMHC promotor should allow for even expression throughout the heart. It would be interesting to evaluate the expression levels of mtHsp70 in each LV region and determine if mtHsp70 overexpression restored mitochondrial function within these particular sub-locales. If mtHsp70 did not restore contractile function within a particular LV region, it would be interesting to evaluate the nuclear-encoded mitochondrial protein import mechanism and the activity of mtHsp70. We speculate that the restoration of cardiac contractile function in Chapter 3 is due to mtHsp70's positive impact on mitochondrial functionality through increased efficiency of nuclear-encoded mitochondrial proteins, which would be critical for stabilization of the mitochondrial proteome in the face of DM. While the type of DM has differential influences on mitochondrial subpopulations, it is interesting to note that ATP production from each subpopulation is likely critical for efficient cardiac contractile function. This indicates that both the SSM and IFM may play a role in preserving cardiac function during pathological insults. Literature suggests that an interconnected mitochondrial network through the mitochondrial reticulum could provide a pathway for energy distribution within the cardiomyocyte (30, 66), thus allowing for the restoration of cardiac contractile function by mtHsp70, despite different mitochondrial subpopulations being affected. Further, Glancy et al. suggest that the contiguous matrix and its elements between the different mitochondrial subpopulations could be a conductive element through this network to allow for the electrical conduction (30). This type of energy distribution could be disrupted during DM and potentially restored with the overexpression of mtHsp70; however, this would need to be assessed.

In summary, the data presented suggest that deficits in the mitochondrial proteome leads to inefficient mitochondrial function, presumably due to deficient nuclear-encoded mitochondrial protein import. In particular, mtHsp70 serves as a central node for restoration of nuclear-encoded mitochondrial protein import, which is essential for maintenance of proper nuclear-encoded protein content within the mitochondrion, particularly in the mitochondrial subpopulation most impacted during the different types of DM. Further, the import of miRNA species into the mitochondria potentially through a complex mechanism of interaction between the RISC and PNPase, could contribute to posttranscriptional regulation and translational repression of proteins encoded by the mitochondrial genome during DM. In conclusion, therapeutic interventions targeted to maintain the mitochondrial proteome through efficient nuclear-encoded mitochondrial protein import and regulation of miRNA import into the mitochondrion during DM may provide protection against cardiac contractile dysfunction in the diabetic heart independent of type of DM.

REFERENCES

1. Diabetes Fact Sheet. *World Health Organization*, 2016.

2. National Diabetes Statistics, edited by Clearinghouse NDI, 2011.

3. The State of Obesity: Better Policies for a Healthier America. 2015.

4. **Adhihetty PJ, Ljubicic V, Menzies KJ, and Hood DA.** Differential susceptibility of subsarcolemmal and intermyofibrillar mitochondria to apoptotic stimuli. *Am J Physiol Cell Physiol* 289: C994-C1001, 2005.

5. **Agnetti G, Bezstarosti K, Dekkers DH, Verhoeven AJ, Giordano E, Guarnieri C, Caldarera CM, Van Eyk JE, and Lamers JM.** Proteomic profiling of endothelin-1-stimulated hypertrophic cardiomyocytes reveals the increase of four different desmin species and alpha-B-crystallin. *Biochim Biophys Acta* 1784: 1068-1076, 2008.

6. **Bandiera S, Mategot R, Girard M, Demongeot J, and Henrion-Caude A.** MitomiRs delineating the intracellular localization of microRNAs at mitochondria. *Free Radic Biol Med* 64: 12-19, 2013.

7. **Bandiera S, Ruberg S, Girard M, Cagnard N, Hanein S, Chretien D, Munnich A, Lyonnet S, and Henrion-Caude A.** Nuclear outsourcing of RNA interference components to human mitochondria. *PloS one* 6: e20746, 2011.

8. **Barrey E, Saint-Auret G, Bonnamy B, Damas D, Boyer O, and Gidrol X.** Pre-microRNA and mature microRNA in human mitochondria. *PloS one* 6: e20220, 2011.

9. **Barringhaus KG and Zamore PD.** MicroRNAs: regulating a change of heart. *Circulation* 119: 2217-2224, 2009.

10. **Baseler WA, Croston TL, and Hollander JM.** Functional Characteristics of Mortalin. In: *Mortalin Biology: Life, Stress and Death*, edited by Kaul SC and Wadhwa R. New York: Springer, 2012, p. 55-80.
11. **Baseler WA, Dabkowski ER, Jagannathan R, Thapa D, Nichols CE, Shepherd DL, Croston TL, Powell M, Razunguzwa TT, Lewis SE, Schnell DM, and Hollander JM.** Reversal of mitochondrial proteomic loss in Type 1 diabetic heart with overexpression of phospholipid hydroperoxide glutathione peroxidase. *Am J Physiol Regul Integr Comp Physiol* 304: R553-565, 2013.
12. **Baseler WA, Dabkowski ER, Williamson CL, Croston TL, Thapa D, Powell MJ, Razunguzwa TT, and Hollander JM.** Proteomic alterations of distinct mitochondrial subpopulations in the type 1 diabetic heart: contribution of protein import dysfunction. *Am J Physiol Regul Integr Comp Physiol* 300: R186-200, 2011.
13. **Baseler WA, Thapa D, Jagannathan R, Dabkowski ER, Croston TL, and Hollander JM.** miR-141 as a regulator of the mitochondrial phosphate carrier (Slc25a3) in the type 1 diabetic heart. *Am J Physiol Cell Physiol* 303: C1244-1251, 2012.
14. **Bauer MF, Sirrenberg C, Neupert W, and Brunner M.** Role of Tim23 as voltage sensor and presequence receptor in protein import into mitochondria. *Cell* 87: 33-41, 1996.
15. **Beitzinger M, Peters L, Zhu JY, Kremmer E, and Meister G.** Identification of human microRNA targets from isolated argonaute protein complexes. *RNA Biol* 4: 76-84, 2007.
16. **Bian Z, Li LM, Tang R, Hou DX, Chen X, Zhang CY, and Zen K.** Identification of mouse liver mitochondria-associated miRNAs and their potential biological functions. *Cell Res* 20: 1076-1078, 2010.

17. **Bohnert M, Rehling P, Guiard B, Herrmann JM, Pfanner N, and van der Laan M.** Cooperation of stop-transfer and conservative sorting mechanisms in mitochondrial protein transport. *Curr Biol* 20: 1227-1232, 2010.
18. **Calin GA and Croce CM.** MicroRNA signatures in human cancers. *Nat Rev Cancer* 6: 857-866, 2006.
19. **Croston TL, Shepherd DL, Thapa D, Nichols CE, Lewis SE, Dabkowski ER, Jagannathan R, Baseler WA, and Hollander JM.** Evaluation of the cardiolipin biosynthetic pathway and its interactions in the diabetic heart. *Life sciences* 93: 313-322, 2013.
20. **Croston TL, Thapa D, Holden AA, Tveter KJ, Lewis SE, Shepherd DL, Nichols CE, Long DM, Olfert IM, Jagannathan R, and Hollander JM.** Functional deficiencies of subsarcolemmal mitochondria in the type 2 diabetic human heart. *Am J Physiol Heart Circ Physiol* 307: H54-65, 2014.
21. **Dabkowski ER, Baseler WA, Williamson CL, Powell M, Razunguzwa TT, Frisbee JC, and Hollander JM.** Mitochondrial dysfunction in the type 2 diabetic heart is associated with alterations in spatially distinct mitochondrial proteomes. *Am J Physiol Heart Circ Physiol* 299: H529-540, 2010.
22. **Dabkowski ER, Williamson CL, Bukowski VC, Chapman RS, Leonard SS, Peer CJ, Callery PS, and Hollander JM.** Diabetic cardiomyopathy-associated dysfunction in spatially distinct mitochondrial subpopulations. *Am J Physiol Heart Circ Physiol* 296: H359-369, 2009.

23. **Dai Q, Escobar GP, Hakala KW, Lambert JM, Weintraub ST, and Lindsey ML.** The left ventricle proteome differentiates middle-aged and old left ventricles in mice. *J Proteome Res* 7: 756-765, 2008.

24. **Das S, Ferlito M, Kent OA, Fox-Talbot K, Wang R, Liu D, Raghavachari N, Yang Y, Wheelan SJ, Murphy E, and Steenbergen C.** Nuclear miRNA regulates the mitochondrial genome in the heart. *Circ Res* 110: 1596-1603, 2012.

25. **Devereux RB, Roman MJ, Paranicas M, O'Grady MJ, Lee ET, Welty TK, Fabsitz RR, Robbins D, Rhoades ER, and Howard BV.** Impact of diabetes on cardiac structure and function: the strong heart study. *Circulation* 101: 2271-2276, 2000.

26. **Distler AM, Kerner J, and Hoppel CL.** Proteomics of mitochondrial inner and outer membranes. *Proteomics* 8: 4066-4082, 2008.

27. **Divakaran V and Mann DL.** The emerging role of microRNAs in cardiac remodeling and heart failure. *Circ Res* 103: 1072-1083, 2008.

28. **Dobson CM.** Protein folding and misfolding. *Nature* 426: 884-890, 2003.

29. **Fillingame RH.** Coupling H+ transport and ATP synthesis in F1F0-ATP synthases: glimpses of interacting parts in a dynamic molecular machine. *J Exp Biol* 200: 217-224, 1997.

30. **Glancy B, Hartnell LM, Malide D, Yu ZX, Combs CA, Connelly PS, Subramaniam S, and Balaban RS.** Mitochondrial reticulum for cellular energy distribution in muscle. *Nature* 523: 617-620, 2015.

31. **Hamblin M, Friedman DB, Hill S, Caprioli RM, Smith HM, and Hill MF.** Alterations in the diabetic myocardial proteome coupled with increased myocardial oxidative stress underlies diabetic cardiomyopathy. *J Mol Cell Cardiol* 42: 884-895, 2007.

32. **Hock J, Weinmann L, Ender C, Rudel S, Kremmer E, Raabe M, Urlaub H, and Meister G.** Proteomic and functional analysis of Argonaute-containing mRNA-protein complexes in human cells. *EMBO Rep* 8: 1052-1060, 2007.

33. **Hollander JM, Thapa D, and Shepherd DL.** Physiological and structural differences in spatially distinct subpopulations of cardiac mitochondria: influence of cardiac pathologies. *Am J Physiol Heart Circ Physiol* 307: H1-14, 2014.

34. **Huang SH, Ratliff KS, and Matouschek A.** Protein unfolding by the mitochondrial membrane potential. *Nature Structural Biology* 9: 301-307, 2002.

35. **Huttemann M, Lee I, Pecinova A, Pecina P, Przyklenk K, and Doan JW.** Regulation of oxidative phosphorylation, the mitochondrial membrane potential, and their role in human disease. *J Bioenerg Biomembr* 40: 445-456, 2008.

36. **Ikeda S, Kong SW, Lu J, Bisping E, Zhang H, Allen PD, Golub TR, Pieske B, and Pu WT.** Altered microRNA expression in human heart disease. *Physiological genomics* 31: 367-373, 2007.

37. **Issartel JP, Dupuis A, Garin J, Lunardi J, Michel L, and Vignais PV.** The ATP synthase (F0-F1) complex in oxidative phosphorylation. *Experientia* 48: 351-362, 1992.

38. **Jadhav VS, Krause KH, and Singh SK.** HIV-1 Tat C modulates NOX2 and NOX4 expressions through miR-17 in a human microglial cell line. *J Neurochem* 131: 803-815, 2014.

39. **Jagannathan R, Thapa D, Nichols CE, Shepherd DL, Stricker JC, Croston TL, Baseler WA, Lewis SE, Martinez I, and Hollander JM.** Translational Regulation of the Mitochondrial Genome Following Redistribution of Mitochondrial MicroRNA in the Diabetic Heart. *Circ Cardiovasc Genet* 8: 785-802, 2015.

40. **Judge S, Jang YM, Smith A, Hagen T, and Leeuwenburgh C.** Age-associated increases in oxidative stress and antioxidant enzyme activities in cardiac interfibrillar mitochondria: implications for the mitochondrial theory of aging. *FASEB J* 19: 419-421, 2005.

41. **Judge S, Jang YM, Smith A, Selman C, Phillips T, Speakman JR, Hagen T, and Leeuwenburgh C.** Exercise by lifelong voluntary wheel running reduces subsarcolemmal and interfibrillar mitochondrial hydrogen peroxide production in the heart. *Am J Physiol Regul Integr Comp Physiol* 289: R1564-1572, 2005.

42. **Kannel WB and McGee DL.** Diabetes and cardiovascular disease. The Framingham study. *JAMA : the journal of the American Medical Association* 241: 2035-2038, 1979.

43. **Kelley DE, He J, Menshikova EV, and Ritov VB.** Dysfunction of mitochondria in human skeletal muscle in type 2 diabetes. *Diabetes* 51: 2944-2950, 2002.

44. **Kren BT, Wong PY, Sarver A, Zhang X, Zeng Y, and Steer CJ.** MicroRNAs identified in highly purified liver-derived mitochondria may play a role in apoptosis. *RNA Biol* 6: 65-72, 2009.

45. **Lesnefsky EJ, Chen Q, Slabe TJ, Stoll MS, Minkler PE, Hassan MO, Tandler B, and Hoppel CL.** Ischemia, rather than reperfusion, inhibits respiration through cytochrome oxidase in the isolated, perfused rabbit heart: role of cardiolipin. *Am J Physiol Heart Circ Physiol* 287: H258-267, 2004.

46. **Lesnefsky EJ, Gudz TI, Moghaddas S, Migita CT, Ikeda-Saito M, Turkaly PJ, and Hoppel CL.** Aging decreases electron transport complex III activity in heart interfibrillar mitochondria by alteration of the cytochrome c binding site. *J Mol Cell Cardiol* 33: 37-47, 2001.

47. **Lesnefsky EJ, Slabe TJ, Stoll MS, Minkler PE, and Hoppel CL.** Myocardial ischemia selectively depletes cardiolipin in rabbit heart subsarcolemmal mitochondria. *Am J Physiol Heart Circ Physiol* 280: H2770-2778, 2001.

48. **Li SZ, Hu YY, Zhao J, Zhao YB, Sun JD, Yang YF, Ji CC, Liu ZB, Cao WD, Qu Y, Liu WP, Cheng G, and Fei Z.** MicroRNA-34a induces apoptosis in the human glioma cell line, A172, through enhanced ROS production and NOX2 expression. *Biochem Biophys Res Commun* 444: 6-12, 2014.

49. **Liu Y, Liu W, Song XD, and Zuo J.** Effect of GRP75/mthsp70/PBP74/mortalin overexpression on intracellular ATP level, mitochondrial membrane potential and ROS accumulation following glucose deprivation in PC12 cells. *Mol Cell Biochem* 268: 45-51, 2005.

50. **Maniataki E and Mourelatos Z.** Human mitochondrial tRNAMet is exported to the cytoplasm and associates with the Argonaute 2 protein. *RNA* 11: 849-852, 2005.

51. **Nichols CE, Shepherd DL, Knuckles TL, Thapa D, Stricker JC, Stapleton PA, Minarchick VC, Erdely A, Zeidler-Erdely PC, Alway SE, Nurkiewicz TR, and Hollander JM.** Cardiac and mitochondrial dysfunction following acute pulmonary exposure to mountaintop removal mining particulate matter. *Am J Physiol Heart Circ Physiol* 309: H2017-2030, 2015.

52. **Nielsen J, Mogensen M, Vind BF, Sahlin K, Hojlund K, Schroder HD, and Ortenblad N.** Increased subsarcolemmal lipids in type 2 diabetes: effect of training on localization of lipids, mitochondria, and glycogen in sedentary human skeletal muscle. *Am J Physiol Endocrinol Metab* 298: E706-713, 2010.

53. **Palmer JW, Tandler B, and Hoppel CL.** Biochemical differences between subsarcolemmal and interfibrillar mitochondria from rat cardiac muscle: effects of procedural manipulations. *Arch Biochem Biophys* 236: 691-702, 1985.

54. **Palmer JW, Tandler B, and Hoppel CL.** Biochemical properties of subsarcolemmal and interfibrillar mitochondria isolated from rat cardiac muscle. *J Biol Chem* 252: 8731-8739, 1977.

55. **Palmer JW, Tandler B, and Hoppel CL.** Heterogeneous response of subsarcolemmal heart mitochondria to calcium. *Am J Physiol* 250: H741-748, 1986.

56. **Pfanner N and Geissler A.** Versatility of the mitochondrial protein import machinery. *Nat Rev Mol Cell Biol* 2: 339-349, 2001.

57. **Pinti MV, Hathaway QA, and Hollander JM.** Role of MicroRNA in Metabolic Shift During Heart Failure. *Am J Physiol Heart Circ Physiol*: ajpheart 00341 02016, 2016.

58. **Ritov VB, Menshikova EV, He J, Ferrell RE, Goodpaster BH, and Kelley DE.** Deficiency of subsarcolemmal mitochondria in obesity and type 2 diabetes. *Diabetes* 54: 8-14, 2005.

59. **Rolo AP and Palmeira CM.** Diabetes and mitochondrial function: role of hyperglycemia and oxidative stress. *Toxicol Appl Pharmacol* 212: 167-178, 2006.

60. **Savel'ev AS, Novikova LA, Kovaleva IE, Luzikov VN, Neupert W, and Langer T.** ATP-dependent proteolysis in mitochondria. m-AAA protease and PIM1 protease exert overlapping substrate specificities and cooperate with the mtHsp70 system. *J Biol Chem* 273: 20596-20602, 1998.

61. **Saveliev AS, Kovaleva IE, Novikova LA, Isaeva LV, and Luzikov VN.** Can foreign proteins imported into yeast mitochondria interfere with PIM1p protease and/or chaperone function? *Arch Biochem Biophys* 363: 373-376, 1999.

62. **Scher AM.** Studies of the electrical activity of the ventricles and the origin of the QRS complex. *Acta Cardiol* 50: 429-465, 1995.

63. **Schnaitman C and Greenawalt JW.** Enzymatic properties of the inner and outer membranes of rat liver mitochondria. *The Journal of cell biology* 38: 158-175, 1968.

64. **Sengupta PP, Korinek J, Belohlavek M, Narula J, Vannan MA, Jahangir A, and Khandheria BK.** Left ventricular structure and function: basic science for cardiac imaging. *J Am Coll Cardiol* 48: 1988-2001, 2006.

65. **Shen X, Zheng S, Thongboonkerd V, Xu M, Pierce WM, Jr., Klein JB, and Epstein PN.** Cardiac mitochondrial damage and biogenesis in a chronic model of type 1 diabetes. *Am J Physiol Endocrinol Metab* 287: E896-905, 2004.

66. **Skulachev VP.** Power transmission along biological membranes. *J Membr Biol* 114: 97-112, 1990.

67. **Srinivasan H and Das S.** Mitochondrial miRNA (MitomiR): a new player in cardiovascular health. *Can J Physiol Pharmacol* 93: 855-861, 2015.

68. **Sripada L, Tomar D, Prajapati P, Singh R, Singh AK, and Singh R.** Systematic analysis of small RNAs associated with human mitochondria by deep sequencing: detailed analysis of mitochondrial associated miRNA. *PloS one* 7: e44873, 2012.

69. **Sripada L, Tomar D, and Singh R.** Mitochondria: one of the destinations of miRNAs. *Mitochondrion* 12: 593-599, 2012.

70. **Stojanovski D, Johnston AJ, Streimann I, Hoogenraad NJ, and Ryan MT.** Import of nuclear-encoded proteins into mitochondria. *Exp Physiol* 88: 57-64, 2003.

71. **Stojanovski D, Pfanner N, and Wiedemann N.** Import of proteins into mitochondria. *Methods in cell biology* 80: 783-806, 2007.

72. **Thapa D, Nichols CE, Lewis SE, Shepherd DL, Jagannathan R, Croston TL, Tveter KJ, Holden AA, Baseler WA, and Hollander JM.** Transgenic overexpression of mitofilin attenuates diabetes mellitus-associated cardiac and mitochondria dysfunction. *J Mol Cell Cardiol* 79: 212-223, 2015.

73. **Truscott KN, Kovermann P, Geissler A, Merlin A, Meijer M, Driessen AJ, Rassow J, Pfanner N, and Wagner R.** A presequence- and voltage-sensitive channel of the mitochondrial preprotein translocase formed by Tim23. *Nat Struct Biol* 8: 1074-1082, 2001.

74. **Turko IV and Murad F.** Quantitative protein profiling in heart mitochondria from diabetic rats. *J Biol Chem* 278: 35844-35849, 2003.

75. **van Dyck L, Neupert W, and Langer T.** The ATP-dependent PIM1 protease is required for the expression of intron-containing genes in mitochondria. *Genes Dev* 12: 1515-1524, 1998.

76. **Van Dyck L, Pearce DA, and Sherman F.** PIM1 encodes a mitochondrial ATP-dependent protease that is required for mitochondrial function in the yeast Saccharomyces cerevisiae. *J Biol Chem* 269: 238-242, 1994.

77. **Voos W, Martin H, Krimmer T, and Pfanner N.** Mechanisms of protein translocation into mitochondria. *Biochim Biophys Acta* 1422: 235-254, 1999.

78. **Wagner I, van Dyck L, Savel'ev AS, Neupert W, and Langer T.** Autocatalytic processing of the ATP-dependent PIM1 protease: crucial function of a pro-region for sorting to mitochondria. *EMBO J* 16: 7317-7325, 1997.

79. **Wang G, Chen HW, Oktay Y, Zhang J, Allen EL, Smith GM, Fan KC, Hong JS, French SW, McCaffery JM, Lightowlers RN, Morse HC, 3rd, Koehler CM, and Teitell MA.** PNPASE regulates RNA import into mitochondria. *Cell* 142: 456-467, 2010.

80. **Wang G, Shimada E, Koehler CM, and Teitell MA.** PNPASE and RNA trafficking into mitochondria. *Biochim Biophys Acta* 1819: 998-1007, 2012.

81. **Williamson CL, Dabkowski ER, Baseler WA, Croston TL, Alway SE, and Hollander JM.** Enhanced apoptotic propensity in diabetic cardiac mitochondria: influence of subcellular spatial location. *Am J Physiol Heart Circ Physiol* 298: H633-642, 2010.

82. **Williamson CL, Dabkowski ER, Dillmann WH, and Hollander JM.** Mitochondria protection from hypoxia/reoxygenation injury with mitochondria heat shock protein 70 overexpression. *Am J Physiol Heart Circ Physiol* 294: H249-256, 2008.

83. **Zarich SW and Nesto RW.** Diabetic cardiomyopathy. *American heart journal* 118: 1000-1012, 1989.

84. **Zhang X, Zuo X, Yang B, Li Z, Xue Y, Zhou Y, Huang J, Zhao X, Zhou J, Yan Y, Zhang H, Guo P, Sun H, Guo L, Zhang Y, and Fu XD.** MicroRNA directly enhances mitochondrial translation during muscle differentiation. *Cell* 158: 607-619, 2014.

Title: Early detection of cardiac dysfunction in the type 1 diabetic heart using speckle-tracking based strain imaging

Author: Danielle L. Shepherd,Cody E. Nichols,Tara L. Croston,Sarah L. McLaughlin,Ashley B. Petrone,Sara E. Lewis,Dharendra Thapa,Dustin M. Long,Gregory M. Dick,John M. Hollander

Publication: Journal of Molecular and Cellular Cardiology

Publisher: Elsevier

Date: January 2016

Order Completed

Thank you for your order.

This Agreement between Danielle L Shepherd ("You") and Elsevier ("Elsevier") consists of your license details and the terms and conditions provided by Elsevier and Copyright Clearance Center.

Your confirmation email will contain your order number for future reference.

Printable details.

License Number	3997400444407
License date	Nov 27, 2016
Licensed Content Publisher	Elsevier
Licensed Content Publication	Journal of Molecular and Cellular Cardiology
Licensed Content Title	Early detection of cardiac dysfunction in the type 1 diabetic heart using speckle-tracking based strain imaging
Licensed Content Author	Danielle L. Shepherd,Cody E. Nichols,Tara L. Croston,Sarah L. McLaughlin,Ashley B. Petrone,Sara E. Lewis,Dharendra Thapa,Dustin M. Long,Gregory M. Dick,John M. Hollander
Licensed Content Date	January 2016
Licensed Content Volume	90
Licensed Content Issue	n/a
Licensed Content Pages	10
Type of Use	reuse in a thesis/dissertation
Portion	full article
Format	both print and electronic
Are you the author of this Elsevier article?	Yes
Will you be translating?	No
Order reference number	

Title of your thesis/dissertation	Cardiac and Mitochondrial Dysfunction during Diabetes Mellitus: Examination of Mitochondrial Import Mechanisms
Expected completion date	Dec 2016
Estimated size (number of pages)	300
Elsevier VAT number	GB 494 6272 12
Requestor Location	Danielle L Shepherd 1 Medical Center Drive PO BOX 9227 MORGANTOWN, WV 26505 United States Attn: Danielle L Shepherd
Total	0.00 USD

ORDER MORE CLOSE WINDOW

Danielle L. Shepherd

OFFICE ADDRESS

Division of Exercise Physiology and
Center for Cardiovascular and
Respiratory Sciences
West Virginia School of Medicine
1 Medical Center Drive
P.O. Box 9227
Morgantown, WV 26506
Tel: (304) 293-7311
Fax: (304) 293-7105
Email: dshepherd@mix.wvu.edu
Personal Email: Danielle.L.Shepherd@gmail.com

EDUCATION

December 2016	**Doctor of Philosophy, Exercise Physiology** Biomedical Sciences, Division of Exercise Physiology Laboratory of Dr. John Hollander West Virginia University School of Medicine Morgantown, West Virginia **Thesis topic:** Cardiac and Mitochondrial Dysfunction during Diabetes Mellitus: Examination of Mitochondrial Import Mechanisms
May 2010	Bachelor of Arts, Psychology Department of Psychology and Neuroscience Minors: Biology and Chemistry Graduated Summa Cum Laude Baylor University Waco, Texas

TEACHING EXPERIENCE/MENTORING

2016	Exercise Science 420-01. Research Design in Exercise Science. Adjunct Professor West Virginia Wesleyan College.
2016	Incoming Biomedical Sciences Graduate Students. Facilitated laboratory skills for new laboratory member, helped to develop projects and protocols: Seth Stine and Quincy Hathaway.
2014	Exercise Physiology 787: Cardiopulmonary Physiology. West Virginia University. Echocardiography and Speckle-Tracking Based Strain Analyses.

2013	Physiology 441: Mechanism of Body Function. West Virginia University. The Digestive System Lecture Series.
2013	Biomedical Sciences 706: Cellular Methods. West Virginia University.
2012-2016	Facilitated laboratory skills and developed projects for Undergraduate and Masters Students: Breanna Nolan, Dave Schnell, Mark Pinti, Kristen Hughes, Kolbi Tonkovich.
2012-2016	West Virginia IDeA Network of Biomedical Research Excellence (WV-INBRE) Undergraduate Summer Research Program. Designed research projects and helped them gain experience in a research laboratory. Mentored Gabrielle LaFata (2012); Danielle Stankus (2013); Danielle Nehilla (2014); Shruthi Skreekumar (2015); Shruthi Skreekumar (2016).
2011-2015	Incoming Biomedical Sciences Graduate Students. Facilitated laboratory skills for rotation students: Blake Moses, Ahmad Hanif, Kyle Mandler, and Erriene Olesh (2011); Ashley Petrone (2012); Tanya Dilan and Dylan Boehm (2014); Seth Stine (2015).
2008-2010	Lab Assistant. Introductory Biology Lab (BIO1105 and BIO1106). Baylor University.

SCIENTIFIC OUTREACH

2016	Children's Discovery Museum of West Virginia. STEM board games. April 23, 2016.
2015	Children's Discovery Museum of West Virginia. Participation in Science Day. What are Germs? October 17, 2015.
2015	Health Sciences and Technology Academy Guest Speaker. University High School, Morgantown, West Virginia. October 5, 2015.
2015	Eastwood Elementary Science Fair 3rd, 4th and 5th Grade Poster Judge and Judge for Excellence in Physiology Research from the American Physiological Society. Eastwood Elementary, Morgantown, West Virginia. June 4, 2015.
2015	Intel International Science and Engineering Fair Grand Award Judge. David L. Lawrence Convention Center, Pittsburgh, Pennsylvania. May 12-13, 2015.
2015	Expanding Your Horizons Conference. Potomac State College, Keyser, West Virginia. April 18, 2015.

2015	How you make slime and making observations. Boys and Girls Club, Brookhaven Elementary School, Morgantown, West Virginia. April 17, 2015.
2015	Dominion West Virginia State Science and Engineering Fair Judge. Fairmont State University, Fairmont, West Virginia. March 28, 2015.
2015, 2016	West Virginia Regional Science Bowl Volunteer. West Virginia University, Morgantown, West Virginia. February 6, 2015; February 5, 2016.
2014	Cheat Lake Elementary Science Fair 2nd and 3rd Grade Poster Judge and Science Activity Coordinator. Cheat Lake Elementary, Morgantown, West Virginia. November 5, 2014.
2014	North Elementary School 3rd Grade Brain Day. Brain Awareness Week. North Elementary School, Morgantown, West Virginia. November 5, 2014.
2014	Watson Elementary School Science Day. 9-weeks Positive Behavior Program. Watson Elementary School, Fairmont, West Virginia. October 24, 2014.
2014	Numbers and Neuroscience Night. Mountainview Elementary School, Morgantown, West Virginia. March 5, 2014.

LEADERSHIP/SERVICE POSITIONS

2016	Appalachian Regional Cell Conference (ARCC) Co-organizer/Consultant. October 1, 2016.
2015	Appalachian Regional Cell Conference (ARCC) Co-organizer/Consultant. November 21, 2015.
2014	Appalachian Regional Cell Conference (ARCC)-sponsored by the American Society for Cell Biology – Invited Poster Judge. November 8, 2014.
2014	West Virginia University Research Induction Ceremony Invited Member of Stage Party for Ethical Oath Recitation and Coating Ceremony. October 24, 2014.
2014 – 2015	Health Sciences Center Graduate Student Organization President. West Virginia University School of Medicine.

2014	Van Liere Selection Committee and Oral Presentation Judge, West Virginia University.
2013	Appalachian Regional Cell Conference (ARCC)-sponsored by the American Society for Cell Biology – Invited Poster Judge and Co-organizer/Consultant. October 26, 2013.
2013	West Virginia University Research Induction Ceremony Invited Member of Stage Party for Ethical Oath Recitation and Coating Ceremony. October 25, 2013.
2013 - Present	Biomedical Sciences Graduate Program Review Committee. West Virginia University School of Medicine.
2013 - 2014	Incoming Student Mentorship Program Coordinator (Recruitment periods in Spring 2013 and 2014). West Virginia University School of Medicine.
2013 - 2014	Health Sciences Center Graduate Student Organization Vice President. West Virginia University School of Medicine.
2012	Co-PI for Appalachian Regional Cell Conference (ARCC)-sponsored by the American Society for Cell Biology – Lead Organizer.
2012	Invited/Scheduled Dr. Ronglih Liao to speak for Cell Biology Training Program, West Virginia University.
2011 - 2013	Graduate Student Organization Leader. Social Committee Chair. West Virginia University School of Medicine.
2011	Search Committee Member for Assistant Director of Graduate Education for West Virginia University Health Sciences Center.
2011 - 2014	Ph.D. Student Recruitment Ambassador/Coordinator. West Virginia University School of Medicine.
2010 - Present	Class Representative for Biomedical Sciences Incoming 2010 class, West Virginia University.

HONORS/AWARDS

2016	Induction into the E.J. Van Liere Research Society. West Virginia University, Morgantown, West Virginia. July 21, 2016.
2016	Peer Science Award for Favorite Poster Presentation. Mitochondrial Biology Symposium: Novel Roles of Mitochondria in Health and

Disease. National Institutes of Health, Bethesda, Maryland. May 19-20, 2016.

2016 — 2nd Place 3 Minute Thesis Competition for West Virginia University. West Virginia University, Morgantown, West Virginia. April 7, 2016.

2016 — 1st Place 3 Minute Thesis Competition Finalist for Health Sciences Center. West Virginia University, Morgantown, West Virginia. March 8, 2016.

2015 — 3rd Place Video Competition. Share Your Science Video Contest, American Society for Cell Biology.

2015 — 1st Place Poster Presentation, Appalachian Regional Cell Conference, Huntington, West Virginia. Title of work: Import of microRNA378 into Cardiac Mitochondria: How do they get in?

2015 — 1st Place Poster Presentation, West Virginia Clinical and Translational Science Institute Annual Meeting, Charleston, West Virginia. Title of work: A New Clinical Predictor of Disease Development in the Type 2 Diabetic Patient?

2015 — 2014-2015 Kenneth D. Gray Student Leadership Award, West Virginia University.

2015 — 3 Minute Thesis Competition Finalist. How the heart works during diabetes. West Virginia University. Morgantown, West Virginia. April 9, 2015.

2014 — 2014 APS Endocrinology and Metabolism Section Campbell Award Poster Competition. Federation of American Societies for Experimental Biology (FASEB). Title of work: The Type 2 Diabetic Patient and Cardiac Mitochondrial Dysfunction: A new perspective.

2013-2015 — Scholarship Winner for the American Association for the Advancement of Science/Science Program for Excellence in Science.

2013 — Science, Technology, Engineering, and Mathematics Entrepreneurship Essentials Workshop Scholarship. College of Business and Economics, Center for Executive Education. West Virginia University. Morgantown, West Virginia.

2013 — 2013 Mead Johnson Research Award in Endocrinology and Metabolism. The American Physiological Society. Federation of American Societies for Experimental Biology (FASEB). Title of work: Heat Shock Protein 27 (hsp27) Translocation to the

	Mitochondria is Associated with Protection Against Diabetic Cardiomyopathy.
2013	1st Place Oral Presentation, Van Liere Convocation, West Virginia University. Title of Podia Presentation: Mitochondrial Translocation and Phosphorylation: What's the Hsp27 connection?
2012	American Society for Cell Biology Grant for One Day Local Meeting- Appalachian Regional Cell Conference.
2012	Invited/Scheduled Dr. Ronglih Liao to speak for Cell Biology Training Program, West Virginia University.
2012	1st Place Poster Presentation, Van Liere Convocation, West Virginia University. Title of work: Conventional echocardiography and speckle-tracking based strain imaging of the type I diabetic heart.
2012	West Virginia University School of Medicine Biomedical Sciences Travel Award. Travel award used to attend FASEB conference. Title of work: Longitudinal assessment of type I diabetes mellitus using conventional echocardiography and speckle-tracking based strain imaging.
2010	Inducted into Phi Beta Kappa at Baylor University.
2006-2010	Dean's List at Baylor University.

SPECIALIZED TRAINING

2011	Workshop on Surgical Techniques in the Laboratory Mouse. The Jackson Laboratory. Bar Harbor, Maine.

PROFESSIONAL SOCIETIES/ORGANIZATIONS

2013-2015	American Women in Science
2013-2015	American Association for the Advancement of Science
2012-2016	American Heart Association
2012-2014	American Physiological Society
2012-2013, 2015-2017	American Society for Cell Biology
2011-Present	Center for Cardiovascular and Respiratory Sciences, West Virginia University.

2010-Present Cell Biology Training Program, West Virginia University.

GRANTS RECEIVED

American Heart Association One Year Predoctoral Fellowship
American Heart Association (14PRE19890020)
Role: Principal Investigator
Funded: July 1, 2014 – June 30, 2015

West Virginia University Student Government Association Grant
Role: President of the Health Sciences Center Graduate Student Organization
Funded: October 2014 – May 2015

ASCB Grant for one day local meeting – Appalachian Regional Cell Conference
Role: Student Organizer/Consultant
Funded: July 1, 2014 – December 31, 2014

ASCB Grant for one day local meeting – Appalachian Regional Cell Conference
Role: Student Organizer/Consultant
Funded: July 1, 2013 – December 31, 2013

NIH Predoctoral Training Grant in Cardiovascular and Pulmonary Diseases (T32)
National Institute of Health (5T32HL090610-03)
Role: Predoctoral Trainee
Funded: July 1, 2012 – July 1, 2014

ASCB Grant for one day local meeting – Appalachian Regional Cell Conference
Role: Principal Investigator
Funded: July 1, 2012 – December 31, 2012

VOLUNTEER WORK

2015 – 2016	Relay for Life Monongalia County, West Virginia.
2015 – 2016	Girls on the Run. Monongalia County, West Virginia.
2015	Walt Disney World Marathon Weekend Volunteer. January 8, 2015.
2014 – 2016	Operation Christmas Child. Volunteer throughout the year organizing and preparing for Christmas.
2010 – 2014	Labor of Love Ministries. Morgantown, West Virginia.

PRESENTATIONS

Invited Podia Presentations

MicroRNAs in the Mitochondrion. Mitochondria and Metabolism Working Group, West Virginia University, Morgantown, West Virginia. September 12, 2016.

How I Got Here, What I do, and How to Make a Difference in STEM. Health Sciences and Technology Academy, University High School, Morgantown, West Virginia. October 5, 2015.

How Can We Help Diabetic Patients? One Beat of the Heart at a Time. 3 Minute Thesis Competition. West Virginia University, Morgantown, West Virginia. April 9, 2015.

Examination of Novel Echocardiographic Analyses and Mitochondrial Dysfunction in the Diabetic Heart. Davis and Elkins Biology and Environmental Sciences Forum, Davis and Elkins College, Elkins, West Virginia. March 12, 2015.

Distinct Myocardial Strain Profiles in Type 1 versus Type 2 Diabetes: Differences in how they pump. Van Liere Convocation, West Virginia University. February 26, 2015.

Hyperglycemia and Hemoglobin A1c: Clinical predictors of mitochondrial dysfunction in diabetic patients. Appalachian Regional Cell Conference, Marshall University. November 8, 2014.

Mitochondrial Translocation and Phosphorylation: What's the Hsp27 connection? Van Liere Convocation, West Virginia University. February 28, 2013.

Poster Presentations

Shepherd D.L., Baseler W.A., Dabkowski E.R., Nichols C.E., Thapa D., Croston T.L., Hollander J.M. Mitochondrial Proteomic Alterations in the Diabetic Heart: A Central Role for Protein Import. NHLBI/NIDDK 2016 Mitochondrial Biology Symposium: Novel Roles in Health and Disease. May 19, 2016.

Shepherd D.L., Sreekumar S., Nichols C.E., Hollander J.M. Import of microRNA378 into Cardiac Mitochondria: How do they get in? Appalachian Regional Cell Conference. November 21, 2015.

Shepherd D.L., Croston T.L., Holden A.A., Tveter K.J., Thapa D., Nichols C.E., Long D.M., Olfert I.M., Hollander J.M. Mitochondrial Dysfunction: A New Clinical Predictor of Disease Development in the Type 2 Diabetic Patient? West Virginia Clinical and Translational Science Institute Annual Meeting. October 2015.

Shepherd D.L., Nichols C.E., Thapa D., Hollander J.M. Distinct Myocardial Strain Profiles in Type 1 versus Type 2 Diabetes: Differences in how they pump. Van Liere Convocation, West Virginia University. February 2015.

Shepherd D.L., Croston T.L., Holden A.A., Tveter K.J., Thapa D., Nichols C.E., Long D.M., Olfert I.M., Hollander J.M. Hyperglycemia and Hemoglobin A1c: Can They Serve as Clinical

Predictors of Cardiac Mitochondrial Dysfunction in the Type 2 Diabetic Patient? Appalachian Regional Cell Conference, Marshall University. November 2014.

Shepherd D.L., Croston T.L., Holden A.A., Tveter K.J., Thapa D., Nichols C.E., Long D.M., Olfert I.M., Hollander J.M. Mitochondrial Dysfunction in the Type II Diabetic Patient: A different viewpoint. American Association of Pharmaceutical Scientists, West Virginia University. May 2014.

Shepherd D.L., Croston T.L., Holden A.A., Tveter K.J., Thapa D., Nichols C.E., Long D.M., Olfert I.M., Hollander J.M. The Type 2 Diabetic Patient and Cardiac Mitochondrial Dysfunction: A new perspective. FASEB J. 2014 *28:688.10*

Shepherd D.L., Croston T.L., Holden A.A., Tveter K.J., Thapa D., Nichols C.E., Long D.M., Olfert I.M., Hollander J.M. Cardiac Mitochondrial Dysfunction in the Type 2 Diabetic Patient: A new perspective. Van Liere Convocation, West Virginia University. February 2014.

Shepherd D.L., Croston T.L., Holden A.A., Tveter K.J., Thapa D., Nichols C.E., Hollander J.M. Human and Mouse Type 2 Diabetes Mellitus and the Mitochondrial Proteome: The beginning to therapeutic possibilities. American Association of Pharmaceutical Scientists, Duquesne University. November 2013.

Shepherd D.L., Croston T.L., Holden A.A., Tveter K.J., Thapa D., Nichols C.E., Hollander J.M. Human and Mouse Cardiac Dysfunction during Type 2 Diabetes Mellitus: Effects on the mitochondrial proteome. Appalachian Regional Cell Conference, West Virginia University in Charleston, WV. October 2013.

Shepherd D.L., Croston T.L., Lewis S.E., Nichols C.E., Thapa D., Jagannathan R., Hollander J.M. Hsp27 Phosphorylation and Mitochondrial Translocation: What's the type 1 diabetic story? American Association of Pharmaceutical Scientists, West Virginia University. May 2013.

Shepherd D.L., Croston T.L., Lewis S.E., Nichols C.E., Thapa D., Jagannathan R., Hollander J.M. Mitochondrial Translocation and Phosphorylation: What's the Hsp27 connection? Van Liere Convocation, West Virginia University. 2013.

Shepherd D.L., Croston T.L., Lewis S.E., Nichols C.E., Thapa D., Jagannathan R., Hollander J.M. Heat Shock Protein 27 (hsp27) Translocation to the Mitochondria is Associated with Protection Against Diabetic Cardiomyopathy. FASEB J. 2013 *27:1209.3*

Shepherd D.L., Croston T.L., Lewis S.E., Nichols C.E., Thapa D., Jagannathan R., Hollander J.M. Mitochondrial Translocation of Heat Shock Protein 27 (hsp27) Protects Against Diabetic Cardiomyopathy. Appalachian Regional Cell Conference, West Virginia University in Charleston, WV. October 2012.

Shepherd D.L., Croston T.L., McLaughlin S.L. Baseler W.A., Nichols C.E., Thapa D., Lewis S.E., Hollander J.M. Longitudinal assessment of type I diabetes mellitus using conventional echocardiography and speckle-tracking based strain imaging. FASEB J. 2012 *26:1054.11*

Shepherd D.L., Croston T.L., Nichols C.E., Baseler W.A., Thapa D., Hollander J.M. Conventional echocardiography and speckle-tracking based strain imaging of the type I diabetic heart. Van Liere Convocation, West Virginia University. 2012.

PUBLICATIONS

Manuscripts

Shepherd, D.L., Hathaway, Q.A., Nichols, C.E., Hughes, K.M., Pinti, M.V., Stine, S.M., Hollander, J.M. Mitochondrial Proteome Disruption in the Diabetic Heart: A Central Role for Mitochondrial Heat Shock Protein 70 (mtHsp70) in Proteome Restoration. Submitted/Under Review Diabetes, 2016.

Hathaway, Q.A., Nichols, C.E., **Shepherd, D.L.**, Stapleton, P.A., McLaughlin S.L., Stricker, J.C., Rellick, S.L., Pinti, M.V., Abukabda, A.B., McBride, C.R., Yi, J., Stine, S.M., Nurkiewicz, T.R., Hollander, J.M. Maternal Engineered Nanomaterial Exposure Disrupts Progeny Cardiac Function and Bioenergetics. Submitted/Under Review AJP Heart and Circulatory Physiology, 2016.

Corbin, D.R., Rehg, J.E., **Shepherd, D.L.,** Zhang, Y.M., Rock C.O., Hollander, J.M., Jackowski, S., Leonardi, R. Excess Coenzyme A Reduces Skeletal Muscle Performance and Strength in Mice Overexpressing Human PANK2. Submitted/Under Review Mol Genet Metab, 2016.

Nichols, C.E., **Shepherd, D.L.,** Thapa, D., Yi, J., Dabkowski, E.R., Nurkiewicz, T.R., Hollander, J.M. Reactive Oxygen Species Damage Drives Cardiac and Mitochondrial Dysfunction Following Acute Nano-Titanium Dioxide Inhalation Exposure. In Preparation, 2016.

Shepherd D.L., Croston T.L., Nichols C.E., McLaughlin S.L., Lewis S.E., Thapa D., Dick G.M., Hollander J.M. Early Cardiac Dysfunction in the Type 1 Diabetic Heart Using Speckle-Tracking-Based Strain Imaging. J Mol Cell Cardiol 2015 Dec 3;90:74-84.

Nichols C.E., **Shepherd D.L.**, Knuckles T.L., Thapa D., Stricker J.C., Stapleton P.A., Minarchick V.C., Erdely A., Zeidler-Erdley P.C., Alway S.A., Nurkiewicz T.R., Hollander J.M. Cardiac and Mitochondrial Dysfunction Following Acute Pulmonary Exposure to Mountaintop Removal Mining Particulate Matter. Am J Physiol Heart Circ Physiol. 2015 Dec 15;309(12):H2017-30.

Jagannathan R., Thapa D., Baseler W., **Shepherd D.**, Croston T., Nichols C., Lewis S., Hollander J. Translational Regulation of the Mitochondrial Genome Following Redistribution of Mitochondrial MicroRNA (MitomiR) in the Diabetic Heart. Circ Cardiovasc Genet. 2015 Dec;8(6):785-802.

Thapa D., Nichols C.E., Lewis S.E., **Shepherd D.L.**, Jagannathan R., Croston T.L., Tveter K.J., Holden A.A., Baseler W.A., Hollander J.M. Transgenic overexpression of mitofilin attenuates diabetes mellitus-associated cardiac and mitochondria dysfunction. J Mol Cell Cardiol. 2015 Feb;79:212-23.

Stapleton P.A., Nichols C.E., Yi J., McBride C.R., Minarchick V.C., **Shepherd D.L.**, Hollander J.M., Nurkiewicz T.R. Microvascular and Mitochondrial Dysfunction in the Female F1 Generation after Gestational TiO2 Nanoparticle Exposure. Nanotoxicology. 2015:9(8):941-51.

Hollander J.M., Thapa D., **Shepherd D.L.** Physiological and Structural Differences in Spatially Distinct Subpopulations of Cardiac Mitochondria: Influence of Pathologies. Am J Physiol Heart Circ Physiol 2014 Jul 1;307(1):H1-14. *Highlighted as a Featured Article on the American Journal of Physiology Heart and Circulatory Physiology Home Page, September 2014.

Croston T.L., Holden A.A., Tveter K.J., Thapa D., Lewis S.E., **Shepherd D.L.**, Nichols C.E., Long D.M., Olfert I.M., Jagannathan R., Hollander J.M. Functional Deficiencies of Subsarcolemmal Mitochondria in the Type 2 Diabetic Human Heart. Am J Physiol Heart Circ Physiol 2014 Jul 1;307(1):H54-65.

Croston T.L., **Shepherd D.L.**, Jagannathan R., Thapa D., Nichols C.E., Dabkowski E.R., Lewis S.E., Hollander J.M. Evaluation of the cardiolipin biosynthetic pathway and its interactions in the diabetic heart. Life Sci 2013 Sep;93(8):313-22.

Baseler W.A., Dabkowski E.R., Jagannathan R., Thapa D., Nichols C.E., **Shepherd D.L.**, Croston T.L., Powell M., Razunguzwa T.T., Lewis S.E., Schnell D.M., Hollander J.H. Reversal of Mitochondrial Proteomic Loss in Type 1 Diabetic Heart with Overexpression of Phospholipid Hydroperoxide Glutathione Peroxidase. Am J Physiol Regul Integr Comp Physiol 2013 Apr;304(7):R553-65.

Book Chapters

Shepherd D.L. Paying It Forward: Engaging the Next Generation of Professional Students In C. McMaster and C. Murphy (Eds.), Graduate Study in the USA: Surviving and Succeeding (Pages 71-77). New York: Peter Lang. 2016.

Abstracts

Sreekumar S., **Shepherd D.L.**, Hathaway Q.A., Stine S.M., Hollander, J.M. Import of miR378 into Diabetic Cardiac Mitochondria: The importance of PNPase and RISC association. West Virginia IDeA Network of Biomedical Research Excellence, West Virginia University. August 2016.

Shepherd D.L., Baseler W.A., Dabkowski E.R., Nichols C.E., Thapa D., Croston T.L., Hollander J.M. Mitochondrial Proteomic Alterations in the Diabetic Heart: A Central Role for Protein Import. NHLBI/NIDDK 2016 Mitochondrial Biology Symposium: Novel Roles in Health and Disease. May 19, 2016.

Shepherd D.L., Nichols C.E., Sreekumar S., Hollander J.M. Import of microRNAs into Cardiac Mitochondria: How Do They Get In? Van Liere Convocation, West Virginia University. March, 2016.

Nichols C.E., Hollander J.M., Engels K., McBride C.R., Yi J., **Shepherd D.L.**, Abukabda A.B., Stapleton P.A., Nurkiewicz T.R. Maternal Engineered Nanomaterial Inhalation During Gestation Alters the Fetal Transcriptome. Society of Toxicology March 2016.

Shepherd D.L., Sreekumar S., Nichols C.E., Hollander J.M. Import of microRNA378 into Cardiac Mitochondria: How do they get in? Appalachian Regional Cell Conference. November 21, 2015.

Shepherd D.L., Croston T.L., Holden A.A., Tveter K.J., Thapa D., Nichols C.E., Long D.M., Olfert I.M., Hollander J.M. Mitochondrial Dysfunction: A New Clinical Predictor of Disease Development in the Type 2 Diabetic Patient? West Virginia Clinical and Translational Science Institute Annual Meeting. October 2015.

Sreekumar S., Nichols C.E., **Shepherd D.L.**, Hollander, J.M. Import Mechanism of miR378 into Cardiac Mitochondria. West Virginia IDeA Network of Biomedical Research Excellence, West Virginia University. August 2015. **Taken to Undergraduate Research Day at the Capitol, West Virginia, February 25, 2016.

Nichols C.E., Thapa D., **Shepherd D.L.**, Knuckles T.L., Erdely A., Zeidler-Erdely P.C., Nurkiewicz T.R., Hollander J.M. Mitochondrial microRNA Dysregulation Contributes to Acute Cardiac Dysfunction following Pulmonary Mountaintop Mining Particulate Matter Exposure. Society of Toxicology. March 2015.

Shepherd D.L., Nichols C.E., Thapa D., Hollander J.M. Distinct Myocardial Strain Profiles in Type 1 versus Type 2 Diabetes: Differences in how they pump. Van Liere Convocation, West Virginia University. February 2015.

Nichols C.E., Thapa D., **Shepherd D.L.**, Knuckles T.L., Erdely A., Zeidler-Erdely P.C., Nurkiewicz T.R., Hollander J.M. MicroRNA Dysregulation and Cardiac Dysfunction following Mountaintop Mining Particulate Exposure. Van Liere Convocation, West Virginia University. February 2015.

Shepherd D.L., Croston T.L., Holden A.A., Tveter K.J., Thapa D., Nichols C.E., Long D.M., Olfert I.M., Hollander J.M. Hyperglycemia and Hemoglobin A1c: Can They Serve as Clinical Predictors of Cardiac Mitochondrial Dysfunction in the Type 2 Diabetic Patient? Appalachian Regional Cell Conference, Marshall University. November 2014.

Shepherd D.L., Croston T.L., Holden A.A., Tveter K.J., Thapa D., Nichols C.E., Long D.M., Olfert I.M., Hollander J.M. Mitochondrial Dysfunction in the Type II Diabetic Patient: A different viewpoint. American Association of Pharmaceutical Scientists, West Virginia University. May 2014.

Nichols C.E., Erdely A., **Shepherd D.L.**, Thapa D., Salmen R., McLoughlin C., Sager T., Roberts J.R., Hollander J.M. Pulmonary Exposure to Carbon-Based Nanomaterials induces Spatially-distinct Cardiac Mitochondrial Dysfunction. AESOT. May 2014.

Shepherd D.L., Croston T.L., Holden A.A., Tveter K.J., Thapa D., Nichols C.E., Long D.M., Olfert I.M., Hollander J.M. The Type 2 Diabetic Patient and Cardiac Mitochondrial Dysfunction: A new perspective. FASEB J. 2014 *28:688.10.*

Nichols C.E., Erdely A., **Shepherd D.L.**, Thapa D., Salmen R., McLoughlin C., Sager T., Roberts J.R., Hollander J.M. Spatially-distinct cardiac mitochondrial dysfunction following pulmonary exposure to various carbon-based nanomaterials. Toxicologist 2014 *138(1):127.*

Shepherd D.L., Croston T.L., Holden A.A., Tveter K.J., Thapa D., Nichols C.E., Long D.M., Olfert I.M., Hollander J.M. Cardiac Mitochondrial Dysfunction in the Type 2 Diabetic Patient: A new perspective. Van Liere Convocation, West Virginia University. February 2014.

Thapa D., Nichols C.E., **Shepherd D.L.,** Hollander J.M. Overexpression of mitofilin restores cardiac contractile function during a type 1 diabetic insult. Van Liere Convocation, West Virginia University. February 2014.

Nichols C.E., Erdely A., **Shepherd D.L.,** Thapa D., Salmen R., McLoughlin C., Sager T., Roberts J.R., Hollander J.M. Carbon-based nanomaterials impact cardiac mitochondrial function following pulmonary exposure. Van Liere Convocation, West Virginia University. February 2014.

Shepherd D.L., Croston T.L., Holden A.A., Tveter K.J., Thapa D., Nichols C.E., Hollander J.M. Human and Mouse Type 2 Diabetes Mellitus and the Mitochondrial Proteome: The beginning to therapeutic possibilities. American Association of Pharmaceutical Scientists, Duquesne University. November 2013.

Shepherd D.L., Croston T.L., Holden A.A., Tveter K.J., Thapa D., Nichols C.E., Hollander J.M. Human and Mouse Cardiac Dysfunction during Type 2 Diabetes Mellitus: Effects on the mitochondrial proteome. Appalachian Regional Cell Conference, West Virginia University in Charleston, WV. October 2013.

Nichols C.E., **Shepherd D.L.**, Croston T.L., Thapa D., Lewis S.E., Jagannathan R., Yi J., Nurkiewicz T.R., Hollander J.M. Acute Nanoparticle Inhalation Provokes Diastolic Stress and Cardiac Mitochondrial Dysfunction. Appalachian Regional Cell Conference, West Virginia University in Charleston, WV. October 2013.

Thapa D., Croston T.L., **Shepherd D.L.**, Nichols C.E., Lewis S.E., Jagannathan R., Hollander J.M. Role of mitofilin in mitochondrial structure and function during a type 1 diabetic insult. Appalachian Regional Cell Conference, West Virginia University in Charleston, WV. October 2013.

Shepherd D.L., Croston T.L., Lewis S.E., Nichols C.E., Thapa D., Jagannathan R., Hollander J.M. Hsp27 Phosphorylation and Mitochondrial Translocation: What's the type 1 diabetic story? American Association of Pharmaceutical Scientists, West Virginia University. May 2013.

Shepherd D.L., Croston T.L., Lewis S.E., Nichols C.E., Thapa D., Jagannathan R., Hollander J.M. Mitochondrial Translocation and Phosphorylation: What's the Hsp27 connection? Van Liere Convocation, West Virginia University. March 2013.

Nichols C.E., **Shepherd D.L.**, Croston T.L., Thapa D., Lewis S.E., Jagannathan R., Yi J., Nurkiewicz T.R., Hollander J.M. Nano-Titanium Dioxide Inhalation Exposure induces Cardiac and Spatially-Distinct Mitochondrial Dysfunction. Van Liere Convocation, West Virginia University. March 2013.

Shepherd D.L., Croston T.L., Lewis S.E., Nichols C.E., Thapa D., Jagannathan R., Hollander J.M. Heat Shock Protein 27 (hsp27) Translocation to the Mitochondria is Associated with Protection Against Diabetic Cardiomyopathy. FASEB J. 2013 *27:1209.3.*

Nichols C.E., **Shepherd D.L.**, Croston T.L., Thapa D., Lewis S.E., Jagannathan R., Yi J., Nurkiewicz T.R., Hollander J.M. Acute Inhalation Exposure of Nano-Titanium Dioxide induces Cardiac and Mitochondrial Dysfunction in Mice. FASEB J. 2013 *27:890.9.*

Jagannathan R., Thapa D., Baseler W.A., **Shepherd D.L.**, Croston T.L., Nichols C.E., Lewis S.E., Hollander J.M. Translational regulation of the mitochondrial genome following redistribution of mitochondrial microRNA (MitomiR) in the diabetic heart. FASEB J. 2013 *27:701.10.*

Lewis S.E., Dabkowski E.R., Baseler W.A., **Shepherd D.L.**, Croston T.L., Thapa D., Nichols C.E., Hollander J.M. Impact of mitochondria phospholipid hydroperoxide glutathione peroxidase (mPHGPx) overexpression on the type 1 diabetic heart. FASEB J. 2013 *27:1209.2.*

Thapa D., Jagannathan R., Croston T.L., Baseler W.A., Nichols C.E., **Shepherd D.L.**, Lewis S.E., Hollander J.M. Interaction of mitofilin with respiratory complexes in mitochondrial subpopulations. FASEB J. 2013 *27:1126.6.*

Croston T.L., Holden A.A., Tveter K., Lewis S.E., Thapa D., **Shepherd D.L.**, Nichols C.E., Jagannathan R., Hollander J.M. Diabetic mouse hearts: a good predictor for the human population? FASEB J. 2013 *27:701.9.*

Fancher I.S., Croston T.L., **Shepherd D.L.**, Dick G.M., Hollander J.M. Cardiac interfibrillar mitoK_{ATP} channels are sensitive to diazoxide and have a regulatory subunit profile distinct from subsarcolemmal mitoK_{ATP}. FASEB J. 2013 *27:1209.16.*

Shepherd D.L., Croston T.L., Lewis S.E., Nichols C.E., Thapa D., Jagannathan R., Hollander J.M. Mitochondrial Translocation of Heat Shock Protein 27 (hsp27) Protects Against Diabetic Cardiomyopathy. Appalachian Regional Cell Conference, West Virginia University in Charleston, WV. October 2012.

Croston T.L., **Shepherd D.L.**, Baseler W.A., Dabkowski E.R., Thapa D., Nichols C.E., Jagannathan R., Lewis S.E., Hollander J.M. Cardiolipin impacts mitochondrial functional integrity in diabetic cardiomyopathy. Appalachian Regional Cell Conference, West Virginia University in Charleston, WV. October 2012.

Nichols C.E., Croston T.L., **Shepherd D.L.**, Thapa D., LaFata G.L., Lewis S.E. Knuckles T.L., McCawley M., Hendryx M., Nurkiewicz T.R., Hollander J.M. Mountain-top mining particulate exposure decreases function and increases apoptotic propensity of distinct subcellular species

of cardiac mitochondria. Appalachian Regional Cell Conference, West Virginia University in Charleston, WV. October 2012.

Thapa D., Baseler W.A., Jagannathan R., Dabkowski E.R., Croston T.L., Nichols C.E., **Shepherd D.L.**, Lewis S.E., Hollander J.M. Cardiomyocytes enrichment with miR-141 regulates ATP content. Appalachian Regional Cell Conference, West Virginia University in Charleston, WV. October 2012.

Shepherd D.L., Croston T.L., McLaughlin S.L. Baseler W.A., Nichols C.E., Thapa D., Lewis S.E., Hollander J.M. Longitudinal assessment of type I diabetes mellitus using conventional echocardiography and speckle-tracking based strain imaging. FASEB J. 2012 *26:1054.11.*

Nichols C.E., **Shepherd D.L.**, Croston T.L., Thapa D., Lewis S.E., Jinghai Y., McBribe C., Nurkiewicz T.R., Hollander J.M. Acute inhalation exposure of titanium dioxide nanoparticles induces diastolic dysfunction and mitochondrial dysfunction in mice. AESOT. April 2012.

Nichols C.E., Baseler W.A., Thapa D., LaFata G.L., Croston T.L., **Shepherd D.L.**, Lewis S.E., Knuckles T.L. McCawley M., Hendryx M., Nurkiewicz T.R., Hollander J.M. Effect of mountain-top mining particulate exposure on function and apoptotic propensity of distinct subcellular species of mitochondria. AESOT. April 2012.

Nichols C. E., Baseler W.A., Thapa D., LaFata G.L., Croston T.L., **Shepherd D.L.**, Lewis S.L., Knuckles T.L., McCawley M., Hendryx M., Nurkiewicz T.R., Hollander J.M. Mountain-top mining particulate matter exposure increases markers of mitochondrially-driven apoptosis in rat cardiac tissue. FASEB J. 2012 *26:1036.15.*

Shepherd D.L., Croston T.L., Nichols C.E., Baseler W.A., Thapa D., Hollander J.M. Conventional echocardiography and speckle-tracking based strain imaging of the type I diabetic heart. Van Liere Convocation, West Virginia University. February 2012.

Croston T.L., **Shepherd D.L.**, Baseler W.A., Dabkowski E.R., Thapa D., Nichols C.E., Jagannathan R., Lewis S.E., Hollander J.M. Influence of diabetic cardiomyopathy on cardiolipin biosynthesis. Van Liere Convocation, West Virginia University. February 2012.

Nichols C. E., Baseler W.A., Thapa D., LaFata G.L., Croston T.L., **Shepherd D.L.**, Lewis S.L., Knuckles T.L., McCawley M., Hendryx M., Nurkiewicz T.R., Hollander J.M. Effect of mountain-top mining particulate exposure on mitochondria function and apoptotic propensity. Van Liere Convocation, West Virginia University. February 2012.

Baseler W.A., Dabkowski E.R., Jagannathan R., Thapa D., Nichols C.E., **Shepherd D.L.**, Croston T.L., Schnell D.M., Hollander J.M. Overexpression of phospholipid hydroperoxide glutathione peroxidase (MPHGPx) attenuates cardiac mitochondrial proteomic loss and reverses protein import detriments observed with type 1 diabetes mellitus. FASEB J. 2012 *26:1127.4.*

Thapa D., Baseler W.A., Jagannathan R., Dabkowski E.R., Croston T.L., Nichols C.E., **Shepherd D.L.**, Lewis S.E., Hollander J.M. miRNA-141 is a potential regulator of the mitochondrial phosphate carrier (slc25a3) in the type 1 diabetic heart. FASEB J. 2012 *26:869.11.*

Croston T.L., **Shepherd D.L**, Baseler W.A., Dabkowski E.R., Thapa D., Nichols C.E., Jagannathan R., Lewis S.E., Hollander J.M. Examination of cardiolipin biosynthesis in the diabetic heart FASEB J. 2012 *26:lb746.*

Jagannathan R., Baseler W.A., Thapa D., Croston T.L., **Shepherd D.L.**, Nichols C.E., Hollander J.M. HDAC6 regulates mitochondrial oxidative phosphorylation by ATP synthase β subunit acetylation in diabetic cardiomyopathy. FASEB J. 2012 *26:869.13.*

Fancher I.S., Baseler W.A., Croston T.L., Thapa D., **Shepherd D.L.**, Nichols C.E., Jagannathan R., Asano S., Lewis S.E., Dick G.M., Hollander J.M. Differential expression of mitoKATP subunits in cardiac mitochondrial subpopulations and the influence of Type I diabetes mellitus. FASEB J. 2012 *26:1057.6.*

REFERENCES

1. **John M. Hollander, Ph.D.** Mentor, Associate Professor, Director of Graduate Studies, Division of Exercise Physiology, West Virginia University
   Email: jhollander@hsc.wvu.edu

2. **Fred L. Minnear, Ph.D.** Professor Emeritus (retired June 2015). Formerly Professor of Physiology and Pharmacology, Assistant Vice President for Graduate Education, and the West Virginia Clinical and Translational Science Institute's Clinical Research, Education, Mentoring and Career Development Core Director.
   Email: fminnear@hsc.wvu.edu

3. **Glenn Dillon, Ph.D.** University of North Texas Vice Provost for Health Institutes. Formerly West Virginia University Vice President for Health Sciences Center Research and Graduate Education.
   Email: Glenn.Dillon@unthsc.edu